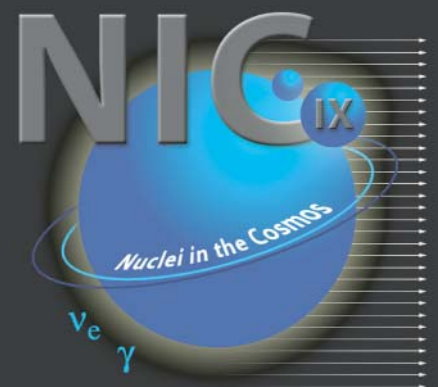


# Nuclei in the Cosmos IX

CERN, GENEVA, SWITZERLAND ● 25 – 30 June 2006



## AGENDA & ABSTRACTS



[www.cern.ch/nic9](http://www.cern.ch/nic9)

# Nuclei in the Cosmos – IX

## Agenda & Abstracts

CERN, Geneva, Switzerland  
25-30 June, 2006

### International Advisory Board

M. Aliotta (University of Edinburgh, UK)  
C. Angulo (Université Louvain-la-Neuve, Belgium)  
L. Buchmann (TRIUMF, Canada)  
A. Davis (University of Chicago, USA)  
R. Diehl (MPI-Munich, Germany)  
R. Gallino (University of Torino, Italy)  
M. Heil (Forschungszentrum Karlsruhe/  
GSI Darmstadt, Germany)  
W. Hillebrandt (MPI-Garching, Germany)  
T. Kajino (NAO-Tokyo, Japan)  
P. Koehler (Oak Ridge National Laboratory, USA)  
S. Kubono (University of Tokyo, Japan)  
D. Lambert (University of Austin, USA)  
K. Langanke (GSI Darmstadt, Germany)  
J. Lattanzio (Monash University, Australia)  
N. Prantzos (Institute of Astrophysics,  
Paris, France)  
C. Rolfs (Ruhr-Universität, Bochum, Germany)  
H. Schatz (MSU, USA)  
C. Spitaleri (Catania, Italy)  
F.-K. Thielemann (Universität Basel, Switzerland)  
C. Volpe (IPN-Orsay, France)  
M. Wiescher (University of Notre Dame, USA)  
S.E. Woosley (University of California,  
Santa Cruz, USA)

### Local Organizing Committee

A. Mengoni (CERN-n\_TOF/IAEA)  
– Conference Chair  
M. Lindroos (CERN-ISOLDE)  
– Scientific Secretary  
J.D. Auria (Simon Fraser University/CERN)  
P. Butler (CERN-ISOLDE)  
L.M. Fraile (CERN-ISOLDE)  
M. Hass (CERN-ISOLDE/  
Weizmann Institute, Israel)  
M. Hjorth-Jensen (University of Oslo/  
CERN-ISOLDE/MSU)  
F. Käppeler (Forschungszentrum Karlsruhe,  
Germany)  
K.-L. Kratz (Universität Mainz, Germany)  
G. Meynet (Geneva Observatory, Switzerland)  
K. Riisager (University of Aarhus/CERN-ISOLDE)

### Secretariat

Tina Osborne & Jennifer Weterings  
CERN CH-1211 Geneva 23  
SWITZERLAND  
Phone: +41 22 767 5828  
email: tina.osborne@cern.ch, jenny.weterings@cern.ch

[www.cern.ch/nic9](http://www.cern.ch/nic9)  
[nic9@cern.ch](mailto:nic9@cern.ch)

# ABSTRACTS

Edited by E. Uberseder<sup>1</sup>, S. Bisterzo<sup>1</sup>, C. Domingo Pardo<sup>1</sup>, F. Käppler<sup>1</sup>, and A. Mengoni<sup>2</sup>  
<sup>1</sup>Forschungszentrum Karlsruhe and <sup>2</sup>IAEA Vienna

# Contents

<b>1</b>	<b>Stars: observations, evolution &amp; nucleosynthesis</b>	<b>8</b>
1.1	Nuclear astrophysics with $\gamma$ -ray line observations . . . . .	8
1.2	From massive stars to supernovae . . . . .	8
1.3	The $rp$ process and X-ray bursts . . . . .	8
<b>2</b>	<b>Experiments in nuclear astrophysics I</b>	<b>8</b>
2.1	Underground nuclear astrophysics . . . . .	8
2.2	The $^{26}\text{Al}(p, \gamma)^{27}\text{Si}$ reaction in novae . . . . .	9
2.3	Direct measurement of the $^{18}\text{F}(p, \alpha)^{15}\text{O}$ reaction for application to nova $\gamma$ -ray emission. . . . .	9
2.4	Measuring difficult reaction rates involving radioactive beams: a new approach .	10
<b>3</b>	<b>Nuclei far from stability</b>	<b>10</b>
3.1	Nuclear-physics data for modeling of the $r$ process . . . . .	10
3.2	Progress in the investigation of nuclei approaching the $r$ -process waiting point A = 195 . . . . .	11
3.3	Building nuclei from the ground up . . . . .	11
3.4	Mass measurements of exotic nuclei and their role in stellar nucleosynthesis . .	12
<b>4</b>	<b>Big-Bang nucleosynthesis</b>	<b>12</b>
4.1	Recent results in Big-Bang nucleosynthesis . . . . .	12
4.2	Is deuterium cosmological? . . . . .	12
4.3	New measurement of the cross section of the Big Bang nucleosynthesis reaction $\text{D}(\alpha, \gamma)^6\text{Li}$ and its astrophysical impact . . . . .	13
<b>5</b>	<b>Element production &amp; stellar evolution: MP &amp; UMP stars</b>	<b>13</b>
5.1	$r$ -Process enhanced metal-poor stars . . . . .	13
5.2	The origins of carbon and neutron-capture element enhancements in metal-poor stars . . . . .	14
5.3	Mass loss at very low metallicity: Impacts on nucleosynthesis and GRB progenitors	14
5.4	Chemical compositions derived from near ultra-violet observations of low-metallicity stars: New insights into the sites of neutron-capture nucleosynthesis processes .	14
5.5	The frequency of carbon-enhanced Stars in HERES and SDSS . . . . .	14
<b>6</b>	<b>Evidence of nucleosynthesis in stars and presolar grains</b>	<b>15</b>
6.1	Heavy elements in presolar grains: Constraints on conditions in asymptotic giant branch stars . . . . .	15
6.2	On the stellar sources of presolar graphite in primitive meteorites . . . . .	15
6.3	Isotopic composition of presolar spinel grain OC2: Constraining intermediate-mass asymptotic giant branch models . . . . .	16
6.4	Magnetic mixing and nucleosynthesis in AGB stars . . . . .	16
6.5	Accelerator mass spectrometry and nuclear astrophysics . . . . .	16
<b>7</b>	<b>Experiments in nuclear astrophysics: indirect methods</b>	<b>17</b>
7.1	Indirect techniques in nuclear astrophysics - ANCs and THM . . . . .	17
7.2	Reaction rate of $^{15}\text{O}(\alpha, \gamma)^{19}\text{Ne}$ via indirect measurements . . . . .	17
7.3	Study of astrophysically important resonant states in $^{26}\text{Si}$ by the $^{28}\text{Si}(^4\text{He}, ^6\text{He})^{26}\text{Si}$ reaction . . . . .	17
7.4	Influences on the triple $\alpha$ process beyond the Hoyle state . . . . .	18
7.5	Experimental determination of reaction rates via Coulomb dissociation . . . . .	19
<b>8</b>	<b>Experiments in nuclear astrophysics II</b>	<b>19</b>
8.1	$\alpha$ -Induced reactions in stellar burning . . . . .	19
8.2	$^{12}\text{C}(\alpha, \gamma)^{16}\text{O}$ . . . . .	19
8.2.1	Measuring $^{12}\text{C}(\alpha, \gamma)^{16}\text{O}$ with ERNA . . . . .	19

8.2.2	Measurement of the cascade cross section to the 6.049-MeV state in $^{16}\text{O}$ in $^{12}\text{C}(\alpha, \gamma)^{16}\text{O}$ . . . . .	20
8.3	$^{40}\text{Ca}(\alpha, \gamma)^{44}\text{Ti}$ . . . . .	20
8.3.1	Study of the $^{40}\text{Ca}(\alpha, \gamma)^{44}\text{Ti}$ reaction at stellar temperatures with DRAGON . . . . .	20
8.3.2	The supernova-nucleosynthesis $^{40}\text{Ca}(\alpha, \gamma)^{44}\text{Ti}$ reaction . . . . .	21
<b>9</b>	<b>Element production, stellar evolution, and stellar explosions</b> . . . . .	<b>21</b>
9.1	New ideas in the theory of core-collapse supernova explosions . . . . .	21
9.2	The role of neutrinos in explosive nucleosynthesis . . . . .	22
9.3	The first nova explosions . . . . .	22
9.4	Neutrinos and nucleosynthesis in $\gamma$ -ray bursts . . . . .	22
9.5	Presupernova evolution and explosive nucleosynthesis of massive stars . . . . .	23
<b>10</b>	<b>Element production &amp; stellar evolution II</b> . . . . .	<b>23</b>
10.1	Globular clusters : Ideal laboratories to test hydrogen-burning nucleosynthesis and hydrodynamics in stars? . . . . .	23
10.2	Neutron-capture elements in globular cluster M15 . . . . .	23
10.3	Chemical evolution of C-Zn and $r$ -process elements produced by the first generation stars . . . . .	24
10.4	Reaction rate uncertainties and the operation of the NeNa and MgAl chains during HBB in intermediate-mass AGB stars . . . . .	24
10.5	The new solar chemical composition: Does the Sun have a sub-solar metallicity? . . . . .	25
<b>11</b>	<b>Nuclear theory in astrophysics</b> . . . . .	<b>25</b>
11.1	Direct Reactions in/for Nuclear Astrophysics . . . . .	25
11.2	Cross sections of light-ion reactions calculated from ab initio wave functions . . . . .	26
11.3	Nuclear models for light systems . . . . .	26
11.4	Modified nuclear lifetime in hot dense plasmas . . . . .	26
11.5	Enhanced electron screening in nuclear reactions and radioactive decays . . . . .	27
<b>12</b>	<b>Cosmology &amp; BBN</b> . . . . .	<b>27</b>
12.1	Dark matter, dark energy & particle physics . . . . .	27
12.2	Type Ia supernovae as standard candles . . . . .	27
12.3	When stars attack! Live radioactivities as signatures of nearby supernovae . . . . .	27
12.4	Electron capture reactions in neutron star crusts: Deep heating and observational constraints . . . . .	28
12.5	Nuclear physics issues in the supernova hot bubble $r$ process: What we know and what we need to find out . . . . .	28
<b>13</b>	<b>Experiments in nuclear astrophysics III</b> . . . . .	<b>29</b>
13.1	AMS measurements of stellar cross sections across the nuclear chart . . . . .	29
13.2	Proton resonance scattering of $^7\text{Be}$ . . . . .	29
13.3	Improving the rate of the triple alpha reaction . . . . .	29
13.4	High-precision mass measurements for reliable nuclear-astrophysics calculations . . . . .	30
13.5	$\alpha$ -Capture reactions and the $\alpha$ -nucleus optical potential for $p$ -process nucleosynthesis . . . . .	30
<b>14</b>	<b>Experiments in nuclear astrophysics IV</b> . . . . .	<b>31</b>
14.1	Neutron capture cross section measurements for nuclear astrophysics at n_TOF . . . . .	31
14.2	Re/Os clock . . . . .	31
14.2.1	Measurements of the $(n, \gamma)$ and $(n, n')$ reaction cross sections on $^{186,187,189}\text{Os}$ and $^{187}\text{Re}$ - $^{187}\text{Os}$ cosmochronology . . . . .	31
14.2.2	Experimental challenges for the Re/Os clock . . . . .	32
14.3	Photodissociation measurements . . . . .	32
14.3.1	Electromagnetic excitations in nuclei: from photon scattering to photodissociation . . . . .	32

14.3.2	Photodissociation as a tool for nuclear astrophysics . . . . .	33
14.3.3	Photodisintegration of $^{181}\text{Ta}$ leading to the isomeric state $^{180}\text{Ta}^m$ . . . . .	33
14.4	Neutron capture measurements on the <i>s</i> -process termination isotopes lead and bismuth . . . . .	34
<b>15</b>	<b>Galactic &amp; stellar evolution</b>	<b>34</b>
15.1	Early galactic chemical evolution: The Milky Way in a cosmological context . .	34
15.2	Neutron capture processes in the early Galaxy . . . . .	34
15.3	Constraints on the yields of the first supernovae in the Universe . . . . .	35
15.4	AGB stars evolution and nucleosynthesis . . . . .	35
<b>16</b>	<b>Evolution &amp; evidence of nucleosynthesis in stars: AGBs</b>	<b>35</b>
16.1	3D hydrodynamical models of the core helium flash . . . . .	35
16.2	The <i>s</i> process in massive stars: The contribution from shell C-burning . . . . .	36
16.3	Light and heavy elements nucleosynthesis in low mass AGB stars . . . . .	36
<b>17</b>	<b>Experiments and theory in nuclear astrophysics</b>	<b>36</b>
17.1	The role of fission in <i>r</i> -process nucleosynthesis . . . . .	36
17.2	Nucleosynthesis in neutrino heated matter . . . . .	37
17.3	Studies of radioactive nuclei and their role in the cosmos . . . . .	37
<b>18</b>	<b>Poster session, 26 June</b>	<b>38</b>
18.1	Abundances of Mn, Co and Eu in a sample of 20 F-G disk stars: The influence of hyperfine structure splitting . . . . .	38
18.2	Coherent effects in nuclear pasta matter . . . . .	38
18.3	Pre-supernova models at low metallicities . . . . .	39
18.4	Breakup and competing processes in reactions involving weakly bound nuclei . .	39
18.5	$^{18}\text{F}(\alpha, p)^{21}\text{Ne}$ reaction: Neutron source for <i>r</i> process in supernovae . . . . .	40
18.6	Abundance clues to the nature of the “main” and the “weak” <i>r</i> -process . . . . .	40
18.7	$^{22}\text{Ne}$ : A primary source of neutrons for the <i>s</i> -process and a major neutron poison in CEMP AGB stars . . . . .	40
18.8	Structure of doorway states above the $K^\pi=8^+$ , $t_{1/2} \approx 2.0 \times 10^5$ yr isomer in $^{186}\text{Re}$ and their impact on the accuracy of the $^{187}\text{Re}/^{187}\text{Os}$ cosmochronometer . . . . .	41
18.9	Indirect techniques in nuclear astrophysics . . . . .	42
18.10	Measurement of the stellar $(n, \gamma)$ cross section of $^{54}\text{Fe}$ . . . . .	42
18.11	First measurements of the total and partial stellar neutron cross sections to the <i>s</i> -process branching-point $^{79}\text{Se}$ . . . . .	43
18.12	Present status of the KADoNiS database . . . . .	43
18.13	Light from the ashes: Explosion physics and nucleosynthesis from the X-ray spectra of type Ia supernova remnants . . . . .	44
18.14	Lead abundance and the weak <i>r</i> process in the metal-poor star K462 (M15) . .	44
18.15	Excitation functions of $(p, n)$ reactions on $^{115}\text{Sn}$ , $^{116}\text{Sn}$ and $^{120}\text{Sn}$ . . . . .	44
18.16	The production of germanium in asymptotic giant branch stars . . . . .	45
18.17	<i>r</i> -Process nucleosynthesis in Alfvén wave-driven proto-neutron star winds . . . .	45
18.18	Experimental determination of the $^{41}\text{Ca}(n, \alpha)^{38}\text{Ar}$ reaction cross section as a function of neutron energy . . . . .	45
18.19	Towards a direct measurement of the $^{15}\text{O}(\alpha, \gamma)^{19}\text{Ne}$ cross section: A first approach using the $^{15}\text{O}+\alpha$ elastic scattering . . . . .	46
18.20	Gravitational wave emission during the transition from rapidly differentially rotating neutron stars to strange stars . . . . .	46
18.21	Can supernova neutrino nucleosynthesis constrain neutrino oscillation parameters? .	47
18.22	<i>r</i> -Process nucleosynthesis in a collapsar . . . . .	47
<b>19</b>	<b>Poster session, 27 June</b>	<b>47</b>
19.1	Non-extensive statistical effects on the nuclear equation of state and on nuclear astrophysical problems . . . . .	47
19.2	Present-day carbon abundances from early-type stars . . . . .	48

19.3	Metastability of electron-nuclear astrophysical plasmas . . . . .	48
19.4	Neutron capture studies with a short flight path . . . . .	48
19.5	Quantitative spectroscopy of Deneb . . . . .	48
19.6	New Experiments on neutron rich $r$ -process Ge-Br isotopes at the NSCL/MSU .	49
19.7	CNO production in the first generation stars . . . . .	49
19.8	Heavy element nucleosynthesis in the MHD jet explosions of core-collapse super- novae . . . . .	49
19.9	Photodisintegration of $^{80}\text{Se}$ , $^{94}\text{Zr}$ , and $^{108}\text{Pd}$ as a probe of neutron capture for radioactive nuclei . . . . .	50
19.10	Observational constraints on the cosmology with a decaying cosmological term .	50
19.11	The $s$ -process branching at $^{186}\text{Re}$ revised . . . . .	50
19.12	Measurement of the stellar $(n, \gamma)$ cross section of $^{182}\text{Hf}$ . . . . .	51
19.13	Light element production in the circumstellar matter of type Ic supernovae at low metallicity . . . . .	51
19.14	Exotic cooling of neutron stars with different surface compositions . . . . .	52
19.15	Phase-transition phenomenology of frustrated nuclear matter in compact stars .	52
19.16	Dielectronic recombination rates in astrophysical plasmas . . . . .	53
19.17	Universality of the $p$ process . . . . .	53
19.18	Cosmic clock and thermometer for neutrino process . . . . .	53
19.19	High-resolution spectroscopy of cool extremely metal-poor carbon-rich stars . .	54
19.20	Extraction of resonant component from spin-polarization observables . . . . .	54
19.21	Equation of state and neutrino signal from collapsing stellar cores . . . . .	54
19.22	Asymmetric collapsing supernovae explosion with rotation . . . . .	55
19.23	Experimental studies of shell-model basis states near $^{132}\text{Sn}$ . . . . .	55
19.24	New study of the astrophysical reaction $^{13}\text{C}(\alpha, n)^{16}\text{O}$ via the $^{13}\text{C}(^7\text{Li}, t)^{17}\text{O}$ transfer reaction . . . . .	55
19.25	Measurement of $^3\text{He}(\alpha, \gamma)^7\text{Be}$ with ERNA recoil separator . . . . .	55
19.26	First experimental constraints on the interference of $3/2^+$ resonances in the $^{18}\text{F}(p, \alpha)^{15}\text{O}$ reaction . . . . .	56
19.27	Nuclear superfluidity and the cooling time of neutron stars . . . . .	56
19.28	Low-mass AGB stars abundance predictions with improved stellar cross sections	57
19.29	SNRs as probes of chemical composition of interstellar medium . . . . .	57
19.30	Nucleosynthesis of binary low mass zero-metallicity stars . . . . .	58
19.31	Synthesis of CNO elements in standard BBN . . . . .	58
19.32	Shell model spin and parity dependent nuclear level densities for nuclear reaction rates . . . . .	59
19.33	Nucleosynthesis and mixing in rotating AGB stars at low metallicity . . . . .	59
19.34	The $^{25}\text{Al}(p, \gamma)^{26}\text{Si}$ reaction rate in novae . . . . .	59
19.35	The QSE-reduced nuclear network for supernovae nucleosynthesis . . . . .	60
19.36	Investigation of nucleosynthesis capture reactions by using $^8\text{Li}$ radioactive beam transfer reactions . . . . .	60
<b>20 Poster session, 28 June</b>		<b>61</b>
20.1	Level structure of $^{19}\text{Ne}$ from studies of the $^{17}\text{O}(^3\text{He}, n)^{19}\text{Ne}$ reaction . . . . .	61
20.2	The $rp$ process in core-collapse supernovae . . . . .	61
20.3	The weak $r$ -process in core-collapse supernovae . . . . .	62
20.4	Elastic scattering of $^8\text{B}$ on Pb, liquid hydrogen, and liquid helium targets and the $^7\text{Be}(p, \gamma)^8\text{B}$ S-factor . . . . .	62
20.5	Low energy nuclear reaction measurements using monolithic silicon telescope . .	63
20.6	Photonuclear reactions of light nuclei studied with high-intensity real photon beams	63
20.7	Supernova physics with a low-energy $\beta$ -beam . . . . .	63
20.8	The detailed abundance patterns of light neutron-capture elements in very metal- poor stars . . . . .	64
20.9	Neutrino opacities in a relativistic non interacting neutron gas . . . . .	64
20.10	Mass measurement of neutron-deficient nuclei close to the $N = Z$ line . . . . .	64
20.11	Hydrodynamic models of type I X-ray bursts . . . . .	65
20.12	Enhanced $d(d, p)t$ cross section in metallic environments . . . . .	65

20.13	Thermonuclear burning ignition and propagation along the surface of neutron stars during X-ray bursts . . . . .	65
20.14	Measurement of the partial $(n, \gamma)$ cross section to $^{176}\text{Lu}^m$ at $s$ -process temperatures	66
20.15	Mapping of the $^{12}\text{C}^*$ and $^9\text{B}^*$ states of astrophysical interest via the $^{10}\text{B}(^3\text{He}, p\alpha\alpha)\alpha$ reaction . . . . .	66
20.16	Fission fragments of actinide and superheavy nuclides in primordial solar system material and problem of their origin . . . . .	67
20.17	A nonperturbative field-theoretical model for nuclear matter without the $\sigma$ and $\omega$	68
20.18	Spectroscopic analyses of subluminescent B stars in binaries . . . . .	68
20.19	A new approach to the solution of large thermonuclear burning networks . . . . .	69
20.20	Experiments and observations of light $r$ -process nuclei . . . . .	69
20.21	Neutrino nucleosynthesis of the exotic nuclei $^{138}\text{La}$ and $^{180}\text{Ta}$ by charged current reactions . . . . .	69
20.22	Measurement of the $^{62}\text{Ni}(n, \gamma)^{63}\text{Ni}$ reaction cross section at $3 < E_n < 100$ keV . . . . .	70
20.23	Study of unbound $^{19}\text{Ne}$ states via the proton transfer reaction $^2\text{H}(^{18}\text{F}, \alpha+^{15}\text{O})n$	71
20.24	Multiple particle break-up studies in the neutron rich Li isotopes . . . . .	71
20.25	Activation method for cross section measurements related to $p$ -process nucleosynthesis . . . . .	72
20.26	Activation measurement of the $^{19}\text{F}(n, \gamma)^{20}\text{F}$ cross section at $kT = 25$ keV . . . . .	72
20.27	The late-time supernova evolution induced by anisotropic neutrino radiation and the $r$ -process environment . . . . .	72
20.28	Nucleosynthesis in AGB stars: results from the STARS code . . . . .	73
20.29	E2 and E1 cross section of the $^{12}\text{C}(\alpha, \gamma)^{16}\text{O}$ reaction obtained at $E_{\text{cm}} = 1.6$ and $1.4$ MeV . . . . .	73
20.30	Signatures of AGB nucleosynthesis in dwarf galaxies . . . . .	74
20.31	Single point off-center helium ignitions as origin of some type Ia supernovae . . . . .	74
20.32	Fission recycling in the $r$ process and formation of the second peak with $A \sim 130$	74
20.33	Neutrino-induced nucleosynthesis as a probe into the mechanism of supernovae	75
20.34	Nuclear structure properties of neutron-rich $r$ -process isotopes . . . . .	75
20.35	Measurement of the temperature dependence of $^7\text{Be}$ decay in different chemical environments . . . . .	75
20.36	Astrophysics at the future Rare Isotope Accelerator . . . . .	76
20.37	Neutron capture during the freeze-out of the $r$ process . . . . .	76
20.38	Astrophysical implications of the $^{139}\text{La}(n, \gamma)$ and $^{151}\text{Sm}(n, \gamma)$ cross sections measured at n-TOF* . . . . .	77
<b>21</b>	<b>Poster session, 29 June</b>	<b>77</b>
21.1	New features in the computational infrastructure for nuclear astrophysics . . . . .	77
21.2	Monte Carlo simulations of Type I X-ray burst nucleosynthesis . . . . .	78
21.3	High precision measurements along the $rp$ -process path . . . . .	78
21.4	On the contribution of classical novae to the $^{26}\text{Al}$ content of the Galaxy . . . . .	79
21.5	Neutrino-induced fission on nuclei near the $r$ -process paths . . . . .	79
21.6	Study of the $^{10}\text{B}(p, \alpha)^7\text{Be}$ reaction through the Trojan Horse Method . . . . .	79
21.7	Neutrino-nucleus cross sections and their role in supernovae* . . . . .	79
21.8	Determination of the astrophysical S factor for the $^{12}\text{N}(p, \gamma)^{13}\text{O}$ reaction from the proton transfer reaction $^{14}\text{N}(^{12}\text{N}, ^{13}\text{O})^{13}\text{C}$ . . . . .	80
21.9	Lifetime of the 4.03 MeV state in $^{19}\text{Ne}$ and the $^{15}\text{O}(\alpha, \gamma)^{19}\text{Ne}$ reaction rate . . . . .	80
21.10	Microdynamical effects on momentum distribution in stellar plasmas . . . . .	81
21.11	Quantum mechanical ab-initio simulation of the electron screening effect in metal deuteride crystals . . . . .	81
21.12	About possible explanations to the lines of radioactive elements in the spectrum of Przybylski's star . . . . .	82
21.13	Heaviest $s$ -process elements in the atmospheres of barium stars . . . . .	82
21.14	Evidence of Na enhancement in Hyades giants from high-resolution spectroscopy	82
21.15	Multi-channel R-matrix analysis of CNO cycle reactions . . . . .	83

21.16	Efficient approximations of neutrino physics for three-dimensional simulations of stellar core collapse . . . . .	83
21.17	Abundances of heavy metals and lead isotopic ratios in subluminoous B stars . .	83
21.18	Direct measurement of stellar neutron capture rates of $^{14}\text{C}$ and comparison with the Coulomb breakup method . . . . .	84
21.19	The roles of nuclear physics during stellar core collapse . . . . .	84
21.20	Neutrinos, fission cycling, and the $r$ process . . . . .	84
21.21	Nucleosynthesis in early proton-rich supernova winds . . . . .	85
21.22	Compound-nuclear reaction cross sections via Surrogate measurements . . . . .	85
21.23	Experimental nuclear astrophysics with recoil mass separators . . . . .	86
21.24	A high resolution spectroscopic study of seven metal-deficient stars . . . . .	86
21.25	Laminar flame acceleration by neon enrichment in white dwarf supernovae . . .	86
21.26	Closing the Cold CNO Cycle: A new measurement of $^{19}\text{F}(p, \gamma)$ . . . . .	87
21.27	Precision mass measurements of neutron-rich nuclei from Ge to Pd and their $r$ -process implications . . . . .	87
21.28	Measurement of transfer reactions on neutron-rich fission fragments in inverse kinematics . . . . .	88
21.29	$r$ -Process experimental campaign at the National Superconducting Cyclotron Laboratory (NSCL/MSU) . . . . .	88
21.30	Experimental nuclear level densities and interpretation within the microcanonical ensemble . . . . .	89
21.31	Determination of low $^7\text{Be}$ activity as a tool to measure the $^3\text{He}(\alpha, \gamma)^7\text{Be}$ cross section . . . . .	89
21.32	CARINA: a European network for nuclear astrophysics . . . . .	89
21.33	Nucleosynthesis in Super AGB stars . . . . .	90
<b>22</b>	<b>Poster session, 30 June</b>	<b>90</b>
22.1	On the origin of the high helium sequence in $\omega$ Centauri . . . . .	90
22.2	A charge breeder for nuclear astrophysics experiments? . . . . .	91
22.3	Neutron capture cross sections of the Zr isotopes: probing neutron exposure and neutron flux in red giants . . . . .	91
22.4	$^{25}\text{Al}+p$ elastic scattering with CRIB . . . . .	91
22.5	Isospin symmetry in nucleon- and $\alpha$ -decays of mirror nuclei and its astrophysical applications . . . . .	92
22.6	Primordial magnetic field constrained from CMB anisotropies, and its generation and evolution before, during and after the BBN . . . . .	92
22.7	Neutrino signal of supernova shock wave propagation: MSW distortion of the spectra and nucleosynthesis . . . . .	93
22.8	The effective long range interaction and resonances in the $n\alpha\alpha$ system at astrophysical energies . . . . .	93
22.9	A case for fast stellar rotation at very low metallicities: C and N in very metal poor halo stars . . . . .	94
22.10	Suppression of the neutron channel in low energy d+d reactions within metallic media . . . . .	94
22.11	Nuclear reaction and structure databases of the National Nuclear Data Center .	94
22.12	Neutrons and features of primordial nucleosynthesis . . . . .	95
22.13	The TRIUMF annular chamber of tracking and identification of charged particles (TACTIC) . . . . .	95
22.14	The influence of electron screening on half-lives . . . . .	96
22.15	$\beta$ -Beam born neutrino – an alternative to double $\beta$ -decay to determine the Majorana neutrino mass. . . . .	96
22.16	Can radiative decay of long-lived particles after the BBN solve the cosmological $^6\text{Li}$ problem? . . . . .	96
22.17	Dating of the $^{60}\text{Fe}$ -peak in a deep sea manganese crust . . . . .	97
22.18	Chemical mixing in galactic BA-type supergiants . . . . .	97
22.19	Neutrino-nucleus inelastic scattering reactions for core-collapse supernovae . . .	97

---

22.20	Quantitative spectroscopy of BA-type supergiants: Observational constraints on massive star evolution in the local group . . . . .	98
22.21	Towards global optical $\alpha$ potentials: Study of the $^{89}\text{Y}(\alpha, \alpha)^{89}\text{Y}$ elastic scattering . . . . .	99
22.22	Mass measurements of radionuclides near the endpoint of the $rp$ process at SHIP-TRAP . . . . .	99
22.23	Mass measurements of $^{22}\text{Mg}$ and $^{26}\text{Si}$ via $(p, t)$ reactions and Penning traps . . . . .	100
22.24	On the $\alpha$ -particle semi-microscopic optical potential at low energies . . . . .	100
22.25	Time of flight mass measurements in the neutron rich Fe region . . . . .	101
22.26	Decay studies at the end of the $rp$ process . . . . .	101
22.27	Fragmentation spectra of strange quark matter in a type-II supernova scenario . . . . .	102
22.28	Level structure of $^{21}\text{Mg}$ : Nuclear and astrophysical implications . . . . .	102
22.29	Proton induced reaction cross sections of the Ge isotopes . . . . .	102
22.30	Neutron decay array for $\beta$ -delayed neutron decay studies . . . . .	102
22.31	The $^{13}\text{C}(\alpha, n)^{16}\text{O}$ reaction rate at stellar temperatures . . . . .	102
22.32	Analysis of the $^{16}\text{O}(d, p)^{17}\text{O}$ and $^{16}\text{O}(d, n)^{17}\text{F}$ transfer reactions to determine astrophysical direct capture cross sections . . . . .	103
22.33	Sensitivity of type I X-ray bursts to $rp$ -process reaction rates . . . . .	103
22.34	Neon abundances in B-stars of the Orion association: Solving the solar neon problem? . . . . .	104
22.35	Nucleosynthesis relevant conditions in neutrino-driven supernova outflows . . . . .	104
22.36	Electron capture rates for neutron star crusts . . . . .	104

## 1 Stars: observations, evolution & nucleosynthesis

### 1.1 Nuclear astrophysics with $\gamma$ -ray line observations

DIEHL, Roland

MPE Garching, Germany

Gamma-ray spectrometers with high spectral resolution are operating in space since 2002: RHESSI and SPI on INTEGRAL. Understanding the instrumental response and backgrounds is major effort but a prerequisite of detailed science interpretations. While  $^{44}\text{Ti}$  from core collapse supernovae could not be detected, this still adds constraints to Cas A  $^{44}\text{Ti}$  ejection. Diffuse nucleosynthesis is studied through  $^{26}\text{Al}$ ,  $^{60}\text{Fe}$ , and positron annihilation  $\gamma$ -ray measurements. With SPI on INTEGRAL, the  $\gamma$ -ray line from decay of radioactive  $^{26}\text{Al}$  could be measured at unprecedented spectroscopic precision. This made possible a new determination of the total mass of  $^{26}\text{Al}$  produced by stellar sources throughout the Galaxy, and an analysis of the properties of the interstellar medium around  $^{26}\text{Al}$  sources.  $^{60}\text{Fe}$  is clearly detected with SPI, its intensity ratio to  $^{26}\text{Al}$  is confirmed to be on the lower side of theoretical predictions. Nucleosynthesis sources are probably minor contributors to Galactic positrons, as deduced from the bulge-centered spatial distribution of the annihilation  $\gamma$ -ray emission.

### 1.2 From massive stars to supernovae

HEGER, Alexander

Los Alamos/UC St Cruz, USA

I will give a review on the evolution of massive stars and their paths to supernovae. Depending on their initial parameters, e.g. initial mass, metallicity, mass loss, and rotation, different kinds of supernovae are the result: normal core collapse supernovae, collapsar-powered supernovae like  $\gamma$ -ray bursts, or even pair-instability supernovae. Similarly varied are the possible remnants of these supernovae and their nucleosynthesis. While the lowest mass stars may have only very little ejecta, the most massive pair-instability supernovae may eject as much as hundred solar masses in metals, out of which up to half can be radioactive  $^{56}\text{Ni}$ . I will present recent results of extended grids of nucleosynthesis of stars of low metallicity.

### 1.3 The $rp$ process and X-ray bursts

SCHATZ, Hendrik

National Superconducting Cyclotron Laboratory, Michigan State University, USA

Accreting neutron stars in X-ray binaries provide a unique laboratory for thermonuclear burning at extreme temperature and density conditions. A range of newly discovered, and largely puzzling, observables needs to be understood and interpreted. A key in this endeavor is the understanding of the underlying nuclear physics of unstable nuclei that span the entire range from the proton drip line to the neutron drip line. X-ray bursts and the  $rp$  process play a central role in this context. I will discuss recent advances in our understanding of these systems from the observational, theoretical, and the experimental side. Concerning the latter, particular attention is paid to advances in the capabilities of radioactive beam facilities such as the National Superconducting Cyclotron Laboratory at Michigan State University, where indirect methods have been developed to better constrain thermonuclear reaction rates at X-ray burst conditions.

## 2 Experiments in nuclear astrophysics I

### 2.1 Underground nuclear astrophysics

COSTANTINI, Heide<sup>1</sup> for the LUNA collaboration

<sup>1</sup>Universities of Genova/Italy and Notre Dame/USA

Cross section measurements for quiescent stellar H and He burning are hampered mainly by extremely low counting rates and cosmic background. Some of the main reactions of the H-burning

phase have been measured at the LUNA facility (Laboratory for Underground Nuclear Astrophysics) taking advantage of the very low background environment of the Underground Gran Sasso National Laboratory in Italy. An overview of the adopted experimental techniques will be given together with the latest results on the  $^{14}\text{N}(p, \gamma)^{15}\text{O}$  reaction and the status of the ongoing experiments. Furthermore, a brief summary of possible future experimental methods coupling low background environments and advanced detector techniques will be presented.

## 2.2 The $^{26}\text{Al}^g(p, \gamma)^{27}\text{Si}$ reaction in novae

RUIZ, C.<sup>1</sup>, PARIKH, A.<sup>2</sup>, BUCHMANN, L.<sup>1</sup>, CAGGIANO, J.<sup>1</sup>, DAVIDS, B.<sup>1</sup>, DAVIS, C.<sup>1</sup>, HUTCHEON, D.H.<sup>1</sup>, OTTEWELL, D.F.<sup>1</sup>, RUPRECHT, G.<sup>1</sup>, TRINCZEK, M.<sup>1</sup>, VOCKENHUBER, C.<sup>1</sup>, CLARK, J.<sup>2</sup>, DEIBEL, C.<sup>2</sup>, LEWIS, R.<sup>2</sup>, PARKER, P.<sup>2</sup>, WREDE, C.<sup>2</sup>, CHEN, A.A.<sup>3</sup>, OUELLET, C.V.<sup>3</sup>, PEARSON, J.<sup>3</sup>, CRAWFORD, H.<sup>4</sup>, D'AURIA, J.M.<sup>4</sup>, ERIKSON, L.<sup>5</sup>, GREIFE, U.<sup>5</sup>, FOGARTY, L.<sup>6</sup>, JEWETT, C.<sup>5</sup>, FREKERS, D.<sup>7</sup>, and JOSÉ, J.<sup>8</sup>

<sup>1</sup>TRIUMF, Vancouver, BC V6T 2A3, Canada, <sup>2</sup>Wright Nuclear Structure Laboratory, Yale University, New Haven, CT 06520-8124, USA, <sup>3</sup>McMaster University, Hamilton, ON, Canada, <sup>4</sup>Simon Fraser University, Burnaby, BC V5A 1S6, Canada, <sup>5</sup>Dept. of Physics, Colorado School of Mines, Golden, CO 80401, USA, <sup>6</sup>National University of Ireland, Maynooth, Co. Kildare, Ireland, <sup>7</sup>Institute für Kernphysik, Westfälische Wilhelms-Universität Münster, Münster, Germany, <sup>8</sup>IEEEEC-UPC, Barcelona, Catalunya, Spain

The strength of the 188 keV resonance in the  $^{26}\text{Al}^g(p, \gamma)^{27}\text{Si}$  reaction has been measured directly in inverse kinematics using the DRAGON recoil separator at TRIUMF-ISAC. Radioactive  $^{26}\text{Al}$  beams with peak intensities of  $5 \times 10^9$  ions/sec were utilised in conjunction with a windowless, recirculating hydrogen gas target. Recoil  $^{27}\text{Si}$  ions were separated and detected with a double-sided silicon strip detector in coincidence with capture  $\gamma$ -rays at the target position in a highly efficient BGO detector array. Background from random coincidence was separated using time-of-flight through the length of the separator. Measured silicon charge state distributions using a  $^{28}\text{Si}$  beam, combined with stopping power information measured in the gas target allowed determination of the strength of this resonance at the level of <20% error. In addition, the resonance energy was measured via the distribution of  $\gamma$ -ray hits in the BGO array, leading to the conclusion that it is lower than previously thought. The 188 keV resonance dominates the reaction rate at typical Oxygen-Neon Nova temperatures and the formation of  $^{26}\text{Al}$  in Novae depends sensitively on the value of this rate. We have found a value of resonance strength differing from the only existing unpublished measurement that has been used in the reaction networks so far in Nova nucleosynthesis models. The results of the experiment will help determine the importance of Novae as originators of Galactic  $^{26}\text{Al}$  compared to other sources, and we discuss the implications of the measurement in this context.

## 2.3 Direct measurement of the $^{18}\text{F}(p, \alpha)^{15}\text{O}$ reaction for application to nova $\gamma$ -ray emission.

DE SEREVILLE, Nicolas<sup>1</sup>, ANGULO, Carmen<sup>1</sup>, LAIRD, Alison<sup>2</sup>, LEFEBVRE, Anne<sup>3</sup>, LELEUX, Pierre<sup>1</sup>, MUMBY-CROFT, P.<sup>2</sup>, ORR, Nigel<sup>4</sup>, ROBERTSON, Doug<sup>5</sup>, VAUGHAN, Kelly<sup>2</sup>, TATIS-CHEFF, Vincent<sup>3</sup>, COC, Alain<sup>3</sup>, ACHOURI, Lynda<sup>4</sup>, CASAREJOS, Enrique<sup>1</sup>, DAVINSON, Thomas<sup>5</sup>, FIGUERA, Pierpaolo<sup>6</sup>, FOX, Simon<sup>2</sup>, HAMMACHE, Fairouz<sup>7</sup>, and KIENER, Jürgen<sup>3</sup>

<sup>1</sup>Université catholique de Louvain, <sup>2</sup>University of York, <sup>3</sup>Centre de Spectrometrie Nucléaire et de Spectrometrie de Masse, <sup>4</sup>Laboratoire de Physique Corpusculaire, <sup>5</sup>University of Edinburgh, <sup>6</sup>Laboratori Nazionali del Sud, <sup>7</sup>Institut de Physique Nucléaire d'Orsay

The  $^{18}\text{F}$  nucleus is one of the radioactive isotope produced during nova explosions. It is of particular interest since it is producing most of the 511 keV  $\gamma$ -ray emission of novae that could be detected with the INTEGRAL satellite or with future  $\gamma$ -ray telescopes. The amount of  $^{18}\text{F}$  synthesized still suffers from large uncertainties due to missing nuclear information concerning the destruction reaction  $^{18}\text{F}(p, \alpha)^{15}\text{O}$ . In particular, the interference sign between three  $3/2^+$  resonances in  $^{19}\text{Ne}$ , situated slightly above the proton threshold (8 keV and/or 38 keV) and at higher energy (665 keV), is unknown. The maximum effect of these interferences is in the energy range corresponding to the region of the Gamow peak and has a strong impact on the  $^{18}\text{F}(p, \alpha)^{15}\text{O}$  rate. We report on the direct measurement of the  $^{18}\text{F}(p, \alpha)^{15}\text{O}$  cross section at low energies (down to 400 keV in

the center of mass) that we performed at the Louvain-la-Neuve CRC-RIB facility with the high intensity and high purity  $^{18}\text{F}$  beam ( $t_{1/2} = 110$  min). Total cross sections for the different incident energies will be presented and compared to previous experimental data, followed by an R-matrix analysis aiming at the determination of the interference sign of the relevant resonances.

## 2.4 Measuring difficult reaction rates involving radioactive beams: a new approach

D'AURIA, John<sup>1</sup>, RUBBIA, Carlo<sup>2</sup>, LINDROOS, Mats<sup>2</sup>, JOSÉ, Jordi<sup>3</sup>, and BUCHMANN, Lothar<sup>4</sup>  
<sup>1</sup>Simon Fraser University, <sup>2</sup>CERN, <sup>3</sup>Institut d'Estudis Espacialde Catalunya (IEEC), <sup>4</sup>TRIUMF

Rates of sub-barrier, radiative capture reactions involving radioactive reactants, needed for understanding various astrophysics explosive scenarios, are often quite difficult to measure directly at relevant stellar temperatures. In general relatively intense radioactive beams ( $>10^{11}/\text{s}$ ) are needed for these inverse kinematic studies, as cross sections are very low. A new production approach is proposed herein that would supply such required intensities in a relatively straightforward fashion. While this system may have many applications, one area could be increasing our understanding of classical novae and X-ray bursts.  $^{25}\text{Al}(p, \gamma)$ ,  $^{30}\text{P}(p, \gamma)$ , and  $^{15}\text{O}(\alpha, \gamma)^{19}\text{Ne}$  are key reactions in our understanding of nova outbursts and/or X-ray bursts and their nucleosynthetic imprints in the Galactic abundances. The first one is important for the synthesis of  $^{26}\text{Al}$ , since it determines the amount of nuclear flow that bypasses  $^{26}\text{Al}$  synthesis through the isomeric state,  $^{25}\text{Al}(p, \gamma)^{26}\text{Si}(\beta^+)^{26m}\text{Al}$ . Hence, reliable predictions of the contribution of novae to the Galactic  $^{26}\text{Al}$  content depend critically on this rate. In turn,  $^{30}\text{P}(p, \gamma)$  determines the path through the Si-Ca region in nova outbursts, and therefore, is crucial in the synthesis of these intermediate-mass elements, and for the location of the nucleosynthesis endpoint in such explosions. Moreover, competition between  $^{30}\text{P}(p, \gamma)$  and  $^{30}\text{P}(\beta^+)$  determines the final amount of  $^{30}\text{Si}$ , an important signature that helps to identify presolar meteoritic grains of a likely nova paternity. The  $^{15}\text{O}(\alpha, \gamma)^{19}\text{Ne}$  reaction is believed to be the breakout path of the hot CNO cycle in an X-ray burst leading to the  $rp$  process. It is important to our understanding of ignition temperatures for the  $rp$  process to know the absolute value of this rate, rather than an upper limit. In this presentation a new approach to the production of required radioactive beam intensities is described which may lead to measurements of the rates of these key reactions.

## 3 Nuclei far from stability

### 3.1 Nuclear-physics data for modeling of the $r$ process

KRATZ, Karl-Ludwig

Institut für Kernchemie, Universität Mainz, Germany

Nucleosynthesis theory predicts that about half of the chemical elements above iron are formed in explosive stellar scenarios by the  $r$  process, i.e. a combination of rapid neutron captures, inverse photo-desintegrations, and slower beta-decays, beta-delayed processes, as well as fission and possibly interactions with neutrinos. A correct modeling of this process, therefore, requires the knowledge of nuclear properties very far from stability and a detailed description of the astrophysical environments. With respect to nuclear data, after an initial period of measuring "waiting-point" nuclei with magic neutron numbers, recent investigations have paid special attention to shape transitions and the erosion of classical shell gaps with possible occurrence of new magic numbers. The status of experimental and theoretical nuclear data on masses and beta-decay properties will be briefly reviewed, and consequences on the overall  $r$ -process matter flow up to the cosmochronometers  $^{232}\text{Th}$  and  $^{238}\text{U}$  will be discussed.

### 3.2 Progress in the investigation of nuclei approaching the $r$ -process waiting point $A = 195$

KURTUKIAN-NIETO, Teresa<sup>1</sup>, BENLLIURE, Jose<sup>1</sup>, SCHMIDT, Karl-Heinz<sup>2</sup>, HENZLOVA, D.<sup>2</sup>, JURADO, B.<sup>2</sup>, PEREIRA, J.<sup>1</sup>, REJMUND, F.<sup>3</sup>, YORDANOV, O.<sup>2</sup>, AUDOUIN, L.<sup>3</sup>, BECKER, F.<sup>2</sup>, BLANK, B.<sup>4</sup>, CASAREJOS, E.<sup>1</sup>, CORTINA-GIL, D.<sup>1</sup>, FERNANDEZ-ORDOÑEZ, M.<sup>1</sup>, and GIOVINAZZO, J.<sup>4</sup>

<sup>1</sup>Universidad de Santiago de Compostela, Spain, <sup>2</sup>GSI Darmstadt, Germany, <sup>3</sup>Institute de Physique Nucléaire, Orsay, France, <sup>4</sup>CENBG Bordeaux-Gradignan, France

The complete understanding of the  $r$ -process still remains a challenge not only because of the identification of the possible astrophysical sites but also because of the interpretation of the observed abundances. With respect to this latter point, one of the main problems we have to overcome to fully understand the observed  $r$ -process abundances is the lack of information on the nuclei participating in this process, in particular for the heaviest ones. The main reason for this is that the heavy nuclei involved in the  $r$ -process are so neutron-rich that until now they have been far from any experimental access. During the last years promising results have been obtained investigating the properties of medium-mass neutron-rich nuclei close to the waiting point  $A = 130$  [1] while the waiting point around  $A = 195$  remains a completely unexplored territory. Nevertheless, the possibility to accelerate heavy ions at relativistic energies has allowed the investigation of reactions mechanisms leading to the production of heavy neutron-rich nuclei such as cold-fragmentation reactions [2]. In this work we report on an experiment performed with the FRS at GSI to explore the production of heavy neutron-rich nuclei close to the neutron shell  $N = 126$  and to measure their beta half-lives. We used cold-fragmentation reactions induced by a  $^{208}\text{Pb}$  beam at 1 AGeV impinging a Be target to produce heavy neutron-rich nuclei south of lead. The isotopic identification of the projectile residues was achieved by determining both the atomic number and the mass-over-charge ratio of each nucleus by measuring their magnetic rigidity, time-of-flight and energy loss. The identified nuclei were implanted in an active catcher made of four  $5 \times 5 \text{ cm}^2$  Double-Side Silicon Strip Detectors 1 mm thick. The position and time correlations between the implanted nuclei and the subsequent beta decay allowed the determination of the beta half-lives. In this measurement we were able to identify for the first time around 30 new neutron-rich nuclei approaching the neutron shell  $N = 126$ . In addition, the half-life of some of them has been determined. These half-lives have been compared with model calculations [3,4] which in general do not reproduce the measured values. This work opens new perspectives for further detailed spectroscopic investigations coupling with gammas that will allow us better understand the structure and decay properties of the  $A = 195$  waiting point nuclei.

[1] Dillmann I., Kratz K.-L., et al. Phys. Rev. Lett. 91, 162503 (2003)

[2] Benlliure J., et al. Nucl. Phys. A 660, 87, (1999)

[3] Tachibana T. et al. Proc. Int. Conf. on Exotic Nuclei and Masses, A 660, Arles, 763 (1995)

[4] P. Müller et al. Atomic Data and Nuclear Data Tables, 66, 131 (1997)

### 3.3 Building nuclei from the ground up

DEAN, David and HAGEN, G.

Oak Ridge National Laboratory

Investigations of rare isotopes in the laboratory are opening the way to understand and clarify the properties of all nuclei and bulk nuclear matter. In this talk I will assess where we stand today in solving the nuclear problem and how future rare isotope facilities will impact our understanding of nuclei and our ability to predict nuclear properties in stellar and other environments. The first part of the nuclear problem concerns our ability to describe complex nuclei from the ground up using as input the basic interactions among protons and neutrons. Indeed, our community is on the verge of discovering how light nuclear systems are built from bare nuclear interactions that have their roots in QCD. I will describe this exciting frontier of research through illustrating recent progress in the nuclear implementation of coupled-cluster methods, a quantum many-body technique that enjoys great success in quantum chemistry. After describing the basic coupled-cluster ideas, I will illustrate their power by reporting on results of ground and excited state calculations for oxygen and calcium nuclei.

*This research is supported by the Office of Nuclear Physics, Office of Science of the U.S. Department of Energy under Contract Number DE-AC05-00OR22725 with UT-Battelle, LLC (Oak Ridge National Laboratory).*

### 3.4 Mass measurements of exotic nuclei and their role in stellar nucleosynthesis

LUNNEY, David

Université de Paris Sud, France

The mass of nuclides far from stability provides information on decay and reaction energies that is crucial for modeling stellar nucleosynthesis. Low production rates, short half-lives, and the inherent precision required make masses perhaps the most difficult nuclear quantity to measure. The minuteness of the binding energy has also contributed to confounding attempts at reliable theoretical mass predictions. This talk will introduce the role played by masses in astrophysics and then quickly review and compare the (growing) multitude of mass-measurement programs now active worldwide. The evaluation process that links reaction, decay and binding energies is also described with its production of a benchmark for the development of the the mass models required by nucleosynthesis networks.

## 4 Big-Bang nucleosynthesis

### 4.1 Recent results in Big-Bang nucleosynthesis

COC, Alain

CSNSM,CNRS/IN2P3 and Université Paris Sud, France

Primordial nucleosynthesis (BBN) has been used for the determination of the baryonic density of the universe. It has now been superseded, for this purpose, by the more precise determination provided by the analysis of the CMB anisotropies by WMAP. Nevertheless, BBN is still very interesting as when we look back into the history of the universe, this is the last era for which, in principle, we know all the physics. Deviations from BBN predictions can hence give hints on non-standard Big Bang models. It is thus important that nuclear reactions involved in BBN be known with good accuracy. Two recent nuclear physics experiments have improved the reliability of lithium yield calculations in standard big-bang nucleosynthesis. The cross section for the  ${}^7\text{Be}(d, p)2\alpha$  reaction has been directly measured at BBN energies at Louvain-la-Neuve. A Coulomb break-up experiment has provided a better determination of the  $\text{D}(\alpha, \gamma){}^6\text{Li}$  cross section over a wide energy range. Nevertheless, the discrepancy between the primordial  ${}^7\text{Li}$  abundance deduced from halo stars observations and BBN remains and the BBN  ${}^6\text{Li}$  production is still orders of magnitudes below the reported  ${}^6\text{Li}$  observations in some halo stars. Now that the baryonic density is accurately provided by the analysis of the CMB anisotropies, BBN can be used to constrain non-standard models: scalar-tensor theories of gravity for instance.

### 4.2 Is deuterium cosmological?

LUBOWICH, Donald<sup>1</sup>, PASACHOFF, Jay<sup>2</sup>, HENKEL, Christian<sup>3</sup>, MILLAR, Tom<sup>4</sup>, and ROBERTS, Helen<sup>5</sup>

<sup>1</sup>Hofstra University, Hempstead, New York, <sup>2</sup>Williams College, Williamstown, Massachusetts, <sup>3</sup>Max-Planck-Institut für Radioastronomie, Bonn, Germany, <sup>4</sup>Queen's University Belfast, Belfast, Northern Ireland, <sup>5</sup>The University of Manchester, Manchester, UK

All the astronomical observations of deuterium are consistent with a cosmological origin of D. Deuterium has been extensively studied because it is not produced via stellar nucleosynthesis and is thought to be primarily produced via the Big-Bang so its abundance will only decrease with time unless there are additional sources of D. The D/H ratio is an important prediction of standard and non-homogeneous Big-Bang models because the abundance of D depends critically on the temperature and baryonic density during the epoch of nucleosynthesis (first 1000 seconds). In homogeneous inflationary or other flat models, the D/H ratio gives the amount of dark matter and

an upper limit to the number of neutrino families. Any Galactic source of D would undermine its use to estimate the baryonic density of the universe and place constraints on Big-Bang nucleosynthesis models. D nucleosynthesis models have included supernovae, supernovae shock-waves, cosmic-ray spallation reactions, accretion disks around neutron stars or black holes,  $\gamma$ -ray photospallation reactions, stellar flares, and a large proton flux during an early active phase of the Galaxy as possible sources for deuterium. If D is produced via any stellar or Galactic nucleosynthesis process, then its abundance would be a maximum value in the Galactic center (which is the most active and heavily processed region of the Galaxy). We review observations of deuterium in the Galaxy, external galaxies, active galaxies, and in quasar absorption systems, including our own observations. D has been detected in molecular clouds, diffuse clouds, HI regions, and HII region from observations of deuterated molecules, Lyman lines, Balmer lines, QSO absorption lines, and the DI 92-cm hyperfine-structure line. The Galactic D/H ratios range from 2 ppm in the Galactic center to 23 ppm towards the anticenter (12 kpc from the GC). The QSO D/H ratios range from 20–30 ppm. Deuterium has not been detected in planetary nebulae, SNRs, or AGN. Because the D/H ratio is lowest value in the Galactic center yet increases with distance from the Galactic center, D is not produced via stellar or galactic activity (massive stars and star formation, cosmic rays, or stellar flares). Thus the observed D is cosmological with the observed D abundances reduced by astration, infall, mixing, and depletion onto grains.

### 4.3 New measurement of the cross section of the Big Bang nucleosynthesis reaction $D(\alpha, \gamma)^6\text{Li}$ and its astrophysical impact

HAMMACHE, Fairouz<sup>1</sup>, GALAVIZ, Daniel<sup>2</sup>, SÜMMERER, Klaus<sup>3</sup>, TYPEL, Stefan<sup>3</sup>, UHLIG, Florian<sup>3</sup>, and the S246 collaboration<sup>4</sup>

<sup>1</sup>IPN-Orsay, <sup>2</sup>TU-Darmstadt, <sup>3</sup>GSI-Darmstadt, <sup>4</sup>GSI, IPN-Orsay, TU-Darmstadt, CSNSM, Ruhr-Universität Bochum, Forschungszentrum Rossendorf, Philipps Universität Marburg, Riken, Santiago de Compostela

The recent observations of non-negligible amounts of  $^6\text{Li}$  in old halo stars [1] have renewed interest in the Big-Bang Nucleosynthesis (BBN) of  $^6\text{Li}$ . The deduced primordial  $^6\text{Li}$  abundance was found to be unexpectedly large compared to the BBN predictions. One important ingredient in the BBN predictions is the low-energy  $D(\alpha, \gamma)^6\text{Li}$  cross section. Up to now, the only available experimental result [2] for this cross section introduced an error of about a factor of 20 in the  $^6\text{Li}$  abundance at the energies of astrophysical interest ( $E_{\text{cm}} < 300$  keV). This uncertainty arises from the discrepancy between the theoretical low energy dependence of the S-factor and the experimental data. Accordingly, new measurements of the cross section of the  $D(\alpha, \gamma)^6\text{Li}$  reaction using Coulomb dissociation of  $^6\text{Li}$  at 150 A MeV have been performed recently at GSI. The preliminary GSI results, which indicate a drop of the S-factor as predicted by theory [3], will be presented as well their impact on the calculated  $^6\text{Li}$  abundance as a function of the baryon-to-photon ratio etc.

[1] M. Asplund *et al.*, astro-ph/0510636, *Astrophys. J.* (in press)

[2] J. Kiener *et al.*, *Phys. Rev. C* 44, 2195 (1991)

[3] A. Kharbach *et al.*, *Phys. Rev. C* 58, 1066 (1998)

## 5 Element production & stellar evolution: MP & UMP stars

### 5.1 *r*-Process enhanced metal-poor stars

COWAN, John

University of Oklahoma, USA

Abundance observations indicate the presence of rapid-neutron capture (i.e., *r*-process) elements in old Galactic halo and globular cluster stars. These observations provide insight into the nature of the earliest generations of stars in the Galaxy – the progenitors of the halo stars – responsible for neutron-capture synthesis of the heavy elements. The large star-to-star scatter observed in the abundances of neutron-capture element/iron ratios at low metallicities – which disappears with increasing metallicity or  $[\text{Fe}/\text{H}]$  – suggests the formation of these heavy elements (presumably from certain types of supernovae) was rare in the early Galaxy. The stellar abundances also indicate

a change from the  $r$  process to the slow neutron capture ( i.e.,  $s$ -) process at higher metallicities in the Galaxy and provide insight into Galactic chemical evolution. Finally, the detection of thorium and uranium in halo and globular cluster stars offers an independent age-dating technique that can put lower limits on the age of the Galaxy, and hence the Universe.

## 5.2 The origins of carbon and neutron-capture element enhancements in metal-poor stars

RYAN, Sean<sup>1</sup>, TSANGARIDES, Stelios<sup>2</sup>, and AOKI, Wako<sup>3</sup>

<sup>1</sup>University of Hertfordshire, UK, <sup>2</sup>Cyprus, <sup>3</sup>National Astronomical Observatory of Japan

We will report on high resolution spectroscopy of an extensive sample of metal-poor stars in which enhancements of C have been observed. We conclude that 70-80% of such stars also have neutron-capture element enhancements. Most of these stars, though not all, can be explained by the accretion of material from an AGB companion in which the  $s$  process was active. Surprisingly, we find empirical evidence for a correlation between Eu and Ba production, which implies greater Eu production by the  $s$ -process than calculations of  $s$ -process networks currently predict. The other 20- 30% of the stars appear to be congenitally C-rich, and may provide valuable information on the C yields of metal-poor populations.

## 5.3 Mass loss at very low metallicity: Impacts on nucleosynthesis and GRB progenitors

MEYNET, Georges, MAEDER, André, and SYLVIA, Ekstrom

Geneva Observatory

Massive stars with no or very little amount of metals are generally considered as having very weak stellar winds. We reconsider here this question through stellar models accounting for the effects of axial rotation and show that rotating models of massive stars might lose a significant fraction of their initial mass through mass loss. The physical mechanisms triggering these mass losses and the chemical composition of the stellar winds will be discussed. Consequences of these models for nucleosynthesis and the nature of the GRB progenitors will be presented.

## 5.4 Chemical compositions derived from near ultra-violet observations of low-metallicity stars: New insights into the sites of neutron-capture nucleosynthesis processes

IVANS, Inese

Carnegie Observatories & Princeton University

Numerous signatures of  $r$ - and  $s$ -process nucleosynthesis can be observed in the photospheres of stars. To date, however, the stellar abundance determinations of many of the elements have been scarce because a large portion of the dominant atomic transitions reside in the UV. To be reported in the context of other recent results of neutron-capture studies, are the abundances (or upper limits) of Nb, Pd, Ag, Yb, Hf, Pt, Pb, and other neutron-capture elements for a sample of stars observed with the near-UV sensitive detector on the High Resolution Echelle Spectrometer of the Keck I telescope.

## 5.5 The frequency of carbon-enhanced Stars in HERES and SDSS

BEERS, Timothy<sup>1</sup>, LUCATELLO, Sara<sup>2</sup>, MARSTELLER, Brian<sup>1</sup>, SIVARANI, Thirupathi<sup>1</sup>, BARKLEM, Paul<sup>3</sup>, CHRISTLIEB, Norbert<sup>3</sup>, MASSERON, Thomas<sup>4</sup>, ROSSI, Silvia<sup>5</sup>, and KNAPP, Gillian<sup>6</sup>

<sup>1</sup>Michigan State University and JINA, <sup>2</sup>University of Padova, Italy, <sup>3</sup>Uppsala University, Sweden, <sup>4</sup>University of Montpellier, France, <sup>5</sup>IAG, University of Sao Paulo, Brazil, <sup>6</sup>Princeton University

Recent large surveys of metal-poor stars in the Galaxy have revealed that a surprising fraction of them are enhanced in their carbon-to-iron ratios by factors of from 10-10,000 relative to the solar

ratio. Although most of the stars in the metallicity interval  $-2.7 < [\text{Fe}/\text{H}] < -2.0$  are likely to have arisen from asymptotic giant branch processing (and subsequent dumping via mass transfer to a surviving companion), there exist many stars with  $[\text{Fe}/\text{H}] < -3.0$  (including the two lowest  $[\text{Fe}/\text{H}]$  stars known, with  $[\text{Fe}/\text{H}] < -5.0$ ) that cannot be accounted for by this process. Rather, primordial (or nearly primordial) progenitors are implicated. We report on the existing information from present surveys, including cool giants from the recently completed HERES (Hamburg/ESO R-process Enhanced Star) survey, and from warm turnoff stars from SDSS-I. We will also describe the results that will come from the recently-funded extension of the SDSS, which includes the program SEGUE = Sloan Extension for Galactic Understanding and Exploration. SEGUE will identify some 20,000 stars with  $[\text{Fe}/\text{H}] < -2.0$ , several thousand of which are expected to be carbon enhanced. New carbon-enhanced models have been used in the analyses of these spectra, and we consider the impact of these models on the derived  $[\text{Fe}/\text{H}]$ ,  $[\text{C}/\text{Fe}]$ , and in some cases,  $[\text{N}/\text{Fe}]$ , that are derived.

## 6 Evidence of nucleosynthesis in stars and presolar grains

### 6.1 Heavy elements in presolar grains: Constraints on conditions in asymptotic giant branch stars

DAVIS, Andrew<sup>1</sup>, BARZYK, Julia<sup>1</sup>, SAVINA, Michael<sup>2</sup>, PELLIN, Michael<sup>2</sup>, AMARI, Sachiko<sup>3</sup>, ZINNER, Ernst<sup>3</sup>, LEWIS, Roy<sup>1</sup>

<sup>1</sup>University of Chicago, <sup>2</sup>Argonne National Laboratory, <sup>3</sup>Washington University

Presolar SiC grains come from a variety of kinds of stars, but the most common type, the mainstream grains, are believed to have formed in the outflows of low mass, carbon-rich asymptotic giant branch (AGB) stars. Measurements of the isotopic composition of the *s*-process elements Sr, Zr, Mo, Ru and Ba in individual mainstream SiC grains allow constraints of the range of conditions used in stellar models of AGB stars.

### 6.2 On the stellar sources of presolar graphite in primitive meteorites

ZINNER, Ernst, AMARI, Sachiko, and JADHAV, Manavi

Washington University

Primitive meteorites contain graphite spherules whose anomalous isotopic compositions indicate a stellar origin [1]. Because the isolation of presolar graphite grains is difficult, they have been less well studied than presolar SiC and presolar oxide grains. It has been known that the isotopic compositions of presolar graphite grains depends on their density, but detailed isotopic measurements have been made only on low-density ( $< 2 \text{ g/cm}^3$ ) individual grains [2]. The NanoSIMS ion microprobe has enabled us to measure O and Si isotopic ratios in graphite grains with a range of densities from the carbonaceous chondrites Murchison and Orgueil [3-5]. These measurements confirm that low-density grains originated from supernovae and indicate that most high-density ( $> 2 \text{ g/cm}^3$ ) grains come from C-rich AGB stars of low metallicity. Low-density grains and a few grains of higher density are characterized by large  $^{18}\text{O}$  and  $^{28}\text{Si}$  excesses that are signatures of Type II supernovae. Many high-density grains have high  $^{12}\text{C}/^{13}\text{C}$  ratios ( $> 300$ ) and large excesses in  $^{30}\text{Si}$  and smaller ones in  $^{29}\text{Si}$ . These are best explained by low-metallicity AGB stars. In these stars the enrichments of the envelope in the heavy Si isotopes and in  $^{12}\text{C}$ , products of nucleosynthesis in the He shell, are much larger than those expected for solar-metallicity parent stars. The high  $^{12}\text{C}/^{13}\text{C}$  ratios imply also high C/O ratios, which cause the preferential condensation of graphite grains over SiC grains. The Ne-E(L) component, almost pure  $^{22}\text{Ne}$ , which is characteristic of presolar graphite and led to its discovery [6], apparently has two sources [7]. In SN grains it is due to the decay of short-lived ( $T_{1/2} = 2.6 \text{ yr}$ )  $^{22}\text{Na}$ , which condenses into the grains, whereas in AGB grains it is due to the abundant  $^{22}\text{Ne}$  in the He shell, produced by  $\alpha$ -captures on  $^{14}\text{N}$ , the result of previous H burning in the CNO cycle.

[1] Hoppe P. et al. (1995) *Geochim. Cosmochim. Acta* 59, 4029-4056.

[2] Travaglio C. et al. (1999) *Astrophys. J.* 510, 325-354.

[3] Amari S. et al. (2004) *Meteorit. Planet. Sci.* 39, A13.

- [4] Amari S. et al. (2005) Meteorit. Planet. Sci. 40, A15.
- [5] Jadhav M. et al. (2006) New Astron. Rev. submitted.
- [6] Amari S. et al. (1990) Nature 345, 238-240.
- [7] Amari S. (2006) New Astron. Rev. submitted.

### 6.3 Isotopic composition of presolar spinel grain OC2: Constraining intermediate-mass asymptotic giant branch models

LUGARO, Maria<sup>1</sup>, KARAKAS, Amanda<sup>2</sup>, and NITTLER, Larry<sup>3</sup>

<sup>1</sup>University of Utrecht, <sup>2</sup>McMaster University, <sup>3</sup>Carnegie Institution of Washington

Presolar spinel (MgAl<sub>2</sub>O<sub>4</sub>) grains have been recently discovered in meteorites and represent the most abundant type of presolar oxides. The O, Mg and Al isotopic compositions of the vast majority of presolar oxide grains indicate that these grains originated in red giant and asymptotic giant branch (AGB) stars of masses lower than approximately 3 solar masses. Grain OC2 has a unique composition, showing most extreme O and Mg isotopic ratios among presolar oxide grains: <sup>17</sup>O/<sup>16</sup>O three times higher than solar, <sup>18</sup>O/<sup>16</sup>O 26 times lower than solar, and excesses in <sup>25</sup>Mg and <sup>26</sup>Mg of (43 ± 1)% and (117 ± 1)%, respectively, with respect to solar. Its origin has thus been tentatively attributed to an AGB star of intermediate mass, around 5 solar masses. In intermediate-mass AGB stars the heavy Mg isotopes are produced in the He intershell by α-capture reactions on <sup>22</sup>Ne, while the O and Al compositions are mostly determined by proton captures at the base of the convective envelope (hot bottom burning). Using detailed models of AGB stars of different masses and metallicities that include Vassiliadis & Wood mass-loss rates and time-dependent convective mixing during the nucleosynthesis postprocessing, we analyze the O, Mg and Al compositions in AGB stars and discuss them in the light of the extremely precise measurements of the composition of grain OC2.

### 6.4 Magnetic mixing and nucleosynthesis in AGB stars

BUSSO, Maurizio

University of Perugia, Department of Physics

AGB stars are the site of important nucleosynthesis phenomena, started by p, n, and α captures. In recent years detailed observational constraints have helped in specifying the yields from such evolved red giants concerning both heavy nuclei produced by slow neutron captures in the He-intershell zone, and intermediate-mass nuclei ( $A = 13 - 27$ ) affected by proton captures in and above the H burning shell. Unfortunately, theoretical predictions for both sets of nuclei still depend on unknown mixing mechanisms. These last have to provide sufficient proton injection into the He intershell to form there an amount of <sup>13</sup>C suitable to trigger the production of neutrons for the *s* process (through the <sup>13</sup>C(α, n)<sup>16</sup>O reaction). They have also to guarantee mass circulations above the H shell (called cool bottom processes) to mix into the envelope newly formed <sup>13</sup>C, <sup>14</sup>N, <sup>17</sup>O, <sup>26</sup>Al. We shall show that the known mechanism of magnetic buoyancy from a toroidal magnetic field (generated by the poloidal field of a rotating star) is sufficient to account for the above mixing requirements, at suitable efficiencies, in a natural and necessary way. The basic mechanism is the creation of buoyant field tubes, perturbed by undulatory instabilities in the classical Parker's description of a stellar dynamo.

### 6.5 Accelerator mass spectrometry and nuclear astrophysics

KORSCHINEK, Gunther

Fachbereich Physik, Technische Universität München, Munich, Germany

Accelerator Mass Spectrometry (AMS) is an extremely sensitive method for determination of rare ions. Besides ongoing applications in quite different scientific fields it is still a rather new tool in nuclear astrophysics. In this presentation I will show the reasons for this unique sensitivity and where are the limits: from the table top machine too a large facility. Applications in nuclear astrophysics range from direct determination of nuclear synthesis in the past until measurements of relevant cross sections. Examples of recent and also ongoing measurements will be discussed.

## 7 Experiments in nuclear astrophysics: indirect methods

### 7.1 Indirect techniques in nuclear astrophysics - ANCs and THM

TRIBBLE, Robert

Texas A&M University, USA

A puzzle in  $\gamma$ -ray astronomy has been the lack of a signal from the decay of  $^{22}\text{Na}$  in novae sites. The isotope should be produced in the Ne-Na cycle following the proton capture reaction  $^{21}\text{Na}(p, \gamma)^{22}\text{Mg}$  and then the  $\beta$  decay of  $^{22}\text{Mg}$  to  $^{22}\text{Na}$ . A reaction that could play a role in understanding the lack of a signal in  $\gamma$ -ray astronomy is  $^{22}\text{Mg}(p, \gamma)^{23}\text{Al}$ . Depending on the stellar conditions, this reaction could reduce the amount of  $^{22}\text{Na}$  that occurs in novae. Little is known about the reaction rate for proton capture on  $^{22}\text{Mg}$ . Furthermore, there is a question about the spin-parity of the ground state of  $^{23}\text{Al}$ , which can change the reaction rate by more than an order of magnitude depending on whether the ground state is  $1/2^+$  or  $5/2^+$ . Two separate experiments have been carried out at the Texas A&M University Cyclotron Institute to better understand this reaction rate. We have obtained the asymptotic normalization coefficient for  $^{22}\text{Mg}+p$  to  $^{23}\text{Al}$  using the  $^{13}\text{C}(^{22}\text{Ne}, ^{23}\text{Ne})^{12}\text{C}$  reaction and mirror symmetry. We also have determined the spin-parity for the ground state of  $^{23}\text{Al}$  by observing its  $\beta$  decay to  $^{23}\text{Mg}$ . With this new information, we can now determine the direct capture rate for this reaction, which fixes the stellar reaction rate and provides a basis for evaluating the importance of the capture reaction in depleting  $^{22}\text{Na}$  in novae.

### 7.2 Reaction rate of $^{15}\text{O}(\alpha, \gamma)^{19}\text{Ne}$ via indirect measurements

TAN, Wanpeng, GÖRRES, Joachim, DALY, Jason, COUDER, Manoel, LEBLANC, Paul, O'BRIEN, Shawn, BEARD, Mary, COUTURE, Aaron, FALAHAT, Sacha, LEE, HyeYoung, PALUMBO, Annalia, STECH, Edward, STRANDBERG, Elizabeth, UGALDE, Claudio, and WIESCHER, Michael

University of Notre Dame

$^{15}\text{O}(\alpha, \gamma)^{19}\text{Ne}$  is one of the main breakout reactions from the hot CNO cycles, which triggers the thermonuclear runaways or X-ray bursts occurring in accreting neutron stars. A recent study has shown that this reaction is critical for the burst amplitude and periodicity of X-ray bursters. However, a direct measurement of this reaction rate at astrophysically relevant temperatures is not feasible yet due to the lack of very high intensity radioactive  $^{15}\text{O}$  beams. There has been considerable effort in the past to investigate this reaction rate indirectly by obtaining  $\gamma$  and  $\alpha$  decay widths of the  $\alpha$ -unbound states in  $^{19}\text{Ne}$ . While this approach has been successful for investigating higher energy resonances, the critical level at 4.03 MeV remains unknown. This leaves the reaction rate largely uncertain since previous attempts have only provided limits on its  $\gamma$  width and its  $\alpha$  decay branching ratio. In this talk we present new experimental work conducted at the University of Notre Dame. Lifetimes of the 4.03 MeV state and other relevant states in  $^{19}\text{Ne}$  have been measured successfully using the  $^{17}\text{O}(^3\text{He}, n-\gamma)$  reaction. We will also present the results of our recent measurement of the  $\alpha$ -decay branching ratios.  $\alpha$ -unbound states in  $^{19}\text{Ne}$  were populated via the reaction  $^{19}\text{F}(^3\text{He}, ^3\text{H}-\alpha)$  and triton- $\alpha$  coincidences were observed using a low energy particle detection Silicon array and the TWINSOL facility. The experimental results and the astrophysical implications will be discussed in the presentation.

### 7.3 Study of astrophysically important resonant states in $^{26}\text{Si}$ by the $^{28}\text{Si}(^4\text{He}, ^6\text{He})^{26}\text{Si}$ reaction

KWON, Young Kwan<sup>1</sup>, LEE, Chun Sik<sup>1</sup>, MOON, Jun Young<sup>1</sup>, LEE, Ju Hahn<sup>1</sup>, KIM, Jang Youl<sup>1</sup>, KUBONO, Shigeru<sup>2</sup>, IWASA, Nahohito<sup>3</sup>, INAFUKU, Kiyohiko<sup>3</sup>, YAMAGUCHI, Hidetoshi<sup>2</sup>, HE, JianJun<sup>2</sup>, SAITO, Akito<sup>2</sup>, WAKABAYASHI, Yasuo<sup>4</sup>, HUIKAWA, Hisashi<sup>2</sup>, AMADIO, Guilherme<sup>2</sup>, LE HONG, Khiem<sup>5</sup>, TANAKA, Masahiko<sup>6</sup>, CHEN, Alan A.<sup>7</sup>, KIM, Aram<sup>8</sup>, and KATO, Seigo<sup>9</sup>

<sup>1</sup>Department of Physics, Chung-Ang University, Seoul 156-756, Republic of Korea, <sup>2</sup>Center for Nuclear Study, Graduate School of Science, University of Tokyo, Wako Branch at RIKEN, Wako, Saitama 351-0198, Japan, <sup>3</sup>Department of Physics, Tohoku University, Sendai, Miyagi 980-8578, Japan, <sup>4</sup>Department of Physics, Kyushu University, Fukuoka 812-8581, Japan, <sup>5</sup>Institute of Physics and Electronics, Hanoi,

Vietnam, <sup>6</sup>The Institute of Particle and Nuclear Study, The High Energy Accelerator Organization (KEK), Tsukuba 305-0801, Japan, <sup>7</sup>Department of Physics and Astronomy, McMaster University, Hamilton ON, L8S 4M1, Canada, <sup>8</sup>Department of Physics, Ewha Womans University, Seoul 120-750, Republic of Korea, <sup>9</sup>Department of Physics, Yamagata University, Yamagata 990-8560, Japan

The emission of 1.809 MeV  $\gamma$ -rays from the first excited state of  $^{26}\text{Mg}$  followed by beta-decay of  $^{26}\text{Al}$  in its ground state ( $^{26}\text{Al}^g$ ) has been identified by  $\gamma$ -ray telescopes such as the Compton Gamma-Ray Observatory (CGRO). To resolve controversy over the possible sources of the observed 1.809 MeV  $\gamma$ -rays, one needs accurate knowledge of the production rate of  $^{26}\text{Al}$ . The  $^{25}\text{Al}(p, \gamma)^{26}\text{Si}$  reaction, which is the competition reaction for production of  $^{26}\text{Al}^g$  is one of the important subjects to be investigated. Iliadis et al. suggested that the  $^{25}\text{Al}(p, \gamma)^{26}\text{Si}$  reaction is dominated by the  $3^+$  unnatural parity state under explosive hydrogen burning conditions. Recent studies of  $^{28}\text{Si}(p, t)^{26}\text{Si}$ ,  $^{24}\text{Si}(^3\text{He}, n\gamma)^{26}\text{Si}$ , and  $^{29}\text{Si}(^3\text{He}, ^6\text{He})^{26}\text{Si}$  reduced the uncertainties in the  $^{26}\text{Si}$  levels above the proton threshold and identified new states as candidates for the unnatural parity state. However, no spin assignment could be obtained directly from the angular distribution measurement. In this work, the astrophysically important  $^{26}\text{Si}$  states were studied via the  $^{28}\text{Si}(^4\text{He}, ^6\text{He})^{26}\text{Si}$  reaction, which can excite unnatural parity states directly, in contrast to the  $(p, t)$  reaction that can not excite unnatural parity states. We have performed an angular distribution measurement using the high resolution QDD spectrograph (PA) at Center for Nuclear Study (CNS), University of Tokyo. The experimental results and data analysis will be presented.

## 7.4 Influences on the triple $\alpha$ process beyond the Hoyle state

DIGET, Christian A.

University of Aarhus

The triple  $\alpha$  process, the fusion of three  $\alpha$  particles, is responsible for the main stellar production of  $^{12}\text{C}$ . It is known that the rate of this process is dominated by the 7.65 MeV resonance predicted by Hoyle and identified in 1953 [1]. At present two reaction rates are widely employed [2,3]. Work is ongoing to improve these rates both at the most important temperature range [4], and for temperatures where other natural parity resonances in  $^{12}\text{C}$  play a role [5] which is where the two existing rates actually differ. To clarify the latter, we present a detailed experimental analysis of the  $0^+$  and  $2^+$  strength in the triple  $\alpha$  continuum above the Hoyle state and investigate their influence on the triple  $\alpha$  process. Since the  $0^+$  and  $2^+$  states in question show a strong coupling to the triple  $\alpha$  continuum, they are broad and not easily distinguished among the other states in this  $^{12}\text{C}$  energy region. Our approach is to selectively feed the states through the beta decay of  $^{12}\text{N}$  and  $^{12}\text{B}$ , and we detect the subsequent triple  $\alpha$  breakup to identify the states. A new experiment (IG301) with improved detector setup has been performed at the IGISOL separator, Finland, to allow a detailed analysis of the properties of the states. We use a setup of segmented silicon detectors to measure triple  $\alpha$  coincidences with a sufficient detection efficiency in most regions of three particle phase space. This has for example permitted us to observe previously unknown breakup channels involving the  $^8\text{Be}$   $2^+$  excited state. Since the  $^{12}\text{C}$  states overlap in energy and some have the same spin and parity they interfere. This is evident from the data and our analysis takes this into account. In this way we determine: properties of the states; their interference; and their coupling to the possible breakup channels  $^8\text{Be}(0^+)+\alpha$  and  $^8\text{Be}(2^+)+\alpha$ . With this knowledge we investigate the influence from these states and breakup channels on the reaction rate of the triple  $\alpha$  process, and thus explore the influences on the triple  $\alpha$  process beyond the Hoyle state.

[1] F. Hoyle, *Astrophysical Journal Supplement Series* 1, 121 (1954)

[2] G.R. Caughlan and W.A. Fowler, *Atomic Data and Nuclear Data Tables* 40, 283 (1988)

[3] C. Angulo et al., *Nuclear Physics A* 656, 3 (1999)

[4] S.M. Austin, *Nuclear Physics A* 758, 375c (2005)

[5] H.O.U. Fynbo et al., *Nature* 433, 136 (2005)

## 7.5 Experimental determination of reaction rates via Coulomb dissociation

MOTOBAYASHI, Tohru

RIKEN Nishina Center for Accelerator-Based Science, Japan

Intermediate-energy Coulomb dissociation using fast radioactive-isotope (RI) beams has been employed to study astrophysical  $(p, \gamma)$  reactions. This method has the advantages of large cross sections and high experimental efficiency. Several experiments have been performed so far at fragmentation-based RI-beam facilities like, GSI, MSU, and RIKEN. The most studied case is for the  ${}^7\text{Be}(p, \gamma){}^8\text{B}$  reaction, which is important in estimating the high-energy neutrino flux from the sun. Coulomb dissociation experiments provide an opportunity to determine the cross section independent to direct capture measurements. To extract accurate results, possible contributions of nuclear breakup, higher order processes, possible mixture of different multiplicity contribution mixed into the dominant E1 contribution are being investigated both experimentally and theoretically.

## 8 Experiments in nuclear astrophysics II

### $\beta$ Decay of highly charged ions

BOSCH, Fritz

GSI Darmstadt, Germany

Ion storage rings and ion traps have provided for the first time the opportunity to investigate beta decay of highly charged atoms, i.e. with only a few or even none bound electrons. The impact of this new field of research for nuclear astrophysics and, in particular, for  $s$ -process nucleosynthesis in hot stellar plasmas is obvious. In this talk an overview is given on the activities in this field during the last decade at the ion storage-cooler ring ESR of GSI, with the emphasis on bound-state beta decay and its astrophysical implications. Moreover, first results of a new technique, single-ion decay spectroscopy, will be presented and analyzed, i.e. the direct observation of two-body beta decays (bound-state beta decay and orbital electron capture) of single, stored and cooled ions at well-defined atomic charge states.

### 8.1 $\alpha$ -Induced reactions in stellar burning

GÖRRES, Joachim

University of Notre Dame and Joint Institute for Nuclear Astrophysics, USA

Alpha-induced reactions play an important role in a variety of astrophysical environments. They provide the neutron sources for the main  $s$  process which takes place in highly convective AGB stars and for the weak process during core Helium burning in massive stars. In addition, alpha induced reactions on  ${}^{15}\text{O}$  and  ${}^{18}\text{Ne}$  provide a break-out from the CNO cycle which is important for the dynamics of explosive Hydrogen burning. To illuminate experimental difficulties in determining reaction rates results of recent and ongoing experiments will be presented and future developments at the Nuclear Structure Laboratory at Notre Dame will be discussed.

### 8.2 ${}^{12}\text{C}(\alpha, \gamma){}^{16}\text{O}$

#### 8.2.1 Measuring ${}^{12}\text{C}(\alpha, \gamma){}^{16}\text{O}$ with ERNA

SCHÜRMAN, Daniel

Ruhr-Universität Bochum

The fusion of carbon and helium via  ${}^{12}\text{C}(\alpha, \gamma){}^{16}\text{O}$  in the helium burning phase of red giant stars is generally accepted to be a key reaction of nuclear astrophysics. Although there exist several direct and indirect measurements, the cross section in the Gamow peak is still not known sufficiently well. A new measurement of the  ${}^{12}\text{C}(\alpha, \gamma){}^{16}\text{O}$  reaction cross section has been done using the European Recoil separator for Nuclear Astrophysics ERNA. In ERNA the reaction is performed

in inverse kinematics, i.e. guiding a  $^{12}\text{C}$  beam on a  $^4\text{He}$  gas target. In the recoil separator the high intensity beam is filtered from the oxygen recoil nuclei using velocity and momentum filters. ERNA also needs to provide the necessary acceptances in angle and energy needed to cover the kinematics governed by the  $\gamma$ -ray emission. At the end of the separator the recoil nuclei are freely (i.e. without coincidence conditions) detected in a  $\Delta\text{E-E}$  ionization chamber telescope. Assuming full acceptances for the chosen charge state one therefore measures the total cross section. Additional measurement of the coincident  $\gamma$ -rays will provide information on the different capture amplitudes. The key parameters of the recoil separator, i.e. the acceptance of the recoil nuclei and the suppression of the incoming beam, are discussed. The results of the measurements of the total cross section of  $^{12}\text{C}(\alpha, \gamma)^{16}\text{O}$  in the energy range of 1.9 - 5 MeV are presented and compared to R-Matrix calculations.

### 8.2.2 Measurement of the cascade cross section to the 6.049-MeV state in $^{16}\text{O}$ in $^{12}\text{C}(\alpha, \gamma)^{16}\text{O}$

MATEI, C.<sup>1</sup>, BUCHMANN, L.<sup>2</sup>, HANNES, W.R.<sup>3</sup>, HUTCHEON, D.A.<sup>2</sup>, RUIZ, C.<sup>4</sup>, D'AURIA, J.<sup>4</sup>, BRUNE, C.R.<sup>1</sup>, CHEN, A.A.<sup>5</sup>, LAMEY, M.<sup>4</sup>, LI, ZH.<sup>2</sup>, LIU, WP.<sup>6</sup>, OTTEWELL, D.<sup>2</sup>, PEARSON, J.<sup>5</sup>, RUPRECHT, G.<sup>2</sup>, TRINCZEK, M.<sup>4</sup>, VOCKENHUBER, C.<sup>4</sup>, and WREDE, C.<sup>4</sup>

<sup>1</sup>Ohio University, Athens, OH, <sup>2</sup>TRIUMF, 4004 Wesbrook Mall, Vancouver, British Columbia, Canada, V6T 2A3, <sup>3</sup>University of Konstanz, Department of Physics, Germany, <sup>4</sup>Simon Fraser University, Burnaby, British Columbia, Canada, <sup>5</sup>McMaster University, Hamilton, Ontario, Canada, <sup>6</sup>China Institute of Atomic Energy, Beijing, P. R. China

The cascade through the 6.049-MeV  $J^\pi=0^+$  state  $^{16}\text{O}$  of has rarely been discussed as contributing to the  $^{12}\text{C}(\alpha, \gamma)^{16}\text{O}$  cross section at low energies largely due to experimental difficulties in observing this transition. We report here first measurements of this transition in  $^{12}\text{C}(\alpha, \gamma)^{16}\text{O}$  using the DRAGON recoil separator facility at TRIUMF. The experiment was performed in inverse kinematics with an incident  $^{12}\text{C}$  beam on a windowless  $^4\text{He}$  gas target, covering center of mass energies between 2.2 MeV and 5.42 MeV. The coincidence setup included a BGO array around the gas target and a DSSS Detector for the detection of  $^{16}\text{O}$  recoil particles at the focal plane of DRAGON. To derive actual cross sections, the acceptance of DRAGON including the BGO array has been simulated in GEANT. The transition strength has been derived and analyzed in the R-matrix formalism. Information on the 6.92-MeV cascade transition and the ground state transition were also obtained from the same data set. We derived the  $^{12}\text{C}(\alpha, \gamma)^{16}\text{O}$  total cross section and found it in good agreement with a recently reported measurement.

## 8.3 $^{40}\text{Ca}(\alpha, \gamma)^{44}\text{Ti}$

### 8.3.1 Study of the $^{40}\text{Ca}(\alpha, \gamma)^{44}\text{Ti}$ reaction at stellar temperatures with DRAGON

VOCKENHUBER, C.<sup>1</sup>, OUELLET, C. V.<sup>2</sup>, BUCHMANN, L.<sup>1</sup>, CAGGIANO, J.<sup>1</sup>, CHEN, A. A.<sup>2</sup>, D'AURIA, J. M.<sup>3</sup>, DAVIDS, B.<sup>1</sup>, FOGARTY, L.<sup>1</sup>, FREKERS, D.<sup>4</sup>, HUSSEIN, A.<sup>5</sup>, HUTCHEON, D. A.<sup>1</sup>, KUTSCHERA, W.<sup>6</sup>, OTTEWELL, D.<sup>1</sup>, PAUL, M.<sup>7</sup>, PEARSON, J.<sup>2</sup>, RUIZ, C.<sup>1</sup>, RUPRECHT, G.<sup>1</sup>, TRINCZEK, M.<sup>1</sup>, and WALLNER, A.<sup>6</sup>

<sup>1</sup>TRIUMF, Vancouver, BC, Canada, <sup>2</sup>McMaster University, Hamilton, ON, Canada, <sup>3</sup>Simon Fraser University, Burnaby, BC, Canada, <sup>4</sup>Institut für Kernphysik, Universität Münster, Germany, <sup>5</sup>University of Northern British Columbia, Prince George, BC, Canada, <sup>6</sup>VERA, Institut für Isotopenforschung und Kernphysik, Universität Wien, Austria, <sup>7</sup>Racah Institute of Physics, Hebrew University, Jerusalem, Israel

$^{44}\text{Ti}$  (60.0 yr half-life) is one of the few short-lived radionuclides, which has been detected in space by  $\gamma$ -ray astronomy and thus confirm ongoing nucleosynthesis. Since it is produced predominantly in supernovae during the alpha-rich freezeout, its measured abundance can be used to constrain supernova models. The  $^{40}\text{Ca}(\alpha, \gamma)^{44}\text{Ti}$  reaction plays a key role in  $^{44}\text{Ti}$  production. It has been studied partly in the past by prompt  $\gamma$ -ray measurements. A recent integral measurement over a larger temperature regime by off-line counting of  $^{44}\text{Ti}$  nuclei with AMS showed a significantly larger  $^{44}\text{Ti}$  yield compared to previous results from prompt  $\gamma$ -ray measurements. We have measured this reaction in inverse kinematics at the recoil mass spectrometer DRAGON, located at the ISAC facility at TRIUMF (Vancouver, Canada). High-purity  $^{40}\text{Ca}$  beam (less than 0.5%  $^{40}\text{Ar}$

contamination) was accelerated to energies of 0.8 - 1.2 MeV/amu impinging on a windowless He gas target surrounded by a high-efficiency BGO  $\gamma$ -detector array.  $^{44}\text{Ti}$  recoils are then separated from the  $^{40}\text{Ca}$  beam by the recoil mass spectrometer and identified in an ionization chamber. The advantage of direct detection of  $^{44}\text{Ti}$  recoils and prompt  $\gamma$  rays allows a detailed study of this reaction over a large energy range with sufficient resolution to resolve individual resonances. In this presentation, we report on the status of our investigations, which begins at the strong isospin triplet around  $E_x = 9.2$  MeV and continues from here to lower energies covering a temperature regime of  $T_9 \approx 1.5$  to 2.5 relevant for supernova nucleosynthesis.

### 8.3.2 The supernova-nucleosynthesis $^{40}\text{Ca}(\alpha, \gamma)^{44}\text{Ti}$ reaction

PAUL, Michael<sup>1</sup>, NASSAR, Hisham<sup>1</sup>, SAVARD, Guy<sup>2</sup>, VONDRASEK, Richard<sup>2</sup>, GORIELY, Stephane<sup>3</sup>, HEGGER, Alexander<sup>4</sup>, HASS, Michael<sup>5</sup>, JANSSENS, Robert V.F.<sup>2</sup>, KASHIV, Yoav<sup>1</sup>, OFAN, Avishai<sup>1</sup>, PARDO, Richard<sup>2</sup>, and REHM, K. Ernst<sup>2</sup>

<sup>1</sup>Hebrew University, Jerusalem, Israel 91904, <sup>2</sup>Argonne National Laboratory, Illinois 60439, <sup>3</sup>Universite Libre de Bruxelles, 1050 Brussels, Belgium, <sup>4</sup>Los Alamos National Laboratory, NM 87545, USA, <sup>5</sup>Weizmann Institute, Rehovot, Israel 76100

The  $^{44}\text{Ti}$  ( $t_{1/2}=59$  y) nuclide is considered an important signature of core-collapse supernova (SN) nucleosynthesis and has recently been observed as live radioactivity by  $\gamma$ -ray astronomy from the Cas A SN remnant. We investigated in the laboratory the major  $^{44}\text{Ti}$  production reaction,  $^{40}\text{Ca}(\alpha, \gamma)^{44}\text{Ti}$  ( $E_{cm} \sim 0.6 - 1.2$  MeV/u), by off-line counting of  $^{44}\text{Ti}$  nuclei using accelerator mass spectrometry [1]. The observed yield is significantly higher than inferred from previous prompt- $\gamma$  spectroscopy experiments. The present data strongly support the BRUSLIB statistical model [2] which incorporates a microscopic model of nuclear level densities and of the  $\gamma$ -ray strength function, and a global  $\alpha$ -nucleus optical-model potential. Comparison of the data with the statistical model confirms the strong suppression in yield expected for  $(\alpha, \gamma)$  reactions on self-conjugate ( $N = Z$ ) nuclei. The derived astrophysical rate of the  $^{40}\text{Ca}(\alpha, \gamma)^{44}\text{Ti}$  reaction is a factor 5-10 higher than calculated in current models. We will present results of stellar calculations in spherical hydrodynamics, as those described in [3] but using this reaction rate, showing an increase of the calculated SN  $^{44}\text{Ti}$  yield by a factor  $\sim 2$  over current estimates. An increase by a factor of  $\sim 2$  in  $^{44}\text{Ti}$  is found also in the calculated fall back material. The yields calculated by multi-dimensional SN explosion calculations proposed to explain the observed  $^{44}\text{Ti}$  yield of Cas A, in which parts of deeper layers can be ejected while some of the outer layers fall back, are expected to be enhanced in  $^{44}\text{Ti}$  as well.

*This work was supported in part by the US- DOE, Office of Nuclear Physics, under Contract No. W-31-109-ENG-38, the DOE Program for Scientific Discovery through Advanced Computing (SciDAC; DE-FC02-01ER41176), by DOE contract W-7405-ENG-36 to the Los Alamos National Laboratory, and by the USA-Israel Binational Science Foundation (BSF).*

[1] H. Nassar et al., Phys. Rev. Lett., to be published.

[2] M. Arnould and S.Goriely, Nucl. Phys. A, to be published.

[3] T. Rauscher et al., Astrophys. J., 576, 323 (2002).

## 9 Element production, stellar evolution, and stellar explosions

### 9.1 New ideas in the theory of core-collapse supernova explosions

BURROWS, Adam

University of Arizona

Core-collapse supernova explosions are fundamentally aspherical and require multi-dimensional radiation/hydrodynamical tools to address them. Recent simulations have hinted that the inner core of the protoneutron star executes vigorous g-mode oscillations that damp by the emission of acoustic power. I will present results from our recent 2D simulations that explore such core pulsations, the generation of sound, neutrino emissions, and explosion. The sound pulses radiated from the core steepen into shock waves that merge as they propagate into the outer mantle and

deposit their energy and momentum with high efficiency. All models we address explode with the aid of such acoustic power, but what the ultimate role of sound may be in the supernova phenomenon remains to be seen. I will address the implications of the new simulations for the mechanism of supernova explosions, the r-process, pulsar kicks, supernova blast morphology, and the gravitational radiation signatures of the deaths of massive stars and I will provide a roadmap for future theoretical explorations to test, verify, or refute the new ideas that are emerging.

## 9.2 The role of neutrinos in explosive nucleosynthesis

FRÖHLICH, Carla<sup>1</sup>, THIELEMANN, Friedrich-Karl<sup>1</sup>, MARTÍNEZ PINEDO, Gabriel<sup>2</sup>, and LIEBENDÖRFER, Matthias<sup>1</sup>

<sup>1</sup>University of Basel, <sup>2</sup>GSI

A new nucleosynthesis process, that we denote  $\nu p$ -process, will be presented. It occurs in supernovae (and possibly  $\gamma$ -ray bursts) when strong neutrino fluxes create proton-rich ejecta. In this process, antineutrino absorptions in the proton-rich environment produce neutrons that are immediately captured by neutron-deficient nuclei. This allows for the nucleosynthesis of nuclei with mass numbers  $A > 64$ . Making this process a possible candidate to explain the origin of the solar abundances of the light  $p$  nuclei (such as <sup>92,94</sup>Mo and <sup>96,98</sup>Ru). This process also offers a natural explanation for the large abundance of Sr seen in an hyper-metal-poor star.

## 9.3 The first nova explosions

JOSÉ, Jordi<sup>1,3</sup>, HERNANZ, Margarita<sup>1,2</sup>, GARCÍA-BERRO, Enrique<sup>1,3</sup>, and GIL-PONS, Pilar<sup>3</sup>

<sup>1</sup>Institut d'Estudis Espacials de Catalunya, <sup>2</sup>Consejo Superior de Investigaciones Científicas (CSIC), <sup>3</sup>Univ. Politècnica de Catalunya

Classical nova outbursts are powered by thermonuclear runaways (hereafter, TNRs) that take place in the hydrogen-rich accreted envelopes of white dwarfs in close binary systems. Extensive numerical simulations of nova outbursts have shown that the accreted envelopes attain peak temperatures ranging between 100 and 400 MK for about several hundred seconds, and therefore, their ejecta is expected to show signatures of a significant nuclear activity. Indeed, it has been claimed that novae can play a certain role in the enrichment of the interstellar medium through a number of intermediate-mass elements. This includes <sup>17</sup>O, <sup>15</sup>N and <sup>13</sup>C, systematically overproduced in huge amounts with respect to solar abundances, with a lower contribution in a number of other species with  $A < 40$ , such as <sup>7</sup>Li, <sup>19</sup>F, or <sup>26</sup>Al. Estimates of the contribution of novae to the Galactic abundances usually rely on poorly known quantities, and implicitly assume that novae have been the same sort of objects during the whole Galaxy's history: that is, an explosion on a particular white dwarf, of a given mass and luminosity, is today similar to those contaminating the interstellar medium in the early epochs of the Galaxy. In this presentation, we analyse the first nova explosions and demonstrate that these objects were more important contributors to the Galactic abundances in the past.

## 9.4 Neutrinos and nucleosynthesis in $\gamma$ -ray bursts

SURMAN, Rebecca<sup>1</sup> and MCLAUGHLIN, Gail<sup>2</sup>

<sup>1</sup>Union College, <sup>2</sup>North Carolina State University

$\gamma$ -ray bursts, while rare, may be important contributors to galactic nucleosynthesis. Here we consider the types of nucleosynthesis that can occur as material is ejected from a  $\gamma$ -ray burst accretion disk. We calculate the composition of material within the disk as it dissociates into protons and neutrons and then use a parameterized outflow model to follow nuclear recombination in the wind. From the resulting nucleosynthesis we delineate the disk and outflow conditions in which iron peak,  $r$ -process, or light  $p$ -process nuclei may form. In all cases the neutrinos have an important impact on the final abundance distributions.

## 9.5 Presupernova evolution and explosive nucleosynthesis of massive stars

LIMONGI, Marco<sup>1</sup> and CHIEFFI, Alessandro<sup>2</sup>

<sup>1</sup>INAF-Osservatorio Astronomico di Roma, <sup>2</sup>INAF-Istituto di Astrofisica Spaziale e Fisica Cosmica

I will review the presupernova evolution and the associated explosive nucleosynthesis of massive stars with mass loss in the mass interval between 11 and 120  $M_{\odot}$ . For the solar metallicity models I will address the following topics: 1) the evolutionary properties of Wolf-Rayet stars and their comparison with observations; 2) the chemical yields provided by a generation of core collapse supernovae; 3) the contribution of these stars to the production of  $^{26}\text{Al}$  and  $^{60}\text{Fe}$  in the Galaxy. For the zero metallicity models I will mainly discuss their chemical yields and their connection with "normal" and C-rich extremely metal poor stars.

## 10 Element production & stellar evolution II

### 10.1 Globular clusters : Ideal laboratories to test hydrogen-burning nucleosynthesis and hydrodynamics in stars?

CHARBONNEL, Corinne

Geneva Observatory, Geneva, Switzerland & CNRS, France

Galactic globular clusters (GC) stars exhibit abundance patterns which are not shared by their field counterparts, e.g. the well-documented O-Na and Mg-Al anticorrelations. Recent observations provided compelling evidence that these abundance anomalies were already present in the intracluster gas from which the observed stars formed. A widely held hypothesis is that the gas was polluted early in the history of the GC by material processed through H-burning at high temperature and then lost by stars more massive than the presently observed long-lived stars. However the "polluters" have not been unambiguously identified yet. Most studies have focused on AGB stars, but rotating massive stars present an interesting alternative. In this talk we try to answer to the following question : "Are GC ideal laboratories to test hydrogen-burning nucleosynthesis and hydrodynamics in stars?" We critically analyse the pros and cons of both potential stellar polluters. We discuss the constraints that the observational data bring on the stellar nucleosynthesis and hydrodynamics as well as on nuclear reaction rates.

### 10.2 Neutron-capture elements in globular cluster M15

OTSUKI, Kaori<sup>1</sup>, AOKI, Wako<sup>2</sup>, HONDA, Satoshi<sup>2</sup>, TRURAN, Jim<sup>1</sup>, MATHEWS, Grant<sup>3</sup>, KAJINO, Toshitaka<sup>4</sup>, DWARKADAS, Vikram<sup>1</sup>, and MEDINA, Anibal<sup>1</sup>

<sup>1</sup>University of Chicago, <sup>2</sup>National Astronomical Observatory of Japan, <sup>3</sup>University of Notre Dame, <sup>4</sup>National Astronomical Observatory of Japan

We report on observations of six giants in the globular cluster M15 (NGC 7078). The Subaru/HDS was used to measure neutron-capture elemental abundances. Previous studies have reported a significant star-to-star variation in the neutron-capture elemental abundances of M15, and deduced that their origin was from the  $r$  process. Our abundance analyses based on high-quality blue spectra confirm the scatter in the abundances of heavy neutron-capture elements (e.g., Eu). Observed [La/Eu] ratios indicate there are no significant  $s$ -process contributions. We have found, for the first time, that there are anti-correlations between the abundance ratios of light to heavy neutron-capture elements ([Y/Eu] and [Zr/Eu]) and heavy ones (e.g., Eu). This indicates that light neutron-capture elements in these stars cannot be explained by only a single  $r$  process, but another process that has significantly contributed to the light neutron-capture elements is required to have occurred in M15. We will also discuss possible  $r$ -process enrichment model to explain our results.

### 10.3 Chemical evolution of C-Zn and *r*-process elements produced by the first generation stars

ISHIMARU, Yuhri<sup>1</sup>, WANAJO, Shinya<sup>2</sup>, and PRANTZOS, Nikos<sup>3</sup>

<sup>1</sup>Academic Support Center, Kogakuin University, <sup>2</sup>Research Center for the Early Universe, Graduate School of Science, University of Tokyo, <sup>3</sup>Institut d'Astrophysique de Paris

Metal-poor stars record enrichment history of the Galaxy at the early epoch. Abundance analysis of these stars reveals large star-to-star scatters in *r*-process elements. This may be interpreted as a result of incomplete mixing of the interstellar medium (ISM) at the beginning of the Galaxy. However, recent studies also show considerable small dispersions for abundance ratios of C-Zn [1]. We construct an inhomogeneous chemical evolution model, assuming supernova induced star formation. Then we discuss whether inhomogeneity of the ISM consistently accounts for observed differences between *r*-process and lighter elements, using several latest sets of supernova yields for metal-poor stars. If metal-poor stars are enriched by only one or a few supernovae, huge dispersions in *r*-process elements possibly imply that their yields are highly dependent on supernova progenitor masses. However, the site of *r*-process is still uncertain even from nucleosynthesis studies. We, then, attempt to determine the site of *r*-process, using an inhomogeneous chemical evolution model. In our previous study, we have shown that values of [Eu/Fe] of three metal poor stars given by Subaru observation strongly support the model where the *r*-process site is assumed as the low mass-end of supernova progenitors, such as 8 - 10  $M_{\odot}$  stars. On the other hand, a large dispersion has been found in [Sr/Ba] at lower metallicity (e.g., [2] and [3]), suggesting that lighter elements such as Sr does not come from a universal process, which produces Ba and Eu, but from 'weak' *r*-process. We show that this scenario well explains observations, when weak *r*-process produces  $\approx 60\%$  of Sr but only  $\approx 1\%$  of Ba in metal-poor stars. Intermediate mass elements between Sr and Ba must provide clues to understand the nucleosynthesis of weak *r*-process. We estimate Pd abundances of very metal-poor stars, using Subaru and also show that weak *r*-process pattern gradually decreases with atomic mass from Sr to Ba.

[1] Cayrel et al., A&A 416 (2004) 1117

[2] Ryan et al., A&AS 120 (1996) 120C

[3] Honda et al., ApJSS 152 (2004) 113

### 10.4 Reaction rate uncertainties and the operation of the NeNa and MgAl chains during HBB in intermediate-mass AGB stars

IZZARD, Robert<sup>1</sup>, LUGARO, Maria<sup>1</sup>, KARAKAS, Amanda<sup>2</sup>, and ILIADIS, Christian<sup>3</sup>

<sup>1</sup>University of Utrecht, <sup>2</sup>McMaster University, <sup>3</sup>University of North Carolina

We study the effect of uncertainties in the proton-capture reaction rates on nucleosynthesis due to the operation of the NeNa and MgAl chains during hot bottom burning (HBB) in intermediate-mass asymptotic giant branch (AGB) stars. This kind of nucleosynthesis is associated with the production of sodium, of the radioactive nucleus  $^{26}\text{Al}$  and of the heavy magnesium isotopes, and it is possibly responsible for the O, Na, Mg and Al abundance anomalies observed in globular cluster stars. We model HBB with an analytic code based on full stellar evolution models. In this way we can calculate a very large number of stars in a relatively quick time (e.g.  $10^6$  stars in 12 hours). We have computed stellar models at two different metallicities (0.02 and 0.004) and two masses (5 and 6 solar masses). We vary in turn each of the p-capture rates involved in the NeNa and MgAl chains of factors corresponding to their current uncertainties in the range of temperatures relevant for HBB ( $T_9 \approx 0.06 - 0.1K$ ). We find large uncertainties, variations of up to one order of magnitude, in the final yields of  $^{23}\text{Na}$  and  $^{22}\text{Ne}$ ,  $^{26}\text{Al}$ ,  $^{27}\text{Al}$ , and  $^{24}\text{Mg}$ , because of uncertainties in the  $^{22}\text{Ne}(p, \gamma)^{23}\text{Na}$ ,  $^{25}\text{Mg}(p, \gamma)^{26}\text{Al}$ ,  $^{26}\text{Al}(p, \gamma)^{27}\text{Si}$ ,  $^{26}\text{Mg}(p, \gamma)^{27}\text{Al}$  and  $^{23}\text{Na}(p, \gamma)^{24}\text{Mg}$  reaction rates. The uncertainty ranges increase with decreasing metallicity and increasing mass of the star, because the temperature at the base of the convective envelope increases in these cases, making HBB more efficient. We are in the process of modelling stars of lower metallicity (0.0001), where the effect of HBB is even greater. Current work also involves the computation of models in which we vary all the reaction rates in the same model. We then calculate the variation of each isotopic yield due to the uncertainties associated with all the reaction rates involved in the NeNa and MgAl chains.

## 10.5 The new solar chemical composition: Does the Sun have a sub-solar metallicity?

ASPLUND, Martin

Australian National University

In the Sun, the convection zone reaches up to the solar atmosphere and can thus directly influence the emergent spectrum. Traditionally, the effects of convection has been modelled with the local mixing length theory in 1D hydrostatic model atmospheres for stars like the Sun. In a different approach, we have performed realistic time-dependent, 3D, radiative-hydrodynamical simulations of the outer layers of the solar convection zone, including the atmosphere. Both the different mean stratification and the presence of atmospheric inhomogeneities in 3D impact the spectral line formation. We have applied this 3D solar model atmosphere to the problem of the solar chemical composition while adopting the best possible atomic and molecular line data and taking into account departures from LTE in the line formation when necessary. The inferred C, N, O and Ne abundances are all significantly lower than estimated from previous 1D modelling by 0.2-0.3 dex. These results have significant implications for a range of topics in contemporary astrophysics, including causing a severe headache for helioseismology. In this review talk I will present an overview of our analysis, give arguments why our results are trustworthy and discuss some of their ramifications.

## 11 Nuclear theory in astrophysics

### 11.1 Direct Reactions in/for Nuclear Astrophysics

BERTULANI, Carlos

Department of Physics, University of Arizona, Tucson, AZ

Precise nuclear reaction rates are needed for a detailed description of the production of elements in primordial nucleosynthesis and during the hydrostatic burning of stars to constrain the astrophysical models. The relevant reactions are extremely difficult to measure directly in the laboratory at the small astrophysical energies [1]. In recent years several indirect methods have been developed and applied to extract low-energy astrophysical S factors. Here, the methods of Coulomb dissociation, of the asymptotic normalization coefficient (ANC) and the Trojan-Horse method will be discussed. The application of these indirect methods requires a combination of experimental and theoretical efforts. This contribution focuses on the underlying reaction theories that have to be understood well in order to assess the precision and limitations of the various approaches [2]. Studying nuclear structure and nuclear reactions within a consistent approach is a complicated issue in nuclear physics. Here I will report on an attempt to reconcile structure and reactions in the No-Core Shell-Model (NCSM). The principal foundation of the NCSM is the use of effective interactions appropriate for the large, but finite, basis spaces employed in the calculations. These effective interactions are derived from the underlying realistic inter-nucleon potentials by a unitary transformation in a way that guarantees convergence to the exact solution as the basis size increases. It is a challenging task to extend ab initio nuclear structure approaches to the description of nuclear reactions. I will present the first calculations of the  ${}^7\text{Be}(p, \gamma){}^8\text{B}$  S-factor starting from the ab initio NCSM wave functions of  ${}^7\text{Be}$  and  ${}^8\text{B}$  bound states [3]. These wave functions were obtained in basis spaces up to  $10\hbar\omega$  and used to calculate channel cluster form factors (overlap integrals) of the  ${}^8\text{B}$  ground state with  ${}^7\text{Be}+p$ . Due to the use of the harmonic oscillator (HO) basis, the overlap integrals have incorrect asymptotic properties. We fix this problem in two alternative ways. First, by a Woods-Saxon potential solution fit to the interior of the NCSM overlap integrals. Second, by a direct matching with the Whittaker function. The corrected overlap integrals are then used for the  ${}^7\text{Be}(p, \gamma){}^8\text{B}$  S-factor calculation.

[1] C.A. Bertulani, Phys. Lett. B 585 (2004) 35

[2] C.A. Bertulani, Phys. Rev. Lett. 94, 072701 (2005)

[3] P. Navratil, C.A. Bertulani, and E. Caurier, Phys. Lett. B 634 (2006) 191; Phys. Rev. C, in press.

## 11.2 Cross sections of light-ion reactions calculated from ab initio wave functions

FORSSÉN, Christian<sup>1</sup>, NAVRATIL, Petr<sup>1</sup>, ORMAND, W. Erich<sup>1</sup>, and CAURIER, Etienne<sup>2</sup>

<sup>1</sup>Lawrence Livermore National Laboratory, <sup>2</sup>IREC CNRS Strasbourg

I will discuss present attempts to employ many-body nuclear structure information in nuclear reaction calculations. The foundation of our approach is the ab initio no-core shell model (NCSM), which is a well-established theoretical framework aimed at an exact description of nuclear structure starting from high-precision interactions between the nucleons. We are now able to extract translationally invariant cluster form factors from the NCSM many-body wave functions, and subsequently use them in cross section calculations. I will show some of our first results from studies of the radiative capture reactions  ${}^3\text{He}(\alpha, \gamma){}^7\text{Be}$  and  ${}^{10}\text{Be}(n, \gamma){}^{11}\text{Be}$ . The former reaction corresponds to the most important uncertainty in solar model predictions of neutrino fluxes, while the latter represents a possible breakout from the standard primordial nucleosynthesis in inhomogeneous Big Bang scenarios.

*This work was partly performed under the auspices of the U.S. Department of Energy by the University of California, Lawrence Livermore National Laboratory under contract No. W-7405-Eng-48. Support from the LDRD contract No. 04-ER-058 is acknowledged.*

## 11.3 Nuclear models for light systems

DESCOUEMONT, Pierre

Physique Nucléaire Théorique et Physique Mathématique, Université Libre de Bruxelles, Belgium

First we present general properties of low-energy reactions between light nuclei. Different theoretical approaches are briefly described. We present recent results on the  ${}^{18}\text{F}(p, \alpha){}^{15}\text{O}$  reaction, obtained in a microscopic cluster model. We point out that some  $1/2^+$  resonances, generally disregarded, may play a role. The spectroscopic properties of  ${}^{19}\text{Ne}$ , and charge symmetry between  ${}^{19}\text{Ne}$  and  ${}^{19}\text{F}$  are also discussed. Another application deals with the  ${}^{14}\text{C}(n, \gamma){}^{15}\text{C}$  reaction, where we use the Asymptotic Normalization Constant (ANC) method. By using recent data on  ${}^{14}\text{O}+p$  elastic scattering, we show that some indirect results on  ${}^{14}\text{C}(n, \gamma){}^{15}\text{C}$  are inconsistent with charge symmetry.

## 11.4 Modified nuclear lifetime in hot dense plasmas

GOSSELIN, Gilbert, MEOT, Vincent, and MOREL, Pascal

Commissariat à l'énergie atomique (CEA)

In hot dense plasmas, the electronic environment in the immediate vicinity of the nucleus is modified, and thus, the plasma conditions influence key processes driving the lifetime of a nuclear level [1]. A correct lifetime prediction requires every de-excitation process to be evaluated jointly with its corresponding excitation process. For heavy nuclei, the nuclear lifetime of discrete levels is often strongly dependent on internal conversion, which involves bound electrons. In plasma, many of these electrons are no longer in a bound state and the internal conversion rate can be significantly reduced. Its coupling with its inverse process, nuclear excitation by electron capture (NEEC), can lead to greatly increased nuclear lifetimes. In some cases, an atomic transition can be coupled with a nuclear transition in a process called nuclear excitation by electron transition (NEET) if their energies are closely matched [2]. This can accelerate the de-excitation of the excited nuclear level, and reduce its lifetime. We developed a model able to deal with these processes in plasma under thermodynamic equilibrium. It evaluates internal conversion as well as NEEC and NEET rates in plasma. Depending on the particular situation, we use either an average atom description or a multi configuration Dirac Fock (MCDF) approach to describe the electronic environment of the atom. Large variations of several excited nuclear level lifetimes have been predicted. A complete description of the nuclear lifetime must also include some other nuclear levels through which indirect nuclear excitation or de-excitation may occur. This particular situation may provide a fast method to populate or depopulate nuclear isomers [3].

[1] M. R. Harston and J. F. Chemin, Phys. Rev. C 59, 2462 (1999)

[2] P. Morel, V. Meot, G. Gosselin, D. Gogny and W. Younes, Phys. Rev. A 69, 063414 (2004)

- [3] G. Gosselin and P. Morel, Phys. Rev. C 70, 064603 (2004)

## 11.5 Enhanced electron screening in nuclear reactions and radioactive decays

CZERSKI, Konrad<sup>1</sup>, HEIDE, Peter<sup>2</sup>, HUKU, Armin<sup>2</sup>, and RUPRECHT, Götz<sup>3</sup>

<sup>1</sup>Institute of Physics, University of Szczecin, Szczecin, Poland, <sup>2</sup>Institut für Atomare Physik und Fachdiagnostik, Technische Universität Berlin, Berlin, Germany, <sup>3</sup>TRIUMF, Vancouver, Canada

In recent years, an enhanced electron screening in metallic environments has been demonstrated by many groups in experimental investigations of low-energy nuclear reactions. Similarly, first radioactive decay experiments in metallic materials have been performed to possibly observe an alteration of the decay constant due to electron screening. Both kinds of experiments are of fundamental importance for nuclear astrophysics since the metallic quasi-free electrons represent a model for dense astrophysical plasmas and thus the corresponding theories can be experimentally verified. Here, the self-consistent dielectric function theory will be applied to determine electron screening energies in different metallic materials. The results will be compared with the experimental values obtained for different nuclear reactions and some predictions for radioactive decay experiments will be presented. Furthermore, several solid state effects which can lead to an increase of the screening energy will be discussed. Special interest will be devoted to the temperature dependence of the electron screening effect.

## 12 Cosmology & BBN

### 12.1 Dark matter, dark energy & particle physics

ELLIS, John

CERN, Switzerland

### 12.2 Type Ia supernovae as standard candles

GARNAVICH, Peter

University of Notre Dame, USA

Type Ia supernovae are believed to be thermonuclear explosions of carbon-oxygen white dwarf stars. Observationally they show a wide range of light curve shapes and peak luminosities at optical wavelengths. Fortunately their peak brightness correlates with the decline rate of their light curve making them "standardizable" candles with a precision of 7 to 10% in distance. At near infrared wavelengths, type Ia supernovae appear to be closer to true standard candles and also less susceptible to dust extinction. Observations between 1 and 3 microns may be the ideal way to use type Ia supernovae as accurate cosmological probes. The origin of the diversity in type Ia supernovae remains an interesting problem. The peak brightness is controlled by the mass of radioactive nickel produced in the explosion, but what determines the nickel yield? Possibilities include the heavy metal content of the progenitor star or the mass of the star that produced the white dwarf. Both possibilities are examined by studying the characteristics of the galaxies that host type Ia events.

### 12.3 When stars attack! Live radioactivities as signatures of nearby supernovae

FIELDS, Brian and ATHANASSIADOU, Themis

University of Illinois

Supernovae are critical for life in many ways, e.g., their nucleosynthesis is the dominant cosmic source of heavy elements essential for planet formation and ultimately for biology. Yet supernovae take a more sinister shade when they occur closer to home, because an explosion inside a certain "minimum safe distance" would pose a grave threat to life on Earth. We will discuss these cosmic

insults to life, and ways to determine whether a supernova occurred nearby over the course of the Earth's existence. We will then present recent evidence that a star exploded near the Earth about 3 million years ago. Radioactive  $^{60}\text{Fe}$  atoms have been found in ancient samples of deep-ocean material, and are likely to be debris from this explosion. Recent, high-quality data confirm this radioactive signal, representing a major step forward for this field. We will present simulations of the supernova impact on the Solar System and delivery of ejecta into Earth's orbit. We will show how sea sediments can be used for nuclear astrophysics "archaeology": terrestrial samples of supernova debris allow direct laboratory probes of nucleosynthesis products from an individual explosion.

#### 12.4 Electron capture reactions in neutron star crusts: Deep heating and observational constraints

BROWN, Edward<sup>1</sup>, GUPTA, Sanjib<sup>1</sup>, SCHATZ, Hendrik<sup>1</sup>, MÜLLER, Peter<sup>2</sup>, and KRATZ, Karl-Ludwig<sup>3</sup>

<sup>1</sup>Michigan State University/Joint Institute for Nuclear Astrophysics, <sup>2</sup>Los Alamos National Laboratory, <sup>3</sup>Universität Mainz

Many neutron stars accrete H- and He-rich matter from a stellar companion. Over the lifetime of the binary, enough matter can be transferred to replace the crust of neutron star. As the material is compressed, the rising electron Fermi energy induces electron captures. We calculate the evolution of a fluid element being compressed to neutron drip under conditions appropriate for the crust of an accreting neutron star. We consider different initial distributions of nuclei (X-ray burst and superburst ashes) and allow for electron captures into excited states. The heating from these reactions sets the temperature of the neutron star crust at depths where explosive burning of carbon (observed as a superburst) occurs, thus providing a possible constraint on the heating from these captures. A second constraint comes from neutron stars that accrete intermittently; when the accretion halts, the surface is detectable with X-ray telescopes such as Chandra and XMM. We calculate the evolution of the X-ray luminosity following the end of an accretion outburst using our new crust models.

#### 12.5 Nuclear physics issues in the supernova hot bubble $r$ process: What we know and what we need to find out

MATHEWS, Grant

Center for Astrophysics (CANDU), Department of Physics, University of Notre Dame, Notre Dame, USA

Core-collapse supernovae are some of the most spectacular events in the universe, yet they are still poorly understood in their detailed dynamics. In this talk we summarize the current state of the field and highlight new developments based upon the multi-dimensional behavior of the matter, neutrinos and magnetic fields during the collapse. We will discuss the crucial neutrino-energized high-entropy bubble which forms above the proto neutron star and its possible role in the nucleosynthesis of heavy nuclei by rapid neutron capture (the  $r$  process). We will present results of detailed studies of the key nuclear physics issues which remain to be addressed including which nuclear reactions, beta decay rates, nuclear masses, and nuclear structure information are most crucial. We will also summarize crucial neutrino interaction processes along with the remaining nuclear equation of state issues.

## 13 Experiments in nuclear astrophysics III

### 13.1 AMS measurements of stellar cross sections across the nuclear chart

WALLNER, Anton<sup>1</sup>, DILLMANN, Iris<sup>2</sup>, GOLSER, Robin<sup>1</sup>, KÄPPELER, Franz<sup>2</sup>, KUTSCHERA, Walter<sup>1</sup>, PRILLER, Alfred<sup>1</sup>, STEIER, Peter<sup>1</sup>, PAUL, Michael<sup>3</sup>, and VOCKENHUBER, Christof<sup>4</sup>  
<sup>1</sup>Institut für Isotopenforschung und Kernphysik, VERA, Univ. Wien, <sup>2</sup>Institut für Kernphysik, Forschungszentrum Karlsruhe, <sup>3</sup>Racah Institute of Physics, Hebrew University, <sup>4</sup>TRIUMF, Vancouver

Accurate and precise cross-section data are the key ingredients to our understanding of stellar nucleosynthesis. Common techniques for these data comprise online time-of-flight measurements of reaction cross sections as well as offline methods like the activation technique. In cases of longer-lived nuclides or nuclides with an unfavourable decay scheme, counting atoms directly rather than their decay rates, is the far more sensitive method. Accelerator mass spectrometry (AMS) offers a powerful tool to measure cross sections independent on half-lives of reaction products. At the Vienna Environmental Research Accelerator (VERA) we are pursuing a program to study cross sections relevant to nuclear astrophysics. In this context, various samples are irradiated in a quasi-stellar neutron spectrum of  $kT = 25$  keV produced with the  ${}^7\text{Li}(p, n){}^7\text{Be}$  reaction at the 3.7 MV Van de Graaff accelerator of Forschungszentrum Karlsruhe. The subsequent AMS measurements are performed at VERA. The main challenge in AMS is to discriminate isotopic and isobaric interferences. By extensive background studies the required sensitivity for cross section measurements has been demonstrated for various isotopes prior to the AMS measurements. So far, the reactions  ${}^9\text{Be}(n, \gamma){}^{10}\text{Be}$ ,  ${}^{13}\text{C}(n, \gamma){}^{14}\text{C}$ ,  ${}^{40}\text{Ca}(n, \gamma){}^{41}\text{Ca}$ ,  ${}^{54}\text{Fe}(n, \gamma){}^{55}\text{Fe}$ , and  ${}^{209}\text{Bi}(n, \gamma){}^{210}\text{Bi}$  have been investigated. For some of these reactions no experimental results exist up to now. The implications of measured cross sections for various nucleosynthesis scenarios will be discussed.

### 13.2 Proton resonance scattering of ${}^7\text{Be}$

YAMAGUCHI, Hidetoshi<sup>1</sup>, SAITO, A.<sup>1</sup>, TOGANO, Y.<sup>2</sup>, IWASA, N.<sup>3</sup>, INAFUKU, K.<sup>3</sup>, NIIKURA, M.<sup>1</sup>, KHIEM, L.H.<sup>4</sup>, HE, J.J.<sup>1</sup>, WAKABAYASHI, Y.<sup>1</sup>, AMADIO, G.<sup>1</sup>, FUJIKAWA, H.<sup>1</sup>, KUBONO, S.<sup>1</sup>, TERANISHI, T.<sup>5</sup>, KWON, Y.K.<sup>6</sup>, and NISHIMURA, S.<sup>7</sup>

<sup>1</sup>CNS, Univ. of Tokyo, <sup>2</sup>Department of Physics, Rikkyo University, <sup>3</sup>Department of Physics, Tohoku Univ., <sup>4</sup>National Centre for Natural Science and Technology, Vietnam, <sup>5</sup>Department of Physics, Kyushu Univ., <sup>6</sup>Department of Physics, Chung-Ang Univ., <sup>7</sup>RIKEN

We have studied the proton resonance scattering of  ${}^7\text{Be}$  by using a pure  ${}^7\text{Be}$  beam produced at CRIB (CNS Radioactive Ion Beam separator; CNS stands for Center of Nuclear Study, University of Tokyo). The excitation function of  ${}^8\text{B}$  was measured up to the excitation energy of 6.8 MeV, using the thick-target method. The excited states of  ${}^8\text{B}$  higher than 3.5 MeV were not known by the past experiments. This proton elastic scattering is also of importance in relation with the  ${}^7\text{Be}(p, \gamma){}^8\text{B}$  reaction, which is a key reaction in the standard solar model. The latest results of our measurement will be presented.

### 13.3 Improving the rate of the triple alpha reaction

TUR, Clarisse<sup>1</sup>, WUOSMAA, Alan<sup>2</sup>, and AUSTIN, Sam<sup>1</sup>

<sup>1</sup>Michigan State University/NSCL, <sup>2</sup>Western Michigan University

The rate of the triple alpha process, which plays a central role in the production of  ${}^{12}\text{C}$  in stars, is known with an accuracy of about 12%. Variations within the  $\pm 12\%$  errors can cause significant changes in the determination of the mass of the iron core in core-collapse supernovae (type II) and the composition of the material later ejected in the interstellar medium, as well as a factor of two change in the surface abundance of  ${}^{12}\text{C}$  in light ABG stars. The present triple alpha experiment aims therefore at reducing the uncertainty on the knowledge of this rate to about 6% by measuring more accurately than has been done in the past the pair branch for the 7.654 MeV state in  ${}^{12}\text{C}$ . This state is excited by inelastic proton scattering, taking advantage of a strong resonance at an excitation energy of 10.6 MeV and a scattering angle of 135 degrees in the lab. The protons are produced by using the Tandem accelerator at Western Michigan University. A reduction in the

$\gamma$ -ray background is achieved by a coincidence requirement between a thin scintillator tube and the large block of plastic scintillator surrounding it. The pair branch is then given by the ratio of the number of electron-positron pairs detected in the plastic scintillators in coincidence with the protons scattered at 135 degrees to the total number of such scattered protons. The experimental status will be presented.

### 13.4 High-precision mass measurements for reliable nuclear-astrophysics calculations

HERLERT, Alexander<sup>1</sup>, BARUAH, Sudarshan<sup>2</sup>, BREITENFELDT, Martin<sup>2</sup>, BLAUM, Klaus<sup>3</sup>, DELAHAYE, Pierre<sup>4</sup>, DWORSCHAK, Michael<sup>3</sup>, GEORGE, Sebastian<sup>3</sup>, GUÉNAUT, Céline<sup>5</sup>, HAGER, Ulrike<sup>6</sup>, HERFURTH, Frank<sup>7</sup>, KELLERBAUER, Alban<sup>4</sup>, KLUGE, H.-Jürgen<sup>7</sup>, LUNNEY, Dave<sup>5</sup>, SCHWEIKHARD, Lutz<sup>2</sup>, and YAZIDJIAN, Chabouh<sup>7</sup>

<sup>1</sup>European Organization for Nuclear Research (CERN), <sup>2</sup>Ernst-Moritz-Arndt-University, Institute of Physics, 17487 Greifswald, Germany, <sup>3</sup>Johannes Gutenberg-University, Institute of Physics, 55099 Mainz, Germany, <sup>4</sup>CERN, Physics Department, 1211 Geneva 23, Switzerland, <sup>5</sup>CSNSM-IN2P3-CNRS, 91405 Orsay-Campus, France, <sup>6</sup>University of Jyväskylä, Department of Physics, 40014 Jyväskylä, Finland, <sup>7</sup>GSI, Planckstr. 1, 64291 Darmstadt, Germany

The nuclear mass is an important parameter in nuclear physics and astrophysics. The experimental determination of precise and accurate values is a challenge, especially for short-lived radionuclides far away from the valley of stability with low production yields as well as half-lives down to the millisecond time scale. However, these mass values are required for testing and modeling nucleosynthesis theories that describe how elements and nuclides are formed in stellar evolution, e.g., violent processes like supernova explosions. For the calculations of the various pathways from hydrogen to the heavier elements the nuclear properties of a large number of nuclides need to be known [1,2]. Especially in the case of the r-process, where elements heavier than iron are formed by rapid neutron capture, nuclear structure data of neutron-rich nuclides far from the valley of stability are required. The path of the r-process is determined by and reflects nuclear structure. For example at the neutron shell N=50 it crosses through the waiting point nuclide <sup>80</sup>Zn. Slight deviations in the nuclear physics parameters can lead to large discrepancies in the modeling of the subsequent nucleosynthesis processes. One crucial parameter is the mass of the nuclides, which enters into the determination of neutron separation energies and the Q-values for the beta decays as well as interaction cross-sections. They are thus essential for the study of the r-process and other astrophysical aspects. With the Penning trap mass spectrometer ISOLTRAP at ISOLDE/CERN very precise and accurate mass measurements with relative mass uncertainties down to  $\Delta m/m=8 \times 10^{-9}$  can be achieved. Recently, the atomic masses of the neutron-rich zinc isotopes <sup>71-81</sup>Zn have been measured. For the first time the masses of <sup>79</sup>Zn and <sup>81</sup>Zn have been determined. The new experimental data allow the investigation of nuclear structure at the neutron shell N=50 for low Z. The possible impact on nuclear astrophysics and further examples are discussed.

[1] M. Mukherjee et al., Phys. Rev. 93, 150801 (2004)

[2] D. Rodriguez et al., Phys. Rev. Lett. 93, 161104 (2004)

### 13.5 $\alpha$ -Capture reactions and the $\alpha$ -nucleus optical potential for *p*-process nucleosynthesis

HARISSOPULOS, Sotirios<sup>1</sup>, DEMETRIOU, Paraskevi<sup>2</sup>, SPYROU, Artemisia<sup>2</sup>, LAGOYANNIS, Anastasios<sup>2</sup>, AXIOTIS, Michael<sup>2</sup>, BECKER, Hans Werner<sup>3</sup>, and ROLFS, Claus<sup>4</sup>

<sup>1</sup>Institute of Nuclear Physics, NCSR "Demokritos", <sup>2</sup>Institute of Nuclear Physics, NCSR "Demokritos", Athens, Greece., <sup>3</sup>DTL, Ruhr-Universität Bochum, Bochum, Germany. <sup>4</sup>EP3, Ruhr-Universität Bochum, Bochum, Germany.

The *p* process is the production mechanism for a certain number of proton-rich, stable nuclei, that cannot be produced by neutron captures. These 35 nuclei, lying between Se and Hg, are referred to as *p* nuclei. The most favoured scenarios for the *p* process involve the photodisintegration of intermediate and heavy elements at high temperatures (2-3 billion degrees Kelvin) that can be achieved only during the explosive burning phases of massive stars. One of the persistent puzzles

of the current abundance calculations, is the underproduction of the Mo-Ru region. These discrepancies could be due to uncertainties in the astrophysical models or in the nuclear physics data used. During the photodisintegration process, neutron, proton and  $\alpha$  emission compete with one another and with  $\beta$ -decays. A  $p$ -process network calculation involves almost 20000 reactions. However, only very few of these reactions can or have been measured in the laboratory, so the network calculations rely largely on theoretical estimates of the relevant reaction rates. Considerable effort has been devoted in the recent years to determine the nuclear properties entering the theoretical calculations of reaction rates. One such property is the  $\alpha$ -nucleus optical model potential (OMP) which is poorly known at low energies close to the Coulomb barrier. The uncertainties in the  $\alpha$  OMP, lead to large uncertainties in the  $\alpha$ -induced reaction cross sections and inverse processes (up to a factor 10), and can therefore affect the  $p$ -process network calculations. This has motivated us to carry out a systematic investigation of low-energy  $\alpha$ -induced reactions on nuclei of relevance to the  $p$  process. Experiments have been carried out at the Dynamitron accelerator of the University of Bochum. At the same time, we have updated a recent global,  $\alpha$ -nucleus OMP based on the double-folding method, on all existing data on  $\alpha$ -nucleus reactions. In this paper, we shall report on our new measurements and present detailed comparisons with calculations using the improved  $\alpha$ -nucleus OMP. The impact on  $p$ -nuclei abundances and perspectives will also be discussed.

## 14 Experiments in nuclear astrophysics IV

### 14.1 Neutron capture cross section measurements for nuclear astrophysics at n\_TOF

HEIL, Michael<sup>1</sup> for the n\_TOF collaboration

<sup>1</sup>Forschungszentrum Karlsruhe, Institut für Kernphysik, Germany

The neutron time of flight (n\_TOF) facility at CERN is a neutron spallation source with a flight path of 187 m. A proton beam from the CERN PS with an energy of 20 GeV, an intensity of  $7 \times 10^{12}$  protons/pulse and a pulse width of 6 ns is focused on a lead spallation module. A white neutron beam is produced which covers fully the energy range of interest for capture cross section measurements relevant in nuclear astrophysics, in particular for  $s$ -process nucleosynthesis. The measuring station at 187 m from the spallation module allows for time-of-flight measurements with very high energy resolution in a low-background environment. The extremely high instantaneous neutron flux and the low repetition frequency of the proton beam is best suited for capture cross section measurements on radioactive samples. This contribution gives an overview of the neutron capture measurements on isotopes of Mg, Zr, La, Sm, Os, Pb, and Bi relevant for nuclear astrophysics.

### 14.2 Re/Os clock

#### 14.2.1 Measurements of the $(n, \gamma)$ and $(n, n')$ reaction cross sections on $^{186,187,189}\text{Os}$ and $^{187}\text{Re}$ - $^{187}\text{Os}$ cosmochronology

SEGAWA, Mariko<sup>1</sup>, NAGAI, Yasuki<sup>1</sup>, TEMMA, Yasuyuki<sup>1</sup>, MASAKI, Tomohiro<sup>2</sup>, SHIMA, Tatushi<sup>1</sup>, OHTA, Takeshi<sup>1</sup>, NAKAYOSI, Akira<sup>1</sup>, NISHIYAMA, Jun<sup>3</sup>, and IGASHIRA, Masayuki<sup>3</sup>

<sup>1</sup>Research Center for Nuclear Physics, Osaka University, <sup>2</sup>Kobe University, <sup>3</sup>Research Laboratory for Nuclear Reactors, Tokyo Institute of Technology

$^{187}\text{Re}$ - $^{187}\text{Os}$  pair is known as the most promising nuclear cosmochronometer with considerable potential. This is because  $^{187}\text{Re}$   $\beta$ -decays with the half-life of  $42.3 \pm 1.3$  Gyr,  $^{187}\text{Re}$  is produced only by the rapid neutron capture process nucleosynthesis, and both  $^{186}\text{Os}$  and  $^{188}\text{Os}$  are produced only by the slow neutron capture process nucleosynthesis. However, there remains a non-trivial problem related to an excited neutron capture reaction of  $^{187}\text{Os}$  at a stellar temperature. Namely,  $^{187}\text{Os}$  is produced and depleted by the slow process nucleosynthesis. Hence, it is necessary to obtain both the production and depletion rates of  $^{187}\text{Os}$  to derive the excess abundance of  $^{187}\text{Os}$ , which can be attributable to  $\beta$ -decay from  $^{187}\text{Re}$ . While,  $^{187}\text{Os}$  is depleted not only by its ground state neutron capture reaction but also by an excited state neutron capture reaction of  $^{187}\text{Os}$ .

Note that  $^{187}\text{Os}$  has a low-lying excited state at  $E_x = 10$  keV, and the state could be significantly populated at a stellar temperature  $kT \sim 30$  keV [1]. Hence, it is necessary to know the excited state neutron capture cross section for  $^{187}\text{Os}^*$  to estimate the depletion rate of  $^{187}\text{Os}$  [2]. In order to deduce neutron capture cross section for  $^{187}\text{Os}^*$ , it has been suggested to measure the neutron inelastic scattering cross section for  $^{187}\text{Os}$  off the ground state of  $^{187}\text{Os}$  to its excited 10 keV state. The measurement of the inelastic scattering cross section of the ground state in  $^{189}\text{Os}$  has been also suggested to derive the neutron capture cross section for the first excited state of  $^{187}\text{Os}^*$ , since the spin-parities of the ground state in  $^{189}\text{Os}$  is the same as that of the first excited in  $^{187}\text{Os}$ . In the present study, we have measured the neutron capture reaction cross sections for  $^{186}\text{Os}$ ,  $^{187}\text{Os}$  and  $^{189}\text{Os}$  accurately and neutron inelastic scattering reaction cross-section for  $^{187}\text{Os}$  in the neutron energy range from 10 to 100 keV. The measurements of the neutron capture reactions have been carried out by detecting a prompt  $\gamma$ -ray from the reaction by means of an anti-Compton NaI(Tl) spectrometer. The  $(n, n')$  reaction cross section for  $^{187}\text{Os}$  has been measured by means of  $^6\text{Li}$ -glass scintillation detectors. These results will be discussed.

[1] D. D. Clayton, *Astrophys. J.* 139, 637 (1964)

[2] W. A. Fowler, *Revs. Mod. Phys.*, Vol. 56, No2. Part1. April 1984.

### 14.2.2 Experimental challenges for the Re/Os clock

MOSCONI, Marita<sup>1</sup>, HEIL, Michael<sup>1</sup>, KÄPPELER, Franz<sup>1</sup>, PLAG, Ralf<sup>1</sup>, MENGONI, Alberto<sup>2</sup>, FUJII, Kaori<sup>3</sup>, GALLINO, Roberto<sup>4</sup>, and the n\_TOF collaboration

<sup>1</sup>Forschungszentrum Karlsruhe GmbH (FZK), <sup>2</sup>International Atomic Energy Agency, Vienna, <sup>3</sup>Istituto Nazionale di Fisica Nucleare, Trieste, <sup>4</sup>Università di Torino

The stellar neutron capture cross sections of  $^{186}\text{Os}$  and  $^{187}\text{Os}$  are fundamental for the Re/Os cosmo-chronometer for defining the s-process abundance of  $^{187}\text{Os}$ . Subtraction of the s component from the solar  $^{187}\text{Os}$  abundance yields the radiogenic contribution to  $^{187}\text{Os}$  due to the  $\beta$ -decay of  $^{187}\text{Re}$  ( $t_{1/2} = 42.3$  Gy) since the onset of r-process nucleosynthesis. The laboratory cross section of  $^{187}\text{Os}$  requires a significant correction for the effect of low-lying excited state at 9.75 keV, which is strongly populated under stellar conditions. This theoretical correction can be improved by an experimental cross section for inelastic scattering to the 9.75 keV state. High resolution time-of-flight measurements of  $(n, \gamma)$  cross sections of  $^{186,187,188}\text{Os}$  from 1 eV to 1 MeV at CERN n\_TOF facility are reported. The inferred stellar cross sections differ from previously recommended values. In addition, the inelastic scattering cross section has been measured at 30 keV neutron energy via time-of-flight at the Karlsruhe 3.7 MV Van de Graaff. The implications of these results for the Re/Os clock are discussed.

## 14.3 Photodissociation measurements

### 14.3.1 Electromagnetic excitations in nuclei: from photon scattering to photodissociation

BEYER, R., DÖNAU, F., SCHWENGER, R., WAGNER, A., ERHARD, M., GROSSE, E., JUNGHANS, A.R., KOSEV, K., NAIR, C., NANKOV, N., RUSEV, G., and SCHILLING, K.D.  
Institut für Kern- und Hadronenphysik Forschungszentrum Rossendorf

In explosive nucleosynthesis temperatures are high enough for photo dissociation reaction to occur, e.g. leading to the production of  $p$ -process nuclei. In order to understand the details of element production and element disruption we started an experimental program at the new bremsstrahlung facility of the superconducting electron accelerator ELBE of FZ-Rossendorf, Dresden. The bremsstrahlung facility and the detector setup are designed such that the scattering of photons from nuclei and the photo dissociation of nuclei around the particle separation energies can be studied under optimized background conditions. The results of photon scattering experiments from the  $Z = 42$  nuclei  $^{92,98,100}\text{Mo}$  and the  $N = 50$  nuclei  $^{88}\text{Sr}$ ,  $^{89}\text{Y}$ , and  $^{90}\text{Zr}$  will be shown and compared to calculations based on a random-phase approximation method for deformed nuclei. In activation measurements with bremsstrahlung at end point energies from 10.5 to 16 MeV ( $\gamma, p$ ), ( $\gamma, n$ ) and ( $\gamma, \alpha$ ) reactions of  $^{92,100}\text{Mo}$  have been studied. The results are compared to recent

astrophysical network calculations to investigate if the underproduction of Mo and Ru isotopes in the  $p$  process is due to incorrect nuclear reaction rates.

### 14.3.2 Photodissociation as a tool for nuclear astrophysics

MÜLLER, Sebastian, HASPER, Jens, LINDENBERG, Kai, KERN, Linda, SONNABEND, Kerstin, and ZILGES, Andreas

Institut für Kernphysik, TU Darmstadt

Photodissociation cross sections play an important role in our understanding of nucleosynthesis in the mass region above  $A > 60$ . The bulk of these heavy nuclei are produced by neutron capture reactions during the  $s$  and  $r$  process. The so-called branching points of the  $s$ -process have typical half-lives on the order of a few days up to a few hundred years. The direct measurement of neutron capture cross sections of the short-living is not feasible. However, some of the long-living ones were measured successfully [1,2]. We try to constrain theoretical predictions of the capture cross section by measuring the inverse  $(\gamma, n)$  cross section directly above the neutron threshold. A current result, the cross section of  $^{186}\text{Re}(n, \gamma)$  will be shown and its influence on the Re/Os-chronometer will be discussed [3]. About 32 neutron deficient nuclei with masses  $A > 60$  cannot be produced by neutron capture reactions. These so-called  $p$  nuclei are produced by photodisintegration reactions during the  $p$  process. The  $p$  process takes place at temperatures of about 2.5 GK. At this temperature the photons stemming from the thermal photon bath induce  $(\gamma, n)$ ,  $(\gamma, \alpha)$ , and  $(\gamma, p)$  reactions. We can emulate thermal photon spectra in the needed energy range to deduce directly the ground state reaction rates [4]. We will show recent results for neutron deficient nuclei with  $Z > 78$  [5]. One of the remaining puzzles is the abundance of the neutron deficient Molybdenum isotopes. These abundances are underestimated by all network calculations by at least one order of magnitude. We measured the coulomb dissociation cross section of  $^{92,93,94,100}\text{Mo}$  at the LAND setup at GSI. This cross section can be converted into a photodissociation cross section. For comparison, the photodissociation cross section of  $^{100}\text{Mo}$  will be measured at the S-DALINAC using real photons. The last part of this presentation will be about the status of the quasi-monochromatic photon source NEPTUN at the S-DALINAC. The high resolution photon tagger NEPTUM at the S-DALINAC is designed to measure  $(\gamma, n)$  cross sections with an energy resolution of about 0.25% in the energy range between 8 MeV and 20 MeV.

- [1] K. Wisshak, F. Voss, F. Käppeler, M. Krčeka, S. Raman, A. Mengoni, and R. Gallino, Phys. Rev. C 73, 015802 (2006)
- [2] U. Abbondando et al. Report CERN-SL-2002-053 ECT, CERN (2003)
- [3] S. Müller, A. Kretschmer, K. Sonnabend, A. Zilges and D. Galaviz, Phys. Rev. C, in press
- [4] P. Mohr, K. Vogt, M. Babilon, J. Enders, T. Hartmann, C. Hutter, T. Rauscher, S. Volz and A. Zilges Phys. Lett B 488, 127 (2000)
- [5] K. Sonnabend, K. Vogt, D. Galaviz, S. Müller and A. Zilges, Phys. Rev. C 70, 035802 (2004)

### 14.3.3 Photodisintegration of $^{181}\text{Ta}$ leading to the isomeric state $^{180}\text{Ta}^m$

UTSUNOMIYA, Hiroaki and GOKO, S.

Konan University, Konan, Japan

Photoneutron cross sections for  $^{180}\text{Ta}^m$  were determined from simultaneous measurements of total cross sections ( $\sigma^{\text{tot}}$ ) and ground-state cross sections ( $\sigma^{\text{gs}}$ ) for  $^{180}\text{Ta}$  in photodisintegration of  $^{181}\text{Ta}$  with laser Compton-backscattered  $\gamma$  rays. Techniques of direct neutron counting and photoactivation were used for the measurement of  $\sigma^{\text{tot}}$  and  $\sigma^{\text{gs}}$ , respectively. The partial cross sections for the isomeric state serves as a novel probe of the nuclear level density of  $^{180}\text{Ta}$ . Implications for the  $p$ - and  $s$ -process nucleosynthesis of  $^{180}\text{Ta}^m$  are given.

## 14.4 Neutron capture measurements on the *s*-process termination isotopes lead and bismuth

DOMINGO PARDO, Cesar<sup>1</sup> for the n\_TOF collaboration

<sup>1</sup>Instituto de Física Corpuscular (IFIC) UV-CSIC

Resonance cross sections relevant for the termination of the *s*-process reaction path have been determined for <sup>204,206,207</sup>Pb and <sup>209</sup>Bi at the CERN neutron time-of-flight spectrometer n\_TOF. The measurements were carried out in the neutron energy range from 1 eV up to 500 keV. By using a system of C<sub>6</sub>D<sub>6</sub>-detectors with optimized neutron sensitivity, the main corrections of previous measurements related to neutron scattered backgrounds could be practically eliminated. Other corrections were thoroughly treated by control measurements with additional samples for determination of the ambient background and of background from in-beam  $\gamma$ -rays as well as by detailed analyses via Monte Carlo simulations. The final resonance parameters of the four isotopes and the Maxwellian averaged cross sections will be reported and their implications for the *s*-process abundance contributions in the Pb/Bi region will be discussed.

*This work has been partially supported by the EC (contract FIKW-CT-200000107) and by the National Institutions partners in the n\_TOF Collaboration*

## 15 Galactic & stellar evolution

### 15.1 Early galactic chemical evolution: The Milky Way in a cosmological context

PRANTZOS, Nikos

IAP, Paris, France

I will present an overview of recent work on the early chemical evolution of galaxies. Available information on the early Milky Way (derived from observations of abundances, abundance ratios, metallicity distributions, etc.) will be compared to information about the distant Universe (derived from metallicity, star formation rate, supernova rates, abundance patterns, etc. as a function of redshift).

### 15.2 Neutron capture processes in the early Galaxy

AOKI, Wako

National Astronomical Observatory of Japan

High resolution spectroscopy for very metal-poor stars have revealed that some fraction of objects have large excesses of neutron-capture elements, whose abundance patterns agree very well with that of the *r*-process component of solar-system material [1]. However, recent abundance studies show the existence of objects that have quite different abundance patterns. One is the class of objects that have very large enhancements of light neutron-capture elements. Although the nucleosynthesis process responsible for such chemical composition is still unknown, observational studies for this process have made substantial progresses in the past few years: (1) Such objects appear even in the extremely low metallicity range ( $[\text{Fe}/\text{H}] \leq -3.0$ ), while the stars having large excesses of heavy neutron-capture elements appear in the metallicity range of  $[\text{Fe}/\text{H}] \geq -3.0$  [2]. A large excess of the light neutron-capture element Sr is found even in the most iron-deficient star HE1327-2326 [3]. (2) An evidence of this process is found in metal-poor globular cluster stars [4]. These observational facts indicate that the process was efficient in general in the very early Galaxy. (3) The detailed elemental abundance pattern (Sr-Yb) was determined for the metal-poor star HD122563, a star that might well preserve the yields of this process [5]. The abundances of elements between the 1st and 2nd abundance peak of neutron-capture elements continuously decrease in this object. This result provides strong constraints on modeling the process responsible for production of light neutron-capture elements in the early Galaxy, which is presumably related to early generation supernovae. Another is the class of carbon-enhanced metal-poor stars that exhibit large excesses of Eu as well as *s*-process elements (e.g. Ba, Pb). Although contributions of

nucleosynthesis in AGB stars are assumed because of the excesses of *s*-process elements, standard *s*-process models cannot explain the Eu enhancement. Our recent study determined the abundances of Os and Ir for one star in this group (CS31062-050), confirming the excesses of *r*-process elements. Discovery of such objects and measurements of their detailed abundance patterns have impact on the studies of the origins of *r*-process elements.

- [1] C. Sneden *et al.*, ApJ, 467, 819 (1996)
- [2] W. Aoki *et al.*, ApJ 632, 611 (2005)
- [3] A. Frebel *et al.*, Nature 434, 871 (2005)
- [4] K. Otsuki *et al.*, ApJL, in press
- [5] S. Honda *et al.*, ApJ, in press

### 15.3 Constraints on the yields of the first supernovae in the Universe

CAYREL, Roger

Observatoire de Paris, Paris, France

Thanks to extensive surveys and to a new generation of 8 to 10 m telescopes, it has been possible to study an important sample of extremely metal-poor stars reflecting the ejectas of the first supernovae. Whereas the classical population II, with metallicities of the order of 1/100th of the solar metallicity, has rather stable abundance ratios reflecting type II SNe ejectas, a few stars with much lower metallicities present extremely different patterns, signature of specific nucleosynthetic processes. We shall review these differences, and describe the theoretical proposals attempting to explain these newly observed yields.

### 15.4 AGB stars evolution and nucleosynthesis

HERWIG, Falk

Theoretical Astrophysics Group, Los Alamos National Laboratory, USA

AGB stars are the nuclear production phase of low- and intermediate mass stars. The double-shell burning of He and H around the electron degenerate core drives a rich pattern of nucleosynthesis, including the slow neutron capture process, as well as the formation of neutron rich isotopes. This nucleosynthesis is now observationally accessible in extremely metal poor stars, in particular the carbon enhanced *s*- process rich stars in binaries. Models of AGB star evolution and nucleosynthesis include a wide range of approaches: parameterized *s*-process post-processing, stellar evolution models with various assumptions on stellar mixing as well as, more recently, hydrodynamic simulations of He-shell flash convection. New studies have been carried out to investigate the sensitivity of mixing and element production to nuclear reaction rates.

(*LA-UR-05-0900, LA-UR-05-8084, LA-UR-04-5295*)

## 16 Evolution & evidence of nucleosynthesis in stars: AGBs

### 16.1 3D hydrodynamical models of the core helium flash

LATTANZIO, John<sup>1</sup>, DEARBORN, David<sup>2</sup>, EGGLETON, Peter<sup>2</sup>, and DOSSA, Don<sup>2</sup>

<sup>1</sup>Monash University, <sup>2</sup>Lawrence Livermore National Laboratory

We present fully three dimensional models of the core helium flash in low mass stars. These hydrodynamical models show that the simple 1D hydrostatic models are not too misleading! New results, for rotating models, will be reported.

## 16.2 The $s$ process in massive stars: The contribution from shell C-burning

PIGNATARI, Marco<sup>1</sup>, HEGER, Alexander<sup>2</sup>, GALLINO, Roberto<sup>1</sup>, BALDOVIN, Carla<sup>1</sup>, WIESCHER, Michael<sup>3</sup>, and HERWIG, Falk<sup>2</sup>

<sup>1</sup>Università di Torino, <sup>2</sup>Los Alamos National Laboratory, <sup>3</sup>University of Notre Dame

In the evolution of massive stars the  $s$  process is activated at different temperatures, during He-burning and during C-burning. In the convective carbon shell, the  $s$  process affects the  $s$  yields from previous core He-burning, and the final results carry the signatures of both neutron exposures. A detailed analysis of the  $s$  process in massive stars is presented, in particular at the end of shell carbon burning, when the  $s$  process efficiency could rapidly increase with the local temperature.

## 16.3 Light and heavy elements nucleosynthesis in low mass AGB stars

CRISTALLO, Sergio<sup>1</sup>, STRANIERO, Oscar<sup>1</sup>, GALLINO, Roberto<sup>2</sup>, PIERSANTI, Luciano<sup>1</sup>, and DOMINGUEZ, Inma<sup>3</sup>

<sup>1</sup>Osservatorio Astronomico di Teramo (INAF, Italy), <sup>2</sup>Università di Torino, Torino, Italy, <sup>3</sup>Universidad de Granada, Granada, Spain

We present a new set of low mass AGB Stars models having the same mass ( $2 M_{\odot}$ ) and different metallicities ( $Z = 10^{-4}$ ,  $Z = 10^{-3}$ , and  $Z = 1.5 \times 10^{-2}$ , corresponding to the most recent evaluation of the solar metallicity). For each mass we present the evolution from the Pre-Main-Sequence up to the end of the thermally pulsing AGB phase. The introduction of an exponential decay of the convective velocities at the inner border of the convective envelope allows the formation of a tiny  $^{13}\text{C}$  pocket after Third-Dredge-Up episodes, whose extension in mass decreases along the AGB path. Detailed pulse by pulse surface enrichments and final yields at different metallicities, using a full nuclear network directly incorporated in the FRANEC stellar evolutionary code, are presented and discussed in detail. We follow the production of both light and heavy elements describing nuclear chains responsible for their production and show new results for the synthesis of radioactive isotopes such as  $^{26}\text{Al}$  and  $^{60}\text{Fe}$ .

# 17 Experiments and theory in nuclear astrophysics

## 17.1 The role of fission in $r$ -process nucleosynthesis

KELIĆ, Aleksandra

GSI Darmstadt

Fission can have an important influence on the termination of the  $r$  process and on the abundances of long-lived actinides, which are relevant for determining the age of the Universe. Fission can also influence the abundances of nuclei in the region  $A \sim 90$  and 130 due to the fission cycling. In order to quantitatively understand the fission role in the  $r$  process, two important pieces of information are needed: the fission-barrier heights and mass- and charge-distributions of the fission fragments. Unfortunately, experimental information is only available for nuclei in a limited region of the nuclide chart, and for heavy  $r$ -process nuclei one has to rely on theoretical predictions. Recently, important progress has been made in developing full microscopic approaches to nuclear fission. Nevertheless, due to the complexity of the problem, this type of calculations are still difficult to apply to heavy nuclei and, moreover, the precision of these models is often still low. In this contribution we will concentrate on macroscopic-microscopic approaches that could help us to understand the contribution of fission to the  $r$  process. Firstly, using available experimental data on saddle-point and ground-state masses, we will present a detailed study on the predictions of different models concerning the isospin dependence of saddle-point masses [1]. It will be shown that several models yield unrealistic barriers for very neutron-rich nuclei. Secondly, we will present a model for calculating mass- and charge- distributions of fission fragments, that can correctly predict the transition from double-humped to single-humped distributions with decreasing mass of the fissioning system and increasing excitation energy in the light actinides. This model has

recently [2] been used to calculate fission-fragment distributions in neutrino-induced fission of  $r$ -process nuclei.

[1] A. Kelić and K.-H. Schmidt, accepted by Phys. Lett. B

[2] A. Kelić et al, Phys. Lett. B 616 (2005) 48

## 17.2 Nucleosynthesis in neutrino heated matter

MARTÍNEZ PINEDO, Gabriel

GSI Darmstadt

Independently of the still unclear explosion mechanism for core-collapse supernovae there will be matter ejected under strong neutrino fluxes. Depending of the spectral properties of both neutrinos and antineutrinos the composition of the matter goes from proton rich to neutron rich. Current supernova simulations suggest that the early ejecta is proton rich while at latter times we expect neutron-rich ejecta. Proton-rich ejecta constitute the site a new kind of  $\nu p$ -process that is catalyzed by antineutrino absorptions in protons and that we denote as  $\nu p$ -process. The combination of proton-rich ejecta and mildly neutron-rich ejecta could explain the production of several light  $p$ -nuclei in particular  $^{92,94}\text{Mo}$  and  $^{96,98}\text{Ru}$  and at the same time explain the elemental abundances of Sr, Y and Zr seen in metal poor stars. The  $r$  process is expected to occur in neutron rich ejecta. Depending in the conditions even the heavier  $r$ -process elements can be produced. In this case fission can play a major role in understanding the production of  $r$ -process elements. In this talk I will discuss the current theoretical and experimental uncertainties related to nucleosynthesis in neutrino heated matter and in particular the role of fission (neutron induced, neutrino induced and  $\beta$ -delayed) in  $r$ -process nucleosynthesis.

## 17.3 Studies of radioactive nuclei and their role in the cosmos

BLACKMON, Jeff C.<sup>1</sup> for the RIBENS Collaboration

<sup>1</sup> Oak Ridge National Laboratory, USA

Radioactive nuclei play an important role in many astrophysical phenomena, particularly in stellar explosions where the rates of nuclear reactions can be much faster than the lifetimes of most radioactive isotopes. Accelerated beams of radioactive ions are being used to address uncertainties in some key reaction rates. We will review recent progress in the field, focusing on results from the Holifield Radioactive Ion Beam Facility (HRIBF) at Oak Ridge National Laboratory. The production of gamma-rays from electron-positron annihilation in novae is particularly sensitive to the rate of the  $^{18}\text{F}(p, \alpha)^{15}\text{O}$  reaction. Uncertainties have remained in the  $^{18}\text{F}(p, \alpha)^{15}\text{O}$  reaction rate due to the uncertain contributions of low-energy resonances and the nature of interferences between resonances. We will report on recent measurements of the  $^{18}\text{F}(p, \alpha)^{15}\text{O}$  cross section at the HRIBF using an experimental approach similar to previous measurements [1]. The new data provide some of the first constraints on the nature of interferences between resonances in the  $^{18}\text{F}(p, \alpha)^{15}\text{O}$  reaction. We will present a novel experimental technique that we have developed to allow improved sensitivity for studies of low energy ( $p, \alpha$ ) resonances. In this new approach a heavy ion beam bombards a large, windowless chamber filled with hydrogen gas. Alpha particles and recoiling heavy ions are detected in coincidence in arrays of silicon strip detectors operating inside the hydrogen gas. While each element of the detector array simultaneously views reaction products over a wide range of angles, the relative kinematics of the two reaction products allows the vertex of the reaction to be accurately determined on an event-by-event basis. We will present results from a measurement applying this technique to the 183-keV resonance in the  $^{17}\text{O}(p, \alpha)^{14}\text{N}$  reaction that was first reported using a more conventional approach last year [2]. The strength of this resonance is also crucial for understanding the production of  $^{18}\text{F}$  in novae as well as the Galactic origins of the rare  $^{17}\text{O}$  isotope. This approach will next be applied to low energy resonances in  $^{18}\text{F}(p, \alpha)^{15}\text{O}$ . Results from recent measurements using  $^7\text{Be}$  beams at the HRIBF will also be presented. Accurate measurements of the neutrino flux originating from the decay of  $^8\text{B}$  in the solar core provide a powerful probe of the properties of the solar interior and neutrinos themselves [3]. While recent measurements have substantially improved our understanding of the  $^7\text{Be}(p, \gamma)^8\text{B}$  reaction rate that impacts the interpretation of solar neutrino observations [4], the experimental situation is less than completely resolved. We are performing direct measurements of the  $^7\text{Be}(p, \gamma)^8\text{B}$  cross section

in inverse kinematics, using a radioactive  ${}^7\text{Be}$  beam on a windowless hydrogen gas target. This alternative approach at direct measurement of the  ${}^7\text{Be}(p, \gamma){}^8\text{B}$  cross section is interesting since it provides an independent check on potential systematic uncertainties. We will present results from the first measurements at the HRIBF that have demonstrated the advantages and limitations of the approach, though not yet competitive statistically with  ${}^7\text{Be}$  target experiments. We will also present measurements of  ${}^7\text{Be}+p$  elastic and inelastic scattering cross sections at center-of-mass energies ranging between 0.5 to 3.4 MeV that provide new information on the properties of excited states in  ${}^8\text{B}$  and  ${}^7\text{Be}+p$  s-wave phase shifts, which can influence extrapolations of the  ${}^7\text{Be}(p, \gamma){}^8\text{B}$  cross section to solar energies in some models [5].

*Oak Ridge National Laboratory is managed by UT-Battelle, LLC, for the U.S. Department of Energy under Contract No. DE-AC05-00OR22725.*

- [1] D.W. Bardayan *et al.*, Phys. Rev. Lett. 89, 262501 (2002)
- [2] A. Chafa *et al.*, Phys. Rev. Lett. 95, 031101 (2005)
- [3] S.N. Ahmed *et al.*, Phys. Rev. Lett. 92, 181301 (2004)
- [4] A.R. Junghans *et al.*, Phys. Rev. C 65, 065803 (2003), and references therein
- [5] P. Descouvemont, Phys. Rev. C 70, 065802 (2004)

## 18 Poster session, 26 June

### 18.1 Abundances of Mn, Co and Eu in a sample of 20 F-G disk stars: The influence of hyperfine structure splitting

DEL PELOSO, Eduardo<sup>1</sup>, CUNHA, Katia<sup>1</sup>, DA SILVA, Licio<sup>1</sup>, and PORTO DE MELLO, Gustavo<sup>2</sup>  
<sup>1</sup>Observatorio Nacional/MCT, <sup>2</sup>Observatorio do Valongo/UFRJ

We present Mn, Co, and Eu abundances for a sample of 20 disk F and G dwarfs and subgiants with metallicities in the range  $-0.8 \leq [\text{Fe}/\text{H}] \leq +0.3$ . We investigate the influence of hyperfine structure (HFS) on the derived abundances of Mn and Co by using HFS data from different sources in the literature, as well as calculated HFS from interaction factors A and B. Eu abundances were obtained from spectral synthesis of one Eu II line that takes into account HFS from a series of recent laboratory measurements. For the lines analysed in this study, we find for manganese that the differences between abundances obtained with different HFSs are no greater than 0.10 dex. Our cobalt abundances are even less sensitive to the choice of HFS than Mn, presenting a 0.07 dex maximum difference between determinations with different HFSs. However, the cobalt HFS data from different sources are significantly different. Our abundance results for Mn offer an independent confirmation of literature results, favouring type Ia supernovae as the main nucleosynthesis site of Mn production, in contrast to trends of Mn versus metallicity previously reported in the literature. For Co, we obtain  $[\text{Co}/\text{Fe}] \approx 0.0$  in the range  $-0.3 < [\text{Fe}/\text{H}] < +0.3$  and  $[\text{Co}/\text{Fe}]$  rising to a level of +0.2 when  $[\text{Fe}/\text{H}]$  decreases from -0.3 to -0.8, in disagreement with recent results in the literature. The observed discrepancies may be attributed to the lack of HFS in the works we used for comparison. Our results for Eu are in accordance with low-mass type II supernovae being the main site of r-process nucleosynthesis.

### 18.2 Coherent effects in nuclear pasta matter

PEREZ GARCIA, Angeles  
 University of Salamanca, Spain

At densities below nuclear saturation density a non uniform arrangement of nuclear matter is allowed. This type of matter, known as pasta matter. It is believed to exist in the crust of neutron stars and supernova matter. Coherent scattering of neutrinos, produced in the early stages of a supernova, can happen. We study the coherent response of the medium by using molecular dynamics simulations. We perform an analysis of the static structure of pasta matter in the spin/isospin channels.

### 18.3 Pre-supernova models at low metallicities

HIRSCHI, Raphael<sup>1</sup> and MEYNET, Georges<sup>2</sup>

<sup>1</sup>University of Basel, <sup>2</sup>Geneva Observatory

We will present recent results from single rotating massive stellar models at low metallicities. We describe the evolution and stellar yields of the models and compare them with observations of long and soft GRBs and very metal poor stars. Predicted GRB rates as a function of metallicity will be given. Rotation enables a high production of primary nitrogen at very low metallicities, which is observed in EMP stars. Rotation also increases mass loss in very low metallicity stars with  $M \geq 60 M_{\odot}$ . It therefore opens the possibility of SNIb,c (and maybe GRBs) production at very low metallicities from single massive stars.

### 18.4 Breakup and competing processes in reactions involving weakly bound nuclei

SZANTO DE TOLEDO, Alejandro, SOUZA, F.A., CARLIN, N., LIGUORI NETO, R., DE MOURA, M.M., MUNHOZ, M.G., SUAIDE, A.A.P., SZANTO, E.M., TAKAHASHI, J., and BECK, C.

Departamento de Fisica Nuclear, Instituto de Fisica da Universidade de São Paulo, C.P. 66318,5315-970 São Paulo, S.P., Brasil

The study of the reaction dynamics involving weakly bound nuclei became one of the most intriguing and challenging problems in low energy nuclear physics. The cross section enhancement generally observed at sub-barrier energies is understood in terms of dynamical processes arising from couplings to collective inelastic excitations of the target and/or projectile [1]. In the case of reactions, where at least one of the colliding nuclei has a sufficiently low binding energy, breakup becomes an important process. Some of the conflicting experimental and theoretical results reported recently were clarified [2-4]. However, the interplay between fusion and breakup processes, which exhibit different behavior depending on the energy regime, still presents important open questions. This is of fundamental importance in astrophysical processes, which occur mostly outside the valley of stability, and consequently involve unstable nuclei. A final tuning for the coupling of the breakup channel, as well as the correct description of the reaction dynamics, requires the explicit measurement of precise elastic scattering data as well as yields leading to breakup. The investigation of the [ ${}^6,7\text{Li} + {}^{59}\text{Co}, {}^{115}\text{In}$ ] breakup processes is used to understand the influence of breakup on the fusion cross section. Experimental results are compared to predictions of Coupled Channel Calculations. The identification of the breakup products has been achieved measuring the three body final state correlations. Coincidence data are used to determine the process Q-value in order to gate exclusively on the projectile breakup channel. Furthermore, the system excitation energy as well as the relative energy of the projectile fragments are used to identify the exit channel with no ambiguity. Based on those filters, angular correlations are obtained to identify the different processes. This is complemented by measurements of the relative energy of the fragments using different rest frame references (target, projectile, target + fragment) in order to disentangle the contribution of breakup, incomplete fusion, and/or transfer-reemission. These experimental results are compared to three body kinematics calculations. This procedure in unfolding the several light particle emission processes has not been exploited so far in the literature.

- [1] M. Dasgupta *et al.*, Ann. Rev. Nucl. Part. Sci. 48, 401 (1998) and references therein
- [2] K. Hagino *et al.*, Phys. Rev. C 61, 037602 (2000) and references therein
- [3] C. Beck *et al.*, Phys. Rev. C 67, 54602 (2003)
- [4] A. Diaz Torres *et al.* Phys.Rev. C 68, 44607 (2003)

### 18.5 $^{18}\text{F}(\alpha, p)^{21}\text{Ne}$ reaction: Neutron source for $r$ process in supernovae

LEE, Hye Young<sup>1</sup>, O'BRIEN, S.<sup>1</sup>, PALUMBO, A.<sup>1</sup>, STECH, E.<sup>1</sup>, STRANDBERG, E.<sup>1</sup>, TAN, W.<sup>1</sup>, WIESCHER, M.<sup>1</sup>, BECKER, H.-W.<sup>2</sup>, ANGULO, C.<sup>3</sup>, CASAREJOS, E.<sup>3</sup>, LELEUX, P.<sup>3</sup>, GROOMBRIDGE, D.<sup>4</sup>, FULTON, B.<sup>4</sup>, LAIRD, A.<sup>4</sup>, ALIOTTA, M.<sup>5</sup>, COUDER, M.<sup>1</sup>, COULTURE, A.<sup>1</sup>, GÖRRES, J.<sup>1</sup>, and LEBLANC, P.<sup>1</sup>

<sup>1</sup>University of Notre Dame, USA <sup>2</sup>Dynamitron Tandem Laboratory, Ruhr-Universität Bochum, Germany,

<sup>3</sup>Centre de Recherches du Cyclotron and Institut de Physique Nucleaire, UCL, Louvain la Neuve, Belgium,

<sup>4</sup>University of York, UK, <sup>5</sup>University of Edinburgh, UK

Recent observation of heavy elements abundance distribution in metal poor old stars gives an indication of the existence of more than one  $r$ -process site. One of models suggested the  $r$ -process nucleosynthesis in the supernova shock passing through the He-rich shell of the pre-supernova star. In this helium rich environment, a possible neutron source for the second  $r$ -process would be the reaction sequence  $^{14}\text{N}(\alpha, \gamma)^{18}\text{F}(\alpha, p)^{21}\text{Ne}(\alpha, n)^{24}\text{Mg}$  with rapid depletion of  $^{14}\text{N}$ . The  $(\alpha, p)$  reaction on  $^{18}\text{F}$  will be faster than  $\beta^+$  decay at the high densities and temperature in the shock. The  $^{18}\text{F}(\alpha, p)^{21}\text{Ne}$  reaction and the inverse reaction  $^{21}\text{Ne}(p, \alpha)^{18}\text{F}$  have been measured in CRC, Louvain-la-neuve and in Notre Dame in the energy range of the Gamow window. Experimental results will be presented and compared with Hauser-Feshbach calculations. The astrophysical implications of the new reaction rates will be discussed.

### 18.6 Abundance clues to the nature of the “main” and the “weak” $r$ -process

KRATZ, Karl-Ludwig<sup>1</sup>, SNEDEN, Chris<sup>2</sup>, TRURAN, James, W.<sup>3</sup>, PFEIFFER, Bernd<sup>1</sup>, FAROUQI, Khalil<sup>1</sup>, COWAN, John, J.<sup>4</sup>

<sup>1</sup>Joh. Gutenberg-Universität Mainz, Germany, <sup>2</sup>Univ. Texas, Austin, TX, <sup>3</sup>Univ. of Chicago, Chicago, IL, <sup>4</sup>Univ. of Oklahoma, Norman, OK

Abundances of neutron-capture elements beyond Ba in several ultra-metal-poor (UMP) halo stars in the early Galaxy accurately replicate the solar system  $r$ -process pattern, whereas the lighter elements show distinct under-abundances. This appears to require contributions from different types of  $r$ -process synthesis events: an early primary “main”  $r$  process and a later secondary “weak”  $r$  process. We examine model predictions, based on the most recent experimental and theoretical nuclear physics quantities, to explore the nuclear and astrophysical implications of the solar and stellar observations. We find that the isotopic fractions of Ba, together with the Ba/Eu elemental abundance ratios in the UMP stars can only be matched by computations in which the neutron densities are  $n_n > 10^{23}$ , whereas the reproduction of the lighter-element pattern requires only conditions of  $n_n < 10^{23}$ . Further, our calculations indicate that it is difficult to decouple full production of the 2<sup>nd</sup>  $r$ -process abundance peak from the observed full solar pattern beyond Ba. Finally, in the  $n_n$  ranges required for production for the observed solar / stellar 3<sup>rd</sup>  $r$ -process peak, our prediction of inter-peak element Hf follows closely those of the 3<sup>rd</sup> peak elements Os through Pb, Bi. This suggests that abundance comparisons of Hf to lower- $Z$  rare-earth elements and to 3<sup>rd</sup>-peak elements, as well as to the Th, U cosmochronometers, can shed further light on claims of invariance in the entire heavy end of the  $r$ -process abundance pattern.

### 18.7 $^{22}\text{Ne}$ : A primary source of neutrons for the $s$ -process and a major neutron poison in CEMP AGB stars

GALLINO, Roberto<sup>1</sup>, BISTERZO, Sara<sup>1,2</sup>, KÄPPELER, Franz<sup>2</sup>, CRISTALLO, Sergio<sup>3</sup>, and STRANIERO, Oscar<sup>3</sup>

<sup>1</sup>Dip. Fisica Generale, University of Torino, Torino, Italy, <sup>2</sup>Forschungszentrum Karlsruhe, Institut für Kernphysik, D-76021 Karlsruhe, Germany, <sup>3</sup>INAF-Osservatorio di Teramo, Teramo, Italy

In AGB stars of low mass and very low metallicity,  $[\text{Fe}/\text{H}] < -2$ , a large abundance of  $^{12}\text{C}$  is mixed with the envelope by each third dredge up episode. The further activation of the H burning shell at the bottom of the envelope converts almost all CNO nuclei into  $^{14}\text{N}$ . Thus the H-burning ashes contain  $^{14}\text{N}$  from the original CNO nuclei, plus an increasing amount of primary  $^{14}\text{N}$ . During

the subsequent convective thermal instability in the He shell, all  $^{14}\text{N}$  nuclides present in the He intershell are converted to  $^{22}\text{Ne}$  by double alpha capture on  $^{14}\text{N}$  during the early development of the thermal instability. At the peak temperature reached at the base of the thermal pulse, the  $^{22}\text{Ne}(\alpha, n)^{25}\text{Mg}$  reaction is partly activated, giving rise to an efficient neutron exposure feeding the s-process. At the same time, although the neutron capture cross section of  $^{22}\text{Ne}$  is very small [ $\text{MACS}(^{22}\text{Ne}, 30\text{keV})=0.059\pm 0.0057$  mbarn, Beer et al. 1991],  $^{22}\text{Ne}$  acts as a major poison against the s-process. This poison effect is substantial also in case of addition of a  $^{13}\text{C}$ -pocket with a range of neutron exposure efficiencies. Some fraction of primary  $^{16}\text{O}$  is also made in the thermal pulse by alpha capture on  $^{12}\text{C}$  (with mass fraction  $X(^{16}\text{O}) = 0.04$ , while  $X(^{12}\text{C}) = 0.20$ ). Besides  $^{12}\text{C}$  and  $^{22}\text{Ne}$ , a number of light isotopes are largely produced in a primary way, among which  $^{19}\text{F}$  (from neutron capture on  $^{18}\text{O}$ , and other channels as well),  $^{21}\text{Ne}$ ,  $^{23}\text{Na}$ , and some  $^{24}\text{Mg}$ ,  $^{25}\text{Mg}$ ,  $^{26}\text{Mg}$ . An effort should be devoted to the measurement of the MACS of all the light isotopes involved with improved accuracy, in order to better constrain both the s-process efficiency and the production of light isotopes in these stars.

### 18.8 Structure of doorway states above the $K^\pi=8^+$ , $t_{1/2} \approx 2.0 \times 10^5$ yr isomer in $^{186}\text{Re}$ and their impact on the accuracy of the $^{187}\text{Re}/^{187}\text{Os}$ cosmochronometer

KONDEV, Filip G.<sup>1</sup>, DRACOU LIS, George D.<sup>2</sup>, WATANABE, Hiroshi<sup>2</sup>, WILSON, Anna N.<sup>2</sup>, LANE, Gregory J.<sup>2</sup>, BYRNE, Aidan<sup>2</sup>, CARPENTER, Michael P.<sup>1</sup>, DAVIDSON, Paul M.<sup>2</sup>, HUGHES, Richard O.<sup>2</sup>, JANSSENS, Robert V.F.<sup>1</sup>, KIBEDI, Tibor<sup>2</sup>, and NIEMINEN, Paivi<sup>2</sup>

<sup>1</sup>Argonne National Laboratory, <sup>2</sup>Australian National University

The amount of  $^{187}\text{Os}$  in meteorites that results from  $\beta$ -decay of the long-lived ( $t_{1/2}=4.35 \times 10^{10}$  yr [1])  $^{187}\text{Re}$  nuclide has been used in dating of the r-process. In order to reduce the nuclear physics uncertainties for this cosmochronometer, a correction is needed to the  $^{187}\text{Re}$  abundance that arises from the fact that  $^{186}\text{Re}$  has an  $8^+$  isomeric state ( $t_{1/2} \approx 2.0 \times 10^5$  yr,  $E_x=149$  keV) [1], sufficiently long-lived that sequential neutron captures  $^{185}\text{Re}(n, \gamma)^{186}\text{Re}^m(n, \gamma)^{187}\text{Re}$  can contribute to the s-process production. The branch through the isomer has been ignored in the past owing to the lack of experimental data. Studies have recently been reported using the activation technique [2], but these are sensitive to the half-life of the isomer, which is not known accurately. In order to evaluate the production (and destruction) cross-section for the isomer following neutron capture reactions, detailed information on the disposition of the experimental states above the  $8^+$  isomer in  $^{186}\text{Re}$  is required. The identification and characterization of such doorway states would stimulate future capture cross sections measurements using a neutron-induced, prompt  $\gamma$ -ray spectroscopy technique that is independent of the isomer lifetime. We have pursued studies of  $^{186}\text{Re}$  using the  $^{186}\text{W}(d, 2n)$  reaction and  $\gamma$ -ray spectroscopy with the main aim of characterising states above the  $8^+$  isomer. DC beams from the 14UD Pelletron accelerator of the Australian National University were incident on a 6 mg/cm<sup>2</sup> thick target that was isotopically enriched in  $^{186}\text{W}$ . Gamma rays were detected using the CAESAR array comprising 9 Compton-suppressed Ge detectors and one LEPS Ge spectrometer. Excitation functions in the 11.9-20.0 MeV range and  $\gamma$ - $\gamma$  coincidence measurements at 12.5 MeV (near the barrier) and 14.5 MeV (to enhance the population of the  $8^+$  isomer) were carried out. In addition, preliminary studies using the Gammasphere spectrometer in conjunction with time-correlated,  $\gamma$ -ray coincidence techniques have been initiated at Argonne National Laboratory. In a recent experiment, a 820 MeV pulsed beam (1 ns on/820 ns off) of  $^{136}\text{Xe}$  from the ATLAS accelerator was used to bombard an enriched  $^{185}\text{Re}$  target, populating many nuclei in the region near  $^{186}\text{Re}$  using multi-nucleon transfer reactions. Results from these measurements will be presented and discussed with emphasis on the properties of states above the  $8^+$  isomer in  $^{186}\text{Re}$  and their impact on the production of the isomer in stellar environments. The astrophysical relevance of other long-lived isomers in neighboring nuclei will be also reviewed.

*This work was supported by the U.S. Department of Energy, Office of Nuclear Physics under Contracts No. W-31-109-ENG-38, the ANSTO program for Access to Major Research Facilities, grant No. 02/03-H-05 and the Australian Research Council projects DP0343027 and DP0345844.*

[1] R.B. Firestone and V.S. Shirley, Table of Isotopes (Wiley, New York, 1996)

[2] T. Hayakawa et al., Astrophys. J. 628 533 (2005).

## 18.9 Indirect techniques in nuclear astrophysics

MUKHAMEDZHANOV, Akram Zhanov

Texas A&M University

It is very difficult or often impossible to measure under lab conditions nuclear cross sections at astrophysically relevant energies. That is why different indirect techniques are used to extract astrophysical information. In this talk two different experimental possibilities to get astrophysical information using radioactive and stable beams will be addressed.

1. The asymptotic normalization coefficient (ANC) method has proven to be a powerful indirect technique to get astrophysical S factors. Often this method requires the use of radioactive beams. The ANC method is especially powerful when subthreshold states contribute to the process. The role of subthreshold states as bound states and resonances will be discussed. I will demonstrate the application of the ANC technique for the most important reaction of the CNO cycle,  $^{14}\text{N}(p, \gamma)^{15}\text{O}$  and the first reaction of the Ne-Na cycle  $^{20}\text{Ne}(p, \gamma)^{21}\text{Na}$ . In both cases the subthreshold states dominate the radiative capture process. It is believed that the  $^{13}\text{C}(\alpha, n)^{16}\text{O}$  reaction is a major source of neutrons for the s-process in low-mass stars at the asymptotic giant branch (AGB). I will demonstrate the first application of the ANC method to determine a very important astrophysical factor for astrophysical rearrangement reaction. The  $^{13}\text{C}(\alpha, n)^{16}\text{O}$  reaction proceeds through the subthreshold state 6.356 MeV in  $^{17}\text{O}$ , just 3 keV below the threshold. The astrophysical factor is governed by the ANC for the  $^{13}\text{C} + \alpha \rightarrow ^{17}\text{O}(6.356 \text{ MeV}; s1/2)$  virtual synthesis. The ANC for this state has been measured using the sub-Coulomb  $\alpha$ -transfer  $^{13}\text{C}(^6\text{Li}, d)^{17}\text{O}(6.356 \text{ MeV}; s1/2)$  in inverse kinematics and the astrophysical factor has been calculated down to zero energy. Our astrophysical factor  $S(0)$  is almost 50% larger than the NACRE compilation. It is the first accurate determination of the astrophysical factor for the neutron generator in AGB stars.

2. "Trojan Horse" is another powerful indirect method, which allows one to extract the astrophysical factors for direct and resonant nuclear reactions at astrophysically relevant energies. Using a few-body approach one can obtain a relationship between the measured  $3 \rightarrow 2$  cross section and the extracted binary reaction  $2 \rightarrow 2$  cross section. I will discuss the relationship between the half-off-the-energy-shell astrophysical factor determined from the Trojan Horse method (THM) and the on-shell astrophysical factor. I will address also the impact of the initial and final state interactions on the energy dependence of the astrophysical factor extracted from the Trojan Horse reaction. The main advantage of the THM is that this method allows one to determine the astrophysical factors between bare nuclei down to zero energy. By comparing the astrophysical factor determined from the THM with the direct one, one can extract the electron screening potential. Experimental kinematics for the THM will be discussed and the astrophysical factors for the rearrangement direct and resonant reactions determined using the Trojan Horse method will be presented.

## 18.10 Measurement of the stellar $(n, \gamma)$ cross section of $^{54}\text{Fe}$

COQUARD, Laurent<sup>1</sup>, DILLMANN, Iris<sup>1,2</sup>, WALLNER, Anton<sup>3</sup>, KÄPPELER, Franz<sup>1</sup>, and KUTSCHERA, Walter<sup>3</sup>

<sup>1</sup>Institut für Kernphysik, Forschungszentrum Karlsruhe, D-76021 Karlsruhe, Germany, <sup>2</sup>Departement Physik und Astronomie, Universität Basel, CH-4056 Basel, Switzerland, <sup>3</sup>Vienna Environmental Research Accelerator, Institut für Isotopenforschung und Kernphysik, Universität Wien, A-1090 Wien, Austria

The activation technique, a well established tool for measurements of stellar neutron capture cross sections, has been combined with accelerator mass spectrometry (AMS) for investigating the  $(n, \gamma)$  cross section of  $^{54}\text{Fe}$ . In this case, direct off-line counting of the produced activity is compromised by the long half-life (2.73 yr) and missing  $\gamma$ -ray transitions. Thus our measurement is based on the detection of  $^{55}\text{Fe}$  atoms directly via AMS, which has the advantage of being independent of both, uncertain half-lives and decay intensities. Two samples consisting of natural iron have been irradiated for 16 days and 10 days, respectively, at the Karlsruhe 3.7 MV Van-de-Graaff accelerator in a quasi-stellar neutron spectrum of  $kT = 25$  keV produced by the  $^7\text{Li}(p, n)^7\text{Be}$  reaction. The subsequent AMS measurements were performed at the Vienna Environmental Research Accelerator (VERA), which is based on a 3-MV pelletron and a negative ion sputter source. By selecting  $^{55}\text{Fe}$  (3+) ions it was demonstrated that VERA provides a high particle transmission in combination with a very low detection limit. The determination of the stellar neutron cross section via

the activation technique and AMS represents an important complement to previous time-of-flight measurements, since this independent approach implies different systematic uncertainties, much higher sensitivity, and includes the contribution from the direct capture channel as well.

### 18.11 First measurements of the total and partial stellar neutron cross sections to the *s*-process branching-point $^{79}\text{Se}$

DILLMANN, Iris<sup>1</sup>, RUGEL, Georg<sup>2</sup>, FAESTERMANN, Thomas<sup>2</sup>, HEIL, Michael<sup>3</sup>, KÄPPELER, Franz<sup>3</sup>, KNIE, Klaus<sup>2</sup>, KORSCHINEK, Gunther<sup>2</sup>, POUTIVTSEV, Michail<sup>2</sup>, and WALLNER, Anton<sup>4</sup>

<sup>1</sup>Institut für Kernphysik, Forschungszentrum Karlsruhe, D-76021 Karlsruhe, Germany and Departement Physik und Astronomie, Universität Basel, CH-4056 Basel, Switzerland, <sup>2</sup>Fakultät für Physik, TU München, D-85747 München, Germany, <sup>3</sup>Institut für Kernphysik, Forschungszentrum Karlsruhe, D-76021 Karlsruhe, <sup>4</sup>Vienna Environmental Research Accelerator, Institut für Isotopenforschung und Kernphysik, Universität Wien, A-1090 Wien, Austria

Although  $^{79}\text{Se}$  represents an important branching in the *s* process, the stellar neutron capture cross section to this isotope has not been measured yet and has to rely on predictions derived by the Hauser-Feshbach theory. Its terrestrial half-life of about 295000 yr is drastically reduced under stellar conditions by thermal population of the low-lying isomeric state at  $E(\gamma) = 96$  keV, allowing beta-decays to compete with neutron captures at temperatures above  $1.5 \cdot 10^8$  K. The strength of the resulting branching is reflected in the *s*-only isotopes  $^{80}\text{Kr}$  and  $^{82}\text{Kr}$ . Analysis of the local abundance pattern in the mass region  $A = 80 - 82$  yields the effective half-life of  $^{79}\text{Se}$  at the *s*-process site. Since the temperature dependence is well-known, the branching can also be interpreted as an *s*-process thermometer. We have measured the partial cross section to the 3.92 min isomeric state and the total capture cross section to the 295000 yr ground state by activation of natural Se samples (23.77%  $^{78}\text{Se}$ ) in the quasi-stellar neutron spectrum of the  $^7\text{Li}(p,n)^7\text{Be}$  source at the Karlsruhe 3.7 MV Van-de-Graaff accelerator. The cross section to the isomeric state has been determined in short activations via  $\gamma$  spectroscopy of the 96 keV transition. For the measurement of the total cross section a CdSe sample was irradiated for 13 days, and the number of  $^{79}\text{Se}$  atoms produced was counted via accelerator mass spectrometry (AMS) using the gas-filled analyzing magnet system (GAMS) at the Maier-Leibnitz-Laboratory of the Munich Universities. Our measurement yields a much lower total capture cross section than the recommended value of  $109 \pm 41$  mbarn from the Bao et al. compilation. The isomeric ratio decreases from 0.88 at  $kT = 0.025$  eV to 0.65 at  $kT = 25$  keV.

### 18.12 Present status of the KADoNiS database

DILLMANN, Iris<sup>1,2</sup>, PLAG, Ralf<sup>1</sup>, HEIL, Michael<sup>1,3</sup>, KÄPPELER, Franz<sup>1</sup>, THIELEMANN, Friedrich-Karl<sup>2</sup>, and RAUSCHER, Thomas<sup>2</sup>

<sup>1</sup>Institut für Kernphysik, Forschungszentrum Karlsruhe, D-76021 Karlsruhe, Germany, <sup>2</sup>Departement Physik und Astronomie, Universität Basel, CH-4056 Basel, Switzerland, <sup>3</sup>GSI Darmstadt, D-64291 Darmstadt, Germany

The “Karlsruhe Astrophysical Database of Nucleosynthesis in Stars” (KADoNiS) project is an online database for experimental cross sections relevant to the *s* process and *p* process. It is available under <http://nuclear-astrophysics.fzk.de/kadonis> and consists of two parts. Part 1 is an updated sequel to the well-known Bao et al. compilation, which is online since April 2005. Presented is the status of this update, including a list of unpublished measurements, and the extension to  $(n, p)$  and  $(n, \alpha)$  reactions as in the 1987 version of the Bao et al. compilation. The second part of KADoNiS is a *p*-process library, which includes all available experimental data from  $(p, \gamma)$ ,  $(p, n)$ ,  $(\alpha, \gamma)$ ,  $(\alpha, n)$ ,  $(\alpha, p)$ ,  $(\alpha, \alpha)$ ,  $(n, \alpha)$ , and  $(\gamma, n)$  reactions in or close to the respective Gamow window. Despite the great amount of reactions involved in this reaction network, experimental data is still scarce and up to now restricted to stable targets.

### 18.13 Light from the ashes: Explosion physics and nucleosynthesis from the X-ray spectra of type Ia supernova remnants

BADENES, Carlos<sup>1</sup>, BORKOWSKI, Kazimierz J.<sup>2</sup>, BRAVO, Eduardo<sup>3</sup>, and HUGHES, John P.<sup>1</sup>

<sup>1</sup>Department of Physics and Astronomy, Rutgers University, <sup>2</sup>Department of Physics, North Carolina State University, <sup>3</sup>Department of Physics and Nuclear Engineering, Universitat Politècnica de Catalunya

Despite the continuing efforts of the last decades, many important details concerning the explosion mechanism and nucleosynthetic yields of Type Ia supernovae (SNe) are still the subject of heated debate. We report the results of an ongoing effort to model the X-ray emission from young, ejecta-dominated Type Ia supernova remnants (SNRs) like Tycho and SN1006. We compare the excellent observations provided by XMM-Newton and Chandra for these objects to detailed theoretical models that include the hydrodynamic evolution of the SNR and a self-consistent calculation of the non-equilibrium ionization processes in the shocked plasma. In the case of the Tycho SNR, one particular explosion model (a delayed detonation) is capable of reproducing the fundamental properties of the X-ray emission from O, Si, S, Ar, Ca and Fe in the shocked SN ejecta. Other explosion mechanisms like pure deflagrations, pulsating delayed detonations or sub-Chandrasekhar explosions, can be ruled out with a high degree of confidence.

### 18.14 Lead abundance and the weak $r$ process in the metal-poor star K462 (M15)

HANNAWALD, Michael

Subaru Telescope, NAOJ

Former astrophysical results indicate the existence of (at least) two types of  $r$ - process. The evidence is based on a variety of observations in different fields. The strongest indication comes from the observation of heavy neutron-capture element abundances in very metal-poor halo stars. On the one hand, metallicity- scaled abundances of elements in the Pt peak down to Ba ( $Z = 56$ ) in all halo stars so far investigated are in remarkable agreement with the solar  $N_r$  pattern, while on the other hand the abundances of low- $Z$  neutron-capture elements ( $Z < 56$ ) are under- abundant comparing to solar. New observations of K462 ( $[\text{Fe}/\text{H}] = -2.2$ ) in the globular cluster M15, with  $R > 90000$  and  $S/N > 92$  near  $3500 \text{ \AA}$  to  $212$  near  $5200 \text{ \AA}$  will be presented, showing this expected pattern with the pronounced odd-even- $Z$  staggering of the low- $Z$  abundances. Taking the waiting-point approach of Kratz et al. to fit the  $N_{r,weak}$  pattern in K462, it could be investigated under which stellar conditions the light elements ( $40 < Z < 56$ ) have been synthesized. In total, 17 light elements below Ba and 16 elements beyond Ba could be detected, including Pb. Additionally, an upper limit for U was derived.

### 18.15 Excitation functions of $(p, n)$ reactions on $^{115}\text{Sn}$ , $^{116}\text{Sn}$ and $^{120}\text{Sn}$

SKAKUN, Yevgen<sup>1</sup> and RAUSCHER, Thomas<sup>2</sup>

<sup>1</sup>National Science Center "Kharkiv Institute of Physics and Technology", Kharkiv, Ukraine, <sup>2</sup>Departement für Physik und Astronomie, Universität Basel, Basel, Switzerland

Using an off-line  $\gamma$ -spectrometry technique  $(p, n)$  reaction cross sections of the tin isotopes with  $A=115, 116$  and  $120$ , the first of which is a  $p$ -process isotope, have been measured in the proton energy range between  $4.5$  and  $9.0$  MeV, corresponding to stellar temperatures  $T_9 > 3$ . Thin self-supporting foils of enriched tin isotopes were irradiated at the Kharkiv linear accelerator with proton beam intensities of  $10$  to  $50$  nA. The induced activities were measured with a calibrated Ge(Li)-detector. The cross sections for the production of isomeric states in  $^{116}\text{Sb}$  ( $J^m=8^-$ ,  $J^g=3^+$ ) and  $^{120}\text{Sb}$  ( $J^m=8^-$ ,  $J^g=1^+$ ) were determined separately. The total cross sections of the  $^{120}\text{Sn}(p, n)^{120}\text{Sb}$  reaction are compared with the results of other authors obtained with the neutron registration technique in this incident proton energy range and with the respective results for the astrophysical reaction  $^{119}\text{Sn}(p, \gamma)^{120}\text{Sb}$  [1]. Cross sections, astrophysical S-factors and reaction rates have also been calculated by means of the statistical model code NON-SMOKER [2]. In general, good agreement between theoretical predictions and experimental data was found. The sensitivity of the results on different theory parameters is studied.

[1] F.R. Chloupek *et al.*, Nucl. Phys. A652, 391 (1999)

- [2] T. Rauscher and F.-K. Thielemann, ADNDT 75, 1 (2001)

i

### 18.16 The production of germanium in asymptotic giant branch stars

KARAKAS, Amanda<sup>1</sup>, LUGARO, Maria<sup>2</sup>, and GALLINO, Roberto<sup>3</sup>

<sup>1</sup>McMaster University, <sup>2</sup>University of Utrecht, <sup>3</sup>Università di Torino

Recent observations of planetary nebulae by Sterling, Dinerstein & Bowers [1] have revealed enhancements in the rare element Germanium by factors of 3 to 10. Germanium is a light neutron-capture element that can be produced by the slow-neutron capture (*s*-process) in Asymptotic Giant Branch (AGB) stars. We compute a series of solar metallicity ( $Z = 0.012$ ) AGB models of 1.5, 3, and 5 solar masses that include Vassiliadis & Wood mass-loss rates, and follow the evolution from the main sequence to near the end of the thermally-pulsing AGB phase. Each model has third dredge-up (TDU) and the 5 solar mass model also experiences hot bottom burning at the base of the convective envelope. We include a partial mixing zone of constant mass at the deepest extent of each dredge-up episode. During the interpulse period this mixing zone will produce a  $^{13}\text{C}$  pocket in the top 1/10th of the He-rich intershell, releasing free neutrons, which can be captured by iron-seed nuclei. Using a post-processing code that includes 156 species, 1260 reaction rates, and time-dependent convective mixing, we follow the nucleosynthesis of all stable isotopes up to  $^{75}\text{As}$ , including the five stable Ge isotopes. We present the evolution of Ge as a function of time for each model, compare with results calculated by the code of Gallino et al. [2], and discuss the ability of these models to match the planetary nebulae observations.

- [1] N.C. Sterling, H.L. Dinerstein, and C.W. Bowers, ApJ 578, L55 (2002)

- [2] R. Gallino *et al.*, Ap. J. 497, 388 (1998)

### 18.17 *r*-Process nucleosynthesis in Alfvén wave-driven proto-neutron star winds

SUZUKI, Takeru<sup>1</sup>, NAGATAKI, Shigehiro<sup>2</sup>, and WANAJO, Shin-ya<sup>3</sup>

<sup>1</sup>Department of Physics, Kyoto University, <sup>2</sup>Yukawa Institute, Kyoto University, <sup>3</sup>Resceu, University of Toyko

We investigate possibilities of *r*-process nucleosynthesis in Alfvén wave-driven proto-neutron star (PNS) winds. Alfvén waves excited by surface motions of a PNS propagate outwardly, and they heat and accelerate the wind by their dissipation. Compared with the wind purely driven by the neutrino heating, a larger entropy per baryon and a shorter dynamical time scale are achieved, which favors the *r* process. Wind solutions adopting typical wave parameters show that a PNS with surface field strength,  $\geq 5 \times 10^{14}$  G, gives suitable wind properties for the *r* process. We further carry out nuclear network calculations for some of the wind solutions, focusing on differences of synthesized elements in the Alfvén wave-driven wind from those in the standard neutrino-driven wind. We also discuss different properties of trans-critical and sub-critical flows in the light of the *r* process and possibilities for detecting  $\gamma$ -rays from proto-magnetars.

### 18.18 Experimental determination of the $^{41}\text{Ca}(n, \alpha)^{38}\text{Ar}$ reaction cross section as a function of neutron energy

DE SMET, Liesbeth<sup>1</sup>, WAGEMANS, Cyriel<sup>1</sup>, HEYSE, Jan<sup>2</sup>

<sup>1</sup>University of Gent, <sup>2</sup>IRMM Geel, Belgium

$^{41}\text{Ca}$  is one of the rare nuclei for which not  $(n, \gamma)$  but  $(n, \alpha)$  is the dominant reaction process. According to theoretical calculations, the Maxwellian-averaged  $(n, \alpha)$  cross section at a temperature of  $kT = 20$  keV e.g., is roughly 20 times larger than the corresponding  $(n, \gamma)$  cross section. Such a situation leads to branchings in nucleosynthesis networks, which can strongly influence the reaction flow. In the case of  $^{41}\text{Ca}$ , the nucleosynthesis path deviates from the formation of heavier Ca-isotopes to the Ar synthesis path. So the  $^{41}\text{Ca}(n, \alpha)^{38}\text{Ar}$  reaction cross section directly influences the production of Ca and Ar isotopes, and indirectly the abundance of the rare isotope  $^{36}\text{S}$  [via the reaction  $^{39}\text{Ar}(n, \alpha)^{36}\text{S}$ ]. In this contribution, a new experimental determination of the

$^{41}\text{Ca}(n, \alpha)^{38}\text{Ar}$  reaction cross section at the GELINA neutron facility in Geel (Belgium) will be reported. A dozen of resonances has been observed and for most of them, resonance parameters could be determined. Besides  $(n, \alpha_0)$  transitions, also  $(n, \alpha_1)$  and  $(n, \alpha\gamma)$  transitions have been identified. Also the Maxwellian-averaged  $(n, \gamma)$  cross section has been calculated as a function of stellar temperature, which will improve the accuracy of reaction network calculations.

### 18.19 Towards a direct measurement of the $^{15}\text{O}(\alpha, \gamma)^{19}\text{Ne}$ cross section: A first approach using the $^{15}\text{O}+\alpha$ elastic scattering

ANGULO, Carmen<sup>1</sup>, CASAREJOS, Enrique<sup>1</sup>, COUDER, Manoël<sup>1</sup>, LELEUX, Pierre<sup>1</sup>, VANDERBIST, Frank<sup>1</sup>, DESCOUVEMONT, Pierre<sup>2</sup>, ALIOTTA, Marialuisa<sup>3</sup>, DAVINSON, Thomas<sup>3</sup>, LIU, Zhong<sup>3</sup>, and WOODS, Phillip J.<sup>3</sup>

<sup>1</sup>Université catholique de Louvain, <sup>2</sup>Université Libre de Bruxelles, <sup>3</sup>University of Edinburgh

The  $^{15}\text{O}(\alpha, \gamma)^{19}\text{Ne}$  is of interest in explosive burning occurring in X-ray bursts, as this reaction could be a break-out from the hot CNO cycles to the  $rp$ - process. The  $^{15}\text{O}(\alpha, \gamma)^{19}\text{Ne}$  reaction proceeds through resonances above and close to the  $^{15}\text{O}+\alpha$  threshold, which is situated at 3.529 MeV in  $^{19}\text{Ne}$ ; the strength of these resonances is governed by their  $\alpha$ -width. A conclusion from recent experiments [1-3] is that a direct measurement of the  $^{15}\text{O}(\alpha, \gamma)^{19}\text{Ne}$  cross section in the region of astrophysical interest is currently impossible:  $^{15}\text{O}$  beams of intensity larger than  $10^{11}$  pps on target would be required. This high beam current is one of the main challenges to be tackled in the coming years. However,  $^{15}\text{O}$  beams of lower intensity have been developed [4] and can be used to investigate levels at higher excitation energies to test both, the experimental method and the data-analysis technique. Here we present a measurement of the  $\alpha$ - width of a state at 1.82 MeV above threshold. We have used the elastic resonant method in inverse kinematics using the  $^{15}\text{O}$  beam available at Louvain-la-Neuve, with an intensity of about  $10^7$  pps, and a He gas target limited by Mylar windows [5]. The use of a He gas target leads to some experimental problems that require new data analysis methods. The experimental setup and the data analysis will be presented. The results will be discussed and compared with previous estimates.

[1] B. Davids *et al.*, Phys. Rev. C67 (2003)012801(R)

[2] D.W. Visser *et al.*, Phys. Rev. C69 (2004) 048801

[3] P.V. Magnus *et al.*, Nucl. Phys. A506 (1990) 332

[4] M. Gaelens *et al.*, 15th Int. Conf. on *Applications of Accelerators in Research and Industry*, edited by J.L. Duggan and I.L. Morgan, AIP Conf. Proc. 475 (1999) p305

[5] F. Vanderbist *et al.*, Eur. Phys. J. A (in press)

### 18.20 Gravitational wave emission during the transition from rapidly differentially rotating neutron stars to strange stars

YASUTAKE, Nobutoshi<sup>1</sup>, HASHIMOTO, Masa-aki<sup>1</sup>, KOTAKE, Kei<sup>2</sup>, and YAMADA, Shoichi<sup>2</sup>

<sup>1</sup>Department of Physics, Kyushu University, Japan, <sup>2</sup>Science of Engineering, Waseda University, Japan

We present a scenario of formation of strange stars from rapidly differentially rotating neutron stars via QCD phase transition. Enough energy of  $10^{53}$  ergs could be released that may lead to  $\gamma$ -ray bursts. The liberated energy would become a new energy source for a delayed supernova explosion. Linked with this scenario, we investigate the waveforms of gravitational wave derived from the quadrupole formula. Thus our scenario suggests that the supernova associated with  $\gamma$ -ray bursts could become candidates of targets of future observation of gravitational waves.

## 18.21 Can supernova neutrino nucleosynthesis constrain neutrino oscillation parameters?

YOSHIDA, Takashi<sup>1</sup>, KAJINO, Toshitaka<sup>2</sup>, YOKOMAKURA, Hidekazu<sup>3</sup>, KIMURA, Keiichi<sup>3</sup>, TAKAMURA, Akira<sup>4</sup>, and HARTMANN, Dieter<sup>5</sup>

<sup>1</sup>Astronomical Institute, Graduate School of Science, Tohoku University, <sup>2</sup>National Astronomical Observatory, <sup>3</sup>Department of Physics, Graduate School of Science, Nagoya University, <sup>4</sup>Department of Mathematics, Toyota National College of Technology, <sup>5</sup>Department of Physics and Astronomy, Clemson University

Recent neutrino experiments have confirmed neutrino oscillations and determined most of the neutrino oscillation parameters. However, only an upper limit has been obtained for the mixing angle  $\theta_{13}$  and the mass hierarchy has not yet been clarified. During supernova explosions, a huge neutrino fluence emerges from the cooling proto-neutron star. Theoretical studies of neutrino oscillations show that neutrinos change flavor in the stellar material surrounding the proto-neutron star, which results in modified neutrino energy spectra. The spectral changes in turn affect the neutrino-induced nucleosynthesis. We evaluate the yields of  ${}^7\text{Li}$  and  ${}^{11}\text{B}$  in a supernova taking into account neutrino oscillations by assuming large mixing angle solutions. We investigate the dependence of the yields on the mixing angle  $\theta_{13}$  and the mass hierarchy. In the case of an adiabatic resonance of 13-mixing and a normal mass hierarchy, the yields of  ${}^7\text{Li}$  and  ${}^{11}\text{B}$  are larger than those without oscillations by factors of 1.9 and 1.3, respectively. Other parameter cases yield smaller increases of these yields. We discuss the implied potential constraints of the mixing angle  $\theta_{13}$  and the mass hierarchy from the viewpoint of supernova nucleosynthesis.

## 18.22 *r*-Process nucleosynthesis in a collapsar

NAGATAKI, Shigehiro<sup>1</sup> and WANAJO, Shinya<sup>2</sup>

<sup>1</sup>Yukawa Institute for Theoretical Physics, Kyoto University, <sup>2</sup>The University of Tokyo

Recent progress of numerical simulations on *r*-process nucleosynthesis in a collapsar is presented. The collapsar model of MacFadyen and Woosley [1] with a central black hole of  $3.762 M_{\odot}$  is used as initial condition. Thermal energy is injected around the innermost region, which makes an energetic jet that propagates along the rotational axis. We calculate explosive nucleosynthesis using the post-processing method with a reaction network that contains over 4000 nuclei. It is shown that *r*-process elements are produced in the GRB jets. We also compare the chemical composition in the GRB jets with solar system abundances and discuss whether *r*-process elements in extremely metal poor stars can be explained by GRBs.

[1] A.I. MacFadyen & S.E. Woosley, ApJ 524, 262 (1999)

## 19 Poster session, 27 June

### 19.1 Non-extensive statistical effects on the nuclear equation of state and on nuclear astrophysical problems

LAVAGNO, Andrea  
Politecnico di Torino

Following the basic prescriptions of the Tsallis' non-extensive thermodynamics, we study the relativistic nuclear equation of state in the hadronic and in the quark plasma phase. We show that small deviations from the standard extensive statistics, due to long-range and memory interactions between particles inside an astrophysical plasma, imply remarkable effects for the shape of the equation of state and, as a consequence, for many high-energy astrophysical problems such as the evolution of a newly-born proton-neutron star after a supernova explosion.

## 19.2 Present-day carbon abundances from early-type stars

NIEVA, Maria Fernanda<sup>1,2</sup> and PRZYBILLA, Norbert<sup>1</sup>

<sup>1</sup>Dr. Remeis Sternwarte Bamberg, Sternwartstr. 7, D-96049 Bamberg, Germany, <sup>2</sup>Observatorio Nacional, Rua General Jose Cristino 77, CEP 20921-400, Rio de Janeiro, Brazil

Carbon is one of the most abundant metals in the universe because of its synthesis in the fundamental triple alpha reaction. The knowledge of carbon abundances in different environments is a key ingredient to our understanding of stellar and galacto-chemical evolution. Studies of luminous OB-type stars allow us to address both topics even in galaxies beyond our own. Unfortunately the history of carbon abundance determinations from these objects in the last three decades is one of limited success. Analyses of the strong and weak line spectra of C II as well as C III tend to be largely discrepant. We present results of quantitative spectral analyses based on a sophisticated model atom for non-LTE line formation calculations of C II-IV. As a first application, carbon abundances in a sample of B-type dwarfs and giants in nearby associations and in the field are determined. Consistency is finally achieved for all measurable lines (up to 40) from the three ionization stages. This includes in particular the notorious C II 4267 and 6578/6582 Å features, which are highly important for abundance determinations of fast-rotating and extragalactic objects. The long-standing problem of carbon line formation can now be regarded as solved. A highly homogeneous and slightly sub-solar present-day carbon abundance from young stars in the solar vicinity of  $\log C/H+12 = 8.29 \pm 0.03$  is derived.

## 19.3 Metastability of electron-nuclear astrophysical plasmas

GERVINO, Gianpiero<sup>1</sup>, LAVAGNO, Andrea<sup>2</sup>, and QUARATI, Piero<sup>2</sup>

<sup>1</sup>Università di Torino, <sup>2</sup>Politecnico di Torino

Physical motivations indicating that the electron-nuclear plasma of a stellar core (like the solar core) is not in a global thermodynamical equilibrium but satisfies the conditions of a metastable state are described. Momentum distributions of electrons and ions are power law distributions, rather than the Maxwellian distribution of a global equilibrium state. Some open astrophysical problems are discussed as signals of deviations from global equilibrium description.

## 19.4 Neutron capture studies with a short flight path

WALTER, Stephan<sup>1</sup>, HEIL, Michael<sup>1</sup>, KÄPPELER, Franz<sup>1</sup>, PLAG, Ralf<sup>1</sup>, and REIFARTH, René<sup>2</sup>

<sup>1</sup>Forschungszentrum Karlsruhe, 76021 Karlsruhe, Germany, <sup>2</sup>Los Alamos National Laboratory, Los Alamos, New Mexico, USA

The time of flight method (TOF) is an important tool for the experimental determination of neutron capture cross sections. These data are important for *s*-process nucleosynthesis in general, and for analyses of branchings in the *s*-process reaction path in particular, which yield information on the physical conditions during stellar He burning. In current measurements sample masses of at least several milligrams are required to compensate limitations in the available neutron fluxes. For most of the relevant unstable branch point nuclei, this constraint leads to unacceptable backgrounds due to the decay activity of the sample. A possible solution of this difficulty has been proposed by the NCAP project at the University of Frankfurt. A similar step in this direction is reported here, which aims at enhancing the sensitivity of the Karlsruhe TOF array by reducing the neutron flight path to only a few centimetres. By this approach sample masses in the microgram regime can be used, but the increase in neutron flux is paid with a higher background from the prompt  $\gamma$  flash related to neutron production. Test measurements for background reduction and the prospects for experiments on stable isotopes as well as on a <sup>63</sup>Ni sample ( $t_{1/2} = 100$  yr) are reported.

## 19.5 Quantitative spectroscopy of Deneb

SCHILLER, Florian and PRZYBILLA, Norbert

Dr. Remeis-Observatory Bamberg

We present results from a comprehensive model atmosphere analysis of the A-type supergiant Deneb. Stellar parameters and elemental abundances in this highly luminous object are derived

from non-LTE spectrum synthesis with unprecedented accuracy. Practically all inconsistencies reported in earlier studies are resolved. A self-consistent view of Deneb is thus obtained, allowing us to discuss its evolutionary state in detail by comparison with the most recent generation of evolution models for massive stars. We determined 8525 K for the effective temperature and 1.1 for  $\log g$  reducing the uncertainties to 75 K and 0.05 dex at the 1 sigma-level. The derived CNO abundances indicate mixing with nuclear processed matter. A high N/C ratio of 4.5 suggests a late O-type main sequence progenitor rapidly rotating with more than 300 km/s. Since the spectroscopic mass of 17 solar masses is lower than the derived zero-age main sequence mass of 22 solar masses, significant mass loss must have occurred through stellar winds, strengthened by the effect of centrifugal forces. We have used Deneb as a benchmark for spectroscopic analysis techniques of the whole class of luminous BA-type supergiants. The consistency of our results indicates that BA-type supergiants can now be relied on as important tools for extragalactic stellar astronomy.

### 19.6 New Experiments on neutron rich $r$ -process Ge-Br isotopes at the NSCL/MSU

QUINN, Matthew<sup>1</sup>, WOEHR, Andreas<sup>1</sup>, MANTICA, Paul<sup>2</sup>, PEREIRA-CONCA, Jorge<sup>2</sup>, SCHATZ, Hendrik<sup>2</sup>, HENNRICH, Stefan<sup>3</sup>, KRATZ, Karl-Ludwig<sup>3</sup>, and APRAHAMIAN, Ani<sup>1</sup>

<sup>1</sup>University of Notre Dame, <sup>2</sup>NSCL/MSU, <sup>3</sup>Universität Mainz

Recent measurements at the NSCL/MSU have attempted to determine new half-lives and  $\beta$ -delayed neutron emission probabilities for several isotopes in the neutron rich Ge-Br region. These isotopes are in the region just after the N=50 bottle neck in the classical  $r$  process. These nuclei may be particularly relevant to the high entropy neutrino-wind  $r$  process. Nuclear properties such as  $\beta$  decay half-lives and beta-delayed neutron emission probabilities are critical inputs for  $r$  process models. Isotopes were produced by fragmentation of a 120 MeV/u <sup>136</sup>Xe beam on a Be target at the A1900 fragment separator. Nuclei of interest were implanted into a 40 x 40 segmented double-sided silicon detector, which is part of the Beta Counting System. Surrounding the Beta Counting System were 60 proportional neutron counters seated in a polyethylene block. Setup and preliminary results will be presented.

### 19.7 CNO production in the first generation stars

EKSTRÖM, Sylvia, MEYNET, Georges, and MAEDER, André

Geneva Observatory

Big Bang nucleosynthesis produces only light elements and the very first generation of stars are thus formed from metal-free clouds. They start the production of heavy elements during their life, and enrich the interstellar medium through their explosive death. Stellar evolution models show that the treatment of rotation has important effects on the evolution of those metal-free stars: for example, rotating models produce up to five orders of magnitude more primary nitrogen than non rotating models, due to internal mixing. This will have an impact in the composition of the second generation stars, some of which may now be observed in the Galactic halo. In the case Population III stars were very massive and would end up as direct black holes, rotation again has an interesting effect of enhancing mass loss through centrifugal forces and surface enrichment. CNO composition patterns observed in ultra metal-poor halo stars may be explained by a “wind only” contribution.

### 19.8 Heavy element nucleosynthesis in the MHD jet explosions of core-collapse supernovae

NISHIMURA, Nobuya<sup>1</sup>, HASHIMOTO, Masa-aki<sup>1</sup>, FUJIMOTO, Shinichiro<sup>2</sup>, KOTAKE, Kei<sup>3</sup>, and YAMADA, Shoichi<sup>3</sup>

<sup>1</sup>Kyushu University, <sup>2</sup>Kumamoto National College of Technology, <sup>3</sup>Waseda University

Massive stars with masses larger than 10 M<sub>⊙</sub> evolve until the Fe-core is formed. Since the nuclear reactions in the Fe-core do not proceed further, the core begins to collapse, which leads to the catastrophic explosion. The nucleosynthesis during the evolutions and subsequent explosions is

responsible for the heavy element enrichment in our galaxy. We have investigated heavy element nucleosynthesis during the magneto- hydrodynamical (MHD) explosion of supernova in a massive star. We have consistently calculated all stages of the collapse of the Fe core, the core bounce, and the shock propagation. When the shock wave propagates into the oxygen-neon layers, the  $p$ -process nucleosynthesis is expected to occur. Until now, the  $p$  process has been studied with spherical explosion models [1], where significant deficiencies in some  $p$  elements compared to solar have been found. We present nonspherical effects on the production of  $p$  elements using a pure MHD explosion model.

[1] M. Rayet, M. Arnould, M. Hashimoto, N. Prantzos, & K. Nomoto, *A&A*, 298, 517 (1995)

## 19.9 Photodisintegration of $^{80}\text{Se}$ , $^{94}\text{Zr}$ , and $^{108}\text{Pd}$ as a probe of neutron capture for radioactive nuclei

UTSUNOMIYA, Hiroaki  
Konan University

Photoneutron cross sections were measured for  $^{80}\text{Se}$ ,  $^{94}\text{Zr}$ , and  $^{108}\text{Pd}$  near neutron threshold with laser Compton-backscattered  $\gamma$ -ray beams at AIST. Neutron capture cross sections are evaluated for these three nuclei with the photoreaction data as constraints on the statistical model calculation. Emphasis is placed on the  $s$ -process branching at  $^{79}\text{Se}$ , which is sensitive to stellar temperature.

## 19.10 Observational constraints on the cosmology with a decaying cosmological term

NAKAMURA, Riou<sup>1</sup>, HASHIMOTO, Masa-aki<sup>1</sup>, and ICHIKI, Kiyotomo<sup>2</sup>

<sup>1</sup>Department of Physics, Graduate School of Science, Kyushu University, <sup>2</sup>National Astronomical Observatory of Japan

Recent observations suggest the existence of the cosmological term in the universe. On the other hand, any theories have been proposed to solve the cosmological constant problem. We investigate the evolution of the universe with a decaying cosmological term. In this model, while the cosmological term increases at the early universe, the radiation energy density is lower compared to the model with the cosmological "constant". We find that the effects of the decaying cosmological term on the expansion rate at the redshift  $z < 2$  is negligible. However, the decrease in the radiation density affects the thermal history of the universe; e.g. the photon decoupling occurs at higher  $z$ . We present furthermore the effects of the decaying cosmological term on the anisotropy of the cosmic microwave background.

## 19.11 The $s$ -process branching at $^{186}\text{Re}$ revised

MOHR, Peter<sup>1</sup>, GORIELY, Stephane<sup>2</sup>, SHIZUMA, Toshiyuki<sup>3</sup>, UTSUNOMIYA, Hiroaki<sup>4</sup>, and HAYAKAWA, Takehito<sup>3</sup>

<sup>1</sup>Strahlentherapie, Diakoniekrankenhaus Schwäbisch Hall, <sup>2</sup>Institut d'Astronomie et d'Astrophysique, Université Libre de Bruxelles, <sup>3</sup>Advanced Photon Center, JAEA, <sup>4</sup>Department of Physics, Konan University

The  $s$ -process branching at  $^{186}\text{Re}$  has been studied recently in various experiments [1,2,3]. Photodisintegration cross sections have been measured using monochromatic photons and direct neutron detection [1] and bremsstrahlung and photoactivation [2], and statistical model calculations were used to derive the inverse neutron capture cross section of the unstable nucleus  $^{186}\text{Re}$  in [1,2]. Reliability and limitations of this method are discussed. The  $8^+$  isomer at 149 keV in  $^{186}\text{Re}$  may have noticeable influence on the analysis of  $^{187}\text{Re}(\gamma, n)^{186}\text{Re}$  photoactivation data; this was not taken into account in [1]. Additionally, the role of this isomer in the neutron capture chain  $^{185}\text{Re}(n, \gamma)^{186}\text{Re}^m(n, \gamma)^{187}\text{Re}$  was analyzed in [3]. A recommendation for the Maxwellian-averaged capture cross section of  $^{186}\text{Re}$  is given and compared to recent compilations [4,5]. Within the given uncertainties the  $s$ -process branching at  $^{186}\text{Re}$  remains small.

[1] T. Shizuma et al., *Phys. Rev. C* 72, 025808 (2005)

[2] S. Müller et al., *Phys. Rev. C*, in press; arXiv:astro-ph/0512603

[3] T. Hayakawa et al., *Astroph. J.* 628, 533 (2005)

[4] Z. Y. Bao et al., *At. Data Nucl. Data Tables* 76, 70 (2000)

[5] KADoNiS, <http://nuclear-astrophysics.fzk.de/kadonis/>

### 19.12 Measurement of the stellar $(n, \gamma)$ cross section of $^{182}\text{Hf}$

VOCKENHUBER, C.<sup>1</sup>, DILLMANN, I.<sup>2</sup>, HEIL, M.<sup>2</sup>, KÄPPELER, F.<sup>2</sup>, WINCKLER, N.<sup>2</sup>, KUTSCHERA, W.<sup>3</sup>, WALLNER, A.<sup>3</sup>, BICHLER, M.<sup>4</sup>, DABABNEH, S.<sup>5</sup>, GALLINO, R.<sup>6</sup>, and BISTERZO, S.<sup>2,7</sup>  
<sup>1</sup>TRIUMF, Vancouver, BC, Canada, <sup>2</sup>Institut für Kernphysik, Forschungszentrum Karlsruhe, Karlsruhe, Germany, <sup>3</sup>VERA, Institut für Isotopenforschung und Kernphysik, Universität Wien, Wien, Austria  
<sup>4</sup>Atominstytut der Österreichischen Universitäten, Wien, Austria, <sup>5</sup>Faculty of Applied Sciences, Al-Balqa Applied University, Salt, Jordan, <sup>6</sup>Dipartimento di Fisica Generale, Università di Torino and Sezione INFN di Torino, Torino, Italy and Centre for Stellar and Planetary Astrophysics, Monash University, Victoria, Australia, <sup>7</sup>Dipartimento di Fisica Generale, Università di Torino, Torino, Italy

The stellar neutron capture cross section of the radioactive isotope  $^{182}\text{Hf}$  with a half-life of  $(8.9 \pm 0.1) 10^6$  years [1] has been measured for the first time at  $kT = 25$  keV by means of the activation technique.  $^{182}\text{Hf}$  is particularly interesting for heavy element nucleosynthesis since its stellar production originates from the  $s$  process in AGB stars as well as from the  $r$  process in supernovae or neutron star mergers. High abundances of  $^{182}\text{Hf}$ , which could be inferred from  $^{182}\text{W}$  isotopic anomalies in meteorites, and recently in lunar material [2], are intimately linked to the quest for the formation of the early solar system. In this context, the  $^{182}\text{Hf}(n, \gamma)^{183}\text{Hf}$  reaction determines the  $s$ -process abundance of  $^{182}\text{Hf}$ . The  $(n, \gamma)$  cross section was measured with a  $^{182}\text{Hf}$  sample produced by irradiation of Hf in a high flux reactor more than 30 years ago. The activation measurement was carried out at the Karlsruhe Van de Graaff accelerator using the  $^7\text{Li}(p, n)^7\text{Be}$  reaction for simulating a Maxwellian neutron spectrum corresponding to a thermal energy of  $kT = 25$  keV. In addition, the thermal cross section of  $^{182}\text{Hf}$  was measured at the TRIGA Mark-II reactor of the Atominstytut der Österreichischen Universitäten in Vienna, Austria. The high activity obtained in the reactor irradiation allowed us to improve the decay parameters of  $^{183}\text{Hf}$ , which are required in the analysis of the activations. The results are compared with theoretical predictions, and the astrophysical implications will be discussed.

[1] C. Vockenhuber *et al.*, *Phys. Rev. Lett.* 93 (2004) 172501

[2] T. Kleine *et al.*, *Science* 310 (2005) 1671

### 19.13 Light element production in the circumstellar matter of type Ic supernovae at low metallicity

NAKAMURA, Ko<sup>1</sup>, INOUE, Susumu<sup>2</sup>, WANAJO, Shinya<sup>1</sup>, and SHIGEYAMA, Toshikazu<sup>1</sup>

<sup>1</sup>University of Tokyo, <sup>2</sup>National Astronomical Observatory of Japan

We investigate energetic type Ic supernovae as production sites for  $^6\text{Li}$  and Be in the early stages of the Milky Way. Recent observations have revealed that some very metal-poor stars with  $[\text{Fe}/\text{H}] < -2.5$  possess unexpectedly high abundances of  $^6\text{Li}$ . Some also exhibit enhanced abundances of Be as well as N. From a theoretical point of view, recent studies of the evolution of metal-poor massive stars show that rotation-induced mixing can enrich the outer H and He layers with C, N, and O (CNO) elements, particularly N, and at the same time cause intense mass loss of these layers. Here we consider energetic supernova explosions occurring after the progenitor star has lost all but a small fraction of the He layer. The fastest portion of the supernova ejecta can interact directly with the circumstellar matter (CSM), both composed of He and CNO, and induce light element production through spallation and He-He fusion reactions. We calculate the resulting  $^6\text{Li}/\text{O}$  and  $^9\text{Be}/\text{O}$  ratios in the ejecta+CSM material out of which the very metal-poor stars may form, and find that they are consistent with the observed values if the mass of the He layer remaining on the pre-explosion core is  $0.01 - 0.1 M_{\odot}$ , and the mass fraction of N mixed in the He layer is about 0.01. Further observations of  $^6\text{Li}$ , Be, and N at low metallicity should provide critical tests of this production scenario.

### 19.14 Exotic cooling of neutron stars with different surface compositions

NODA, Tsuneo<sup>1</sup>, HASHIMOTO, Masa-aki<sup>1</sup>, and FUJIMOTO, Masayuki<sup>2</sup>

<sup>1</sup>Department of Physics, Graduate School of Science, Kyushu University, <sup>2</sup>Department of Physics, Faculty of Science, Hokkaido University

The thermal evolution of isolated neutron stars depends on neutrino emission process, equation of states of nuclear matter, and surface composition. Focusing on the neutrino emission process, we can classify in two groups. The first one is the "standard cooling model", which includes modified URCA process and bremsstrahlung process; these processes are believed to operate inside neutron stars. The second group includes exotic processes at high density or high temperature, such as pion condensation or quark beta decay, which is named as "exotic cooling model". Since exotic models accompanies high neutrino emission rates, exotic neutron stars cool much faster than standard ones. We investigate the thermal evolution of isolated neutron stars, using standard and exotic cooling models, and some kinds of surface composition. We employ also nucleon superfluidity models, and we adopt a critical temperature as a density-independent parameter. We find that there are parameter regions, which can be consistent with the observational results.

### 19.15 Phase-transition phenomenology of frustrated nuclear matter in compact stars

NAPOLITANI, Paolo<sup>1</sup>, CHOMAZ, Philippe<sup>1</sup>, GULMINELLI, Francesca<sup>2</sup>, and HASNAOUI, Karim<sup>1</sup>

<sup>1</sup>Ganil - Caen, <sup>2</sup>LPCC - Caen

The aspect, which distinguishes nuclear matter in compact stars with respect to the physics of nuclei, is the form of the Coulomb interaction and, in particular, the presence of electrons and protons in equal proportions. The charge, which is neutral at macroscopic scale due to the presence of opposite charges, fluctuates at microscopic scale, with the consequence of inducing Coulomb-frustration effects, when the density drops below saturation. Such effects correspond to the absence of a state minimizing nuclear and Coulomb interactions simultaneously, as we find it in other more common physical systems, from liquid crystals to protein folding. Frustration is expected to force the appearing of inhomogeneous phases which, at the low temperatures of neutron stars, froze into crystalline structures, called 'pasta' phases. Parallel to the study of cold stellar matter, the understanding of the physics of the hot outer shell of proto-neutron stars is of fundamental importance: the related equation of state as a function of the temperature would give constraints on the description of fundamental phenomena like the opacity to neutrino emission and the cooling process. By constructing an Ising analogue to compact-star matter, we investigated the evolution to high temperature of the frustrated phase transition. In contrast with the physics of nuclei, we found that the introduction of a Coulomb field preserves and even expands the interval of temperatures, where inhomogeneous phases are formed. In the same context, we searched for manifestations of a critical temperature. The phase-transition phenomenology of uncharged nuclear matter is well known and belongs to a class of systems having the same liquid-gas-type thermodynamics; it is related to the divergence of the correlation length at a critical temperature: this means that, at this temperature, the system becomes completely black to any incoming wave. This phenomenon has been searched for in the physics of neutrino transport: at a critical temperature, neutrinos would be completely trapped in the star outer shell with relevant consequences on the conflagration dynamics of the supernova. This scenario is, on the contrary, remarkably different when the Coulomb field is taken into account. The region of phase coexistence does no more end upon a critical point and no critical effects can be expected: stellar matter stays therefore grey at the passage of neutrinos at all temperatures. Formally, nuclear matter in compact stars is no more compatible with the phenomenology of the liquid-gas phase transition. The consequence of this finding is to especially emphasize the need of knowing effective interactions in detail.

### 19.16 Dielectronic recombination rates in astrophysical plasmas

QUARATI, Piero and BACHARI, Fatima  
 Politecnico di Torino

Dielectronic recombination (DR) is the main process in hot and dilute astrophysical plasmas. It is a basic ingredient for the understanding of the dynamics of solar corona and nuclear fusion plasmas and in plasma modeling codes employed for analysis of spectra from astrophysical observations. DR rate coefficients have been measured at heavy-ion storage rings for several ions. Astrophysical observation of X-ray sources are possible with X-ray satellites and spectral lines have been measured in electron beam trap experiments. Plasma conditions in experimental measurements and astrophysical observations may be very different. Nevertheless signatures of departure from Maxwellian distributions of particle in plasmas are present in many different experimental observations and are required to fit the data, both in laboratory and in space. In this work we discuss how recently derived non-extensive distribution functions, differing from Maxwellian, can affect, especially at low temperatures, the expression of the DR rates commonly used up to now and the consequences on the interpretation of the X-ray spectra.

### 19.17 Universality of the $p$ process

HAYAKAWA, Takehito<sup>1</sup>, IWAMOTO, Nobuyuki<sup>2</sup>, KAJINO, Taka<sup>3</sup>, SHIZUMA, Toshiyuki<sup>2</sup>, UMEDA, Hideyuki<sup>4</sup>, and NOMOTO, Ken'ichi<sup>4</sup>

<sup>1</sup>Japan Atomic Energy Agency, Quantum Beam Science Directorate, <sup>2</sup>Japan Atomic Energy Agency, <sup>3</sup>National Astronomical Observatory, <sup>4</sup>University of Tokyo

We investigate the principle of "the universality of the  $p$  process" using core-collapse supernova explosion models. We found two crucial empirical scaling laws in the solar system abundances, which are the evidence that the most probable origin of the  $p$  nuclei is the  $p$  process. There are 22  $p$  nuclei associated with almost pure  $s$  nuclei that have two more neutrons than the  $p$  nuclei. We found the first scaling law that the abundance ratios of  $N(s)/N(p)$ , where  $N$  are the isotopic abundances, are almost constant in a wide region. We also proposed a novel concept of "the universality of the  $p$  process" that the  $N(s)/N(p)$  ratios produced by individual  $p$  processes are constant in a wide region. However, its reason has remained as an open problem. We calculate the  $N(s)/N(p)$  ratios in different astrophysical conditions of progenitor masses, metallicities, and explosion energies. The calculated  $N(s)/N(p)$  ratios are almost constant, independent of the conditions. We conclude that the  $p$ -process episodes with various astrophysical conditions occur but the ratios are independent of the conditions. Three mechanisms contribute the manifestation of the universality. They are a weak  $s$  process before SNe, the ratio independence of nuclear reactions, the shift of  $p$ -process layers. We also find that a large deviation of the  $N(s)/N(p)$  ratio in the solar abundances is a piece of evidence that the weak  $s$  process in massive stars actually happen before SNe. These provide a new insight to the  $p$  process.

### 19.18 Cosmic clock and thermometer for neutrino process

HAYAKAWA, Takehito<sup>1</sup>, SHIZUMA, Toshiyuki<sup>2</sup>, KAJINO, Taka<sup>3</sup>, OGAWA, Kengo<sup>4</sup>, and NAKADA, Hitoshi<sup>4</sup>

<sup>1</sup>Japan Atomic Energy Agency, Quantum Beam Science Directorate, <sup>2</sup>Japan Atomic Energy Agency, <sup>3</sup>National Astronomical Observatory, <sup>4</sup>University of Chiba

A nucleus  $^{138}\text{La}$  is considered to be synthesized mainly by neutrino process in supernova explosions. We here propose a  $^{138}\text{La}$ - $^{138}\text{Ce}$ - $^{136}\text{Ce}$  system as a new nuclear cosmic clock for the neutrino process in supernova explosions. The nucleus  $^{138}\text{La}$  decays to  $^{138}\text{Ce}$  and  $^{138}\text{Ba}$  with a half-life of 105 Gyr. This clock can be applied to a sample affected strongly by a single nucleosynthesis episode such as presolar grains in primitive meteorites. The daughter nucleus  $^{138}\text{Ce}$  is synthesized by the  $p$  process in SNe. Since the manner of the mixing of the  $p$  and neutrino process nuclei in individual grains should be different, the theoretical estimation of the initial abundance is difficult. In our system, the initial abundance of  $^{138}\text{Ce}$  can be calculated by the empirical scaling law between the two  $p$  nuclei, which was found in the solar system. We find that the nuclear structure of  $^{138}\text{La}$  strongly affects to the performance of  $^{138}\text{La}$ , which has not been studied experimentally well. If a beta

unstable isomer in  $^{138}\text{La}$  exists, it is crucial for the neutrino process origin of  $^{138}\text{La}$  because the synthesized  $^{138}\text{La}$  should be also destroyed via the beta decay of the isomer and the production rate may drastically decrease. In such a case, our proposed clock cannot work well but we propose this system as a new cosmic thermometer to measure the temperature of nucleosynthesis site of  $^{138}\text{La}$ . In this case, the initial abundance can also be calculated by the scaling law. Therefore, the nuclear structure is a key to understand the neutrino process and the origin of  $^{138}\text{La}$ . To investigate the possibility of the isomer, we calculate the nuclear structure of  $^{138}\text{La}$  in a shell model. We reproduce the nuclear structures of  $^{140}\text{Pr}$ , which is an isotone of  $^{138}\text{La}$ , and known excited states in  $^{138}\text{La}$ . Our proposals and calculations provide a new vision to the study of the neutrino process.

### 19.19 High-resolution spectroscopy of cool extremely metal-poor carbon-rich stars

ZACS, Laimons<sup>1</sup>, SCHMIDT, Mirosław<sup>2</sup>, DIEBELE, Ilze<sup>1</sup>, and ALKSNIS, Oskars<sup>1</sup>

<sup>1</sup>University of Latvia, <sup>2</sup>N. Copernicus Astronomical Center

The preliminary results of abundance analysis are presented for two extremely metal-poor carbon-rich stars HD112869 and BPS BS17569-0011 with the effective temperatures of about 3700 K. Our LTE abundance analysis support an extremely low metallicity for both stars,  $[\text{Fe}/\text{H}] = -3.0$ , and a significant overabundance of carbon and neutron-capture elements. The  $^{12}\text{C}/^{13}\text{C}$  ratio in the atmosphere of HD112869 is high.

### 19.20 Extraction of resonant component from spin-polarization observables

YAMAGUCHI, Mitsutaka<sup>1</sup>, MAKOTO, Tanifuji<sup>2</sup>, YOSHIHIRO, Tagishi<sup>1</sup>, TATSUYA, Katabuchi<sup>3</sup>, YASUO, Aoki<sup>4</sup>, YOSHINORI, Yamato<sup>4</sup>, TAKASHI, Nagatomo<sup>4</sup>, TOMOYUKI, Iizuka<sup>4</sup>, NAOKO, Yoshimaru<sup>4</sup>, and TAKUYA, Shinba<sup>4</sup>

<sup>1</sup>RIKEN, <sup>2</sup>Rikkyo Univ., <sup>3</sup>Gunma Univ., <sup>4</sup>Tsukuba Univ

Recently, some groups studied about  $^6\text{Li}(d, p)$  and  $^6\text{Li}(d, \alpha)$  reactions near zero energy using for astrophysical interests. These reactions are affected by a resonant level under the reaction threshold. Normally, the resonant component is extracted from cross section data. In this work, we present a way to extract the resonant component from spin-polarization observables.

### 19.21 Equation of state and neutrino signal from collapsing stellar cores

YUDIN, Andrey and NADYOZHIN, Dmitriy

ITEP, Moscow

Starting from the conditions of Nuclear Statistical Equilibrium we investigate the equation of state for stellar matter in a wide range of thermodynamic parameters specific for the gravitational collapse of massive stellar cores. We take a variety of nuclei into account and try to adequately describe their properties placing special emphasis on the partition functions and their high-temperature limit. Also we investigate how the presence of the neutron-rich nuclei, whose properties are not yet well established, can modify the collapse properties. Moreover, we explore the non-ideal effects produced by the Coulomb interaction and suggest the algorithm for the description on multi-component Coulomb systems which holds in different interaction regimes. All these effects are considered in their connection with the collapse dynamics and the properties of attendant neutrino signal. Obtained neutrino light curves and spectra especially that for the electron neutrinos coming from the non-equilibrium neutronization of matter on the early stage of the collapse (first 10-20 ms after bounce) may be of importance both for the detection of the supernova neutrinos on the earth neutrino observatories and for the yields of the neutrino-induced nucleosynthesis.

## 19.22 Asymmetric collapsing supernovae explosion with rotation

MANUKOVSKIY, Konstantin

ITEP, Moscow

Hydrodynamic processes, by which the collapse of stellar core triggers the supernovae explosion, were studied in detail by numerical solution of axially symmetric problem taking into account fast initial rotation of iron core. Simulations showed the propagation of a strong diverging shock wave with a large asymmetry of explosion and with a total post-shock energy comparable to the characteristic energies of observed supernovae. Physical background for the formulation of the problems under consideration is the rotational explosion scenario for collapsing supernovae. According to this scenario supernovae explosion is preceded by the formation of a close binary system of neutron stars through the fragmentation of a rapidly rotating preneutron star. Such neutron star binary evolves to the point of explosion due to the losses of energy and angular momentum via the emission of gravitational waves in the presence of uniform or toroidal atmosphere - another residual of iron core collapse

## 19.23 Experimental studies of shell-model basis states near $^{132}\text{Sn}$

WALTERS, William

University of Maryland

Recent studies of the structure and decay of nuclei near the double-magic nucleus  $^{132}\text{Sn}$  will be described and the observed properties related to calculations of r-process abundances.

## 19.24 New study of the astrophysical reaction $^{13}\text{C}(\alpha, n)^{16}\text{O}$ via the $^{13}\text{C}(^7\text{Li}, t)^{17}\text{O}$ transfer reaction

PELLEGRITI, Maria Grazia<sup>1</sup>, HAMMACHE, Fairouz<sup>1</sup>, AUDOUIN, Laurent<sup>1</sup>, BEAUMEL, Didier<sup>1</sup>, FORTIER, Simone<sup>1</sup>, GAUDEFROY, Laurent<sup>2</sup>, KIENER, Jurgen<sup>3</sup>, LEFEBVRE, Anne<sup>3</sup>, ROUSSEL, Pierre<sup>1</sup>, STANOIU, Mihai<sup>4</sup>, TATISCHEFF, Vincent<sup>3</sup> and VILMAY, Mathieu<sup>1</sup>

<sup>1</sup>IPN-Orsay, IN2P3-Université Paris XI, 91406 Orsay-Campus, France, <sup>2</sup>GANIL-Caen, France, <sup>3</sup>CSNSM, 91405 Orsay-Campus, France, <sup>4</sup>GSI, Postfach 110552, D-64220 Darmstadt, Germany

The cross section of the  $^{13}\text{C}(\alpha, n)^{16}\text{O}$  reaction is a key ingredient for the comprehension of the s-process. This reaction is considered as the main neutron source for the slow (s) process in low-mass AGB stars (1-3 solar mass)[1]. At the energies of astrophysical interest (around 190 keV, corresponding to a temperature of  $10^8$  K), the contribution of the sub-threshold resonance at 6.356 MeV of  $^{17}\text{O}$  to the cross section of  $^{13}\text{C}(\alpha, n)^{16}\text{O}$  reaction should be taken into account. The contribution of this level to the cross section can be evaluated by using its reduced alpha-width. The latter can be extracted from the alpha-spectroscopic factor of the level. Actually, the likely effect of this state is very controversial after the study of this reaction by Kubono et al.[2], via the transfer reaction  $^{13}\text{C}(^6\text{Li}, d)^{17}\text{O}$ . So, a new measurement of the alpha-spectroscopic factor of the 6.356 MeV state of  $^{17}\text{O}$  was performed by studying the  $^{13}\text{C}(^7\text{Li}, t)^{17}\text{O}$  transfer reaction. The experiment has been performed at the Orsay TANDEM by using a  $^7\text{Li}$  beam energy of 28 and 34 MeV respectively. The angular distributions of the emitted tritons have been measured by using the SPLITPOLE spectrometer. The preliminary results of the experiment will be shown and discussed.

[1] R.Gallino et al., *Astrophys. J.* 497 (1998) 388

[2] S.Kubono et al., *Phys. Rev. Lett.* 90 (2003) 159

## 19.25 Measurement of $^3\text{He}(\alpha, \gamma)^7\text{Be}$ with ERNA recoil separator

DI LEVA, Antonino

Experimentalphysik 3, Ruhr Universität Bochum

The  $^3\text{He}(\alpha, \gamma)^7\text{Be}$  reaction plays an important role in the interpretation of the results of the solar neutrino experiments, since the estimate of the oscillation parameters relies on the solar neutrino spectrum, calculated by solar models. The high energy component in this spectrum is mainly

produced by the decay of  ${}^7\text{Be}$  and  ${}^8\text{B}$ . The uncertainty in the  ${}^3\text{He}(\alpha, \gamma){}^7\text{Be}$  cross section is also one of the largest contributions to the uncertainty on the predicted primordial  ${}^7\text{Li}$  abundance in Big Bang Nucleosynthesis calculations. Previous measurements of the  ${}^3\text{He}(\alpha, \gamma){}^7\text{Be}$  cross section have been performed detecting the capture  $\gamma$ -rays or, alternatively, measuring the activity of the synthesized  ${}^7\text{Be}$ . While the results of the two different approaches agree on the energy dependence of the astrophysical  $S$  factor, they disagree in the extrapolated  $S_{34}(0)$  value at a  $3\sigma$  level. A novel approach uses the European Recoil separator for Nuclear Astrophysics (ERNA) to detect directly the  ${}^7\text{Be}$  ions produced in a recirculating  ${}^3\text{He}$  windowless gas target. The total cross section has been measured in the energy range  $E_{cm} = 1.1$  to  $3.15$  MeV. The results are presented and their extrapolation to astrophysical energies is discussed.

### 19.26 First experimental constraints on the interference of $3/2^+$ resonances in the ${}^{18}\text{F}(p, \alpha){}^{15}\text{O}$ reaction

CHAE, K. Y.<sup>1</sup>, BARDAYAN, D. W.<sup>2</sup>, PAIN, S. D.<sup>3</sup>, PAULASKAS, S.<sup>4</sup>, PORTER-PEDEN, M.<sup>5</sup>, SHRINER, J. F.<sup>4</sup>, SMITH, M. S.<sup>2</sup>, THOMAS, J. S.<sup>3</sup>, SMITH, N.<sup>4</sup>, BLACKMON, J. C.<sup>2</sup>, GREGORY, D.<sup>4</sup>, GUIDRY, M. W.<sup>1</sup>, JOHNSON, M. S.<sup>6</sup>, KOZUB, R. L.<sup>4</sup>, LIVESAY, R. J.<sup>5</sup>, MA, Z.<sup>1</sup>, and NESARAJA, C. D.<sup>2</sup>

<sup>1</sup>Department of Physics and Astronomy, University of Tennessee, Knoxville, Tennessee 37996, <sup>2</sup>Physics Division, Oak Ridge National Laboratory, Oak Ridge, Tennessee 37831, <sup>3</sup>Department of Physics and Astronomy, Rutgers University, Piscataway, New Jersey, 08854, <sup>4</sup>Physics Department, Tennessee Technological University, Cookeville, TN 38505, <sup>5</sup>Department of Physics, Colorado School of Mines, Golden, Colorado 80401, <sup>6</sup>Oak Ridge Associated Universities, Bldg 6008, P. O. Box 2008, Oak Ridge, Tennessee 37831

The  ${}^{18}\text{F}(p, \alpha){}^{15}\text{O}$  reaction plays a crucial role in understanding both  $\gamma$ -ray emission from novae during the first several hours after the expansion and heavy element production in the higher temperature environments of x-ray bursts. The interference effects among  $J^\pi = 3/2^+$  resonances in the  ${}^{18}\text{F} + p$  system, however, have never been measured. The interference has a significant effect on the reaction rate at nova temperatures. An excitation function for the  ${}^1\text{H}({}^{18}\text{F}, \alpha){}^{15}\text{O}$  reaction has been measured using radioactive  ${}^{18}\text{F}$  beams at the Holifield Radioactive Ion Beam Facility (HRIBF) in order to study the interference effect. By comparing the measured cross section with theoretical calculations, we could provide the first experimental constraints on the relative signs of reduced widths for all three of the interfering resonances. We shall also discuss new upper limits on the proton widths of other resonances.

*Oak Ridge National Laboratory is managed by UT-Battelle, LLC for the U.S. Department of Energy under contract DE-AC05-00OR22725.*

### 19.27 Nuclear superfluidity and the cooling time of neutron stars

SANDULESCU, Nicolae  
CEA/Bruyeres-le-Chatel

The superfluid properties of the inner crust matter, formed by neutron-rich nuclei immersed in a neutron gas, have a strong influence on the cooling time of neutron stars. This is especially the case of neutron stars which cool rapidly their interiors by direct Urca processes. In my talk I shall discuss the pairing and the thermal properties of the inner crust matter predicted by self-consistent HFB and QRPA calculations based on effective forces tuned on finite nuclei and nuclear matter [1-3]. Thus I shall show how the specific heat of the inner crust depends on temperature, matter inhomogeneity, the screening of the pairing force and the collective excitations of the inner crust baryonic matter. Finally, I shall discuss the cooling times of neutron stars obtained by using the specific heat provided by the HFB and the QRPA calculations.

[1] N. Sandulescu, Phys. Rev. C70 (2004) 025801

[2] N. Sandulescu, Nguyen Van Giai, R.J.Liotta, Phys. Rev. C69 (2004) 045802

[3] E. Khan, N. Sandulescu, Nguyen van Giai, Phys. Rev. C71 (2005) 042801(R)

## 19.28 Low-mass AGB stars abundance predictions with improved stellar cross sections

BISTERZO, Sara<sup>1</sup>, KÄPPELER, Franz<sup>2</sup>, GALLINO, Roberto<sup>1</sup>, TRAVAGLIO, Claudia<sup>3</sup>, and HEIL, Michael<sup>2</sup>

<sup>1</sup>Dipartimento di Fisica Generale, Università di Torino, <sup>2</sup>Institut für Kernphysik, Forschungszentrum Karlsruhe, Postfach 9640, D-76021 Karlsruhe, Germany, <sup>3</sup>Istituto Nazionale di Astrofisica (INAF), Osservatorio Astronomico di Torino

The main-s process component, which produces the s abundances from Sr to Pb/Bi, occurs in low-mass thermally pulsing AGB stars. In this scenario, the  $^{13}\text{C}(\alpha, n)^{16}\text{O}$ , which burns radiatively at  $T_8 \approx 0.9$  keV during the interpulse period, constitutes the major neutron source. A second weaker neutron source, the  $^{22}\text{Ne}(\alpha, n)^{25}\text{Mg}$ , is partially activated during the convective thermal pulses, when the maximum temperature at the bottom of the He-burning shell reaches a value of  $T_8 \approx 3$  keV. Within the stellar model for the AGB phase a large spread of observed heavy element abundances can be described by variations of three free parameters: the initial stellar mass, the initial metallicity, and the s-process efficiency given by the  $^{13}\text{C}$ -pocket. It was shown, for example, that the solar main component can be reproduced by a standard  $^{13}\text{C}$ -pocket (Gallino et al. 1998) [1] and a metallicity of  $[\text{Fe}/\text{H}] = -0.3$  (Arlandini et al. 1999) [2]. Using recently improved stellar  $(n, \gamma)$  cross sections and updated stellar AGB models with a full reaction network, the prediction for the main-s process component are revisited. In this study, the effect of neutron poisons as well as the consequences of the new partial cross sections to the ground and isomeric states of some important branching points are considered and examined in detail. The updated s-process calculations are compared with the GCE model of Travaglio et al. (1999, 2001, 2004) [3], which considers the chemical evolution of stars in the mass range between 1 and 8 solar masses in the three galactic zones (halo, thick and thin disk) over the galactic history. Subtracting of the s-process contributions from the solar abundances yields an improved determination of the r-process abundance distribution in the mass range  $A \lesssim 90$ , which has a profound impact on the spectroscopic analyses of very metal poor stars with pronounced r-process signatures.

[1] Gallino, R., et al. 1998, ApJ 497, 388

[2] Arlandini, C., et al. 1999, ApJ 525, 886

[3] Travaglio, C., et al. 1999, ApJ 521, 691; 2001, ApJ 549, 346; 2004, ApJ 601, 864

## 19.29 SNRs as probes of chemical composition of interstellar medium

TELEZHINSKY, Igor<sup>1</sup>, HNATYK, Bohdan<sup>1</sup>, and PETRUK, Oleh<sup>2</sup>

<sup>1</sup>Astronomical Observatory of Kiev University, <sup>2</sup>Institute for Applied Problems in Mechanics and Mathematics NAS of Ukraine

The Supernova Remnants (SNRs) offer a promising opportunity to investigate the chemical evolution of galaxies. When the shock wave of SNR propagates into the surrounding interstellar medium (ISM), it heats up the gas of ISM. The gas becomes visible in X-Rays and thus can be tested for elements abundances. When the reverse shock wave propagates through the ejecta from the progenitor star we can observe the emission from the elements synthesized during the Supernova explosion. The rigorous calculation of 3D evolution of SNRs in nonuniform ISM is complicated numerical task, realized only in a restricted number of cases. The large-scale gradient of the ISM density essentially affects the evolution of SNRs: the shape of SNR becomes non-spherical and distributions of gas parameters inside the SNR become strongly anisotropic, so Sedov solutions may not be applied. Additional problems are connected with necessity to take into account radiative losses of shocked plasma. We propose the new approximate analytical method for description of 3D radiative hydrodynamic evolution of SNRs in ISM with large-scale density gradient and use it for the analysis of thermal X-ray emission of SNRs. We show that the surface distribution of the X-ray emission is very sensitive to the initial density distribution around the SN progenitor. Emission characteristics give important information about physical conditions inside and outside of the non-spherical SNR thus giving opportunity for good spectra interpretation from where we can obtain information about surrounding elements abundances. The model is especially good if SN explodes on the edge of dark molecular cloud or in stellar clusters where previous SN explosions have taken place. The method also can be used in the theory of cosmic rays (CR) acceleration

in SNRs because it gives right values for the shock wave dynamics and physical conditions at the shock front. Thus non-thermal X- ray and  $\gamma$  ray emission from SNRs can be tested. As experimental background we are planning to use observations of XMM Newton and INTEGRAL space missions.

### 19.30 Nucleosynthesis of binary low mass zero-metallicity stars

LAU, Ho Bun, Herbert and TOUT, Christopher Adams  
Institute of Astronomy, Cambridge

The first generation of stars that formed in the Universe, commonly referred to as Population III stars or zero-metallicity stars, should have the composition indicated by Big Bang nucleosynthesis, so they are essentially made up of hydrogen and helium with minimal traces of lithium. They were responsible for the initial enrichment of the interstellar medium with heavy elements. Hence, the nucleosynthesis and evolution of zero-metallicity stars are important. The formation mechanism of the Population III stars is not well understood, so the initial mass function is not well established. It is possible that the IMF may have a peak at around one solar mass [1] and the stars may also form in binary systems [2]. Because mass loss by stellar winds is proportional to metallicity, mass loss in single stars could be minimal. However, mass loss during binary interactions could produce significant enrichment of the interstellar medium. Moreover, binary mass transfer may explain the existence of low metallicity CN-rich stars. Using the STARS code ([3], [4]) with Stancliffe's nucleosynthesis's routine covering forty-six isotopes [5], a grid of three to seven solar masses zero-metallicity stars is modelled in order to investigate the nucleosynthesis signatures during mass loss. This should simulate the effect of binary mass transfer on the evolution and nucleosynthesis output of binary low mass population III stars.

- [1] Nakamura & Umemura ApJ 548 (2001) 19N
- [2] Saigo et al., ApJ 615L (2004) 65S
- [3] Eggleton, Mon. Not. R. Astron. Soc. 151 (1971) 351
- [4] Pols et al., Mon. Not. R. Astron. Soc. 274 (1995) 964
- [4] Stancliffe et al., Nucl. Phys. A 758 (2005) 569c

### 19.31 Synthesis of CNO elements in standard BBN

IOCCO, Fabio Iocco  
Università di Napoli "Federico II"; KIPAC/SLAC

According to the abundance of CNO elements in the primordial gas, the first generation of stars (PopIII) follows widely different formation and evolutionary paths from later generations. The qualitative prediction of the standard cosmological model is the almost total absence of 'metals' in the pristine gas, although modern and detailed analyses of the reason for that are lacking. We carefully study the production mechanism of CNO elements in the standard version of Primordial Nucleosynthesis (BBN), with the aim to assess a quantitative and robust upper limit to the metallicity of the primordial gas in the standard cosmological scenario. In recent years, the nuclear reaction network of the publicly available and widely used Kawano BBN code has been already enlarged and updated by the Naples Astroparticle group [1,2]. We have further added four formerly neglected unstable nuclides and over two hundred reactions to the code described in [2]. Only minor enhancements have been found of the final abundances of Carbon, Nitrogen or Oxygen isotopes, demonstrating the robustness of the BBN prediction about the possibility of the existence of a pristine metal-free generation of stars. The processes leading to CNO synthesis are clarified, and the interesting differences with the CNO production in stars are outlined. I will report on this analysis performed with the state-of-the art BBN knowledge and the prior on the the baryon abundance imposed by cosmic microwave background anisotropy data.

- [1] A. Cuoco, F. Iocco, G. Mangano, G. Miele, O. Pisanti and P.D. Serpico, "Present status of primordial nucleosynthesis after WMAP: results from a new BBN code" Int. J. Mod. Phys. A 19, 4431 (2004) [astro-ph/0307213]
- [2] P.D. Serpico, S. Esposito, F. Iocco, G. Mangano, G. Miele and O. Pisanti, "Nuclear Reaction Network for Primordial Nucleosynthesis: a detailed analysis of rates, uncertainties and light nuclei yields" JCAP 0412, 010 (2004) [astro-ph/0408076]

### 19.32 Shell model spin and parity dependent nuclear level densities for nuclear reaction rates

HOROI, Mihai

Central Michigan University

We recently developed a strategy, ([1], [2], [3]), of calculating the spin and parity dependent shell model level density for application to astrophysics reaction rates. The main ingredients are: (i) the extension of methods of the nuclear statistical spectroscopy [S.S.M. Wong, Nuclear Statistical Spectroscopy, Oxford, 1986] by exactly calculating the fixed spin- first and second moments, (ii) an exact decomposition of the space of many-body configurations in classes corresponding to different parities and number of harmonic oscillator excitations, (iii) developing new effective interactions for model spaces of interest starting from the G-matrix [4] and fixing/fitting monopole terms or/and linear combinations of two-body matrix elements to known experimental data, and (iv) an accurate estimate of the shell model ground state (g.s.) energy using the exponential convergence method (ECM) ([5], [6]). We present spin and parity dependent nuclear level densities for cases of interest for the rp-process, such as  $^{67}\text{As}$ ,  $^{71}\text{Br}$  and  $^{75}\text{Rb}$ . The calculations are done in the model space built with the  $p_{3/2}$ ,  $p_{1/2}$ ,  $f_{5/2}$ , and  $g_{9/2}$  single particle (s.p.) orbits, which is less affected by the spurious contribution of the shell model center-of-mass excitations.

[1] Nucl. Phys. A 785C (2005) 142

[2] Phys. Rev. C 69 (2004) 041307(R)

[3] Phys. Rev. C 67 (2003) 054309

[4] Phys. Rep. 261 (1995) 125

[5] Phys. Rev. Lett. 82 (1999) 2064

[6] Phys. Rev. C 67 (2003) 034303

### 19.33 Nucleosynthesis and mixing in rotating AGB stars at low metallicity

DECRESSIN, Thibault and CHARBONNEL, Corinne

Geneva Observatory

Models of rotating stars at  $Z = 0.0005$  with masses between 2.5 and 7  $M_{\odot}$  are computed from the pre-main sequence up to the end of the last thermal pulses on the asymptotic giant branch (AGB). We discuss the impact of rotation on nucleosynthesis and mixing especially during central He-burning phase. Rotational mixing allows some carbon and oxygen to be mixed into the H-burning shell where some new primary elements are synthesized. In stars massive enough to allow deep second dredge-up in the early-AGB phase, those elements are revealed at the surface. The TP-AGB phase is also investigated in order to follow the changes due to the interplay between third dredge-up and hot bottom burning on the chemical composition of the surface, and hence, on the wind. We obtain yields from those stars which are discussed in the context of the chemical anomalies seen in globular cluster stars.

### 19.34 The $^{25}\text{Al}(p, \gamma)^{26}\text{Si}$ reaction rate in novae

BARDAYAN, Dan<sup>1</sup>, HOWARD, J.A.<sup>2</sup>, LINGERFELT, E.J.<sup>3</sup>, LIVESAY, R.J.<sup>4</sup>, PAIN, S.D.<sup>5</sup>, SCOTT, J.P.<sup>3</sup>, SMITH, M.S.<sup>1</sup>, THOMAS, J.S.<sup>5</sup>, VISSER, D.W.<sup>6</sup>, BLACKMON, J.C.<sup>1</sup>, BRUNE, C.R.<sup>7</sup>, CHAE, K.Y.<sup>3</sup>, HIX, W.R.<sup>1</sup>, JOHNSON, M.S.<sup>8</sup>, JONES, K.L.<sup>5</sup>, KOZUB, R.L.<sup>2</sup>, and LIANG, J.F.<sup>1</sup>

<sup>1</sup>Oak Ridge National Laboratory, <sup>2</sup>Tennessee Technological University, <sup>3</sup>University of Tennessee, <sup>4</sup>Colorado School of Mines, <sup>5</sup>Rutgers University, <sup>6</sup>University of North Carolina, <sup>7</sup>Ohio University, <sup>8</sup>Oak Ridge Associated Universities

The production of  $^{26}\text{Al}$  in novae is uncertain, in part, because of the uncertain rate of the  $^{25}\text{Al}(p, \gamma)^{26}\text{Si}$  reaction at novae temperatures. This reaction is thought to be dominated by a long-sought  $3^+$  level in  $^{26}\text{Si}$ , and the calculated reaction rate varied by orders of magnitude depending on the energy of this resonance. We present evidence concerning the spin of a level at 5.914 MeV in  $^{26}\text{Si}$  from the  $^{28}\text{Si}(p, t)^{26}\text{Si}$  reaction studied at the Holifield Radioactive Beam Facility at

ORNL. We find that the angular distribution for this level implies either a  $2^+$  or  $3^+$  assignment, with only a  $3^+$  being consistent with the mirror nucleus,  $^{26}\text{Mg}$ . Additionally, we have used the updated  $^{25}\text{Al}(p, \gamma)^{26}\text{Si}$  reaction rate in a nova nucleosynthesis calculation and have addressed the effects of the remaining uncertainties in the rate on  $^{26}\text{Al}$  production. The measurement and calculations will be presented.

*Oak Ridge National Laboratory is managed by UT-Battelle, LLC, for the U.S. Department of Energy under contract DE-AC05-00OR22725.*

### 19.35 The QSE-reduced nuclear network for supernovae nucleosynthesis

PARETE-KOON, Suzanne<sup>1</sup>, HIX, W. Raphael<sup>2</sup>, FREIBURGHAUS, Christian<sup>3</sup>, and THIELE-MANN, Friedrich-Karl<sup>3</sup>

<sup>1</sup>University of Tennessee, <sup>2</sup>University of Tennessee/ Oak Ridge National Laboratory, <sup>3</sup>University of Basel

Iron and neighboring nuclei are formed in the cores of massive stars before core collapse and during supernova outbursts. Because of the larger number of nuclei involved, the computational time needed to model the formation of iron often can exceed that of all other burning stages. The final state is nuclear statistical equilibrium (NSE) where the photodisintegrations are balanced by the light particle capture reactions. NSE grows from and eventually dissolves into several smaller groups of nuclei, which maintain mutual equilibrium (termed quasi-statistical equilibrium, QSE) among themselves. We present a hybrid network equilibrium scheme, which takes advantage of quasi-equilibrium in order to reduce the number of independent variables calculated. This allows accurate prediction of the nuclear abundance evolution, depletionization, and energy generation even at temperatures too low to maintain NSE. During silicon burning the QSE-reduced network runs ten times faster and requires about a third as many variables as a full reaction network without a significant loss of accuracy. These reductions in computational cost make the QSE-reduced network well suited for inclusion within hydrodynamic simulations, particularly in multi-dimensional applications, which have often traced the composition only during NSE and ignored the elemental composition at lower temperatures.

*This work was made possible by funding from the U.S. National Science Foundation (PHY-0244783) and the Scientific Discovery through Advanced Computing Program of the U.S. Department of Energy's Office of Science. ORNL is managed by UT-Battelle, LLC, for the U.S. Department of Energy under contract DE-AC05-00OR22725.*

### 19.36 Investigation of nucleosynthesis capture reactions by using $^8\text{Li}$ radioactive beam transfer reactions

GUIMARAES, Valdir<sup>1</sup>, BARIONI, Adriana<sup>1</sup>, BECCHETTI, Fred D.<sup>2</sup>, JIANG, Hao<sup>2</sup>, CAMARGO, Orli<sup>1</sup>, LICHTENTHALER, Rubens<sup>1</sup>, KOLATA, James J.<sup>3</sup>, AMRO, Hanan<sup>3</sup>, AGUILERA, Eli F.<sup>4</sup>, LIZCANO, David<sup>4</sup>, MARTINEZ-QUIROZ, Enrique<sup>4</sup>, and GARCIA, H.<sup>4</sup>

<sup>1</sup>University of Sao Paulo - Sao Paulo - Brazil, <sup>2</sup>University of Michigan, Ann Arbor - USA, <sup>3</sup>University of Notre Dame - Indiana, USA, <sup>4</sup>Instituto Nacional de Investigaciones Nucleares, Mexico

Nucleosynthesis of light element is impeded due to the stability gap at mass  $A = 8$ . However, in some astrophysical environments, as in the r-process nucleosynthesis, neutron stars and in the inhomogeneous big bang models, this gap can be bridged with reactions involving the unstable nucleus  $^8\text{Li}$ . Some efforts have been devoted to the investigation of two important  $^8\text{Li}$  induced reactions in these scenarios,  $^8\text{Li}(\alpha, n)^{11}\text{B}$  [1,2] and  $^8\text{Li}(n, \gamma)^9\text{Li}$  [3,4]. Due to the low cross section and low intensity of the radioactive  $^8\text{Li}$  beam, the rate for the  $^8\text{Li}(n, \gamma)^9\text{Li}$  capture reaction has been estimated only by indirect methods [3,4], and some uncertainties are still present. Here we present the preliminary results of the investigation of the  $^8\text{Li}(n, \gamma)^9\text{Li}$ ,  $^7\text{Li}(n, \gamma)^8\text{Li}$  and  $^8\text{Li}(p, \gamma)^9\text{Be}$  capture reactions by using the Asymptotic Normalization Coefficient (ANC) method. In this method, the ANC, which normalizes the capture reaction, is obtained from the angular distribution of the  $^9\text{Be}(^8\text{Li}, ^9\text{Li})$ ,  $^9\text{Be}(^8\text{Li}, ^7\text{Li})$  and  $^9\text{Be}(^8\text{Li}, ^9\text{Be})$  transfer reactions. These angular distributions have been measured at Nuclear Structure Laboratory of the University of Notre Dame, USA, using a 27 MeV  $^8\text{Li}$  radioactive beam from the TWINSON [5] system and a 1.4 mg/cm<sup>2</sup> thick  $^9\text{Be}$  target. The  $^8\text{Li}$  scattered particles;  $^7\text{Li}$ ,  $^9\text{Li}$  and  $^9\text{Be}$  reaction products were detected by E-DE silicon detector

telescopes. The ANC values have been obtained from the comparison between the experimental differential cross section and DWBA calculation using the code FRESKO.

- [1] H. Miyatake et al. Nucl. Phys. A738 (2004) 401
- [2] X.Gu, R.N. Boyd et al. Phys. Lett. 343B (1995) 31
- [3] B. Guo et al. Nucl. Phys. A 761 (2005) 162
- [4] H.Kobayashi et al. Phys. Rev. C 67 (2003) 015806
- [5] F. D. Becchetti et al. Nucl. Instr. and Method Res. A 505 (2003) 377

## 20 Poster session, 28 June

### 20.1 Level structure of $^{19}\text{Ne}$ from studies of the $^{17}\text{O}(^3\text{He}, n)^{19}\text{Ne}$ reaction

HORNISH, M.J., BRUNE, C.R., GRIMES, S.M., HADIZADEH, M.H., MASSEY, T.N., VOINOV, A.V., O'DONNELL, J.E., ADEKOLA, A., MATEI, C., and HEINEN, Z.

Ohio University

The astrophysically-relevant region of the level structure of  $^{19}\text{Ne}$  around the proton threshold remains incomplete when considering that analogs for several states in the mirror nucleus  $^{19}\text{F}$  have not yet been identified in  $^{19}\text{Ne}$ . This structure is particularly important to understanding the eventual fate of the long-lived radioisotope  $^{18}\text{F}$  in explosive environments like novae and x-ray bursts, where rates of proton-induced reactions on  $^{19}\text{F}$  depend critically on the properties of  $^{19}\text{Ne}$  excited states above threshold. To study this system, a measurement of the  $^{17}\text{O}(^3\text{He}, n)^{19}\text{Ne}$  reaction has been performed at Ohio University's Edwards Accelerator Laboratory, which features a 4.5-MV tandem Van de Graaff accelerator. Utilizing pulsed beams and neutron time-of-flight techniques, this experiment has been conducted at forward angles with a  $^3\text{He}$  beam energy of 4.2 MeV. This energy has been chosen such that the compound reaction model is the dominant mechanism, which should ensure that this reaction will in principle populate all excited states including any newly observed ones. In addition to precisely determining the excited energies for individual levels, this measurement will provide experimental differential cross sections for individual states that can be compared to calculations employing the Hauser-Feshbach statistical model in an attempt to extract information on the spins of the excited states. The observed  $^{19}\text{Ne}$  level structure from this reaction will be presented and its astrophysical implications will be discussed.

### 20.2 The $rp$ process in core-collapse supernovae

WANAJO, Shinya

University of Tokyo

Recent hydrodynamic simulations of core-collapse supernovae with accurate neutrino transport suggest that the bulk of the neutrino-heated ejecta is proton rich, in which the production of some interesting proton-rich nuclei is expected. However, there are a number of waiting point nuclei with the beta-lives of a few minutes, which prevent the production of heavy proton-rich nuclei beyond iron in explosive events such as core-collapse supernovae. In this study, it is shown that the rapid proton-capture ( $rp$ ) process takes place by bypassing these waiting points via neutron-capture reactions even in the proton-rich environment, if there is an intense neutrino flux as expected during the early phase of the neutrino-driven winds of core-collapse supernovae. The nucleosynthesis calculations are performed using the general relativistic models of neutrino-driven winds with wide range of  $Y_e$  (number of proton per baryon). Comparison of the mass- $Y_e$ -averaged yields to the solar compositions implies that the neutrino-driven winds can be potentially the origin of light p-nuclei up to  $A \approx 110$ , including  $^{92,94}\text{Mo}$  and  $^{96,98}\text{Ru}$  that cannot be explained by other astrophysical sites.

### 20.3 The weak $r$ -process in core-collapse supernovae

WANAJO, Shinya<sup>1</sup> & ISHIMARU, Yuhri<sup>2</sup>

<sup>1</sup>University of Tokyo, <sup>2</sup>Kogakuin University

While the origin of  $r$ -process nuclei remains a long-standing mystery, recent spectroscopic studies of extremely metal-poor stars in the Galactic halo strongly suggest that it is associated with core-collapse supernovae. In addition, recent comprehensive analysis of such stars implies the presence of the “weak”  $r$ -process that is responsible for only lighter nuclei with  $A < 130$ . In this study, we show that the weak  $r$ -process nuclei can be produced in the neutrino winds from a typical proto-neutron star of  $1.4 M_{\odot}$ . This suggests that the significant fraction of weak  $r$ -process elements (Sr, Y, Zr, etc.) originate from “typical” core-collapse supernovae with the progenitor mass range of  $\approx 10 - 20 M_{\odot}$ .

### 20.4 Elastic scattering of $^8\text{B}$ on Pb, liquid hydrogen, and liquid helium targets and the $^7\text{Be}(p, \gamma)^8\text{B}$ S-factor

BISHOP, Shawn<sup>1</sup>, MOTOBAYASHI, T.<sup>1</sup>, AOI, N.<sup>1</sup>, BABA, H.<sup>1</sup>, GOMI, T.<sup>1</sup>, ICHIKAWA, I.<sup>1</sup>, IMAI, N.<sup>2</sup>, IWASA, N.<sup>3</sup>, IWASAKI, H.<sup>2</sup>, KAWAI, S.<sup>4</sup>, KONDO, Y.<sup>5</sup>, NAKUMURA, T.<sup>5</sup>, NAKAO, T.<sup>2</sup>, NISHIMURA, S.<sup>1</sup>, OHNISHI, T.<sup>1</sup>, ONISHI, K.<sup>2</sup>, ONG, H. J.<sup>2</sup>, OTA, S.<sup>6</sup>, PERERA, A.<sup>1</sup>, SHIMOURA, S.<sup>6</sup>, SUZUKI, D.<sup>2</sup>, SUZUKI, H.<sup>2</sup>, SUZUKI, M. K.<sup>2</sup>, TAKEUCHI, S.<sup>1</sup>, TAMAKI, M.<sup>6</sup>, TANAKA, K.<sup>1</sup>, TOGANO, Y.<sup>4</sup>, and YANAGISAWA, Y.<sup>1</sup>

<sup>1</sup>RIKEN, <sup>2</sup>University of Tokyo, <sup>3</sup>Tohoku University, <sup>4</sup>Rikkyo University, <sup>5</sup>Tokyo Institute of Technology,

<sup>6</sup>Tokyo Institute of Technology & Center for Nuclear Study, University of Tokyo

The solar  $^8\text{Be}(p, \gamma)^8\text{B}$  reaction has been the object of intense experimental and theoretical scrutiny for more than 30 years. An outstanding problem in nuclear astrophysics remains the precise determination of the zero-energy astrophysical S factor,  $S(0)$ , for this reaction and, hence, precisely predict the solar neutrino flux to be observed on Earth. Past experiments have used the Coulomb Dissociation (CD) of  $^8\text{B}$  on Pb targets [1,2,3,4] to indirectly measure the low energy radiative capture cross section, thereby determining  $S(0)$ . However, these results have been subject to systematic uncertainties caused by: 1. possible nuclear breakup contributions; 2. higher multipole contributions to the breakup cross section beyond the dominant E1 electromagnetic interaction; 3. optical parameter uncertainties in the  $^8\text{B} + \text{Pb}$  system as, heretofore, no elastic scattering data for this system existed, forcing previous analyses to rely on  $^{17}\text{O} + \text{Pb}$  optical parameter sets; 4. higher order processes. In an effort to extract the nuclear and EL ( $L > 1$ ) contributions to  $^8\text{B}$  dissociation and determine  $S(0)$  with greater precision, we have performed a  $^8\text{B}$  CD experiment, at the RIKEN RIPS facility [5], employing Pb, liquid  $\text{H}_2$  and liquid He secondary targets. Using a  $^8\text{B}$  secondary beam of 150 kcps, and a detector system consisting of two PPAC’s 1.7 m upstream of the secondary target position, and a 1 m<sup>2</sup> plastic scintillator hodoscope 3.98 m downstream of the secondary target position, CD data and elastic scattering data of  $^8\text{B}$  on each of these targets were acquired. Before analyzing the CD data for  $S(0)$ , issue 3 above must first be addressed for the Pb target data. Additionally, the elastic scattering data from these 3 targets will necessarily provide the optical parameter sets that will provide for a fully complete and self-consistent analysis of the CD data and extraction of  $S(0)$ . This poster will outline the experiment and present the elastic scattering analysis for  $^8\text{B}$  on these 3 targets. Additionally, an outline the direction of this new CD study to extract  $S(0)$  for the  $^7\text{Be}(p, \gamma)^8\text{B}$  reaction will be shown.

[1] T. Motobayashi et al., Phys. Rev. Let. 73, 2680, (1994)

[2] T. Kikuchi et al., Phys. Let. B 391, 261, (1997)

[3] N. Iwasa et al., Phys. Rev. Let. 83, 2910, (1999)

[4] F. Schümann et al, Phys. Rev. Let. 90, 232501, (2003)

[5] T. Kubo et al., NIM B70, 309, (1992)

## 20.5 Low energy nuclear reaction measurements using monolithic silicon telescope

NISHIMURA, Shunji  
RIKEN

${}^8\text{Li}(\alpha, n){}^{11}\text{B}$  is recognized as an important reaction for passing through the valley of  $A = 8$  in nucleosynthesis. While, there are some difficulties of measuring the most interesting energy region of data below 1 MeV due to the background particles consists of elastically scattered  ${}^8\text{Li}$  ions, and  $\alpha$  particles as well as the decay products of  ${}^8\text{Li}$ .

A new experimental approach for exploring these low-energy nuclear reactions using a monolithic silicon telescope have been performed at the CNS-CRIB spectrometer. Our preliminary results will be presented.

## 20.6 Photonuclear reactions of light nuclei studied with high-intensity real photon beams

SHIMA, Tatsushi<sup>1</sup>, NAGAI, Yasuki<sup>1</sup>, UTSUNOMIYA, Hiroaki<sup>2</sup>, AKIMUNE, Hidetoshi<sup>2</sup>, MIYAMOTO, Shuji<sup>3</sup>, and MOCHIZUKI, Takayasuh<sup>3</sup>

<sup>1</sup>Research Center for Nuclear Physics, Osaka University, <sup>2</sup>Department of Physics, Konan University, <sup>3</sup>Laboratory of Advanced Science and Technology for Industry, University of Hyogo

Photonuclear reactions, as well as their inverse, radiative capture reactions, of light nuclei are considered to play important roles in various processes of nucleosynthesis in stars and in the early universe. Photonuclear reactions of light nuclei are also of interest, because they are useful to investigate the analogous processes of the neutrino-induced reactions with weak neutral current, which are supposed to play critical roles in the dynamics of Type-II supernova explosions and in neutrino-induced nucleosynthesis. Recently we have developed a new experimental method for high-precision measurement of photonuclear reactions in the energy region of astrophysical importance, based on a high-intensity monochromatic  $\gamma$ -ray beam and an active target technique. In this contribution we will present the performance of the new method and the results of the photonuclear reaction experiments on light nuclei such as D,  ${}^3\text{He}$ ,  ${}^4\text{He}$ , and  ${}^{12}\text{C}$ .

## 20.7 Supernova physics with a low-energy $\beta$ -beam

JACHOWICZ, Natalie<sup>1</sup> and MCLAUGHLIN, Gail<sup>2</sup>

<sup>1</sup>Ghent University, Department of Subatomic and Radiation Physics, <sup>2</sup>Department of Physics, North Carolina State University

Core-collapse supernova neutrino-spectra are of interest not only for understanding the deep interior of astrophysical explosions, but also for understanding the synthesis of many elements made primarily in this environment. A new type of neutrino beam, the  $\beta$  beam, is now under discussion as a next generation neutrino experiment. A low-energy version of this beam has been proposed for a number of astrophysical applications. The energy range of these low-energy neutrino is the same as that of supernova neutrino. We present a theoretical discussion of the importance of low-energy  $\beta$ -beams for improving our interpretation of a future galactic supernova signal. We present a novel method, where fitting 'synthetic' spectra, constructed by taking linear combinations of  $\beta$ -beam spectra, to the original supernova-neutrino spectra reproduces the folded differential cross sections very accurately. Comparing the response in a terrestrial detector to these synthetic responses provides a direct way to determine the main parameters of the supernova-neutrino energy-distribution.

## 20.8 The detailed abundance patterns of light neutron-capture elements in very metal-poor stars

HONDA, Satoshi<sup>1</sup>, AOKI, Wako<sup>1</sup>, ISHIMARU, Yuhri<sup>2</sup>, WANAJO, Shinya<sup>3</sup>, RYAN, Sean<sup>4</sup>, KAJINO, Toshitaka<sup>1</sup>, ANDO, Hiroyasu<sup>1</sup>, and BEERS, Timothy<sup>5</sup>

<sup>1</sup>National Astronomical Observatory of Japan, <sup>2</sup>Kogakuin University, <sup>3</sup>University of Tokyo, <sup>4</sup>University of Hertfordshire, <sup>5</sup>Michigan State University

We report the detailed abundance patterns of neutron-capture elements in very metal-poor stars. Over the past few decades, a considerable number of studies have been conducted on the elemental abundances of r-process. However, there are few objects investigated in the wide range of atomic number. This is because most of interested lines of neutron-capture elements exist in the UV region, which is difficult to access using ground-based telescopes. We select four bright very metal-poor stars and observed the near UV region with Subaru/HDS to obtain the abundance patterns from light to heavy neutron-capture elements. (1) The abundance patterns of heavy neutron-capture elements in two stars among them are quite similar to the pattern of r-process component in the solar system. Light neutron-capture elements of these stars show, however, deviation. These stars probably represent the abundance pattern of the so-called main r-process. (2) Other two have quite low abundances of heavy neutron-capture elements. However, the light neutron-capture elements of these stars show excesses with respect to heavy ones, indicating a contribution of other process than the main r-process. These results will be useful to investigate the r-process nucleosynthesis in the early universe.

## 20.9 Neutrino opacities in a relativistic non interacting neutron gas

VANTOURNHOUT, Klaas and JACHOWICZ, Natalie

Ghent University

Neutrino processes play an important role in a wide variety of astrophysical phenomena. Neutrino emissions are the driving force behind the cooling of a neutron star during the first hundreds of years after its birth. Furthermore, neutrino interactions are crucial in the final stages of core collapse supernovae. For a better understanding of the evolutionary stages of these events, it is necessary to have a detailed knowledge of neutrino transport properties in high density matter. Neutrino transport in supra nuclear-matter has been studied in a variety of models which take the correlations into account. RPA, molecular dynamics and Hartree analysis are some of the used techniques. In our work we focus on the relativistic effects. A fully relativistic description of neutrino opacities in neutron matter shall be presented and compared with its Newtonian counterpart. To this purpose, neutron matter is described as a non interacting Fermi gas in  $\beta$ -equilibrium. Results will be shown for the differential cross sections and dynamical formfactors. The ratio of the latter two makes the hadron current in the weak interaction matrix element visible. Eventually, this triggers a discussion about the necessity of introducing  $Q^2$  dependent form factors and of including a weak magnetic term in the hadron current.

## 20.10 Mass measurement of neutron-deficient nuclei close to the $N = Z$ line

HAGER, Ulrike<sup>1</sup>, KANKAINEN, Anu<sup>1</sup>, POPOV, Andrey<sup>2</sup>, RAHAMAN, Saidur<sup>1</sup>, RINTA-ANTILA, Sami<sup>1</sup>, SAASTAMOINEN, Antti<sup>1</sup>, SONODA, Tetsu<sup>1</sup>, VOROBJEV, Gleb<sup>3</sup>, ÄYSTÖ, Juha<sup>1</sup>, ELISEEV, Sergej<sup>3</sup>, ELOMAA, Viki<sup>1</sup>, ERONEN, Tommi<sup>1</sup>, HAKALA, Jani<sup>1</sup>, JOKINEN, Ari<sup>1</sup>, MOORE, Iain<sup>1</sup>, NOVIKOV, Yuri<sup>4</sup>, and PENTTILÄ, Heikki<sup>1</sup>

<sup>1</sup>University of Jyväskylä, <sup>2</sup>St. Petersburg State University, <sup>3</sup>GSI, <sup>4</sup>GSI, St. Petersburg State University

The masses of neutron-deficient nuclei close to  $A = 80$  are important for modeling the astrophysical rapid proton capture process (rp process) [1]. The rp process occurs as a sequence of  $\beta^+$ -decays and proton captures in various astrophysical sites, such as on the surface of an accreting neutron star. The rp process flows close to the  $N = Z$  nuclei up to  $^{56}\text{Ni}$ . At higher masses, the path will broaden and shift by about one or two units towards stable nuclei. The decay properties of several neutron-deficient nuclei near  $A = 80$  have been studied at the IGISOL facility in a series of experiments [2].

These investigations are now extended to precision mass measurements of the nuclei. The masses of  $^{79,80,81,82,83}\text{Y}$ ,  $^{83,84,85,86,88}\text{Zr}$ ,  $^{85,86,87,88}\text{Nb}$  and  $^{96,98}\text{Mo}$  have been measured in the precision trap of the JYFLTRAP Penning trap at IGISOL. The mass of  $^{84}\text{Zr}$  has been measured for the first time. The accuracy of the QEC values and proton separation energies, which are important for the rp process, could be improved significantly for the studied neutron-deficient nuclei.

[1] R.K. Wallace and S.E. Woosley, *Astrophys. J. Suppl.* 45, 389 (1981)

[2] A. Kankainen et al., *Eur. Phys. J. A* 25, 355 (2005)

## 20.11 Hydrodynamic models of type I X-ray bursts

JOSÉ, Jordi<sup>1</sup> and MORENO, Fermin<sup>2</sup>

<sup>1</sup>Institut d'Estudis Espacials de Catalunya/UPC, <sup>2</sup>Institut d'Estudis Espacials de Catalunya

X-ray bursts are violent events that take place on the H/He-rich envelopes of accreting neutron stars, and are powered by thermonuclear runaways. These cataclysmic events constitute the most frequent source of stellar explosions in the Galaxy (and the fourth most energetic event after  $\gamma$ -ray bursts, supernovae and nova outbursts). In this contribution, we present new hydrodynamical models (1D) of X-ray bursts, from the onset of accretion up to the explosion phase, with special emphasis on the gross observational characteristics of the outburst (light curve, time scale of the burst...) as well as on the associated nucleosynthesis. In particular, we stress the role played by the composition of the envelope and the mass-accretion rate. Current attempts in modeling these explosions in 2D will be also outlined.

## 20.12 Enhanced $d(d,p)t$ cross section in metallic environments

RAIOLA, Francesco

Ruhr Universität Bochum

Understanding the electron screening effect in the laboratory is critical for a correct interpretation of low-energy nuclear reactions in stars. Extensive studies of the electron screening effect in deuterated metals (54 metals) and other environments have been carried out in Bochum in the last 4 years. Experimental results of anomalous enhancements have been interpreted in terms of the Debye plasma model applied to quasi-free metallic electrons. For the  $d(d,p)t$  reaction in metallic environments, the variation of hydrogen solubility in the samples as a function of temperature has also been measured, showing an anti-correlation with screening enhancement as expected. Within this model, the deduced number of valence electrons per metallic atom also agrees with the corresponding number from the Hall coefficient. Recently, the expected temperature dependence of the screening potential has been verified together with the expected  $Zt$  scaling (with the metallic host) of the Debye radius. Preliminary results on the  $^7\text{Li}(p,\alpha)$  and  $^6\text{Li}(p,\alpha)$  reactions in Li insulators, Li metal and PdLi alloys confirm the expected behaviour of the screening effect and further supports the applicability of the Debye model. Indeed, the proposed model also accounts for the high screening potential ( $U_e = 900 \pm 50$  eV) observed in previous studies of the reactions  $^9\text{Be}(p,\alpha)$  and  $^9\text{Be}(p,d)$ , which was not understood at the time. A review of all these results will be presented.

## 20.13 Thermonuclear burning ignition and propagation along the surface of neutron stars during X-ray bursts

GRYAZNYKH, Dmitry A., SIMONENKO, Vadim A., LYKOV, Vladimir A., SHUSHLEBIN, Alexander N., LITVINENKO, Igor A., KARLYKHANOV, Nikolay G., and GRYAZNYKH, Anatoliy I.  
Russian Federal Nuclear Center - Zababakhin Institute of Technical Physics (VNIITF)

There are reliable experimental evidences of high-frequency oscillations during some X-ray bursts in LMXB. These oscillations can be caused by thermonuclear burning wave propagation along the layer of accreted matter on the neutron star surface. However a reliable theoretical explanation for the discrepancy between observed and predicted parameters is still necessary. We studied a mechanism of thermonuclear burning propagation with 2D simulations of simplified problem for pure helium layer along the surface of a neutron star. Mixed Euler-Lagrange code TIGR-3T was used. It includes equilibrium radiative and electron heat transfer, heat release and composition

evolution due to thermonuclear reactions, and subgrid  $K_\epsilon$  turbulence model. The burning wave was simulated for a layer with bottom density of  $1.8 \times 10^7 \text{ g cm}^{-3}$ . It is the lowest density at which nuclear burning on neutron stars has so far been simulated and thus more realistic one. The special conditions on initial temperature perturbation are required: it must be large enough at size and have smooth profile. The burning propagates with speed about  $10^8 \text{ cm/s}$  due to the following mechanism: the portions of burnt material rise and spread over the free surface of the unburnt fuel; the inflowing matter increases the thickness of the layer and pressure at its bottom. As a result, the unburnt fuel is ignited.

### 20.14 Measurement of the partial $(n, \gamma)$ cross section to $^{176}\text{Lu}^m$ at s-process temperatures

WINCKLER, Nicolas<sup>1</sup>, HEIL, Michael<sup>2</sup>, KÄPPELER, Franz<sup>2</sup>, DABABNEH, S.<sup>3</sup>, GALLINO, Roberto<sup>4</sup>, and BISTERZO, Sara<sup>4</sup>

<sup>1</sup>Gesellschaft für Schwerionenforschung mbH (GSI), <sup>2</sup>Institut für Kernphysik, Forschungszentrum Karlsruhe, Postfach 9640, D-76021 Karlsruhe, Germany <sup>3</sup>Faculty of Applied Sciences, Al-Balqa Applied University, Salt 19117, Jordan, <sup>4</sup>Dipartimento di Fisica Generale, Università di Torino and Sezione INFN di Torino, Via P. Giuria 1, I-10125 Torino, Italy and Centre for Stellar and Planetary Astrophysics, Monash University, Victoria 3800, Australia

The s-process reaction path in the vicinity of  $^{176}\text{Lu}$  has attracted considerable interest for a long time. Initially,  $^{176}\text{Lu}$  was considered as a potential s-process chronometer due to its long half life of 36 Gyr. However, it turned out that the hot photon bath at typical s-process temperatures leads to thermally induced transitions between the long-lived ground state and the short-lived isomer (3.68 h), which are otherwise strictly forbidden. In this way the effective half life can be reduced to a few days. Accordingly, the final abundance ratio  $^{176}\text{Hf}/^{176}\text{Lu}$  becomes a sensitive function of temperature and neutron density, which turns  $^{176}\text{Lu}$  into an s-process thermometer. In this context, the isomeric ratio has to be known at the temperatures of the two neutron sources of the main s-process component, i.e. at  $9 \times 10^7 \text{ K}$  ( $kT = 84 \text{ keV}$ ) and  $2.7 \times 10^8 \text{ K}$  ( $kT = 23 \text{ keV}$ ), respectively. The stellar cross section feeding the isomeric state in  $^{176}\text{Lu}$  has been measured at  $kT = 5 \text{ keV}$  and  $25 \text{ keV}$  at the Karlsruhe 3.7 MV Van de Graaff accelerator via the activation technique. With these results and recent TOF data for the total capture cross section, the isomeric ratio was found to be constant in the relevant thermal energy range, in good agreement with a statistical model calculation. In the light of the improved cross section information, the branching at  $^{176}\text{Lu}$  is investigated by a comprehensive s-process analysis to test the temperature conditions during He shell flashes in thermally pulsing low mass asymptotic giant branch stars.

### 20.15 Mapping of the $^{12}\text{C}^*$ and $^9\text{B}^*$ states of astrophysical interest via the $^{10}\text{B}(^3\text{He}, p\alpha)\alpha$ reaction

ALCORTA, Martin<sup>1</sup>, JEPPESEN, Henrik B.<sup>2</sup>, BORGE, Maria Jose G.<sup>1</sup>, FYNBO, Hans O.U.<sup>3</sup>, GARCIA, Gaston<sup>4</sup>, KIRSEBOM, Oliver<sup>3</sup>, MADURGA, Miguel<sup>1</sup>, NYMAN, Goran<sup>5</sup>, OBRADORS, Diego<sup>1</sup>, and TENGBLAD, Olof<sup>1</sup>

<sup>1</sup>Inst. de Estructura de la Materia, CSIC Serrano 113bis, E-28006 Madrid, Spain, <sup>2</sup>CERN, ISOLDE, PH Department, CH-1211 Geneve 23, Switzerland. Inst. de Estructura de la Materia, CSIC Serrano 113bis, E-28006 Madrid, Spain, <sup>3</sup>Inst. for fysik og astronomi, Aarhus Universitat, DK-8000 Aarhus C, Denmark, <sup>4</sup>CMAM, Universidad Autonoma de Madrid, Cantoblanco, 28049 Madrid, Spain, <sup>5</sup>Fundamental Fysik, Chalmers Tekniska Hogskola, S-412 96 Goteborg, Sweden

The  $^3\text{He} + ^{10}\text{B}$  reaction can give us information that is of relevance to nuclear astrophysics. In the  $^{12}\text{C}^* + p$  channel we study resonances in  $^{12}\text{C}$  which are important for determining the rate of the triple- $\alpha$  process responsible for helium burning in stars. In addition, studying the  $^9\text{B}^* + \alpha$  channel can give us information on the states in  $^9\text{B}^*$ , its mirror nucleus, which influences the  $\alpha$ - $\alpha$ -n reaction and therefore also contributes to helium burning. In the past decade there have been a series of experiments performed using beta-decays of short lived isotopes ( $^9\text{C}$ ,  $^9\text{Li}$ ,  $^{12}\text{N}$ ,  $^{12}\text{B}$ ) with the goal of studying resonances in  $^9\text{B}$  [1],  $^9\text{Be}$  [2] and  $^{12}\text{C}$  [3]. The  $^3\text{He} + ^{10}\text{B}$  reaction allows us to gain complementary information on both the  $^9\text{B}$  and  $^{12}\text{C}$  resonances compared to what is

known from  $\beta$ -decay experiments because we can populate states non-accessible to  $\beta$ -decay studies due to energetic limitations and selection rules. As an example we can therefore study resonances with negative parity in  $^{12}\text{C}$  and positive parity in  $^9\text{B}$ , as well as gain information on energy levels situated above the  $Q_\beta$  values. This reaction has been studied once before in the 60's, but with very limited technology. Both the  $p + ^{12}\text{C}^*$  and  $\alpha + ^9\text{B}^*$  channels were identified on-line from the image on an oscilloscope with two particles preselected in hardware coincidence at given angles[4]. With the development of segmented detectors and faster electronics, we have detected 4-particle coincidences in our setup at the 5 MV tandetron in Madrid with a much better resolution. The experimental setup consisted of two 60  $\mu\text{m}$  thick DSSSDs, backed with a 1.5 mm Si-detector and 2.5 mm Si-detectors. The DSSSDs give a granularity of 256  $3 \times 3$  mm pixels. With a solid angle covered of about  $1/9$  of  $4\pi$ , we had a 2-particle detection efficiency of about 1 %, and a 4-particle detection efficiency of approximately 0.015 %. The reaction took place with a beam of  $^3\text{He}$  at 2.45 MeV on a target of  $^{10}\text{B}$  with a thickness of 20  $\mu\text{g}/\text{cm}^2$ . In our data we identified states in  $^{12}\text{C}$  from the ground state up to about 18 MeV, with spins ranging from 0 to 4. Due to our very good resolution, we are able to determine properties of these  $^{12}\text{C}$  resonances, such as their energy, width, and spin-parity. The ground state as well as the 2.34 MeV excited state in  $^9\text{B}$  has also been observed. In this contribution preliminary results from the ongoing analysis will be presented.

[1] U.C. Bergmann et al., Nucl. Phys. A692 (2001) 427

[2] Y. Prezado et al., Phys. Lett. B 618 (2005) 43

[3] H.O.U. Fynbo et al., Nature 433 (2005) 137

[4] M.A. Waggoner et al., Nucl. Phys. 88 (1966) 81

## 20.16 Fission fragments of actinide and superheavy nuclides in primordial solar system material and problem of their origin

GONCHAROV, Georgy

Department of Geochemistry, St.-Petersburg State University

Research for cumulative atomic mass distributions of chemical elements in the different objects of the Solar system in a view of modern systematics of mass distributions of fission fragments for actinide and superheavy elements [1,2] is carried out. It is revealed, that characteristic signatures for asymmetric fission of actinide and superheavy elements have maxima of mass distribution usually explained by the r-process contribution. A decrease of the even-odd effect in distribution of the atomic masses, especially appreciable in the field of heavy nuclei ( $A = 195$ ) owing to reduction of the s-process nuclides contribution, and also characteristic maxima for easy and heavy fission fragments are observed among these signatures. Using of the rules of "unchanged charge density" and equality of  $\beta$ -decay chains for fission fragments has allowed to lead reconstruction of charges and masses of fissioning nuclides. Two basic sources in the production of transiron nuclides with weakened even - odd effect in distribution of their atomic masses is revealed for matter of the Solar system. The first of them, distinguished by Dy, Pt and Te enrichment ( $A = 164, 195$  and  $130$ ), is characteristic for carbonaceous chondrites and the Solar photosphere. The second - having maxima of Sr, Zr and Ba abundances ( $A = 88, 94$  and  $138$ ) is observed in substance of crusts of the Earth and the Moon. The first of above mentioned components, probably, enters into internal zones of the Earth and in crust rocks is fixed by rather small yield of deep mantle component (for example, komatiitic basalts) in crust rocks. Characteristics (mass, a charge, neutron multiplicity) of possible natural superheavy nuclides ( $Z = 114$  and  $Z = 126$ ) was reconstructed on the data for primary cosmic distributions of the atomic masses in carbonaceous chondrites [3]. According to a rule of "unchanged charge density" the maxima near  $A = 88, 94$  and  $138$  can correspond to light and heavy fragments of Th and U nuclear fission after neutron emission. The abundance relations among nuclides of light groups of fission fragments ( $A = 88$  and  $94$ ) are same as well as their parent nuclides - Th and U, accordingly, in the Earth and the Moon crusts. Considering, that heights of fission barriers for Th and U and superheavy elements are in a rather narrow range of values (5.5 - 7 MeV after [4]) it is possible to assume ratios of their primordial abundances equal between total abundances of their fission fragments. The approached calculation shows, that in the rest after the induced fission at supernova explosions and in jet flows from neutron stars should be kept no more than 0.001 of parent nuclei abundances. The received value allows to estimate superheavy elements abundances in various natural objects depending on their lifetimes. Yields of fragments of the

induced fission of actinide and superheavy nuclides are shown in  $^{132}\text{Xe}$ ,  $^{134}\text{Xe}$ ,  $^{136}\text{Xe}$  distributions also. Separation of xenon isotopes in this mass region is possible owing to mixing of the various contributions of fission fragments distributions near  $A = 130$  (for superheavy nuclides) and  $A = 138$  (for actinides). Relative enrichment by  $^{132}\text{Xe}$  in carbonaceous chondrites, iron meteorites, the Solar wind and the Earth atmosphere also can be consequence of the greater contribution of fragments of the induced fission of superheavy nuclides. Enrichment by  $^{134}\text{Xe}$ ,  $^{136}\text{Xe}$  in achondrites, gases of the Earth's crust is consequence of the greater contribution of fragments of the induced fission of actinide nuclides. The given effect amplifies addition of products of spontaneous fission  $^{244}\text{Pu}$  after formation of these objects. It is supposed production of superheavy as well as actinide nuclei could proceed in a crust of a neutron star or in presupernova core in the fusion reactions of iron nuclei closely packed in clusters [3].

[1] E.K. Hulet et. al., Phys. Rev., C 40, 770 (1989)

[2] M.G. Itkis et. al., Yadern. Fiz., 66, 1154 (2003)

[3] G.N. Goncharov, Proc. Int. Symp. 'EXON 2004', World Sc. Publ. Comp., Singapore, 278 (2005)

[4] A. Mamdouh et al., Nucl. Phys., A679, 337 (2001)

## 20.17 A nonperturbative field-theoretical model for nuclear matter without the $\sigma$ and $\omega$

JENA, Saktidhar  
Utkal University

A nonperturbative field-theoretical technique is developed to study the properties of nuclear matter at zero temperature, as well as at finite temperature. A relativistic Lagrangian for pions and nucleons including only the pseudoscalar interaction is considered. A non-relativistic reduction is shown to automatically introduce a Lorentz-scalar, and isoscalar coupling of nucleons with an intermediate correlated pion pair. Equation state for nuclear matter is derived from the dynamics of the interacting system in a self-consistent manner, treating both the nucleons and the pions as quantized fields. The model reproduces the characteristic nuclear matter properties without the necessity of introducing additional sigma and omega fields. The transition temperature for nuclear matter is predicted around 20 MeV. The model is proposed as an alternative to the Walecka's  $\sigma$ - $\omega$  model without having to introduce the hypothetical  $\sigma$  coupling.

## 20.18 Spectroscopic analyses of subluminescent B stars in binaries

GEIER, Stephan<sup>1</sup>, HEBER, Uli<sup>1</sup>, KARL, Christian<sup>1</sup>, and NAPIWOTZKI, Ralf<sup>2</sup>

<sup>1</sup>Dr. Remeis Sternwarte Bamberg, <sup>2</sup>Centre for Astrophysics Research, University of Hertfordshire

We present the results of quantitative spectral analyses of subluminescent B stars from high resolution, high signal-to-noise optical spectra obtained with the ESO VLT and UVES. We derived their atmospheric parameters as well as their elemental abundance patterns and discuss them in the context of diffusion theory. All stars are radial velocity variable on time scales of hours to days, indicating that they reside in close binary systems. The companions are invisible at optical wavelengths. In addition to the radial velocity curves, the projected rotational velocities were measured with high accuracy. The rotation of the short period binaries is very likely tidally locked to the orbit. Adopting a reasonable assumption for the mass of the subluminescent B stars enabled us to derive the masses of the unseen companions. In most cases these masses are typical for white dwarfs. However, we find at least two systems with companion masses beyond the Chandrasekhar limit, indicating that those companions might be neutron stars or even black holes.

## 20.19 A new approach to the solution of large thermonuclear burning networks

GUIDRY, Mike

U. Tennessee, Oak Ridge National Laboratory

Thermonuclear burning networks as large as thousands of isotopes are necessary to describe nucleosynthesis properly in stellar evolution, novae, X-ray bursts, thermonuclear supernovae, core-collapse supernovae, neutron star mergers, and gamma-ray bursts (with these categories perhaps not all orthogonal). These burning networks power the phenomena for the first four cases, and in all cases the spatial and temporal signature of element and energy production may be a critical diagnostic for the mechanism. Standard networks have stability issues associated with the extremely stiff nature of the coupled ODE system that require implicit numerical methods with substantial computational overhead. They do not scale well, with computational time typically increasing as the square or even the cube of network size. As a result, typical simulations with multi-dimensional hydrodynamics couple only highly schematic or truncated networks directly to the actual hydro. I will describe a new stochastic approach that decouples stability from accuracy, permitting a stable explicit integration with large timesteps, even of very stiff systems. Initial tests of the method indicate that it can reproduce standard results as precisely as desired, but with important advantages: (1) The algorithm permits large but stable explicit timesteps tailored to the accuracy appropriate for a particular problem. (2) It scales linearly with network size. (3) It is highly parallel and fault tolerant. (4) Energy production is often calculated well, even for timesteps that are orders of magnitude too large to faithfully reproduce the evolution of smaller mass fractions. I will give examples from nova and X-ray burst simulations illustrating these properties, and discuss our current efforts using this method to couple more realistic networks to multidimensional hydrodynamics for various astrophysical phenomena.

## 20.20 Experiments and observations of light $r$ -process nuclei

MONTES, Fernando

GSI

Nuclear structure properties in the region Sr-Ag influence the creation of elements in the onset of the  $A \approx 130$  peak of the solar  $r$ -process abundance pattern. Since the modeling of the  $r$ -process in this mass region depends heavily on the strength of the shell closure  $N = 82$ , recent experiments measuring  $\beta$ -decay half-lives and  $\beta$ -delayed neutron emission probabilities have been performed to determine whether our understanding of nuclear structure evolution in this mass region is correct. Besides nuclear structure, the region is also interesting because elements  $42 \leq Z \leq 47$  seem to be underabundant in some recent observations of  $r$ -process rich metal-poor stars when compared to the observed solar  $r$ -process abundance pattern. This may suggest that an additional mechanism besides the *strong*  $r$ -process is required to create the missing residual abundances in the region  $Z \leq 47$ . Description of the experimental technique, results and outlook for future experiments will be presented along with the results and discussion of a parameter study performed to find the astrophysical conditions ( $n_n, T, \tau$ ) in which a neutron capture process would produce the necessary residual abundance pattern.

## 20.21 Neutrino nucleosynthesis of the exotic nuclei $^{138}\text{La}$ and $^{180}\text{Ta}$ by charged current reactions

BYELIKOV, Anatoliy<sup>1</sup>, ADACHI, T.<sup>2</sup>, VON BRENTANO, P.<sup>3</sup>, FREKERS, D.<sup>4</sup>, DE FRENNE, D.<sup>5</sup>, FUJITA, H.<sup>6</sup>, FUJITA, Y.<sup>2</sup>, HEGER, A.<sup>7</sup>, JAKOBS, E.<sup>5</sup>, KALMYKOV, Y.<sup>1</sup>, LANGANKE, K.<sup>8</sup>, KOLBE, E.<sup>9</sup>, MARTINEZ-PINEDO, G.<sup>8</sup>, NEGRET, A.<sup>5</sup>, VON NEUMANN-COSEL, P.<sup>1</sup>, POPESCU, L.<sup>5</sup>, RAKERS, S.<sup>4</sup>, RICHTER, A.<sup>1</sup>, SHEVCHENKO, A.<sup>1</sup>, and SHIMBARA, Y.<sup>2</sup>

<sup>1</sup>TU Darmstadt, <sup>2</sup>Osaka University, <sup>3</sup>Universität zu Köln, <sup>4</sup>Universität Münster, <sup>5</sup>Universiteit Gent, <sup>6</sup>University of Witwatersrand, <sup>7</sup>Los Alamos, <sup>8</sup>GSI, <sup>9</sup>Universität Basel

The nucleosynthesis of the exotic heavy odd-odd nuclides  $^{138}\text{La}$  and  $^{180}\text{Ta}$ , amongst the rarest in nature, is a long-standing problem. Both are shielded against the  $r$  process, and  $^{138}\text{La}$  is

bypassed in the  $s$  process, while production of  $^{180}\text{Ta}$  may be possible through neutron capture on the long-lived  $^{179}\text{Ta}$  [1]. The  $p$  process has been suggested as a source of  $^{179}\text{Ta}$ , but  $^{138}\text{La}$  is significantly underproduced in all reasonable scenarios [2]. Another possible source are charged-current neutrino-nucleus reactions [3,4] of the type  $(\nu_e, e^-)$  which would be dominated by the GT response. The main GT resonance lies above the particle threshold and, therefore, does not contribute. At present, the modelling is based on (1p-1h) RPA calculations only, whose capability to describe the response below the main GT resonance is questionable. However, the corresponding GT-strength distributions can be measured with high resolution even in heavy nuclei utilizing the  $(^3\text{He}, t)$  reaction at intermediate energies under zero degree (see e.g. [5]). Measurements of the  $^{138}\text{Ba}(^3\text{He}, t)^{138}\text{La}$  and  $^{180}\text{Hf}(^3\text{He}, t)^{138}\text{Ta}$  reactions have been performed at RCNP, Osaka. The resulting B(GT) strength distributions and their astrophysical implications are presented.

- [1] F. Käppeler et al., Phys. Rev. C 69, 055802 (2004).
- [2] M. Arnould, S. Goriely, Phys. Rep. 384, 1 (2003).
- [3] A. Heger et al., Phys. Lett. B 606 258 (2005).
- [4] S. Goriely et al. Astronomy Astrophys. 375, L35 (2001).
- [5] Y. Kalmykov et al., Phys. Rev. Lett. 96, 012502 (2006).

## 20.22 Measurement of the $^{62}\text{Ni}(n, \gamma)^{63}\text{Ni}$ reaction cross section at $3 < E_n < 100$ keV

NAGAI, Yasuki, TEMMA, Yasuyuki, SEGAWA, Mariko, SHIMA, Tatushi, OHTA, Takeshi, NAKAYOSI, Akira, and FUJIMOTO, Sinya

Research Center for Nuclear Physics, Osaka University

According to a recent nucleosynthetic yield estimation of massive stars of solar metallicity, several Ni isotopes  $^{61}\text{Ni}$ ,  $^{62}\text{Ni}$  and  $^{64}\text{Ni}$  are overproduced, although most calculated isotopic yields from  $A = 16$  to  $A = 90$  are in good agreement with solar abundances [1,2,3]. One of the largest overproduction factors is  $^{62}\text{Ni}$ . The origin of overproduction is considered to be due to residual uncertainties in stellar models and/or nuclear physics inputs such as the neutron capture cross section of Ni isotopes at stellar temperatures. Concerning the neutron capture cross section, quite recently a new MACS of  $28.4 \pm 2.8$  mbarn has been obtained at  $kT = 25$  keV using an activation method [4]. While, we have measured the cross section at  $6 < E_n < 90$  keV by employing a prompt discrete  $\gamma$ -ray detection method using an anti-Compton NaI(Tl) spectrometer. The MACS at 30 keV derived using the result is  $37.0 \pm 3.2$  mbarn, which is 60% larger than the value based on the activation method [5]. Since the cross section of the  $^{62}\text{Ni}(n, \gamma)^{63}\text{Ni}$  is claimed to affect not only for  $^{62}\text{Ni}$  but also for the synthesis of many other isotopes between  $A = 63$  and 80 significantly, it is very important to solve the discrepancy of the reported values mentioned. In the previous measurement, we have not measured the cross section in the neutron energy region at the 4.5 keV strong s-wave resonance state, and we derived the MACS mentioned with use of the evaluated value JENDL together with our data. In the present study, we aimed at measuring the cross section in the neutron energy range from 2 to 100 keV by employing the same prompt gamma-ray detection method mentioned. We will discuss the results of the present experiment.

- [1] F. X. Timmes, S. E. Woosley, and T. A. Weaver, ApJA, 98, 617 (1995)
- [2] T. Rauscher, A. Heger, R.D.Hoffman, and S. E. Woosley, Astrophys. J. 576, 323 (2002)
- [3] S. E. Woosley, A. Heger, T. Rauscher and R. D. Hoffman, Nucl.Phys.A718 (2003) 3c.
- [4] H. Nassar et al., Phys.Rev.Lett.94, 092504-1 (2005).
- [5] A. Tomyo, Y. Temma, M. Segawa, Y. Nagai, H. Makii, T. Shima, T. Ohsaki, and M. Igashira, ApJ. 623, L153 (2005).

## 20.23 Study of unbound $^{19}\text{Ne}$ states via the proton transfer reaction $^2\text{H}(^{18}\text{F}, \alpha+^{15}\text{O})\text{n}$

ADEKOLA, A.<sup>1</sup>, BRUNE, C. R.<sup>1</sup>, HEINEN, Z.<sup>1</sup>, HORNISH, M. J.<sup>1</sup>, MASSEY, T. N.<sup>1</sup>, VOINOV, A. V.<sup>1</sup>, BARDAYAN, D. W.<sup>2</sup>, BLACKMON, J. C.<sup>2</sup>, NESARAJA, C. D.<sup>2</sup>, SMITH, M. S.<sup>2</sup>, CHAE, K.<sup>3</sup>, MA, Z.<sup>3</sup>, CHAMPAGNE, A. E.<sup>4</sup>, VISSER, D. W.<sup>4</sup>, JONES, K. L.<sup>5</sup>, PAIN, S. D.<sup>5</sup>, THOMAS, J. S.<sup>5</sup>, GREIFE, U.<sup>6</sup>, LIVESAY, R.<sup>6</sup>, PORTER-PEDEN, M.<sup>6</sup>, SARAZIN, F.<sup>6</sup>, JOHNSON, M.<sup>7</sup>, DOMIZIOLI, C.<sup>8</sup>, KOZUB, R. L.<sup>8</sup>, MOAZEN, B.<sup>8</sup>, SHRINER, J. F.<sup>8</sup>, and SMITH, N.<sup>8</sup>

<sup>1</sup>Ohio University, <sup>2</sup>Oak Ridge National Laboratory, <sup>3</sup>University of Tennessee, <sup>4</sup>University North Carolina - Chapel Hill, <sup>5</sup>Rutgers, <sup>6</sup>Colorado School of Mines, <sup>7</sup>Oak Ridge Associated Universities, <sup>8</sup>Tennessee Technological University

The nuclear structure of  $^{19}\text{Ne}$  near the proton threshold is of interest for understanding the rates of proton-induced reactions on  $^{18}\text{F}$  in novae. The proton transfer reaction  $^{18}\text{F}(d, n)^{19}\text{Ne}$  has been measured by bombarding a  $720\text{-}\mu\text{g}/\text{cm}^2$   $\text{CD}_2$  target with a 150-MeV  $^{18}\text{F}(9^+)$  beam at ORNL's Holifield Radioactive Ion Beam Facility. The  $^{19}\text{Ne}$  states of interest near the proton threshold decay by breakup into  $\alpha + ^{15}\text{O}$  which were detected in coincidence with position-sensitive E -  $\Delta E$  Si telescopes. The reconstruction of the relative energy reveals the excited states of  $^{19}\text{Ne}$  which are populated. In addition the direction of the undetected neutron can be determined. The mirror reaction  $^2\text{H}(^{18}\text{F}, \alpha+^{15}\text{N})p$  has been measured simultaneously. The implications for the  $^{18}\text{F}(p, \alpha)^{15}\text{O}$  reaction and  $^{19}\text{Ne}$ - $^{19}\text{F}$  mirror symmetry will be discussed.

*Work supported in part by the U.S. Department of Energy and National Science Foundation.*

## 20.24 Multiple particle break-up studies in the neutron rich Li isotopes

MADURGA FLORES, Miguel<sup>1</sup>, GARCIA BORGE, Maria Jose<sup>1</sup>, FYNBO, Hans<sup>2</sup>, JONSON, Bjorn<sup>3</sup>, NYMAN, Goran<sup>3</sup>, PREZADO, Yolanda<sup>4</sup>, and RIISAGER, Karsten<sup>5</sup>

<sup>1</sup>Consejo Superior de Investigaciones Cientificas (CSIC), <sup>2</sup>University of Aarhus, <sup>3</sup>Chalmers University of Technology, <sup>4</sup>Universidad de Santiago, <sup>5</sup>CERN

Light nuclei have been studied intensively as they are good laboratories to understand the nuclear structure and some are relevant for the stellar nucleosynthesis. Near the neutron drip-line, the complexity of their decays represent a challenge for experimentalists to extract structural information of the states involved as the high Q-beta values and low nucleon binding energies open several decay channels. The  $^9\text{Li}$  decay is a perfect example of this behaviour, the levels populated in the daughter,  $^9\text{Be}$ , above the  $\alpha + \alpha + n$  threshold decay preferentially through resonance in  $^8\text{Be}$ , although decay through  $^5\text{He}$  has also been suggested [1,2]. It is of interest determining the different decay channels, as the low-lying unbound states in  $^9\text{Be}$  play a role in the formation of  $^9\text{Be}$  in stellar scenario. The formation of  $^{12}\text{C}$  through  $\alpha(\alpha + n, \gamma)^9\text{Be}$  followed by  $^9\text{Be}(\alpha, n)^{12}\text{C}$  can compete with the triple  $\alpha$  reaction in neutron rich stellar scenarios. The  $^5\text{He}(\alpha, \gamma)^9\text{Be}$  reaction is suggested [2,3] to contribute to the synthesis of  $^9\text{Be}$ , but the lack of experimental information of the  $^9\text{Be}^*$  decay through the  $^5\text{He}$  channel makes very difficult to include this channel in the reaction rate calculations. We report here on the study of the multiple particle break-up of states populated in the  $^9\text{Li}$  and  $^{11}\text{Li}$  beta decays. The aim of the experiment is to disentangle the multiple particle break-up channels taking advantage of the new segmented silicon detectors. The simultaneous detection of the particle energy and direction is crucial to determine the correct decay scheme. The experimental set-up was designed to fulfill this condition and consisted of four DSSSD detectors in a compact cubic geometry. The highly segmented nature of the DSSSD allows to reconstruct the particle momenta from their impinging position and their energy. Previous studies done recently on the  $^9\text{Li}$  and  $^9\text{C}$  decays showed that the complete kinematics analysis of the outgoing particles allows to determine the decay channel unequivocally. In one of our previous studies [4] the decay through the  $^5\text{He}$  resonance of low lying levels in  $^9\text{Be}$  has been successfully identified. We report here on an extension of this work to the break-up of the 2.43 MeV state in  $^9\text{Be}$ , for which the partial branches are well known but the decay mode remains controversial. Furthermore the study of the  $^{11}\text{Be}$  states that break into two charged particles in the final state will be presented. Special attention is given to the  $^6\text{He} + \alpha + n$  channel. The coincidence spectrum and reconstructed excitation energy of this channel will be shown. Identification of the  $2\alpha + 3n$  channel will be discussed.

- [1] G. Nyman et al., Nucl. Phys. A 510 (1990)189.
- [2] L. Buchmann et al., Phys. Rev. C 63 (2001)034303.
- [3] P. Descouvemont, Eur. Phys. J. A. 12 (2001)413.
- [4] Y. Prezado et al., Phys. Lett. B 576 (2003)55; Phys. Lett. B 618 (2005)43.

## 20.25 Activation method for cross section measurements related to $p$ -process nucleosynthesis

ÖZKAN, Nalan  
Kocaeli University

The 35 stable nuclei with the atomic number  $Z < 34$  located at neutron deficient side of valley of beta-stability are called as  $p$ -nuclei and are produced by so called  $p$  process.  $p$ -process nucleosynthesis proceeds mainly via a series of photon induced reactions  $(\gamma, n)$ ,  $(\gamma, p)$ , or  $(\gamma, \alpha)$  in the astrophysical environment. A large reaction network involving thousands of reaction rates is required to describe the  $p$ -process nucleosynthesis. Since, so far most of these reactions are not accessible experimentally, these reaction rates mainly rely on the Hauser Feshbach statistical model. Therefore, cross section measurements for proton and alpha induced reactions are crucial for the  $p$ -process nucleosynthesis and for testing the recent statistical model predictions of Hauser Feshbach. However, most  $\gamma$ -induced reactions are very difficult to measure directly. Instead, they can be measured by activation method and calculated from the inverse of the charge particle induced cross sections using the detailed balance theorem. The primary aim of this paper is to describe the activation method and the status of experimental cross section measurements of radiative particle capture reactions by means of the activation method. The experimental database obtained by activation method up to now and what can be done in the future for the  $p$  process are also given.

## 20.26 Activation measurement of the $^{19}\text{F}(n, \gamma)^{20}\text{F}$ cross section at $kT = 25$ keV

UBERSEDER, Ethan<sup>1</sup>, HEIL, Michael<sup>1</sup>, KÄPPELER, Franz<sup>1</sup>, GÖRRES, Joachim<sup>2</sup>, and WIESCHER, Michael<sup>2</sup>

<sup>1</sup>Forschungszentrum Karlsruhe, <sup>2</sup>University of Notre Dame

Much progress has been made in the study of the production and destruction mechanisms of  $^{19}\text{F}$ . Recent model simulations indicate that the  $^{19}\text{F}(n, \gamma)^{20}\text{F}$  reaction could be the primary destruction channel for fluorine during the thermal pulses of AGB stars, therefore an accurate determination of the neutron capture cross section is of great importance. An activation measurement of the neutron capture cross section of  $^{19}\text{F}$  has been performed at a stellar temperature of  $kT = 25$  keV using the Karlsruhe 3.7 MV Van de Graaff accelerator. The short half life of  $^{20}\text{F}$  ( $t_{1/2} = 11$  s) required the employment of the fast cyclic activation technique. A preliminary analysis indicates a significantly lower neutron capture cross section at  $kT = 25$  keV than is suggested in the current literature. The new measurement also greatly reduces the quoted uncertainty of 20%.

## 20.27 The late-time supernova evolution induced by anisotropic neutrino radiation and the $r$ -process environment

MOTIZUKI, Yuko and MADOKORO, Hideki  
RIKEN

To study the late-time evolution of a core-collapse supernova explosion induced by globally anisotropic neutrino radiation, we have completely revised our hydrodynamical simulation code [1]. In particular, neutrino heating and cooling processes were carefully coordinated for this purpose and the fall back effect was crucially included through the shock heating of the fall-back matter by attacking the hard surface of the protoneutron star. Our special focus will be paid on the late-time evolution of the emerged hot bubble over 10 seconds after the explosion. We will discuss in our 2-D calculations the effect of heating process by electro-neutrino scattering which has been known in the models of spherical explosion [2] to play an important role to generate a great deal of entropy within the bubble, leading to a successful  $r$ -process nucleosynthesis. We will further discuss the

effect of the inner shock heating mentioned above and will compare our 2-D results with those obtained by Fryer and Hungerford [3].

- [1] H. Madokoro, T. Shimizu, and Y. Motizuki, Pub. Astron. Soc. Japan, 56 (2004) 663; H. Madokoro, T. Shimizu, and Y. Motizuki, ApJ 592 (2003), 1035.
- [2] S.E. Woosley et al. ApJ 433 (1994), 229.
- [3] C.L. Fryer and A. Hungerford, in proceedings of the first Argonne/MSU/JINA/INT RIA workshop on the r-process: The astrophysical origin of the heavy elements and related Rare Isotope Accelerator physics, eds. Y.-Z. Qian et al. (World Scientific) pp.234-243 (2004).

## 20.28 Nucleosynthesis in AGB stars: results from the STARS code

STANCLIFFE, Richard<sup>1</sup>, LUGARO, Maria<sup>2</sup>, and TOUT, Christopher<sup>1</sup>

<sup>1</sup>Institute of Astronomy, Cambridge, <sup>2</sup>Sterrenkundig Instituut Utrecht

Recent calculations with the stellar evolution code STARS (Eggleton 1971, Pols et. al. 1995) have yielded interesting results for AGB stars. The code has been shown to predict deeper dredge-up at lower core mass than other evolution codes (Stancliffe, Tout and Pols 2004). If material is dredged-up sooner, it may not have been exposed to temperatures high enough to activate the <sup>22</sup>Ne neutron source and hence could display distinguishable *s*-process signatures. To investigate the nucleosynthesis of light elements, we employ a network of 40 isotopes from D to <sup>34</sup>S plus important iron group isotopes. The *s* process is investigated using a post-processing technique. The results of these nucleosynthesis calculations are compared to known constraints from spectroscopic observations and pre-solar grain measurements.

## 20.29 E2 and E1 cross section of the <sup>12</sup>C( $\alpha, \gamma$ )<sup>16</sup>O reaction obtained at $E_{\text{cm}} = 1.6$ and 1.4 MeV

MAKII, Hiroyuki<sup>1</sup>, NAGAI, Yasuki<sup>2</sup>, SHIMA, Tatushi<sup>2</sup>, SEGAWA, Mariko<sup>2</sup>, UEDA, Hitoshi<sup>2</sup>, MASAKI, Tomohiro<sup>3</sup>, and MISHIMA, Kenji<sup>4</sup>

<sup>1</sup>Japan Atomic Energy Agency, <sup>2</sup>Research Center for Nuclear Physics, Osaka University, <sup>3</sup>Physics department, Kobe University, <sup>4</sup>RIKEN

We have installed a new system to measure the  $\gamma$ -ray angular distributions of the <sup>12</sup>C( $\alpha, \gamma$ )<sup>16</sup>O reaction at the 3.2 MV Pelletron accelerator laboratory at Tokyo Institute of Technology [1]. A typical averaged  $\alpha$ -beam intensity, we can use, is about 8  $\mu$ A at the repetition rate of 4 MHz, and its pulse width is 1.9 ns. The system is comprised of three high efficiency anti-Compton NaI(Tl) spectrometers. Each spectrometer comprises of a central NaI(Tl) detector with a diameter of 22.9 cm and a length of 20.3 cm, and an annular NaI(Tl) detector with an outer diameter of 33 cm and a length of 27.9 cm. With use of the spectrometer together with the intense pulsed beam, we can separate clearly the <sup>12</sup>C( $\alpha, \gamma$ )<sup>16</sup>O reaction events from neutron background events due to the <sup>12</sup>C( $\alpha, \gamma$ )<sup>16</sup>O reaction. In the present study, we have measured the angular distribution of the  $\gamma$ -ray from the  $\alpha$  capture by <sup>12</sup>C feeding to the ground state in <sup>16</sup>O at  $E_{\text{cm}} = 1.6$  MeV and 1.4 MeV by means of the spectrometers. Enriched <sup>12</sup>C targets with thicknesses of 300 to 400  $\mu\text{g}/\text{cm}^2$  have been made to be strong enough against intense  $\alpha$  beams by a thermal cracking of methane gas. The targets were bombarded with intense alpha beams, and they lasted at least for one day without having any problems. The Rutherford backscattering spectrum of  $\alpha$ -particles from the enriched <sup>12</sup>C targets has been measured by means of a Si detector to obtain an incident alpha- beam intensity and the target thickness, and to monitor any change of the targets during beam irradiation. We will discuss the obtained absolute E1 and E2 differential cross sections of the  $\gamma$ -ray determined by taking account of energy and angular dependence of the differential cross section.

- [1] H. Makii et al, Nucl. Instr. Methods. A 547, 411 (2005).

### 20.30 Signatures of AGB nucleosynthesis in dwarf galaxies

FENNER, Yeshe

Harvard-Smithsonian Center for Astrophysics

The chemical evolution of local group dwarf spheroidals and irregulars is simulated using models incorporating feedback from Type II and Ia supernovae. Particular attention is paid to the abundance pattern of heavy neutron-capture elements in order to assess the contribution of AGB stars to metal enrichment in low-mass galaxies. We find that metal-enrichment from low and intermediate-mass stars is needed to explain the *s*-process abundance trends seen in local group dwarf spheroidals, and we discuss the consequences of these results on the nature of the  $^{13}\text{C}$  pocket in AGB stars.

### 20.31 Single point off-center helium ignitions as origin of some type Ia supernovae

FORCADA, Ramon, GARCÍA-SENZ, Domingo, and JOSÉ, Jordi

Universitat Politècnica de Catalunya

We present a set of new hydrodynamical calculations concerning the so-called Sub-Chandrasekhar mass models for Type Ia supernovae. The hydrodynamical evolution after off-center helium runaway is followed using a two-dimensional SPH hydrocode with higher resolution than precedent multi-dimensional calculations. In addition, the better resolution allows us to explore an interesting variation of the standard scenario which arises from the fact that helium may detonate at some height above the interphase between carbon and helium layers. In this case the outcome could be the off-center detonation of carbon near the interphase, leading to a different evolution of the explosion. A comparison between the energetics and ejected isotopic yields of several calculated models is provided.

### 20.32 Fission recycling in the *r* process and formation of the second peak with $A \sim 130$

PANOV, Igor<sup>1</sup> and KORNEEV, Ivan<sup>2</sup>

<sup>1</sup>Institute for Theoretical and Experimental Physics, Moscow, <sup>2</sup>Moscow Institute of Physics and Technology

We discuss the influence of mass predictions and mass distribution of fission products on the formation of heavy elements that occurs on the final stages of the *r* process recycled due to fission in a high neutron density environment (e.g. neutron star mergers). The fission recycling is expected to be of significance when the *r*-process duration becomes long enough to transform the major part of seeds into the transuranium nuclei followed by the restitution of fission fragments into the *r* process. In this case the mass distribution of fission products (along with the consistent nuclear data such as the mass predictions, fission barriers and reaction rates) can be important for the production of nuclei with  $A \sim 130$ . In our *r*-process calculations, we use the new mass-predictions and fission barriers (Myers, Swiatecki, 1999; Mamdouh et al., 2001). The fission rates were taken from Panov et al., 2005. We conclude that a simple two-fission-fragment model can not describe well the position of the second peak of the abundance curve. This peak occurs because the neutron separation energy calculated on the base of new mass predictions depends on neutron excess more smoothly than it was suggested before. As a result, the neutron drip-line turns out to be shifted to heavier nuclei. Thus, more heavier isotopes for the same atomic number are formed and the masses of the most fission fragments exceed 130. Consequently, the shape of the second peak does not reproduce the observed one. We showed that the agreement between calculations and observations can be achieved due to allowing for the instantaneous fission neutrons which were neglected in previous considerations. Finally, a model for neutron multiplicity during fission, based on the nuclear systematics, as well as other channels of removal of the "redundant" mass are discussed.

### 20.33 Neutrino-induced nucleosynthesis as a probe into the mechanism of supernovae

NADYOZHIN, Dmitriy and PANOV, Igor

Institute for Theoretical and Experimental Physics, Moscow

The neutrino nucleosynthesis yields depend on a number of factors. Apart from the onion-like presupernova chemical structure, they are sensitive to temporal and spectral properties of the neutrino "light curve" and to such hydrodynamic parameters as the supernova explosion energy and the delay in passing of the shock wave through successive presupernova chemical shells. Moreover, possible intrusions of other chemicals into the shells (e.g., hydrogen into the helium shell) can appreciably modify the final yields. We report the results of our systematic quantitative study of all these effects with special attention to the supernova explosion energy and characteristic time of the neutrino flux.

### 20.34 Nuclear structure properties of neutron-rich $r$ -process isotopes

WOEHR, Andreas<sup>1</sup>, QUINN, Matthew<sup>1</sup>, APRAHAMIAN, Ani<sup>1</sup>, MANTICA, Paul<sup>2</sup>, PEREIRA CONCA, Jorge<sup>2</sup>, SCHATZ, Hendrik<sup>2</sup>, HENNRICHS, Stefan<sup>3</sup>, KRATZ, Karl-Ludwig<sup>3</sup>, and The NSCL-MSU-03034-05028-COLLABORATION

<sup>1</sup>University of Notre Dame, <sup>2</sup>NSCL, Michigan State University, <sup>3</sup>Institut für Kernchemie, Universität Mainz

Gross  $\beta$ -decay properties, such as half-lives and delayed-neutron emission probabilities of neutron-rich nuclei in the Ge-Kr region may contain first indication of a phase transitions from spherical to deformed shapes. This is a very interesting field of experimental and theoretical investigations of nuclear structure with consequences for nuclear astrophysics. In this regions, the structure of nuclei with unusual combinations of proton and neutron numbers is of particular interest. Rapid phase transitions, exotic symmetries and new pronounced shell gaps leading to new magic numbers may occur in this area. For example, neutron-rich nuclei in the region of the  $Z = 40$  zirconium isotopes offer an unusually large number of shapes, excitation modes and (sub-)shell closures within a small mass range. In the past, the region between the classical shell closure at  $N = 50$ , via the local spherical  $d_{5/2}$  sub-shell at  $N = 56$  and the sudden onset of deformation at  $N = 60$ , up to about neutron mid-shell has been studied mainly at small ISOL facilities [1-2] and by spontaneous-fission of trans-uranium nuclei using  $\gamma$ -detector arrays such as Gammasphere. We have launched an experimental campaign at the A1900 Fragment Separator at the National Superconducting Cyclotron Laboratory (NSCL) of the Michigan State University (MSU) to study neutron-rich isotopes in the Ge-Br and in the Sr-Mo region. Preliminary experimental results as well as studies on how the these gross  $\beta$ -decay properties can influence the modeling of the  $r$  process in this interesting region will be presented.

*This work was supported by: NSF PHY 04-57120 (Notre Dame), NSF PHY02-16783 (JINA), NSF PHY 01-10253 (NSCL) and HGF Vistars (Mainz)*

- [1] Proc. Int. Workshop on Nuclear Structures of the Zirconium Region, April 1988, Bad Honnef, Germany, (J. Eberth, R.A. Meyer, K. Sistemich, Eds.); Research Reports in Physics, Springer Verlag
- [2] Proc. 6th Int. Conf. Nuclei far from Stability and 9th Int. Conf. on Atomic Masses and Fundamental Constants; July 1992, Bernkastel-Kues, Germany; (R. Neugart, A. Woehr, Eds.); Inst. Phys. Conf. Ser. 132 (1993)

### 20.35 Measurement of the temperature dependence of ${}^7\text{Be}$ decay in different chemical environments

LIMATA, Benedicta Normanna

Seconda Università di Napoli and INFN

In stellar environment,  ${}^7\text{Be}$  is produced by  ${}^3\text{He}(\alpha, \gamma){}^7\text{Be}$  and destroyed by  ${}^7\text{Be}(p, \gamma){}^8\text{B}$ , which is responsible of the high energy solar neutrino flux, or, in competition, by its decay to  ${}^7\text{Li}$  by

electron capture. The decay of  ${}^7\text{Be}$  populates either the  ${}^7\text{Li}$  ground state or, in 10% of the cases, the first excited state, which decays to the ground state emitting a 478 keV  $\gamma$ -ray. The decay probability depends on the electronic density at the  ${}^7\text{Be}$  nuclei. The enhancement of the electron screening observed in low energies nuclear reactions induced in metallic targets in the framework of the Drude-Debye model show that the quasi-free electrons in metals modify the electron density around nuclei. In this model, the free metallic electrons screen the nuclear charge at a distance far below the atomic radius. According to the temperature dependence of the Drude-Debye radius, the screening effect is enhanced at low temperature. In order to investigate the effect of the free electron density on the  ${}^7\text{Be}$  decay, the variation of the  ${}^7\text{Be}$   $\gamma$ -emission rate at 10 K respect to room temperature was measured in both metallic and non-metallic environment. The  ${}^7\text{Be}$  samples were obtained implanting a pure radioactive  ${}^7\text{Be}$  ion beam delivered by the CIRCE 3 MV Tandem in Caserta (Italy). The necessary  ${}^7\text{Be}$  was produced via  ${}^7\text{Li}(p,n){}^7\text{Be}$  at the ATOMKI Cyclotron of Debrecen (Hungary).  ${}^7\text{Be}$  implantation was performed in Indium and Palladium metallic targets. A non-metallic sample was obtained using a  ${}^7\text{BeO}$  layer on the surface of a silicon backing. The results of this experiment are presented and discussed.

### 20.36 Astrophysics at the future Rare Isotope Accelerator

SMITH, Michael<sup>1</sup>, SCHATZ, Hendrik<sup>2</sup>, TIMMES, Frank<sup>3</sup>, WIESCHER, Michael<sup>4</sup>, and GREIFE, Uwe<sup>5</sup>

<sup>1</sup>Oak Ridge National Laboratory\*, <sup>2</sup>National Superconducting Cyclotron Laboratory, Michigan State University, and Joint Institute for Nuclear Astrophysics, <sup>3</sup>Los Alamos National Laboratory, <sup>4</sup>Univ. Notre Dame and Joint Institute for Nuclear Astrophysics, <sup>5</sup>Colorado School of Mines

The Astrophysics at RIA (ARIA) Working Group has been established to develop and promote the nuclear astrophysics research anticipated at the Rare Isotope Accelerator (RIA). RIA is a next-generation nuclear science facility in the U.S. that will produce intense beams of unstable nuclei via both projectile fragmentation and ISOL techniques, as well as by a hybrid technique involving fragmentation, gas stopping, ionization, and reacceleration. RIA is currently envisioned to have large experimental halls with state-of-the-art detector systems that access beams with energies ranging from unaccelerated to over 15 MeV/amu. Measurements with unstable beams from RIA beams will enable significant progress in studies of core collapse supernovae, thermonuclear supernovae, X-ray bursts, novae, and other astrophysical sites. The Working Group is discussing the most important science questions to address at RIA, devising sets of representative experiments and associated equipment, and helping to build a broad, interdisciplinary community in nuclear astrophysics to take full advantage of RIA. Details of the science, experiments, facility, organization, and Working Group documents and website ([ariaweb.org](http://ariaweb.org)) will be presented. Many of the issues and science addressed by the Working Group are relevant for other advanced radioactive beam facilities such as the RIKEN RI Beam Factory, the planned GSI FAIR facility, and others.

\* ORNL is managed by UT-Battelle, LLC, for the U.S. Department of Energy under contract DE AC05-00OR22725.

### 20.37 Neutron capture during the freeze-out of the $r$ process

FAROUCI, Khalil<sup>1</sup>, KRATZ, Karl-Ludwig<sup>1</sup>, PFEIFFER, Bernd<sup>1</sup>, THIELEMANN, Friedrich-Karl<sup>2</sup>, and RAUSCHER, Thomas<sup>2</sup>

<sup>1</sup>Johannes Gutenberg-Universität Mainz, <sup>2</sup>Universität Basel

In order to study possible neutron-capture effects during an  $r$  process, it is necessary to perform fully dynamical simulations. We have performed such calculations within the model of an adiabatically expanding high-entropy bubble of a SN II, using improved nuclear-physics data (see [1,2,3]) and temperature-dependent reaction rates including the NON-SMOKER neutron-capture rates (see [4]). In agreement with earlier results (see, e.g. [5]), we find that due to the  $(n, \gamma)$ - $(\gamma, n)$  equilibrium established at the onset of the  $r$  process, only late-time neutron captures during the freeze-out phase are important. Since the uncertainties in the theoretical neutron capture rates are large, we have scaled the "standard" NON-SMOKER rates up and down by a two orders of magnitude, respectively. At low entropy, typical e.g. for the formation of the  $A = 130$  solar-system  $r$ -abundance peak, the freeze-out is fast. Therefore, even a change of all neutron-capture rates

in a range of 4 orders of magnitude will not alter the final abundances significantly. However, the freeze-out at higher entropies, e.g. for conditions that form the REE (rare-earth elements) "pygmy" peak and the  $A = 195$  abundance peak, is lower and can alter the final abundances of heavy nuclei. For example, the abundance "trough" before the 3<sup>rd</sup> peak, obtained when assuming an instantaneous freeze-out, can be filled with such late captures of "primary" neutrons. Furthermore, we have also studied the effects from late re-captures of neutrons emitted after  $\beta$ -decay of short-lived isotopes during the decay back to stability. Similar to the effects observed for the late non-equilibrium capture of the "primary" neutrons, also the delayed neutrons have no effect on the final abundances in the  $A = 130$  peak area, and lead only to minor alterations of the abundances in the heavy REE and the  $A = 195$  peak regions.

- [1] Audi, G. et al. NUBASE Nucl. Phys. A279, 1 (2003)
- [2] Pfeiffer, B. et al., Prog. Nucl. Energy 41, 39 (2002)
- [3] Möller, P. et al., Phys. Rev. C67, 055802 (2003)
- [4] Rauscher, T. and Thielemann, F.-K., Atomic Data Nucl. Data Tables 75, 1 (2000)
- [5] Freiburghaus, C., et al., Ap. J. 516, 381 (1999)

## 20.38 Astrophysical implications of the $^{139}\text{La}(n, \gamma)$ and $^{151}\text{Sm}(n, \gamma)$ cross sections measured at n\_TOF\*

STEFANO, Marrone<sup>1</sup> for the n\_TOF collaboration

<sup>1</sup>INFN-Bari

The  $(n, \gamma)$  cross sections of  $^{139}\text{La}$  and  $^{151}\text{Sm}$  have been measured over a wide energy range at the n\_TOF facility by means of the time-of-flight technique. Neutrons were produced by spallation reactions, and the prompt capture gamma-rays were detected with  $\text{C}_6\text{D}_6$  scintillators. The experimental results are presented with particular emphasis on the deduced Maxwellian averaged cross sections (MACS), which are determined for the full range of thermal energies relevant for  $s$ -process studies. The astrophysical implications of these results will be discussed in detail. Since the small capture cross section of the neutron magic nucleus  $^{139}\text{La}$  acts as a bottleneck for the reaction flow, it leads to the build-up of a large  $s$ -process abundance, well suited for monitoring the  $s$ -process production at different sites. On the other hand, the  $r$  process can be characterized by elements with a very small  $s$ -process component, e.g. by Eu. The cross section of the unstable isotope  $^{151}\text{Sm}$  ( $T_{1/2} = 93$  yr) is important for analyzing the  $s$ -process branchings in the Sm-Eu-Gd region, which can be used for constraining the thermodynamic conditions during the He burning phases in the evolution of low mass stars on the asymptotic giant branch. Combined with recent spectroscopic observations in low metallicity stars, the more accurate  $s$ -process abundance patterns contribute to an improved picture of nucleosynthesis and galactic chemical evolution.

\* This work has been partially supported by the EC (contract FIKW-CT-200000107) and by the National Institutions partners in the n\_TOF Collaboration.

## 21 Poster session, 29 June

### 21.1 New features in the computational infrastructure for nuclear astrophysics

SMITH, Michael S.<sup>1</sup>, LINGERFELT, Eric J.<sup>1,2</sup>, SCOTT, Jason P.<sup>1,2</sup>, KOURA, Hiroyuki<sup>3</sup>, HIX, W. Raphael<sup>1</sup>, ROBERTS, Luke F.<sup>4</sup>, NESARAJA, Caroline D.<sup>1,2</sup>, CHAE, Kyungyuk<sup>1,2</sup>, BAR-DAYAN, Daniel W.<sup>1</sup>, and BLACKMON, Jeffery C.<sup>1</sup>

<sup>1</sup>Physics Division, Oak Ridge National Laboratory\*, <sup>2</sup>Univ. of Tennessee, <sup>3</sup>Advanced Science Research Center, Japan Atomic Energy Agency, <sup>4</sup>Physics Dept., Colorado College

A Computational Infrastructure for Nuclear Astrophysics has been developed to streamline the inclusion of the latest nuclear physics data in astrophysics simulations. The infrastructure is a platform-independent suite of computer codes that is available online at [nucastrodata.org](http://nucastrodata.org). The user-friendly java interface enables users to: upload their nuclear data; perform simple data evaluation tasks; create reaction rates from cross sections and S-factors; create, access, merge, and manage libraries of cross sections and rates; comment on rates and view comments of others; share

rates with others or keep them private; export libraries; setup and run post-processing element synthesis calculations with new rate libraries; and visualize the simulation results with 1D plots and 2D animated nuclide charts. Some of the newest features include: a mass model evaluator which enables theoretical mass models to be compared to each other and to experimental data; the capability to render movies and export for use in presentations; the ability to quickly compare simulation results with different libraries; commenting on rates and libraries with an email-type interface; upgraded tools for parameterizing reaction rates;  $r$ -process and  $\nu - p$  process sample calculations; and the visualization of reaction flux and time derivatives of abundances. The suites features, as well as its current utilization for nova and X-ray burst modeling, will be discussed.

\* ORNL is managed by UT-Battelle, LLC, for the U.S. Department of Energy under contract DE-AC05-00OR22725.

## 21.2 Monte Carlo simulations of Type I X-ray burst nucleosynthesis

ROBERTS, Luke F.<sup>1</sup>, HIX, W. Raphael<sup>2</sup>, SMITH, Michael S.<sup>2</sup>, and FISKER, Jacob L.<sup>3</sup>

<sup>1</sup>Colorado College, <sup>2</sup>Oak Ridge National Laboratory\*, <sup>3</sup>Joint Institute for Nuclear Astrophysics and Dept. of Physics, Univ. of Notre Dame

A Type I X-ray burst (XRB) is a violent thermonuclear runaway producing an explosion on the surface of an accreting neutron star (NS) in a binary star system. The repetitive outbursts are driven by reactions on proton-rich unstable nuclei via the  $\alpha$ - $p$ - and  $rp$ -processes. Large nuclear burning calculations are necessary to determine the energy generation in XRBs that drives the observed X-ray luminosity. Nucleosynthesis calculations can also estimate the possible contribution of these explosions to the abundances of the rare, low-mass  $p$ -nuclides. We have, for the first time, used a Monte Carlo (MC) approach with a post-processing nucleosynthesis code to understand how the uncertainties in the (mostly unmeasured) input reaction rates influence final nuclear abundances and energy generation throughout an XRB. Temperature and density histories for the post processing calculations were taken from a recent self-consistent, general relativistic, one-dimensional XRB model featuring a 298-isotope nuclear network coupled to hydrodynamics with diffusive heat transport and convection [1]. Post processing calculations were performed 50000 times, each time randomly varying the input reaction rates according to roughly estimated uncertainties. Correlations between the input reaction rates and the energy generation during different phases of the burst were determined, along with reaction rate final abundance correlations. These correlations, useful in determining which of the thousands of relevant reaction rates play the most important role in XRBs, will be presented.

\* ORNL is managed by UT-Battelle, LLC, for the U.S. Department of Energy under contract DE-AC05-00OR22725.

- [1] J. L. Fisker, E. Brown, M. Liebendorfer, H. Schatz, F.-K. Thielemann, Nucl. Phys. A 758 (2005) 447c.

## 21.3 High precision measurements along the $rp$ -process path

GALAVIZ, Daniel  
NSCL/MSU

X-ray burst are thermonuclear runaways on the surface of an accreting neutron star in a close binary system. These scenarios are considered to be the site for the so-called rapid proton capture process ( $rp$  process). Starting from the ashes of the CNO-cycle, peak temperatures upto  $3 \times 10^9$  K allow a series of  $(p, \gamma)$  and  $(\alpha, \gamma)$  reactions, leading to the production of heavier proton-rich species. In order to improve the nuclear physics input along the  $rp$ -process path, a new technique has been developed at the NSCL to measure the energy of resonant states above the proton threshold with high precision. The improved information reduces the uncertainty in the calculation of  $(p, \gamma)$  reaction rates on the investigated nuclei. The experimental setup and recently obtained new results are presented, together with their impact on X-ray burst observables.

## 21.4 On the contribution of classical novae to the $^{26}\text{Al}$ content of the Galaxy

HERNANZ, Margarita<sup>1</sup>, SUADES, Moises<sup>1</sup>, DE SEREVILLE, Nicolas<sup>2</sup>, JOSÉ, Jordi<sup>3</sup>, and MARTINEZ PINEDO, Gabriel<sup>4</sup>

<sup>1</sup>Institut d'Estudis Espacials de Catalunya (IEEC/ICE-CSIC), <sup>2</sup>Centre de Recherche du Cyclotron, UCL, <sup>3</sup>Dept. Física i Enginyeria Nuclear (UPC) and IEEC, <sup>4</sup>GSI

A theoretical analysis of the contribution of classical novae to galactic  $^{26}\text{Al}$ , based on the most recent nova yields, will be presented, with special emphasis on the relative contribution of the various scenarios. The relative amount of  $^{26}\text{Al}$  with respect to  $^{60}\text{Fe}$ , as compared with recent observational results from INTEGRAL/SPI, will be used to constrain the nova contribution to  $^{26}\text{Al}$ .

## 21.5 Neutrino-induced fission on nuclei near the $r$ -process paths

BORZOV, Ivan<sup>1,2</sup>, KELIĆ, Alexandra<sup>2</sup>, LANGANKE, Karlheinz<sup>2,3</sup>, MARTINEZ-PINEDO, Gabriel<sup>2</sup>, and ZINNER, Nikolay<sup>3</sup>

<sup>1</sup>IPPE, <sup>2</sup>GSI, <sup>3</sup>IPA, Arhus

Systematic calculations of the neutrino-induced fission [1,2] are performed in a wide region of  $A > 200$  nuclei near the  $r$ -process paths. The  $\beta$ -strength functions of the Gamow-Teller and first-forbidden transitions are calculated within the continuum QRPA approximation based on nuclear ground state description within the density functional approach [2]. A simultaneous calculations of the  $\beta$ -delayed neutron emission,  $\beta$ -delayed and neutron fission cross sections, as well as the distributions of fission fragments and the number of emitted neutrons are done also.

[1] Y.Qian Astron. J.569 (2002) L103

[2] A. Kelic al. Phys.Lett. B616 (2005) 48

[3] I.N. Borzov Phys.ReV. C67 (2003) 025802

## 21.6 Study of the $^{10}\text{B}(p, \alpha)^7\text{Be}$ reaction through the Trojan Horse Method

GIMENEZ DEL SANTO, Marcelo<sup>1</sup>, GAMEIRO MUNHOZ, Marcelo<sup>1</sup>, ROMANO, S.<sup>2</sup>, CHERUBINI, S.<sup>2</sup>, LAMIA, L.<sup>2</sup>, PUGLIA, S.<sup>2</sup>, SPITALERI, C.<sup>2</sup>, TUDISCO, S.<sup>2</sup>, CARLIN, N.<sup>1</sup>, LIGUORI NETO, R.<sup>1</sup>, M. DE MOURA, M.<sup>1</sup>, A. SOUZA, F.<sup>1</sup>, A. P. SUAIDE, A.<sup>1</sup>, M. SZANTO, E.<sup>1</sup>, and SZANTO DE TOLEDO, A.<sup>1</sup>

<sup>1</sup>Universidade de São Paulo - DFN <sup>2</sup>Laboratori Nazionale del Sud - INFN Catania

The astrophysically relevant  $^{10}\text{B}(p, \alpha)^7\text{Be}$  reaction was indirectly studied by means of the Trojan Horse Method using the  $^2\text{H}(^{10}\text{B}, \alpha^7\text{Be})n$  three body reaction. The experiment was performed at the Pelletron-Linac laboratory in Brazil. The accelerator provided a 27 MeV  $^{10}\text{B}$  beam with  $1 \mu\text{A}$  of intensity and the target is made of deuterated polyethylene ( $\text{CD}_2$ ) with approximately  $190 \mu\text{g}/\text{cm}^2$  thickness. The detection setup consists of one  $\Delta E$  gas detector and two position sensitive silicon detectors placed on opposite sides of the beam covering the laboratory angles  $14^\circ \pm 8^\circ$  and  $14^\circ \pm 6^\circ$ . The astrophysical factor  $S(E)$  for the  $^{10}\text{B}(p, \alpha)^7\text{Be}$  reaction will be extracted from the three body reaction at low neutron momentum. We will present preliminary analysis results indicating the presence of resonances that will be very important for the comparison between the  $S(E)$  extracted from this analysis and the direct measurements.

## 21.7 Neutrino-nucleus cross sections and their role in supernovae\*

BLACKMON, Jeff

Oak Ridge National Laboratory, USA

Neutrinos and the weak interaction play a crucial role in core-collapse supernovae. The dynamics of core collapse and shock formation in supernova models is particularly sensitive to weak-interaction (electron capture) rates during core collapse. The intense neutrino flux from the newly formed proto-neutron star carries away 99% of the total energy released in the explosion, and the weak

interaction rates for these neutrinos with nuclei may influence the propagation of the shock wave through the surrounding stellar layers. Neutrino-nucleus interactions also influence the distribution of isotopes that are synthesized and ejected into the interstellar medium. Terrestrial measurements of the neutrino spectra from a nearby supernova could give particularly valuable information on the conditions deep inside the supernova explosion and provide insights into the properties of the neutrinos themselves, but the interpretation of such measurements also requires an accurate understanding of the interaction rates of neutrinos with detector material. Accurate weak interaction rates are therefore crucial for modeling supernovae and for interpreting terrestrial neutrino measurements. However, neutrino interactions at energies relevant for supernovae (tens of MeV) are quite dependent nuclear structure properties that remain largely unknown for most nuclei. The reliability of theoretical models for neutrino cross sections on most nuclei is uncertain and likely depends upon the quality of available nuclear structure information in the region. Thus far, accurate neutrino cross section measurements have been made on only one nucleus,  $^{12}\text{C}$ . A collaboration,  $\nu$ -SNS, has proposed to build a facility for measurements of neutrino-nucleus cross sections at the Spallation Neutron Source (SNS), currently under construction at ORNL. Detectors are currently being designed that would allow for reuse with multiple nuclear targets, allowing for a cost-effective program of neutrino studies on a wide range of nuclei. The charged-current neutrino cross section for any particular target could be measured with 10% accuracy in less than one year of operation with a 20-ton instrument. The proposed experimental program of cross section measurements at the SNS will be discussed. Results from the current R&D program, including Monte Carlo simulations and detector prototypes, will also be presented.

*\*Oak Ridge National Laboratory is managed by UT-Battelle, LLC, for the U.S. Department of Energy under Contract No. DE-AC05-00OR22725.*

## 21.8 Determination of the astrophysical S factor for the $^{12}\text{N}(p, \gamma)^{13}\text{O}$ reaction from the proton transfer reaction $^{14}\text{N}(^{12}\text{N}, ^{13}\text{O})^{13}\text{C}$

BANU, Adriana, AL-ABDULLAH, Tariq, FU, Changbo, GAGLIARDI, Carl A., MUKHAMEDZHANOV, Akram Z., TABACARU, Gabriel, TRACHE, Livius, TRIBBLE, Robert E., and ZHAI, Yongjun J. Cyclotron Institute, Texas A&M University

The reaction rate for the radiative proton capture on the drip line nucleus  $^{12}\text{N}$  is currently under investigation at the Cyclotron Institute/Texas A&M University using an indirect method. This reaction is important in the hot  $pp$  mode nuclear burning in hydrogen-rich massive objects [1]. Primary beam from the K500 superconducting cyclotron is used to produce in-flight secondary radioactive  $^{12}\text{N}$  beam separated with the recoil spectrometer MARS [2]. We are using the  $^{14}\text{N}(^{12}\text{N}, ^{13}\text{O})^{13}\text{C}$  proton transfer reaction to extract the asymptotic normalization coefficient (ANC) for the virtual decay  $^{13}\text{O} \rightarrow ^{12}\text{N} + p$ , and calculate from it the direct component of the astrophysical S-factor. Preliminary results of the investigation are presented.

[1] M. Wiescher et al., *The Astrophysical Journal*, 343: 352-364, 1989.

[2] R.E. Tribble et al., *Nucl. Phys. A* 701, 278c-281c, 2002.

## 21.9 Lifetime of the 4.03 MeV state in $^{19}\text{Ne}$ and the $^{15}\text{O}(\alpha, \gamma)^{19}\text{Ne}$ reaction rate

KANUNGO, Rituparna<sup>1</sup>, ALEXANDER, T. K.<sup>2</sup>, ANDREYEV, A.N.<sup>1,3</sup>, BALL, G.C.<sup>1</sup>, CHAKRAWARTHY, R.S.<sup>1,3</sup>, CHICOINE, M.<sup>4</sup>, CHURCHMAN, R.<sup>1</sup>, DAVIDS, B.<sup>1</sup>, FORSTER, J.S.<sup>4</sup>, GUJRATHI, S.<sup>4</sup>, HACKMAN, G.C.<sup>1</sup>, HOWELL, D.<sup>5</sup>, JOSÉ, J.<sup>6</sup>, LESLIE, J.R.<sup>7</sup>, MORTON, A.C.<sup>1</sup>, PEARSON, C.J.<sup>1</sup>, RESSLER, J.J.<sup>3</sup>, RUIZ, C.J.<sup>1</sup>, SAVAJOLS, H.<sup>1,8</sup>, SCHUMAKER, M.A.<sup>9</sup>, SUBRAMANIAN, M.<sup>1,10</sup>, TANIHATA, I.<sup>1</sup>, WALDEN, P.<sup>1</sup>, and YEN, S.<sup>1</sup>

<sup>1</sup>TRIUMF, Vancouver BC <sup>2</sup>Deep River, ON <sup>3</sup>Simon Fraser University, Burnaby BC, Canada, <sup>4</sup>Department de Physique, Université de Montréal <sup>5</sup>Simon Fraser University, Burnaby BC <sup>6</sup>Institut d'Estudis Espacials de Catalunya, Barcelona; Departament de Física i Enginyeria Nuclear, Universitat Politècnica de Catalunya <sup>7</sup>Department of Physics, Queen's University, Kingston ON <sup>8</sup>GANIL Caen <sup>9</sup>Physics Department, University of Guelph, Guelph ON <sup>10</sup>University of British Columbia, Vancouver BC

Explosive thermonuclear fusion reactions on the surfaces of accreting compact objects in binary star systems cause the astronomical phenomena of novae and X-ray bursts. At these astrophysical

sites explosive hydrogen burning proceeds through the hot CNO cycle.  $^{15}\text{O}(\alpha, \gamma)^{19}\text{Ne}$  has been identified as one of the possible breakout paths from the hot CNO cycle, leading to the *rp*-process which synthesizes heavy nuclei in X-ray bursts. This reaction proceeds mainly through excited states in  $^{19}\text{Ne}$  above the  $^{15}\text{O} + \alpha$  threshold. Thus, the reaction rate depends on the decay widths of these levels. We report here a determination of the decay width of the important level at 4.03 MeV in  $^{19}\text{Ne}$  from a measurement of its lifetime via the Doppler shift attenuation method. The level was populated using the  $^3\text{He}(^{20}\text{Ne}, \alpha)^{19}\text{Ne}$  reaction at 34 MeV with  $^3\text{He}$  implanted Au foil targets. The recoiling  $^{19}\text{Ne}$  nuclei were stopped in the Au foil and the de-excitation  $\gamma$ -rays were detected in coincidence with  $\alpha$  particles. Combining our lifetime measurement with a recent, independent determination of the lifetimes of this and several other near-threshold states in  $^{19}\text{Ne}$ , we update the astrophysical rate of  $^{15}\text{O}(\alpha, \gamma)^{19}\text{Ne}$ .

### 21.10 Microdynamical effects on momentum distribution in stellar plasmas

FERRO, Fabrizio<sup>1</sup>, QUARATI, Piero<sup>2</sup>, BACHARI, Fatima<sup>3</sup>, and MAERO, Giancarlo<sup>4</sup>

<sup>1</sup>Politecnico di Torino - Dipartimento di Fisica and INFN - Sezione di Torino, <sup>2</sup>Politecnico di Torino - Dipartimento di Fisica, and INFN - Sezione di Cagliari, <sup>3</sup>Politecnico di Torino - Dipartimento di Fisica, <sup>4</sup>GSI

We show that, if a random force is present, microscopic dynamics of ion elastic collisions and quantum effects may sensibly modify the momentum distribution of ions and electrons in stellar plasmas. We also show that a few microscopic interactions among the particles, that are significant in very specific energy intervals, lead to peculiar slight corrections to the usual Maxwell-Boltzmann distribution. All these modifications can be easily taken into account by using the non-extensive statistical mechanics. Consequences on the resonant and non-resonant fusion rates are remarkable and may affect strongly some astrophysical processes. Few examples are reported.

### 21.11 Quantum mechanical ab-initio simulation of the electron screening effect in metal deuteride crystals

HUKE, Armin<sup>1</sup>, CZERSKI, Konrad<sup>1,2</sup>, CHUN, Sang-Min<sup>1</sup>, and HEIDE, Peter<sup>1</sup>

<sup>1</sup>Technische Universität Berlin, <sup>2</sup>University of Szczecin

The electron screening energies of the d+d reactions in metallic environments are grossly enhanced by an order of magnitude in comparison to the case of gaseous D-targets. Hitherto theoretical approaches remain far below the measured quantities of about 300 eV. Analytical models can only operate on averaged material properties. Therefore a first effort was undertaken to simulate the pre-reaction impact with an ab-initio quantum mechanical Hartree-Fock calculation which is able to consider the actual crystal structure. The total electrostatic force between the deuteron in its lattice position and an approaching deuteron was successively computed by means of the shifting electron wave functions leading to the screening energy via path integration. The multiple electron wave functions are constructed adiabatically from a limited basis set within a small crystallite. While the results for the screening energy missed the experimental values clearly the numerical model can already show some general tendencies. Electrons from the adjacent metal atoms migrate to the hydrogen atoms as their density distributions show. In order to abandon more of the necessary simplifications in the model the utilization of a massive parallel supercomputer would be required.

### 21.12 About possible explanations to the lines of radioactive elements in the spectrum of Przybylski's star

YUSHCHENKO, Alexander<sup>1</sup>, GOPKA, Vera<sup>2</sup>, GORIELY, Stephane<sup>3</sup>, NAZARENKO, Victor<sup>2</sup>, and SHAVRINA, Angelina<sup>4</sup>

<sup>1</sup>ARCSEC (Astrophysical Research Center for the Structure and Evolution of the Cosmos), Sejong University, <sup>2</sup>Odessa astronomical observatory, <sup>3</sup>Institut d'Astronomie et d'Astrophysique, Universite Libre Bruxelles, <sup>4</sup>Main astronomical observatory Kiev

The spectra of B-F type peculiar stars contains unidentified lines. The most remarkable example is Przybylski's star (HD101065). The abundances of 60 stable elements are investigated in its atmosphere, but near half of the strong lines can not be identified. We investigate the spectrum of the star using high quality VLT observations. It permits us to show the stratification of chemical elements in the atmosphere and build a new atmosphere model of this star. If the unidentified lines in the spectrum are confirmed to originate from unstable elements, the presence of such elements could possibly be explained in three ways:

- 1) Natural radioactive decays of U and Th and other reactions in the layers of atmosphere with overabundances of Th and U.
- 2) Contamination of the atmosphere by a close Supernova event less than a million year ago.
- 3) Spallation reactions at the stellar surface.

We compare the results of observations with calculated abundance and stratifications of chemical elements. To reproduce the abundances a nuclear reaction network including all nuclei with  $8 \leq Z \leq 102$  is used. 3-D hydrodynamical calculations are used to estimate the stratification.

### 21.13 Heaviest *s*-process elements in the atmospheres of barium stars

LAMBERT, David L.<sup>1</sup>, DRAKE, Natalya A.<sup>2</sup>, GOPKA, Vera F.<sup>3</sup>, YUSHCHENKO, Alexander V.<sup>4</sup>, ROSTOPCHIN, Sergey I.<sup>5</sup>, GALAZUTDINOV, Gazinur A.<sup>6</sup>, HAN, Inwoo<sup>6</sup>, and KIM, Kang Meen<sup>6</sup>

<sup>1</sup>Department of Astronomy, University of Texas, <sup>2</sup>Observatorio Nacional/MCT Rio de Janeiro, <sup>3</sup>Astronomical observatory, Odessa National University, <sup>4</sup>ARCSEC (Astrophysical Research Center for the Structure and Evolution of the Cosmos), Sejong University, <sup>5</sup>McDonald Observatory, University of Texas, <sup>6</sup>Korean Astronomy Observatory, Daejeon

Chemical abundance patterns of barium stars HD 16458, HD 101013, and HD 202109 are presented. More than 50 elements were investigated. Special attention is devoted to the elements from Yb to Pb. Spectrum synthesis is used for the abundance calculations. High resolution spectra were obtained at 2.7 meter telescope of the McDonald Observatory (resolving power  $R=60000$ , signal to noise ratio  $S/N > 400$ ) and at 1.8 meter telescope of the Bohyunsan Observatory, Korea ( $R=80000$ ,  $S/N=150-200$ ).

### 21.14 Evidence of Na enhancement in Hyades giants from high-resolution spectroscopy

SCHULER, Simon, KING, Jeremy, and THE, Lih-Sin  
Clemson University

We present our abundance analysis of high-resolution spectra of red giants and main sequence dwarfs in the Hyades open cluster obtained with the 2.7 m Harlan J. Smith telescope and 2dcoude echelle spectrograph at The McDonald Observatory. Initial results indicate a 0.40 dex enhancement of Na in the giants compared to the dwarfs, possibly indicating the mixing of Ne-Na processed material from shell burning regions into the photospheres of the giants. We discuss this scenario in light of our recent study of O abundances in the Hyades, where we found no evidence of mixing-induced O dilution in the photospheres of the giants, and with respect to the abundances of other elements, including Li.

### 21.15 Multi-channel R-matrix analysis of CNO cycle reactions

SIMPSON, Edward<sup>1</sup>, COSTANTINI, Heide<sup>2</sup>, UGALDE, Claudio<sup>3</sup>, GÖRRES, Joachim<sup>4</sup>, CHAMPAGNE, Arthur<sup>3</sup>, TRAUTVETTER, Hanns-Peter<sup>5</sup>, AZUMA, Richard<sup>6</sup>, and WIESCHER, Michael<sup>4</sup>

<sup>1</sup>University of Surrey, <sup>2</sup>INFN, Genova, <sup>3</sup>University of North Carolina, <sup>4</sup>University of Notre Dame, <sup>5</sup>Institut für Experimentalphysik III, Ruhr-Universität Bochum, <sup>6</sup>University of Toronto

The CNO cycle is the main process for hydrogen burning in stars somewhat more massive than the Sun. The reaction cross sections at Gamow energies are typically in the femto to pico-barn range and are consequently very difficult to measure experimentally. The CNO reaction rates are based on extrapolations of experimental data from higher energies. We have been developing a multi-channel R-matrix code to provide a new and more comprehensive tool for fitting experimental data and making extrapolations to lower energies in all reaction and scattering channels. The  $^{14}\text{N}(p,\gamma)^{15}\text{O}$  reaction is the slowest reaction of the CNO cycle and thus it determines the timescale and energy production rate of CNO burning. Furthermore, this reaction plays an important role in the determination of Globular Cluster age, since the position of the turnoff point from the main sequence in the Hertzsprung Russell diagram is defined by the time scale of CNO burning. We have made a reanalysis of the most recent experimental data on the ground state and the 6.18 MeV transition. We will present the results of the R-matrix calculations and discuss the implications and goals for future measurements. In a second study we performed a re-analysis of the  $^{15}\text{N}(p,\gamma)^{16}\text{O}$  and  $^{15}\text{N}(p,\alpha)^{12}\text{C}$  branching point of the CN cycle. The reaction cross sections determine how much catalytic material passes to higher order cycles. This has an effect on the production of heavier elements, particularly  $^{16}\text{O}$  and  $^{17}\text{O}$ . Simultaneous analysis of both reactions for all channels suggests that the ratio  $\Gamma_\gamma/\Gamma_\alpha$  smaller than previously reported.

### 21.16 Efficient approximations of neutrino physics for three-dimensional simulations of stellar core collapse

LIEBENDÖRFER, Matthias<sup>1</sup>, PEN, Ue-Li<sup>2</sup>, and THOMPSON, Christopher<sup>2</sup>

<sup>1</sup>Universität Basel, <sup>2</sup>Canadian Institute for Theoretical Astrophysics

Neutrino transport in spherically symmetric models of stellar core collapse and bounce has achieved a technically complete level, rewarded by the agreement among independent groups that a multi-dimensional treatment of the fluid-instabilities in the post-bounce phase is indispensable to model supernova explosions. While much effort is required to develop a reliable neutrino transport technique in axisymmetry, we explore neutrino physics approximations and parameterizations for an efficient three-dimensional simulation of the fluid-instabilities in the shock-heated matter that accumulates between the accretion shock and the protoneutron star. We demonstrate the reliability of a simple parameterization scheme in the collapse phase and extend our 3D magneto-hydrodynamical collapse simulations to a preliminary postbounce evolution based on a neutrino leakage scheme. The growth of magnetic fields is investigated.

### 21.17 Abundances of heavy metals and lead isotopic ratios in subluminoous B stars

HEBER, Ulrich<sup>1</sup> and O'TOOLE, Simon<sup>2</sup>

<sup>1</sup>Dr.Remeis-Sternwarte, Astronomisches Institut, Universität Erlangen-Nürnberg, <sup>2</sup>Ango Australian Observatory

We present a detailed abundance analysis of high-resolution ultraviolet echelle spectra of five subdwarf B stars obtained using the Space Telescope Imaging Spectrograph onboard the Hubble Space Telescope. The goal of our observations was to test the hypothesis that pulsations in subluminoous B stars are correlated to the surface abundances of iron-group elements. We determined abundances for 25 chemical elements including the iron group and even heavier elements such as tin and lead using LTE curve-of-growth and spectrum synthesis techniques. Abundances for lead isotopes are derived from very resolution spectra using an UV line of triply ionised lead. As Pb terminates the *s*-process sequence Pb isotopic abundance ratios yield important constraints. It is very difficult to measure them in hot stars. For the first time we were able to measure them in two subluminoous B stars and discuss the results.

### 21.18 Direct measurement of stellar neutron capture rates of $^{14}\text{C}$ and comparison with the Coulomb breakup method

REIFARTH, Rene<sup>1</sup>, HEIL, Michael<sup>2</sup>, PLAG, Ralf<sup>2</sup>, BESSERER, Uwe<sup>2</sup>, DABABNEH, Saed<sup>2</sup>, DÖRR, Lothar<sup>2</sup>, GÖRRES, Joachim<sup>3</sup>, HAIGHT, Robert C.<sup>1</sup>, KÄPPELER, Franz<sup>2</sup>, MENGONI, Alberto<sup>4</sup>, O'BRIEN, Shawn<sup>3</sup>, FORSSEN, Christian<sup>5</sup>, PATRONIS, Nikolas<sup>6</sup>, RUNDBERG, Robert S.<sup>1</sup>, WIESCHER, Michael<sup>3</sup>, WILHELMY, Jerry B.<sup>1</sup>, UBERSEDER, Ethan<sup>2</sup>, and BEER, Hermann<sup>2</sup>  
<sup>1</sup>Los Alamos National Laboratory, <sup>2</sup>Forschungszentrum Karlsruhe, <sup>3</sup>University of Notre Dame, <sup>4</sup>CERN, <sup>5</sup>Lawrence Livermore National Laboratory, <sup>6</sup>University of Ioannina

The neutron capture cross section of  $^{14}\text{C}$  has been shown to be important for several neutron driven nucleosynthesis scenarios. Due to the high neutron abundance it is expected that the  $^{14}\text{C}(n, \gamma)$  reaction competes strongly with other reactions. The  $^{14}\text{C}(n, \gamma)$  reaction is also important to validate  $(n, \gamma)$  cross sections obtained via the inverse reaction by the Coulomb breakup method. In principle,  $^{14}\text{C}$  belongs to the few cases where this correspondence can be validated in a convincingly clean way. So far, the example of  $^{14}\text{C}$  is obscured, however, by discrepancies between several experiments and theory. In this contribution we report on a re-analysis of the direct measurements of the  $^{14}\text{C}(n, \gamma)$  reaction presented at the last NIC conference (Vancouver, 2004). The neutron energies used during the experiment ranged from 30 to 800 keV. The earlier presented disagreement between the direct measurements and the Coulomb breakup method has been resolved.

### 21.19 The roles of nuclear physics during stellar core collapse

HIX, W. Raphael<sup>1,2</sup>, MESSER, O.E. Bronson<sup>1</sup>, BAIRD, Mark L.<sup>2</sup>, LENTZ, Eric J.<sup>2</sup>, and MEZ-ZACAPPA, Anthony<sup>1</sup>

<sup>1</sup>Oak Ridge National Laboratory, <sup>3</sup>Univ. of Tennessee

Nuclear physics plays an important role during the collapse of a massive star and the subsequent supernova. Of particular importance during collapse and shock formation are nuclear electron capture and the nuclear equation of state. The nuclear equation of state controls the nature of the bounce which initially forms the supernova shock while electron capture determines the location where the shock forms. Advances in nuclear structure theory have allowed a more realistic treatment of electron capture in supernovae to be developed. With this new treatment of electron capture on heavy nuclei, we have recently shown that electron capture on these nuclei (masses larger than 50) dominates electron capture on free protons, producing significant changes in the hydrodynamics of core collapse and bounce. We will present explorations of the impact of weak interactions with heavy nuclei in supernovae, focusing on the consequences across the range of supernova progenitors. Examination of the sensitivity of these effects to variations in the electron capture rates will also be presented. Additionally, we will present simulations showing the impact of a variety of nuclear equations of state on supernova shock propagation and the interplay between electron capture and the equation of state.

*This work was made possible by funding from the Scientific Discovery through Advanced Computing Program of the U.S. Department of Energy's Office of Science and the U.S. National Science Foundation (PHY-0244783). ORNL is managed by UT-Battelle, LLC, for the U.S. Department of Energy under contract DE-AC05-00OR22725.*

### 21.20 Neutrinos, fission cycling, and the $r$ process

MCLAUGHLIN, Gail<sup>1</sup>, SURMAN, Rebecca<sup>2</sup>, HIX, William Raphael<sup>3</sup>, and BEUN, Joshua<sup>1</sup>

<sup>1</sup>North Carolina State University, <sup>2</sup>Union College, <sup>3</sup>Oak Ridge National Laboratory

It has long been suggested that fission cycling may play an important role in the  $r$ -process. Fission cycling can only occur in a very neutron rich environment. In traditional calculations of the neutrino driven wind of the core collapse supernova, the environment is not sufficiently neutron rich to produce the  $r$ -process elements. However, we present calculations which show that with a reduction of the electron neutrino flux coming from the supernova, fission cycling does occur and furthermore it produces an abundance pattern which is consistent with the observed  $r$ -process abundance pattern in halo stars. Such a reduction can be caused by active-sterile neutrino oscillations or other

new neutrino physics.

### 21.21 Nucleosynthesis in early proton-rich supernova winds

PRUET, Jason<sup>1</sup>, HOFFMAN, Robert<sup>1</sup>, WOOSLEY, Stan<sup>2</sup>, JANKA, Hans-Thomas<sup>3</sup>, and BURAS, Robert<sup>3</sup>

<sup>1</sup>Lawrence Livermore National Laboratory, <sup>2</sup>University of California, Santa Cruz, <sup>3</sup>Max-Planck-Institut für Astrophysik

One of the outstanding unsolved riddles of nuclear astrophysics is the origin of the so called “*p*-process” nuclei from  $A = 92$  to 126. Both the lighter and heavier *p*-process nuclei are adequately produced in the neon and oxygen shells of ordinary Type II supernovae, but the origin of these intermediate isotopes, especially <sup>92,94</sup>Mo and <sup>96,98</sup>Ru, has long been mysterious. Here we explore the production of these nuclei in the neutrino-driven wind from a young neutron star. We consider such early times that the wind still contains a proton excess because the rates for electron-neutrino and positron captures on neutrons are faster than those for the inverse captures on protons. Following a suggestion by Frohlich et al. (2005), we also include the possibility that, in addition to the protons,  $\alpha$  particles, and heavy seed, a small flux of neutrons is maintained by the reaction  $p(\bar{\nu}, \beta^+)n$ . This flux of neutrons, though small, is critical in bridging the long waiting points along the path of the *rp* process by (*n, p*) and neutron capture reactions. Using the unmodified ejecta histories from a recent two-dimensional supernova model by Janka et al. (2003), we find synthesis of proton-rich nuclei up to <sup>102</sup>Pd. However, if the entropy of these ejecta is increased by a factor of two, the synthesis extends to <sup>120</sup>Te. Still larger increases in entropy, that might reflect the role of magnetic fields or vibrational energy input neglected in the hydrodynamical model, result in the production of numerous *r*-, *s*-, and *p*-process nuclei up to approximately  $A = 170$ , even in winds that are proton-rich.

### 21.22 Compound-nuclear reaction cross sections via Surrogate measurements

ESCHER, Jutta, DIETRICH, Frank, FORSSÉN, Christian, GUEORGUIEV, Vesselin, and HOFFMAN, Rob

Lawrence Livermore National Laboratory

Indirect methods play an important role in the determination of nuclear reaction cross sections. Often the cross section needed for a particular application cannot be measured directly since the relevant energy region is inaccessible or the target is too short-lived. This is particularly true for many reactions of interest to astrophysics. An innovative indirect approach to compound-nuclear reactions, first employed in the 1970s [1], has recently been used to obtain cross sections for neutron-induced fission for various thorium, protactinium, uranium, and plutonium targets via “Surrogate” reactions [2-4]. The feasibility of using the Surrogate approach for neutron-induced reactions involving mass 90-100 and rare earth nuclei is currently being tested. The Surrogate reactions method combines experiment with theory to obtain cross sections for compound-nuclear reactions,  $a + A \rightarrow B^* \rightarrow c + C$ , involving difficult-to-produce targets,  $A$ . In the Surrogate approach,  $B^*$  is produced by means of an alternative (“Surrogate”) reaction, e.g.  $d + D \rightarrow b + B^*$ , and the desired decay channel ( $B^* \rightarrow c + C$ ) is observed in coincidence with the outgoing particle  $b$ . The reaction cross section is then obtained by combining the calculated cross section for the formation of  $B^*$  (from  $a + A$ ) with the measured decay probabilities for this state. While the Surrogate method is very general and can in principle be employed to determine cross sections for many types of compound-nuclear reactions on a large variety of targets, there are various issues that require further study, such as the mechanisms for producing highly-excited, unbound configurations in direct reactions (both transfer and inelastic scattering reactions), the damping of such configurations into a compound nuclear system, the population of available angular-momentum values in a compound nucleus, and their impact on the compound-nuclear decay. This presentation will give a brief outline of the Surrogate approach and the challenges involved in carrying out a complete Surrogate treatment. The assumptions underlying the experimental work carried out so far will be detailed and calculations that test the validity of the approximations employed will be presented.

Prospects for using the Surrogate method to obtain cross sections relevant to the astrophysical  $s$  process will be discussed.

- [1] J.D. Cramer and H.C. Britt, Nucl. Sci. and Eng. 41, 177 (1970); H.C. Britt and J.B. Wilhelmy, *ibid.* 72, 222 (1979).
- [2] W. Younes and H.C. Britt, Phys. Rev. C 67, 024610 (2003), *ibid.* 68, 034610 (2003).
- [3] M. Petit et al., Nucl. Phys. A 735, 345 (2004).
- [4] C. Plettner et al., Phys. Rev. C 71, 051602 (2005); J. Burke et al., LLNL report UCRL-TR-214631 (submitted for publication).

### 21.23 Experimental nuclear astrophysics with recoil mass separators

GIALANELLA, Lucio  
INFN Sezione di Napoli

Radiative capture reactions play a fundamental role in nucleosynthesis and stellar evolution. Most of the data available for such reactions has been gained by means of  $\gamma$  spectroscopy. An attractive alternative is given by the direct detection of the nuclei produced in the reactions, which requires the use of a recoil mass separator to separate the reaction products from the intense incident beam. This method allows a direct measurement of the total reaction cross section, regardless of the details of the  $\gamma$ -emission mode, at the price of a quite complicated experimental setup. After the pioneering work done during the 80's, there has been an impressive development of this technique in several laboratories making it now available to study a large number of reactions. This technique will be reviewed and the perspectives in this field will be discussed.

### 21.24 A high resolution spectroscopic study of seven metal-deficient stars

TANNER, John<sup>1</sup> and RYAN, Sean<sup>2</sup>

<sup>1</sup>The Open University, <sup>2</sup>The University of Hertfordshire

We present a high resolution spectroscopic study of seven metal-deficient stars previously identified by a low resolution survey as having  $[\text{Fe}/\text{H}] < -3.00$ . An abundance analysis code (WIDTH6) utilising one dimensional model atmospheres (MARCS and Bell) is used to constrain the stellar parameters (surface gravity, effective temperature, and microturbulence) and to obtain abundances for sixteen different elements. We note the following basic results: (1) Enhanced  $[\text{Mg}/\text{Fe}]$  and  $[\text{Al}/\text{Fe}]$  are observed in one star with  $[\text{Fe}/\text{H}] = -3.36$ . (2) One star shows  $[\alpha/\text{Fe}]$  underabundant for Mg, Ti, and Ca at  $[\text{Fe}/\text{H}] = -2.79$  (3)  $[\text{Eu}/\text{Fe}]$  is observed to be overabundant in one star at  $[\text{Fe}/\text{H}] = -2.86$  signalling  $r$ -process nucleosynthesis. (4) One star shows evidence for possible light neutron-capture activity in  $[\text{Sr}/\text{Ba}]$ .

### 21.25 Laminar flame acceleration by neon enrichment in white dwarf supernovae

CHAMULAK, David<sup>1</sup>, BROWN, Edward<sup>1</sup>, and TIMMES, Francis<sup>2</sup>

<sup>1</sup>Michigan State University, <sup>2</sup>Los Alamos National Laboratory

Type Ia supernovae, the thermonuclear incineration of a C/O white dwarf, are currently used as standard candles for measuring distances to redshifts  $< 1.6$ . Recent observations have suggested that there may be more than one population of progenitor and the peak luminosity at high redshifts may depend on the composition of the white dwarf. Of particular interest is  $^{22}\text{Ne}$ , which is formed from CNO elements during core He burning of the progenitor star and therefore reflects the metallicity of the progenitor. We explore how the rate of burning (the laminar flame speed) depends on the composition of the white dwarf. We find that the laminar flame speed of a C/O mixture is enhanced when it is enriched with small amounts of  $^{22}\text{Ne}$ . Our work applies to the regime where the speed of the newly ignited flame is not yet set by the growth of the Rayleigh-Taylor instability, and possibly also at lower densities (of order 10 million g/cc) where turbulence can disrupt the laminar flame.

## 21.26 Closing the Cold CNO Cycle: A new measurement of $^{19}\text{F}(p, \gamma)$

COUTURE, Aaron<sup>1</sup>, WIESCHER, Michael<sup>2</sup>, GÖRRES, Joachim<sup>2</sup>, STECH, Edward<sup>2</sup>, UGALDE, Claudio<sup>3</sup>, COUDER, Manoel<sup>2</sup>, TAN, Wanpeng<sup>2</sup>, LEE, Hye-Young<sup>2</sup>, and STRANDBERG, Elizabeth<sup>2</sup>

<sup>1</sup>Los Alamos National Laboratory, <sup>2</sup>Univ. of Notre Dame, <sup>3</sup>Univ. of North Carolina

The cold CNO cycle is the primary energy source for main sequence intermediate to heavy mass stars ( $M > 3M_{\odot}$ ). The closure of the cycle has depended on the strength of the  $^{19}\text{F}(p, \alpha)$  reactions to recycle the CNO seed back into the cycle. Since no nucleosynthesis beyond helium is possible at the main sequence burning temperatures, any leakages from the CNO cycle could have a significant impact on post-CNO abundances. The cyclic nature of the process only enhances the effect of a small breakout component. The  $^{19}\text{F}(p, \gamma)$  reaction provides the only breakout path for quiescent hydrogen burning. Prior measurements of  $^{19}\text{F}(p, \gamma)$  were hampered by the strong 6-8 MeV  $\gamma$  background from  $^{19}\text{F}(p, \alpha\gamma)$ . This placed a strong limit on the sensitivity of past measurements. No interference components had been reported in the inter-resonant region by previous authors. A 50% uncertainty is attributed to the stellar reaction rate of  $^{19}\text{F}(p, \gamma)$  due to the uncertainty in the sign of the interference terms. A new detection technique allowed high precision measurements from  $E_p=200-800$  keV at the University of Notre Dame's Nuclear Structure Laboratory. Both resonance parameters and interference components were measured over this energy range. The results of these measurements, including the improved reaction rates, will be presented.

## 21.27 Precision mass measurements of neutron-rich nuclei from Ge to Pd and their $r$ -process implications

JOKINEN, Ari, ELOMAA, Viki-Veikko, HAGER, Ulrike, HAKALA, Jani, RAHAMAN, Saidur, RINTA-ANTILA, Sami, AYSTO, Juha, and ERONEN, Tommi

University of Jyväskylä

In nuclear astrophysics, the binding energies are among the most important ingredients for reliable calculations. They affect the rates of the relevant reactions and they influence the time-scale and energy production of nucleosynthesis. In high temperature conditions, they adjust the balance, which defines the process paths. Precision mass measurements have generally been restricted to stable or long-lived unstable nuclei. In the pioneering work at ISOLTRAP facility, precision measurements were extended to radioactive isotopes [1]. At JYFL we have introduced a unique combination of Penning trap technology and IGISOL-technique. Thus precision studies of atomic masses can now be extended to short-lived exotic isotopes without target-ion source chemistry related restrictions [2]. A Penning trap is well suited for mass spectroscopy, since frequencies of radial eigenmotions in the trap sum up to a cyclotron motion, the frequency which in the given magnetic field is mass dependent ( $\omega_c=(q/m)B$ ). By measuring periodically the cyclotron frequency of the unknown isotope and a well known reference ion, it is possible to deduce the mass of the unknown isotope with accuracy in the range of a few keV. Commissioning of the JYFLTRAP facility has been performed by mass measurements of neutron-rich nuclei in the transitional region from Ge ( $Z=32$ ) to Pd ( $Z=46$ ). This has resulted in more than 100 new atomic masses of neutron-rich nuclei with a precision of 10 keV or better [2,3]. Some of the most exotic isotopes measured were  $^{121}\text{Pd}$ ,  $^{118}\text{Rh}$ ,  $^{110}\text{Mo}$ ,  $^{105}\text{Zr}$ ,  $^{97}\text{Rb}$  and  $^{92}\text{Br}$ . It is worth noting that the latter one is located in the  $r$ -process path in certain scenarios. The studied mass region offers an interesting playground to look for nuclear structure signatures in the mass surface, relevant also for the astrophysical predictions. The results are discussed in comparison with other spectroscopic information and theoretical studies. In addition, we will compare our results with the recent Atomic Mass Evaluation [4] and selected mass predictions used in astrophysical calculations [5].

[1] G. Bollen et al., Nucl. Instr. Meth. A368 (1996) 675

[2] A. Jokinen et al., Int. J. Mass Spectr. (2006), in press.

[3] U. Hager et al, Phys. Rev. Lett (2006), in press.

[4] G. Audi et al., Nucl. Phys A 729 (2003) 3

[5] J.M. Pearson and S. Goriely, Nucl. Phys. A (2006), in press

## 21.28 Measurement of transfer reactions on neutron-rich fission fragments in inverse kinematics

PAIN, Steven<sup>1</sup>, BARDAYAN, D.W.<sup>2</sup>, NESARAJA, C.D.<sup>2</sup>, SMITH, M.S.<sup>2</sup>, THOMAS, J.S.<sup>3</sup>, BLACKMON, J.C.<sup>2</sup>, CHAE, K.Y.<sup>4</sup>, CIZEWSKI, J.A.<sup>3</sup>, JOHNSON, M.S.<sup>5</sup>, JONES, K.L.<sup>3</sup>, KOZUB, R.L.<sup>6</sup>, LIVESAY, R.J.<sup>7</sup>, and MOAZEN, B.H.<sup>4</sup>

<sup>1</sup>Rutgers University, <sup>2</sup>Physics Division, Oak Ridge National Laboratory, Oak Ridge, TN, <sup>3</sup>Department of Physics and Astronomy, Rutgers University, New Brunswick, NJ, <sup>4</sup>Department of Physics and Astronomy, University of Tennessee, Knoxville, TN, <sup>5</sup>Oak Ridge Associated Universities, Oak Ridge, TN, <sup>6</sup>Tennessee Technological University, Cookeville, TN, <sup>7</sup>Department of Physics, Colorado School of Mines, Golden, CO

Due to the paucity of experimental data on the majority of heavy neutron-rich nuclei,  $r$ -process calculations rely significantly on nuclear structure models as input. However, structure models are not well tested in this region, and may be unreliable. The development of rare isotope beams (RIBs) is now allowing the structure of a limited set of  $r$ -process nuclei to be studied. In particular, high quality RIBs have made possible the performance of transfer reactions with unstable nuclei in inverse kinematics. Measurements of  $(d, p)$  reactions on neutron-rich fission fragments yield information on the development of single-neutron structure away from stability, in close proximity to suggested  $r$ -process paths, and are a crucial test of nuclear structure models away from stability. High quality beams of neutron-rich fission fragments around the doubly-magic  $^{132}\text{Sn}$  nucleus are available at the Holifield Radioactive Ion Beam Facility (HRIBF) at Oak Ridge National Laboratory. These can be accelerated to sufficient energy to perform  $(d, p)$  reactions around the Coulomb barrier. A campaign of measurements of  $(d, p)$  reactions on heavy ( $A \sim 132$ ) fission fragments is underway at the HRIBF. Experimentally,  $(d, p)$  reactions on heavy ( $Z \sim 50$ ) fission fragments are complicated by the effects of strongly inverse kinematics, and the relatively low intensities currently obtainable with rare isotope beams. Consequently, ejectile detection with high resolution in position and angle, a high dynamic range and with a large solid-angular coverage is required. The Oak Ridge Rutgers University Barrel Array (ORRUBA) is an array of silicon strip detectors that is under development to meet the challenges. The current status of experiments and the development of ORRUBA will be discussed.

*This work is supported in part by the U.S. Department of Energy under contract numbers DE-FC03-03NA00143 (Rutgers), DE-AC05-00OR22725 (ORNL), DE-FG02-96-ER40955 (TTU), the National Science Foundation, and the LDRD program of ORNL.*

## 21.29 $r$ -Process experimental campaign at the National Superconducting Cyclotron Laboratory (NSCL/MSU)

PEREIRA, Jorge<sup>1</sup>, KRATZ, K.-L.<sup>2</sup>, WOEHR, A.<sup>3</sup>, APRAHAMIAN, A.<sup>3</sup>, ARNDT, O.<sup>2</sup>, BECERRIL, A.<sup>1</sup>, ELLIOT, T.<sup>1</sup>, ESTRADE, A.<sup>1</sup>, GALAVIZ, D.<sup>1</sup>, HENNRICH, S.<sup>2</sup>, KERN, L.<sup>1</sup>, KESSLER, R.<sup>2</sup>, LORUSSO, G.<sup>1</sup>, MANTICA, P.<sup>1</sup>, MATOS, M.<sup>1</sup>, MONTES, F.<sup>1</sup>, PFEIFFER, B.<sup>2</sup>, QUINN, M.<sup>3</sup>, SCHATZ, H.<sup>1</sup>, SHERTZ, F.<sup>3</sup>, SMITH, E.<sup>1</sup>, and WALTERS, W.<sup>4</sup>

<sup>1</sup>National Superconducting Cyclotron Laboratory (NSCL), Michigan State University, East Lansing, MI, USA, <sup>2</sup>Institute für Kernchemie, Universität Mainz, Mainz, Germany, <sup>3</sup>Institute of Structure and Nuclear Astrophysics, Department of Physics, University of Notre Dame, Notre Dame, IN, USA, <sup>4</sup>Department of Chemistry and Biochemistry, University of Maryland, MD, USA

A highly interesting field of experimental and theoretical investigation is the structure of nuclei with unusual combinations of proton and neutron numbers, where rapid phase transitions, exotic symmetries and new pronounced shell gaps leading to new magic numbers may occur. These exotic properties are expected to strongly influence the astrophysical  $r$  process, responsible for the synthesis of a big fraction of heavy-nuclei through the production of extremely neutron-rich isotopes followed by their  $\beta$  decay. Experiments aimed to study the nuclear structure of neutron-rich nuclei far from stability are crucial for understanding the physics that govern the  $r$  process, as well as the sites where the nucleosynthesis of heavy-nuclei occurs. In this context, a JINA/VISTARS  $r$ -process campaign has been launched at the A1900 Fragment Separator at the National Superconducting Cyclotron Laboratory (NSCL) of the Michigan State University. The purpose of this campaign, was to measure the  $\beta$ -decay half-lives and  $P_n$  values of different unknown neutron-rich nuclei in order to investigate first the region between the  $N = 56$  sub-shell closure and the sudden onset

of deformation at  $N = 60$  in the  $A < 100$  region, and second the new shell structures around the possible local, spherical double sub-shell closure at  $Z = 40, N = 70$ , which may help clarify the origin of the calculated  $r$ -process abundance deficiencies around  $A = 110$ . Moreover, the two regions explored in both experiments included some important  $r$ -process waiting-point nuclei, whose  $\beta$ -decay half-lives and  $P_n$ -values are crucial for understanding the  $r$ -process abundance pattern. Details of this campaign will be presented, emphasizing the experimental challenges that had to be faced (from an experimental point of view) in order to explore these two regions.

*US-NSF Joint Institute of Nuclear Astrophysics (JINA)*

*HGF Virtuelles Institut für Struktur der Kerne und Nuklearer Astrophysik (VISTARS)*

### 21.30 Experimental nuclear level densities and interpretation within the microcanonical ensemble

GUTTORMSEN, Magne<sup>1</sup>, CHANKOVA, Rositsa<sup>1</sup>, REKSTAD, John<sup>1</sup>, SCHILLER, Andreas<sup>2</sup>, SIEM, Sunniva<sup>1</sup>, LARSEN, Ann-Cecilie<sup>1</sup>, SYED, Naeem Ul Hasan<sup>1</sup>, VOINOV, Alexander<sup>3</sup>, and AGVAANLUVSAN, Undraa<sup>4</sup>

<sup>1</sup>Department of Physics, University of Oslo, Norway, <sup>2</sup>NSCL, Michigan State University, MI 48824, USA,

<sup>3</sup>Department of Physics, Ohio University, OH 45701, <sup>4</sup>LLNL, 7000 East Avenue, Livermore, CA 94551, USA

Atomic nuclei at low excitation energy are characterized by the motion of pairs of nucleons, known as Cooper pairs, moving in time reversed orbitals. This picture becomes much more complicated as Cooper pairs are broken by collective (Coriolis force) or intrinsic (temperature) excitations. In this talk we will focus on the statistical properties of the system as function of the number of excited nucleons. The Oslo group has investigated level densities for  $\sim 30$  nuclei, from silicon and up to lead. The so-called Oslo method is based on particle- $\gamma$  coincidences in light ion reactions with one charged ejectile. By the use of the Brink-Axel hypothesis, the level density can be extracted from the primary  $\gamma$ -ray spectra, which are measured at all initial excitation energies up to the neutron binding energy. New theoretical descriptions within the microcanonical ensemble are presented.

### 21.31 Determination of low ${}^7\text{Be}$ activity as a tool to measure the ${}^3\text{He}(\alpha, \gamma){}^7\text{Be}$ cross section

GYÜRKY, György<sup>1</sup> for the LUNA Collaboration

<sup>1</sup>Institute of Nuclear Research (ATOMKI)

At the 400 kV LUNA2 accelerator deep underground in Italy's Gran Sasso laboratory a measurement of the  ${}^3\text{He}(\alpha, \gamma){}^7\text{Be}$  cross section is underway. In addition to the in-beam detection the  $\beta$ -delayed  $\gamma$ -activity of the produced  ${}^7\text{Be}$  is counted. The  ${}^3\text{He}(\alpha, \gamma){}^7\text{Be}$  reaction takes place in a differentially pumped windowless  ${}^3\text{He}$  gas target hit by a high intensity  $\alpha$  beam of up to 250  $\mu\text{A}$ . The produced  ${}^7\text{Be}$  nuclei are implanted in the calorimeter surface. The production of parasitic  ${}^7\text{Be}$  by the  ${}^6\text{Li}(d, n){}^7\text{Be}$  reaction as well as  ${}^7\text{Be}$  loss by sputtering and other processes have been tested. After the irradiation, the accumulated activity on the beam stop is measured with well shielded HPGe detectors having extremely good background conditions. The measurements and the data analysis are in progress. Owing to the low background conditions at Gran Sasso, activation data at energies down to  $E_{c.m.} = 100$  keV is feasible to obtain, compared with the lowest energy activation measurement ever made ( $E_{c.m.} = 420$  keV [1]). Here we discuss the technical aspects of the activation measurement such as the gas target set-up, the background conditions, the  $\gamma$  counting and the efficiency calibration of the  $\gamma$  detectors. The first results are also presented.

[1] B. S. Nara Singh et al, Phys. Rev. Lett. 93 (2004) 262503.

### 21.32 CARINA: a European network for nuclear astrophysics

ANGULO, Carmen

Université catholique de Louvain

Nuclear astrophysics has revealed as one of the most exciting areas of interdisciplinary research, in the crossroads of nuclear physics, astrophysics and astronomy. As a driving force for the devel-

opment of the very first Radioactive Ion Beam Facilities, it remains a fundamental research area in many European laboratories and is one of the key research topics in future RIB Facilities in Europe. Coupled to these innovative experimental efforts are substantial communities of theorists, astrophysicists and observers. Input from all of these sectors is necessary to achieve realistic modeling of stellar environments, the ultimate aim being a thorough understanding of the abundance and evolution of the elements and of the processes of energy generation in the Universe. Although the human potential in Europe is considerable, the effort is still dispersed. Within the EURONS project (2005-2008), the CARINA network intends to provide coherence to the research activities in nuclear astrophysics in Europe. CARINA stands for Challenges and Advance Research In Nuclear Astrophysics. Here, the CARINA network will be introduced and the main goals will be presented. More information is available at the website: [www.cyc.ucl.ac.be/CARINA](http://www.cyc.ucl.ac.be/CARINA)

### 21.33 Nucleosynthesis in Super AGB stars

DOHERTY, Carolyn

Monash University

A Super AGB star is one that will undergo complete core hydrogen & helium burning and, due to its high mass (approx  $8.5-11M_{\odot}$ ), it will also ignite carbon off-center. After completion of core carbon burning an inert ONeMg core remains with both hydrogen and helium burning shells above it. As in AGB stars, instabilities in the He shell result in a thermally pulsing (TP) phase with a typical SAGB having in excess of 300 pulses with a pulse period of approx 200-400 years. During the later stages of the TP phase, mass loss is very rapid ( $10^{-4}M_{\odot}$  per year), with these stars ending life as either ONeMg white dwarfs (WDs) or if the core is massive enough, undergoing a SN explosion leaving a neutron star. Here we present nucleosynthetic calculations and yield results for a  $9.5M_{\odot}$ , solar composition Super AGB star model including mass loss. The evolution follows all the way from the pre-main sequence to the end of TP phase, where our star leaves a ONeMg white dwarf after undergoing a planetary nebula phase. Using our nuclear network which includes 74 species and 506 nuclear reactions, we will investigate the processes of dredge up and hot bottom burning, as well as study the effects on yields resulting from variations in some of the more uncertain of the stellar nuclear reaction rates. The results presented here – the abundances and yields of these stars – are useful for a variety of applications such as: studies of core collapse of massive WD in close binary systems (core abundances), outer core abundances necessary for nova outbursts modeling, as well as the more general use of stellar yields for this mass range in Galactic chemical evolution studies.

## 22 Poster session, 30 June

### 22.1 On the origin of the high helium sequence in $\omega$ Centauri

MEYNET, Georges and MAEDER, André

Geneva Observatory

The blue Main Sequence (bMS) of  $\omega$  Cen implies a ratio of helium to metal enrichment  $\Delta Y/\Delta Z \approx 130$ , which is a major enigma. We show that rotating models of low metallicity stars, which account for the anomalous abundance ratios of extremely metal poor stars, are also useful for understanding the very high  $\Delta Y/\Delta Z$  ratio in  $\omega$  Cen. Models of massive stars with moderate initial rotation velocities produce stellar winds with large He- and N-excesses, but without the large C- (and O-) excesses made by very fast rotation, in agreement with the observed chemical abundance ratios in  $\omega$  Cen. Thus, the enrichment of  $\omega$  Cen seems to result mainly from stellar winds, without the usual contributions in heavy elements from supernovae. What is the reason for that? Various possibilities will be presented.

## 22.2 A charge breeder for nuclear astrophysics experiments?

DELAHAYE, Pierre and MARIE-JEANNE, Mélanie  
CERN ISOLDE

At ISOLDE, a PHOENIX ECR charge breeder is being tested for the investigation of the so-called  $1^+ \rightarrow n^+$  scenario for the next generation facilities. As a side objective, its potential use for physics experiments with intense multicharged radioactive ion beams is being investigated. Especially the combination of the ECR charge breeder with a high voltage platform would permit an acceleration of the radioactive ions produced at ISOLDE to total energies up to a few MeV. This opens up possibilities for nuclear astrophysics experiments such as different studies of radiative capture reactions occurring in stellar explosions. This contribution will present the current developments of the ECR charge breeder setup at ISOLDE for its possible use for these physics experiments.

## 22.3 Neutron capture cross sections of the Zr isotopes: probing neutron exposure and neutron flux in red giants

TAGLIENTE, Giuseppe<sup>1</sup> for the n\_TOF Collaboration  
<sup>1</sup>Istituto Nazionale di Fisica Nucleare (INFN)

The understanding of *s*-process nucleosynthesis has recently advanced from a quantitative description of the abundance distribution in the solar system towards a comprehensive picture including all aspects related to stellar and galactic chemical evolution [1]. This development has shown the importance of neutron capture nucleosynthesis for probing the deep interior of red giant stars. In this context, the stellar ( $n, \gamma$ ) cross sections of the Zr isotopes are important for determining the neutron density in the He burning zones of thermally pulsing AGB stars. Furthermore, the small cross section of <sup>90</sup>Zr is required with good accuracy for a quantitative assessment of the bottle-neck effect in the reaction flow due to the neutron magic nuclei with  $N = 50$ . Previous measurements of the stable Zr isotopes in the relevant energy range from 0.1 to 500 keV exhibit uncertainties greater than 10%, and in some cases, discrepancies of up to a factor of two. Based on the characteristic features of the n\_TOF facility at CERN, e.g. the very high instantaneous neutron flux, the high resolution, and the low background conditions [2], accurate measurements of the ( $n, \gamma$ ) cross sections have been performed for all stable Zr isotopes as well as for the radioactive isotope <sup>93</sup>Zr. Compared to previous experiments, systematic uncertainties could be significantly reduced by an optimized experimental setup and a comprehensive analysis of the remaining corrections. Resonance parameters have been extracted from the measured capture yields by means of the R-matrix code SAMMY.

*This work has been partially supported by the EC (contract FIKW-CT-200000107) and by the National Institutions partners in the n\_TOF Collaboration.*

- [1] F. Käppeler, Prog. Nucl. Part. Phys. 43, 419 (1999).
- [2] U. Abbondanno et al. (The n\_TOF Collaboration), CERN n\_TOF Facility: Performance Report, CERN/INTC 2002/037, (2003).

## 22.4 <sup>25</sup>Al+p elastic scattering with CRIB

PEARSON, Jonty<sup>1</sup>, CHEN, Alan<sup>1</sup>, KUBONO, Shigeru<sup>2</sup>, YAMAGUCHI, Hidetoshi<sup>2</sup>, HE, Jianjun<sup>2</sup>, SAITO, Akito<sup>2</sup>, AMADIO, Guilherme<sup>2</sup>, FUJIKAWA, Hisashi<sup>2</sup>, NIIKURA, M<sup>2</sup>, TOGANO, Y<sup>2</sup>, WAKABAYASHI, Y<sup>2</sup>, NISHIMURA, Shunji<sup>3</sup>, MOON, Jun Young<sup>4</sup>, LEE, Ju Hahn<sup>4</sup>, KIM, Jong Chan<sup>5</sup>, CHERUBINI, Silvio<sup>6</sup>, PIZZONE, Roberto<sup>6</sup>, LA COGNATA, M<sup>6</sup>, and TERANISHI, Takashi<sup>7</sup>  
<sup>1</sup>McMaster University, Canada, <sup>2</sup>CNS, University of Tokyo, Japan, <sup>3</sup>RIKEN, Japan, <sup>4</sup>Chung-Ang University, Korea, <sup>5</sup>Seoul National University, Korea, <sup>6</sup>University of Catania, Italy, <sup>7</sup>Kyushu University, Japan

The origin of galactic <sup>26</sup>Al remains a long-standing question in nuclear astrophysics. Within the context of explosive hydrogen burning, the <sup>25</sup>Al( $p, \gamma$ )<sup>26</sup>Si reaction bypasses the production of <sup>26</sup>Al at lower temperatures found in novae, while the same reaction contributes indirectly to <sup>26</sup>Al production at higher temperatures. The present rate of the <sup>25</sup>Al( $p, \gamma$ )<sup>26</sup>Si reaction suffers from significant uncertainties due to the lack of relevant structure information in the compound nucleus <sup>26</sup>Si. A recent <sup>25</sup>Al + p elastic-scattering experiment in inverse kinematics was performed using the CRIB facility at the CNS at the University of Tokyo, Japan. The <sup>2</sup>H(<sup>24</sup>Mg,  $n$ )<sup>25</sup>Al reaction was

used to produce a 7.5 MeV/A  $^{25}\text{Al}$  radioactive beam with intensities of  $\sim 106$  pps at the  $\text{CH}_2$  target position. Protons were detected in silicon EdE telescopes and a center-of-mass energy range of 3 MeV was scanned, reaching up to about 8.5 MeV in excitation energy in  $^{26}\text{Si}$ . In this presentation we report on the status of our investigations and the results so far.

## 22.5 Isospin symmetry in nucleon- and $\alpha$ -decays of mirror nuclei and its astrophysical applications

TIMOFEYUK, Natalia<sup>1</sup>, DESCOUVEMONT, Pierre<sup>2</sup>, and JOHNSON, Ronald C.<sup>1</sup>

<sup>1</sup>University of Surrey, <sup>2</sup>Universite Libre de Bruxelles

It has been realised recently that the amplitudes of one-nucleon decays of two mirror nuclear states into mirror-conjugated channels should be related if charge symmetry of the NN interaction is valid [1]. As a consequence, the ANCs of a pair of particle-bound mirror states can be linked by an approximate model-independent analytical expression for their ratio, given in Ref. [1], which contains only nucleon separation energies, charges of the product nuclei and the range of the strong interaction between the last nucleon and the core. For bound-unbound mirror pairs, mirror symmetry of one-nucleon decay amplitudes manifests itself via a similar link between the width of a proton resonance and the ANC of its mirror bound analog. The link persists for mirror-conjugated  $\alpha$ -particle decays as analytical expressions similar to those for the nucleon decay cases. We test the validity of these analytical formulae against the predictions of a potential model with a charge-independent nuclear interaction and of a many-body microscopic cluster model for several mirror pairs of isotopes from the  $0p$  and  $sd$  shells. We show that these analytical formulae are valid in many cases but that some deviations can be expected for isotopes with strongly deformed cores. In general, the results from microscopic model are not very sensitive to model ingredients and can be used to predict astrophysically relevant cross sections. Thus, the link between mirror ANCs in bound states can be used to predict cross sections for non-resonant proton capture if the mirror neutron ANCs are known. The link between the width of a resonance and the ANC of its bound mirror state can be used to determine capture cross sections which proceed through very narrow resonances. Some particular cases are considered.

- [1] N.K. Timofeyuk, R.C. Johnson and A.M. Mukhamedzhanov, Phys. Rev. Lett. 91, 232501 (2003).

## 22.6 Primordial magnetic field constrained from CMB anisotropies, and its generation and evolution before, during and after the BBN

YAMAZAKI, Dai<sup>1</sup>, ICHIKI, Kiyotomo<sup>2</sup>, KAJINO, Toshitaka<sup>2</sup>, and MATHEWS, Grant<sup>3</sup>

<sup>1</sup>Department of Astronomy, Graduate School of Science, University of Tokyo, <sup>2</sup>Division of Theoretical Astronomy, National Astronomical Observatory Japan, <sup>3</sup>Center for Astrophysics, Department of Physics, University of Notre Dame

Magnetic field plays a very important role in many astronomical phenomena at various scales of the universe. Recent observations of the cosmic microwave background (CMB) have extended measured power spectrum to higher multipoles  $l > \sim 1000$ , and there appears to be possible evidence for excess power on small angular scales. The primordial magnetic field (PMF) can strongly affect the CMB power spectrum and the formation of large scale structure. In this paper, we discuss the CMB temperature anisotropies generated by including a power-law magnetic field at the photon last scattering surface (PLSS). We then deduce an upper limit on the primordial magnetic field based upon our theoretical analysis of the power excess on small angular scales. We have taken into account several important effects such as reionization and the modified matter sound speed in the presence of the magnetic field. An upper limit to the field strength turns out to be  $|B_\lambda| < \sim 4.7$  nG at the present scale of 1 Mpc. This is obtained by comparing the calculated theoretical result including the Sunyaev-Zeldovich (SZ) effect with recent observed data on the small scale CMB anisotropies from the Wilkinson Microwave Anisotropy Probe (WMAP), the Cosmic Background Imager (CBI) and the Arcminute Cosmology Bolometer Array Receiver (ACBAR). We discuss several possible mechanisms for the generation and evolution of the PMF before, during and after the BBN.

## 22.7 Neutrino signal of supernova shock wave propagation: MSW distortion of the spectra and nucleosynthesis

KAWAGOE, Shiou<sup>1</sup>, KAJINO, Toshitaka<sup>2</sup>, SUZUKI, Hideyuki<sup>3</sup>, SUMIYOSHI, Kohsuke<sup>4</sup>, and YAMADA, Shoichi<sup>5</sup>

<sup>1</sup>Department of Astronomical Science, School of Physical Sciences, The Graduate University for Advanced Studies (SOKENDAI), <sup>2</sup>National Astronomical Observatory of Japan, <sup>3</sup>Department of Physics, Faculty of Science and Technology, Tokyo University of Science, <sup>4</sup>Numazu College of Technology, <sup>5</sup>Department of Physics, Faculty of Science and Engineering, Waseda University

There are a lot of mysteries about the mechanism of the collapse-driven supernova explosion and supernova neutrinos. The neutrino oscillation was discovered in various experiments, for example Super Kamiokande and SNO. But, it is still very difficult to determine three neutrino oscillation parameters: the mass difference,  $\Delta m_{13}$ , the mixing angle,  $\theta_{13}$ , and the CP violating phase,  $\delta$ . It is one of the biggest research topics of particle physics, nuclear physics and astrophysics to decide these parameter value. We try to limit the neutrino oscillation parameters from the supernova neutrinos by studying the MSW matter effect. The supernova neutrinos are generated in the core and propagate through the envelope. It is pointed out that shock wave propagation has strong influences on the supernova neutrino oscillation through changing density profile. Using an implicit Lagrangian code for general relativistic spherical hydrodynamics (Yamada, 1997), we succeeded in calculating propagation of shock waves which are generated by adiabatic collapse of iron cores and pass into the stellar envelopes. As the first step, we perform simplified calculations of core collapse and bounce by following adiabatic collapse with fixed electron fraction, because we intend to construct an approximate models of prompt explosion. We adopt the presupernova model of  $15M_{\odot}$  star provided by Woosley and Weaver (WW95). We examined how the influence of the shock wave appears in the neutrino spectrum, using the density profile obtained in our calculation. We confirmed that the influence of the shock wave appears from low-energy side and moves toward high-energy side according to the shock propagation. In addition, we found that this manner of the neutrino signal depends remarkably on the neutrino oscillation parameters. Therefore, there is a possibility of constraining the neutrino oscillation parameters from the supernova neutrino spectrum. We calculate the neutrino signal that will be observed on the Earth. Moreover, there is a possibility of finding the influence on the nucleosynthesis by changing the neutrino spectrum. We report on these results in this paper.

## 22.8 The effective long range interaction and resonances in the $n\alpha\alpha$ system at astrophysical energies

TAKIBAYEV, Nurgali

Kazakh National Pedagogic University

The features of the  $n\alpha\alpha$  system at astrophysical energies ( $\ll 1$  MeV) have been investigated on the basis of Faddeev's equations within the framework of the study of resonance fusion possibility in stellar matter [1]. Focus has been given to the determination and analysis of resonant states of the system. It was found that the series of resonance states appear in the  $n\alpha\alpha$  system at very low energies under certain conditions. The lifetimes of these three body resonances are close to the lifetime of the  $\alpha\alpha$  unstable ground state which has the energy  $\approx 92$  keV and the width  $\approx 6.8$  eV. The  $\alpha$  particles are considered as elementary. Simple forms of  $\alpha\alpha$  and  $n\alpha$  potentials are considered in order to satisfy scattering data at very low energies [2]. It is shown that the effective long range interaction acting as the well-known two body potential  $\sim r^{-2}$  can appear in this model of the  $n\alpha\alpha$  system. It leads to appearance of resonant states in the system. Thomas's and Efimov's effects in three body systems can be cited as typical examples of influence of effective long range interaction [3]. Moreover, the resonance phenomena can take place in a system consisted of one neutron and three or more  $\alpha$  particles at low energy region. The sharp resonance in system consisting of neutron and few  $\alpha$  particles is considered as stimulus to resonance fusion, i.e. this can be a new mode of fusion. Furthermore, the resonance fusion can give results in many astrophysical phenomena.

[1] N. Takibayev, Few-Body Problems in Physics, The Proc. of XIX European Conference on Few Body Problems in Physics, Groningen, The Netherlands 23-27 August 2004, editors N.

Kalantar-Nayestanaki, R.G.E. Timmermans, B.L.G. Bakker, AIP Conf. Proc. 768, p 350, 2005.

[2] N.Takibaev, Physics of Atomic Nuclei, V 68, p 1147, 2005;

[3] F.Pen'kov, N.Takibayev, Physics of Atomic Nuclei, V 57, p 1234, 1994.

## 22.9 A case for fast stellar rotation at very low metallicities: C and N in very metal poor halo stars

CHIAPPINI, Cristina<sup>1</sup>, HIRSCHI, Raphael<sup>2</sup>, MEYNET, Georges<sup>3</sup>, EKSTRÖM, Sylvia<sup>3</sup>, MAEDER, Andre<sup>3</sup>, and MATTEUCCI, Francesca<sup>4</sup>

<sup>1</sup>OAT/INAF and Observatoire de Geneve, <sup>2</sup>Dept. of Physics and Astronomy, University of Basel, <sup>3</sup>Observatoire de Geneve, <sup>4</sup>Dip. di Astronomia, Universita degli Studi di Trieste

We investigate the effect of new stellar models, which take rotation into account, computed for a metallicity  $Z = 10^{-8}$  on the chemical evolution of the earliest phases of the Milky Way. These models are computed under the assumption that the ratio of the initial rotation velocity to the critical velocity of stars is roughly constant with metallicity. This naturally leads to faster rotation at lower metallicity, as metal poor stars are more compact than metal rich ones. We find that the new  $Z = 10^{-8}$  stellar yields have a tremendous impact on the interstellar medium nitrogen enrichment for  $\log(\text{O}/\text{H})+12 < 7$  (or  $[\text{Fe}/\text{H}] < -3$ ). We show that upon the inclusion of the  $Z = 10^{-8}$  stellar yields in chemical evolution models, both high N/O and C/O ratios are obtained in the very-metal poor metallicity range in agreement with observations. Our results give further support to the idea that stars at very low metallicities could have rotational velocities of the order of 600-800 km s<sup>-1</sup>.

## 22.10 Suppression of the neutron channel in low energy d+d reactions within metallic media

CZERSKI, Konrad<sup>1</sup>, DORSCH, Tatjana<sup>2</sup>, HEIDE, Peter<sup>2</sup>, HUKÉ, Armin<sup>2</sup>, MARTIN, Lars<sup>2</sup>, and RUPRECHT, Götz<sup>3</sup>

<sup>1</sup>Institute of Physics, University of Szczecin, Szczecin, Poland, <sup>2</sup>Institut für Atomare Physik und Fachdidaktik, Technische Universität Berlin, Berlin, Germany, <sup>3</sup>TRIUMF, Vancouver, Canada

Study of nuclear reactions taking place in metallic media provides a test for strongly coupled astrophysical plasmas. In the present work, the neutron-proton branching ratio and angular distributions of the  ${}^2\text{H}(d, n){}^3\text{He}$  and  ${}^2\text{H}(d, n){}^3\text{He}$  reactions have been measured using different deuteron-implanted metallic targets at projectile energies ranging between 5 and 60 keV. The experimental data obtained for metals Al, Zr, Pd and Ta agree with those known from gas-target experiments. Contrary, a suppression of the neutron channel connected with an enhanced angular anisotropy of the  ${}^2\text{H}(d, n){}^3\text{He}$  reaction has been observed for the (earth) alkaline metals Li and Sr at deuteron energies below 20 keV. These experimental results can be described using known reaction matrix elements under assumption of quenching of the reaction channels with spin  $S = 0$ . Some reasons for the possible deuteron polarization in metallic media will be discussed.

## 22.11 Nuclear reaction and structure databases of the National Nuclear Data Center

PRITYCHENKO, Boris, ARCILLA, Ramon, HERMAN, Michal, MUGHABGHAB, Said, OBLOZINSKY, Pavel, ROCHMAN, Dimitri, SONZOGNI, Alejandro, TULI, Jagdish, and WINCHELL, David

NNDC, Brookhaven National Laboratory

We discuss nuclear data resources of the National Nuclear Data Center (NNDC) of relevance to nuclear structure, reactions, astrophysics as well as nuclear science applications. These resources include databases, tools and powerful web service at [www.nndc.bnl.gov](http://www.nndc.bnl.gov). Our objective is to provide an overview of nuclear databases, related products, demonstrate new Web service and strengthen contact with the nuclear astrophysics community. Bibliography database Nuclear Science References (NSR) covers more than 80 journals and offers some 180,000 references, providing extremely

effective way of searching scientific literature on a broad range of nuclear physics topics. Experimental nuclear reaction database (CSISRS), covering more than 15,500 experiments and being comprehensive for neutrons and extensive for charged particles, is of relevance to capture and astrophysics. Evaluated Nuclear Data File (ENDF) contains neutron cross sections for 340 isotopes relevant to nuclear technology, including capture in keV region of interest to astrophysics. A new version, ENDF/B-VII, is under development, scheduled for release in 2006. Evaluated Nuclear Structure Data File (ENSDF) represents enormous resource for nuclear structure and  $\gamma$ -ray spectroscopy. It provides information on almost all known nuclei (2,978), including some 140,102 levels and 204,017  $\gamma$  rays. Related database NuDat and highly popular web service offers extensive options for simple and complex retrievals. Other resources of interest include handy booklet Nuclear Wallet Cards with its 7th edition published in May 2005, Atlas of Neutron Resonances scheduled to be published by Elsevier in March 2006 and nuclear data tools.

## 22.12 Neutrons and features of primordial nucleosynthesis

TAKIBAYEV, Nurgali<sup>1</sup> and SPANOVA, Galiya<sup>2</sup>

<sup>1</sup>Kazakh National Pedagogical University, <sup>2</sup>Kazakh National Pedagogical University

Primordial nucleosynthesis is characterized by a considerable quantity of free neutrons. At the early stage of the Universe, when photons and neutrinos were no longer able to prevent nucleosynthesis, the key role in forming the lightest nuclei was given to the neutron component of the matter. Penetrating interactions of neutrons with any nuclei in their surroundings determine the key role of the neutron as a component which leads to chemical equilibrium in nuclear matter. On the contrary, interactions of protons and nuclei are blocked by Coulomb barriers at low temperatures. Neutron enrichment of nuclei of the lightest chemical elements is considered in the frames of the Saha's equations. This method is known in atomic plasma physics as a method of ionization equilibrium. It was used to describe the evolution of the nuclear matter states at the primordial nucleosynthesis stage. Saha's equations define concentrations of different ions and give their functional dependence on temperature change. In our issue the substance components' correlation changes are not due to atom ionization but because of the nuclear reactions with neutrons.

## 22.13 The TRIUMF annular chamber of tracking and identification of charged particles (TACTIC)

RUPRECHT, Götz<sup>1</sup>, AMAUDRUZ, Pierre<sup>1</sup>, BUCHMANN, Lothar<sup>1</sup>, FOX, Simon<sup>2</sup>, FULTON, Brian<sup>2</sup>, GIGLIOTTI, Dario<sup>1</sup>, LAIRD, Alison<sup>2</sup>, MUMBY-CROFT, Paul<sup>2</sup>, OPENSHAW, Robert<sup>1</sup>, PAVAN, Marcello<sup>1</sup>, PEARSON, Jonty<sup>1</sup>, and WALDEN, Patrick<sup>1</sup>

<sup>1</sup>TRIUMF, <sup>2</sup>University of York

Many nuclear reactions important for nucleosynthesis are investigated by transfer reactions using a radioactive ion beam on a gas target such as  $^1\text{H}$ ,  $^2\text{H}$ ,  $^3\text{He}$  and  $^4\text{He}$ . Since these measurements are performed in inverse kinematics, the energies of the ejectiles are usually low with a strong angular dependence in the laboratory system. Therefore, a new kind of detector is needed that allows the detection of low-energy ions from a gas target with good energy and angular resolution and a high angular coverage. TACTIC is a cylindrical time-projection chamber that can utilize the target gas as a drift medium so that no separation window is required. Moreover, the reaction region is still separated from the drift region which allows for higher beam currents which are needed for impact energies far below the Coulomb barrier. The cylindrical design is possible by the application of gas electron-multiplier (GEM) foils for the amplification of the weak electron-drift signals. From the electron-drift times the ion track can be reconstructed while the collected charge provides additional information about the ion species. The status of the detector development will be presented.

### 22.14 The influence of electron screening on half-lives

RUPRECHT, Götz, BUCHMANN, Lothar, HUTCHEON, Dave, OTTEWELL, Dave, RUIZ, Chris, WALDEN, Patrick, and VOCKENHUBER, Christof  
TRIUMF

Electron screening strongly changes nuclear reaction cross sections at energies below 1000 times the screening energy  $U_e$ . Since it has been found that  $U_e$  can be one order of magnitude larger than predicted by theory [1] if the target atoms are hosted in a metallic environment, a change of lifetimes of low-energy  $\beta$  and  $\alpha$  emitters may also be considered if they are situated in a metal. In addition, a temperature dependence of the screening effect has been proposed, changing some half-lives by a factor of 3 and probably more if the metal is cooled [2]. We checked these claims experimentally by measuring the decay rate of  $^{22}\text{Na}$  in a piece of aluminum activated by a 70 MeV proton beam. We observed the  $^{22}\text{Na}$  activity both at room temperature and when cooled down to  $\text{LN}_2$  temperatures. The results will be presented together with models describing the temperature dependence of screening and the maximum effect that can be expected for changes of radioactive decay rates.

[1] Czerski et al., EPL54(2001)449

[2] Raiola et al., JPG31(2005)1141

### 22.15 $\beta$ -Beam born neutrino – an alternative to double $\beta$ -decay to determine the Majorana neutrino mass.

SUJKOWSKI, Ziemowid

Institute for Nuclear Studies

The recent proposal [1] to determine the absolute Majorana neutrino mass with the use of intense  $\beta$ -beams is reviewed. The measurement consists in counting the lepton number violating events induced in a suitable detector by neutrinos produced in a nuclear decay in flight (the so-called  $\beta$  beams). The relativistic boost results in the gain in the content of Majorana neutrinos with helicities responsible for the lepton number violating events as well as in the increase of the interaction cross-section in the detector. A simple formula to calculate this gain is presented. It is shown that in contrast to the neutrino-less double  $\beta$ -decay the results are insensitive to the uncertainties in the nuclear matrix elements. Some examples of the suitable  $\beta$ -decay progenitors ( $\beta^-$  as well as electron capture) are discussed and the relevant cross-sections are given.

*Work in collaboration with L. Lukaszuk and S. Wycech.*

[1] Z. Sujkowski, Proc. Bormio Winter Meeting, 2005, L. Lukaszuk, Z. Sujkowski, S. Wycech, EPJ, in press.

### 22.16 Can radiative decay of long-lived particles after the BBN solve the cosmological $^6\text{Li}$ problem?

KUSAKABE, Motohiko and KAJINO, Toshitaka

Department of Astronomy, Graduate School of Science, University of Tokyo, and National Astronomical Observatory of Japan

Recent spectroscopic observations of metal poor stars have indicated that both  $^7\text{Li}$  and  $^6\text{Li}$  have abundance plateaus with respect to the metallicity of presumably cosmological origin.  $^7\text{Li}$  abundances are about a factor three lower than the primordial abundance predicted in SBBN, and  $^6\text{Li}$  abundances are  $\sim 1/20$  of  $^7\text{Li}$ , whereas SBBN predicts negligible amounts of  $^6\text{Li}$  compared to the detected level. These discrepancies suggest that  $^6\text{Li}$  has another cosmological or Galactic origin and that  $^7\text{Li}$  (and also  $^6\text{Li}$ ) should have depleted from primordial abundance by some post-BBN processes. The radiative or hadronic decay processes of long-lived particles such as SUSY particles are one of the possible processes in the early universe which should affect the cosmological abundances of the light elements. It is expected to provide a possible resolution of these lithium problems. We study this possibility and calculate the non-thermal primordial nucleosynthesis associated with the radiative decay by taking account of the secondary destruction processes of energetic nuclides D, T,  $^3\text{He}$  and  $^6\text{Li}$  which were produced in the primary processes. It is then confirmed that the secondary destruction processes have virtually little effect on the light element abundances so that

the calculated results are very similar to those of previous studies (Ellis et al. 2005, Cyburt et al. 2003). We explore the allowed region of the parameters specifying the properties of long-lived particles. We impose a constraint from observations of CMB spectrum, then the CMB spectrum constrains the abundance of long-lived particles more strongly than those of the effects on the light element abundances when the decay occurs at times later than  $10^{10}$  s. The possible non-thermal production or destruction of  ${}^6\text{Li}$  by the radiative decay is studied. We then found that the non-thermal nucleosynthesis produces  ${}^6\text{Li}$  as much as detected in metal poor halo stars (MPHSs), when the lifetime of unstable particles are  $\sim 10^8 - 10^{12}$  s and their initial abundances with respect to that of photon are  $\sim (10^{-13} - 10^{-12} \text{ GeV})/E_{\gamma 0}$ , where  $E_{\gamma 0}$  is the emitted photon energy in the radiative decay. We thereby propose a nucleosynthetic scenario that the MPHSs have lithium abundances after two different processes. Firstly, a non-thermal cosmological nucleosynthesis associated with radiative decay of unstable particles, and, secondly, the stellar depletion of the primordial lithium abundances might have operated.

### 22.17 Dating of the ${}^{60}\text{Fe}$ -peak in a deep sea manganese crust

KNIE, Klaus<sup>1</sup>, WALLNER, Anton<sup>2</sup>, KORSCHINEK, Gunther<sup>3</sup>, FAESTERMANN, Thomas<sup>3</sup>, and POUTIVTSEV, Mikhail<sup>3</sup>

<sup>1</sup>Technische Universität München, Fakultät für Physik, Garching, Germany and Universität Wien, Institut für Isotopenforschung und Kernphysik, Vienna, Austria, <sup>2</sup>Universität Wien, Institut für Isotopenforschung und Kernphysik, Vienna, Austria <sup>3</sup>Technische Universität München, Fakultät für Physik, Garching, Germany,

In ref. [1] an  ${}^{60}\text{Fe}$  enhancement in a 6-8 mm deep layer of a deep-sea ferromanganese crust from the central Pacific has been reported. This peak has been attributed to a nearby supernova. Here we report on an improved dating of the crust layers in order to get information on the time of the SN explosion. For this purpose, we have measured the cosmogenic radionuclide  ${}^{10}\text{Be}$  by means of accelerator mass spectrometry. Due to radioactive decay, the  ${}^{10}\text{Be}$  concentration decreases with the depth (i.e. age) of the layers; a more accurate age of  ${}^{60}\text{Fe}$  peak has been determined.

[1] K. Knie et al., Phys. Rev. Lett. 93,171103(2004)

### 22.18 Chemical mixing in galactic BA-type supergiants

FIRNSTEIN, Markus

Dr. Remeis-Observatory Bamberg

Abundance patterns of the light elements helium, carbon, nitrogen and oxygen are investigated in several Galactic BA-type supergiants of zero-age main sequence masses between 8 and  $18 M_{\odot}$ . Based on high-resolution and high-S/N Echelle spectra obtained with FOCES on the Calar Alto 2.2m telescope, model atmosphere analyses are performed using state-of-the-art non-LTE spectrum synthesis. Stellar parameters and chemical abundances are determined with high accuracy. This gives tight observational constraints on the evolutionary status of the stars. Objects evolving from the main sequence to the red supergiant stage and those on a blue loop can be distinguished by their mixing signature (pure rotational vs. first dredge-up). The most sensitive tracer of mixing with nuclear processed matter, the N/C ratio, indicates a higher mixing efficiency than predicted by current evolution models of rotating stars with mass-loss.

### 22.19 Neutrino-nucleus inelastic scattering reactions for core-collapse supernovae

SAMPAIO, Jorge<sup>1</sup>, JUODAGALVIS, Andrius<sup>2</sup>, HIX, William Raphael<sup>3</sup>, JANKA, H.-Thomas<sup>4</sup>, LANGANKE, Karlheinz<sup>5</sup>, and MARTÍNEZ-PINEDO, Gabriel<sup>5</sup>

<sup>1</sup>Centro de Física Nuclear da Universidade de Lisboa, Portugal, <sup>2</sup>Institute of Theoretical Physics and Astronomy, Vilnius University, Lithuania, <sup>3</sup>Physics Division, Oak Ridge National Laboratory, USA, <sup>4</sup>Max-Planck-Institut für Astrophysik, Garching, Germany, <sup>5</sup>GSI, Darmstadt, Germany

Neutrinos are responsible for almost all the energy transport in the core-collapse supernova evolution. During collapse they are produced in electron captures and escape the star's core carrying

energy away. With increasing densities neutrino interactions with matter become important in the time-scale of the collapse and eventually an equilibrium between neutrinos and matter is established – neutrino thermalization. So far, supernova simulations have considered neutrino inelastic scattering on electrons and free nucleons as the main mechanism for thermalization, but as Haxton argued in 1988, the excitation of the nuclear giant resonances in the supernova environment can lead to significant cross-sections of inelastic neutrino-nucleus reactions and these should therefore be added in supernova simulations [1]. Moreover, improved models for calculating electron captures rates on nuclei during collapse have shown that these captures dominate captures on free protons [2] and the same might be the case for neutrino-nucleus reactions. The pioneering study of inelastic neutrino-scattering reactions and neutrino absorption-reactions on nuclei in the supernova environment was done by Bruenn and Haxton [3]. In their study the nuclear composition was approximated by a single nucleus –  $^{56}\text{Fe}$  – and the rates were calculated based on a nuclear model appropriate for temperatures  $T = 0$ . They found that inelastic neutrino-nucleus scattering plays a important role in equilibrating neutrinos with matter. More recently, noticeable finite-temperature effects in the low-energy cross-sections were found by Sampaio et al. using results from large-scale Shell-Model calculations of the allowed GT transitions [4]. The study was performed on a restricted number of nuclei suggesting nuclear structure effects on the finite-temperature dependence of the cross-sections. Following up this work, we will present a recent study of neutral-current neutrino-nucleus cross-sections on a large set of nuclei relevant in the supernova composition [5]. The cross-sections are extended to higher neutrino energies adding forbidden transitions to the previous model. These transitions were derived from the Random Phase Approximation with an Independent Particle Model. Results of folded cross-sections over the nuclear composition for a wide range of relevant stellar conditions will be presented. Preliminary results show that NSE-folded cross-sections are mainly dependent on temperature at low neutrino energies. However further studies with a larger set of nuclei are in progress to verify these findings. First estimates of the impact of neutrino-nucleus inelastic scattering reactions on the supernova dynamics are expected to be presented.

[1] W. C. Haxton, Phys. Rev. Lett. 60 (1988) 1999

[2] K. Langanke et al., Phys. Rev. Lett. 90 (2003) 241102

[3] S. W. Bruenn and W. C. Haxton, Astrophys. J. Suppl. ser. 58 (1991) 376

[4] J. M. Sampaio et al., Phys. Lett. B 529 (2002) 19

[5] A. Juodagalvis et al., Nucl. Phys. A 747 (2005) 87

## 22.20 Quantitative spectroscopy of BA-type supergiants: Observational constraints on massive star evolution in the local group

PRZYBILLA, Norbert

Dr. Remeis-Observatory Bamberg

Massive BA-type supergiants are among the visually brightest objects in star-forming galaxies. Modern telescopes of the 8-10 m class facilitate spectroscopy of BA-supergiants throughout the Local Group at sufficient resolution to study stellar parameters and elemental abundances in different galactic environments in great detail. Fundamental stellar parameters and abundances of the light elements are of particular interest for deriving observational constraints on the evolution of massive stars in general, and on mixing processes in particular. Recent progress in quantitative analyses of BA-type supergiants allows for a precise determination of absolute stellar parameters (1- $\sigma$ -uncertainties in effective temperature of 1-2% and in surface gravity of 10-25%) and abundances (typical uncertainties of 10-25%), similar to the accuracy achieved in differential studies of solar-type stars. This provides much tighter observational constraints on surface abundances of He and CNO than previously possible. These are the primary observables for an evaluation of the predictive power of the various stellar evolution computations discussed at present. A status report of an ongoing study of BA-type supergiants in several galaxies of the Local Group is presented, spanning a range of metallicities by one order of magnitude. Emphasis is put in particular on the most luminous objects between 20 to 40  $M_{\odot}$ , where mixing processes are predicted to be most efficient. The empirical findings are discussed in the context of recent evolution models of rotating stars with mass-loss (and magnetic fields).

## 22.21 Towards global optical $\alpha$ potentials: Study of the $^{89}\text{Y}(\alpha, \alpha)^{89}\text{Y}$ elastic scattering

KISS, Gabor<sup>1</sup>, FÜLÖP, Zsolt<sup>1</sup>, SOMORJAI, Endre<sup>1</sup>, GYÜRKY, György<sup>1</sup>, MATE, Zoltan<sup>1</sup>, GALAVIZ, Daniel<sup>2</sup>, MÜLLER, Sebastian<sup>3</sup>, ZILGES, Andreas<sup>3</sup>, AVRIGEANU, Marilena<sup>4</sup>, and MOHR, Peter<sup>5</sup>  
<sup>1</sup>ATOMKI, Institute of Nuclear Research of the Hungarian Academy of Sciences, Debrecen, Hungary,  
<sup>2</sup>NSCL, Michigan State University, USA, <sup>3</sup>Technische Universität Darmstadt, Germany, <sup>4</sup>"Horia Hulubei" National Institute for Physics and Nuclear Engineering, Bucharest, Romania, <sup>5</sup>Strahlentherapie, Diakoniekrankenhaus Schwäbisch Hall, Germany

The modeling of the astrophysical  $p$  process requires a reaction network of thousands of nuclear reactions. The reaction rates on heavy nuclei necessary for obtaining  $p$ -nuclei abundances are calculated from Hauser-Feshbach type statistical models. For reactions involving  $\alpha$  particles, one of the most important input parameters for the calculation is the  $\alpha$ -nucleus optical potential that needs to be known in the low energy region relevant for the  $p$  process. The optical potentials are usually taken from global parameterizations which, however, are tested experimentally only at much higher energies. Therefore, it is necessary to test the global optical potentials at low energies. In recent years, elastic  $\alpha$  scattering experiments have been performed on several isotopes at ATOMKI, Debrecen and the results have been compared with model predictions [1-4]. However, all these measurements have been carried out on even-even nuclei. It is also instructive to see how global optical potentials are able to reproduce experimental data on different isotopes. Therefore, in the present work, angular distribution of the elastic  $\alpha$  scattering on the odd  $Z$ , neutron magic nucleus,  $^{89}\text{Y}$  has been measured at energies of 15.5 and 18.6 MeV with high precision. The results are compared with different global optical potentials. Based on the experimental differential cross sections, a local optical potential has also been constructed for  $^{89}\text{Y}$  using double folding and Woods-Saxon potentials for the real and imaginary parts of the potential, respectively. Details of the experiments, data analysis, and the preliminary results are presented.

- [1] P. Mohr *et al.*, Phys. Rev. C55, 1523 (1997)
- [2] Zs. Fulop *et al.*, Phys Rev. C64, 065805 (2001)
- [3] D. Galaviz *et al.*, Phys Rev. C71, 065802 (2005)
- [4] G. G. Kiss *et al.*, Eur. Phys. J. A27, in press (2006)

## 22.22 Mass measurements of radionuclides near the endpoint of the $rp$ process at SHIPTRAP

BLOCK, Michael<sup>1</sup> for the SHIPTRAP collaboration

<sup>1</sup>Gesellschaft für Schwerionenforschung mbH, Darmstadt

The Penning trap mass spectrometer SHIPTRAP [1] at GSI Darmstadt allows for precision experiments with stopped fusion-evaporation residues after separation by the velocity filter SHIP. To match the energy of the products to the energy acceptance of the traps a buffer gas stopping cell is used, where the fusion products are stopped in at helium pressures of about 50 mbar. An RFQ ion beam cooler is utilized to improve the emittance of the ion beam extracted from the gas cell. In this device the ions are cooled in collisions with buffer gas atoms within a few ms. Then they are extracted as bunched beam. Ions can optionally be stacked in the RFQ cooler. The so prepared ion bunches are injected in the double Penning trap system. It consists of a purification trap for isobar separation and a measurement trap, where the cyclotron frequency of the radionuclides is measured with the time-of-flight ion cyclotron resonance method. In first experiments mass measurements of proton-rich radionuclides around  $^{147}\text{Tm}$  were performed in 2005. The masses of 18 nuclides were measured providing 8 new mass values. In a recent run the masses of radionuclides around  $^{108}\text{Te}$  were measured. The nuclides were produced in the reaction  $^{58}\text{Ni}+^{58}\text{Ni}$  at 3.97 MeV/u. In a 3-day run the masses of 11 nuclides were measured. For the first time the masses of  $^{111}\text{I}$ ,  $^{112}\text{I}$ , and  $^{107}\text{Sb}$  were determined.  $^{107}\text{Sb}$  is one of the nuclides within the SnSbTe cycle. According to reaction network calculation by Schatz *et al.* [2] the rapid proton capture process ends in a closed SnSbTe cycle. To improve such calculations accurate measurements of required input parameters as for instance mass values or proton separation energies are needed. In a future run several of the relevant Sn, Sb and In nuclides can be produced in the reaction  $^{50}\text{Cr}+^{58}\text{Ni}$ . According to the

calculated production cross sections a mass measurements of  $^{106}\text{Sb}$  should be feasible for the first time. In addition, improved mass values are expected for  $^{104,105,106}\text{Sn}$ .

- [1] M. Block *et al.*, Eur. Phys. J. A 25, s1.49 (2005)
- [2] H. Schatz *et al.*, Phys. Rev. Lett. 86, 3471 (2001)

## 22.23 Mass measurements of $^{22}\text{Mg}$ and $^{26}\text{Si}$ via $(p, t)$ reactions and Penning traps

CLARK, Jason<sup>1</sup>, PARIKH, Anuj<sup>1</sup>, BUCHINGER, F.<sup>2</sup>, CAGGIANO, J.A.<sup>1</sup>, CRAWFORD, J.E.<sup>2</sup>, DEIBEL, C.<sup>1</sup>, GREENE, J.P.<sup>3</sup>, GULICK, S.<sup>2</sup>, HARDY, J.C.<sup>4</sup>, HECHT, A.A.<sup>5</sup>, LEE, J.K.P.<sup>2</sup>, LEVAND, A.F.<sup>3</sup>, LEWIS, R.<sup>1</sup>, LUNDGREN, B.F.<sup>3</sup>, PARKER, P.D.<sup>1</sup>, SAVARD, G.<sup>3</sup>, SCIELZO, N.D.<sup>3</sup>, SHARMA, K.S.<sup>6</sup>, TANIHATA, I.<sup>3</sup>, TRIMBLE, W.<sup>3</sup>, WANG, J.C.<sup>6</sup>, WANG, Y.<sup>6</sup>, WREDE, C.<sup>1</sup>, and ZHOU, Z.<sup>3</sup>

<sup>1</sup>Yale University, <sup>2</sup>McGill University, <sup>3</sup>Argonne National Laboratory, <sup>4</sup>Texas A&M University, <sup>5</sup>University of Maryland, <sup>6</sup>University of Manitoba

The success of models used to describe astronomical phenomena such as novae, x-ray bursts, and supernovae is determined by their ability to replicate the observational signatures of these events. Two examples of such observables are the abundances of the isotopes  $^{26}\text{Al}$  and  $^{22}\text{Na}$  which are detected by the  $\beta$ -delayed 1.809 MeV ( $^{26}\text{Al}$ ) and 1.275 MeV ( $^{22}\text{Na}$ )  $\gamma$  rays. Uncertainties in the contribution of novae to the abundances of these nuclides predominantly stem from uncertainties in the  $^{25}\text{Al}(p, \gamma)^{26}\text{Si}$  and  $^{21}\text{Na}(p, \gamma)^{22}\text{Mg}$  reaction rates. Since the reaction rates depend exponentially on the ground-state Q values, the masses of  $^{22}\text{Mg}$  and  $^{26}\text{Si}$  are critical. The Canadian Penning Trap (CPT) mass spectrometer at the Argonne National Laboratory is designed to make precise mass measurements of nuclides with short half-lives. To date, more than 70 radioactive isotopes have been measured with half-lives as short as one second and with a precision  $\delta m/m$  approaching  $10^{-8}$ . Recently, the mass of  $^{22}\text{Mg}$  was determined with both the CPT and the Yale spectrograph. At Yale University, the masses of  $^{22}\text{Mg}$  and  $^{26}\text{Si}$  were determined by measuring the ground-state Q values of the  $^{24}\text{Mg}(p, t)^{22}\text{Mg}$  and  $^{28}\text{Si}(p, t)^{26}\text{Si}$  reactions relative to the  $^{16}\text{O}(p, t)^{14}\text{O}$  reaction with an Enge split-pole spectrograph. The results for the  $^{22}\text{Mg}$  mass excess as measured by these two very different techniques are in excellent agreement  $\Delta = M - A = -400.5(1.0)$  keV [1] and  $-399.73(67)$  keV [2] and provide additional support for the  $^{26}\text{Si}$  mass determined solely at Yale University  $\Delta = -7139.5(1.0)$  keV [1]. This paper will provide a comparison of the experiments at ANL and Yale University used to determine the  $^{22}\text{Mg}$  mass, highlight the  $^{26}\text{Si}$  mass measured with the Yale spectrograph, and discuss the implications on the production of  $^{26}\text{Al}$  and  $^{22}\text{Na}$  in novae.

- [1] A. Parikh *et al.*, Phys. Rev. C 71, 055804 (2005)
- [2] G. Savard *et al.*, Phys. Rev. C 70, 042501 (2004)

## 22.24 On the $\alpha$ -particle semi-microscopic optical potential at low energies

AVRIGEANU, Marilena<sup>1</sup>, LEEB, Helmut<sup>2</sup>, VON OERTZEN, Wolfram<sup>3</sup>, ROMAN, Faustin Laurentiu<sup>1</sup>, and AVRIGEANU, Vlad<sup>1</sup>

<sup>1</sup>"Horia Hulubei" National Institute for Physics and Nuclear Engineering, Bucharest, Romania, <sup>2</sup>Atominstut der Österreichischen Universitäten, Technische Universität Wien, Wien, Austria <sup>3</sup>Freie Universität Berlin, Fachbereich Physics, Arnimallee 14, 14195 Berlin, and Hahn-Meitner-Institut, Glienicker Strasse 100, 14109 Berlin, Germany

The OMP analyses for  $\alpha$ -particles at low energies pointed out two main questions, which are still open, e.g. [1] and Refs. therein, namely (i) the OMP parameter sets obtained from  $\alpha$ -particle elastic scattering at high energies ( $>80$  MeV) do not describe either the low-energy ( $<40$  MeV) elastic scattering or the complete fusion data, and (ii) the statistical  $\alpha$ -particle emission is underestimated by the OMPs that account for elastic scattering on the (cold) ground-state nuclei. In the latter case, the need for new physics in potentials to describe nuclear de-excitation within the statistical model calculations was pointed out [2]. It was thus suggested that particle evaporation occurs from a transient nuclear stratosphere of the emitter nucleus, with a density that differs from cold nuclei [3] and which has not yet relaxed to the density profile expected for complete equilibration

[4]. Therefore, effects due to changes of the nuclear density at a finite temperature have been considered within the double folding (DF) formalism [5] of the  $\alpha$ -nucleus real part of the optical potential. Thus, it is shown that a temperature-dependent nuclear density distribution can be an important aspect to be included in statistical-model calculations even for temperatures  $< 2$  MeV. At the same time, the high precision of recent measurements [6,7] of  $\alpha$ -particle elastic-scattering data makes possible the pointing out of additional features of the  $\alpha$ -particle scattering at low energy and, consequently, of further limits and possible improvement of global OMP parameters obtained previously through semi-microscopic analysis [1,8] of the low-energy  $\alpha$ -particle elastic scattering. The involvement of these potentials for further description of both the scattering and emission of alpha-particles is also discussed in the present work.

- [1] M. Avrigeanu *et al.*, Nucl. Phys. A723, 104 (2003)
- [2] G. La Rana *et al.*, Phys. Rev. C 35, 373 (1987); G.D.J. Moses *et al.*, Phys. Rev. C 36, 422 (1987)
- [3] A.N. Antonov, J. Kanev, I.Zh. Petkov, and M.V. Stoitsov, Il Nuovo Cimento A 101, 525 (1989)
- [4] R. Lacey *et al.*, Phys. Lett. B 191, 253 (1987); G. Bozzolo *et al.*, Phys. Lett. B 219, 161 (1989)
- [5] M. Avrigeanu, W. von Oertzen, and V. Avrigeanu, Nucl. Phys. A764, 246 (2006)
- [6] Zs. Fülöp *et al.*, Phys. Rev. C 64, 065805 (2001)
- [7] D. Galaviz *et al.*, Phys. Rev. C 71, 065802 (2005)
- [8] M. Avrigeanu and V. Avrigeanu, submitted for publication in Phys. Rev. C

## 22.25 Time of flight mass measurements in the neutron rich Fe region

ESTRADE, Alfredo

National Superconducting Cyclotron Laboratory, Michigan State University, 48824 East Lansing, MI, USA

Masses of neutron rich nuclei are a direct input for  $r$ -process calculations, and for calculations of crust processes in accreting neutron stars. Most of the nuclides involved in these processes do not have an experimentally known mass. We recently performed mass measurements by the time of flight technique at the National Superconducting Cyclotron Laboratory at Michigan State University. Details of the experimental technique will be discussed, together with preliminary data from a first experiment in the neutron rich Fe region.

## 22.26 Decay studies at the end of the $rp$ process

SMITH, Edward

The Ohio State University

The  $rp$  process, or rapid proton-capture process, produces proton rich nuclei on the surface of accreting neutron stars. The light curves of type I X-ray bursts are an observable result of the energy produced. In reaction networks, a series of  $(p, \gamma)$  reactions and  $\beta$  decays proceed along a path close to the proton drip-line culminating, for some bursts, in a Sn-Sb-Te cycle. To address uncertainties in the masses near the proton drip-line, we have observed the neutron deficient  $^{103,104,105}\text{Sb}$  isotopes at the National Superconducting Cyclotron Laboratory at Michigan State University. A mixed beam of unstable nuclei was produced at the Coupled Cyclotron Facility and isolated in the A1900 fragment separator. Nuclei were then implanted and decays were observed in the NSCL  $\beta$ -decay end station. We discuss preliminary results on beta-decay properties and the search for proton radioactivity. We also discuss the proposed rf-kicker, a radio frequency fragment separator, which will improve beam purity for future experiments on neutron deficient nuclei at the NSCL.

## 22.27 Fragmentation spectra of strange quark matter in a type-II supernova scenario

PAULUCCI, Laura

Instituto de Fisica, Universidade de Sao Paulo

We present and discuss calculations of strange matter fragmentation expected in the ejecta from type II supernovae. Relevant issues such as the dynamical evolution of the ejecta and interactions with the outgoing stellar shells are addressed with the aim of understanding the mass distribution and energy spectra at the sources. We attempt to relate the results with the problem of propagation through the ISM and ultimately, predict the contribution to the putative flux of strangelets probed by several experiments.

## 22.28 Level structure of $^{21}\text{Mg}$ : Nuclear and astrophysical implications

MURPHY, Alexander

University of Edinburgh

Resonant elastic scattering of a radioactive  $^{20}\text{Na}$  beam incident upon protons in a polyethylene target has been used to probe the level structure of  $^{21}\text{Mg}$  above the proton decay threshold. Three states have been observed and their properties deduced through analysis based on the R-Matrix formalism. The results improve and extend previous studies of this nucleus. An estimate of the  $^{20}\text{Na}(p, \gamma)^{21}\text{Mg}$  reaction rate, including these new data, suggests this reaction will not play a significant role in explosive hydrogen burning in astrophysical sites such as novae and X-ray bursts.

## 22.29 Proton induced reaction cross sections of the Ge isotopes

FÜLÖP, Zsolt

ATOMKI, Debrecen, Hungary

As a continuation of a systematic study of charged particle capture reactions relevant to the astrophysical  $p$  process, the proton induced reaction cross sections of different Ge isotopes have been measured using the activation technique. Natural Ge targets have been irradiated with proton beams from the Van de Graaff and cyclotron accelerators of ATOMKI. The cross sections of the reactions  $^{70}\text{Ge}(p, \gamma)^{71}\text{As}$ ,  $^{73}\text{Ge}(p, \gamma)^{74}\text{As}$ , and  $^{76}\text{Ge}(p, n)^{76}\text{As}$  have been derived by measuring the  $\gamma$  radiation following the  $\beta$  decay of the reaction products. The measurements have been carried out between 1.6 and 4.4 MeV in 400 keV steps covering the relevant energy range (Gamow window) for these reactions. The final analysis of the experimental results is still in progress. Preliminary results are presented here and compared with the predictions of the Hauser-Feshbach statistical model calculations using the NON-SMOKER code.

## 22.30 Neutron decay array for $\beta$ -delayed neutron decay studies

LUROSSO, Giuseppe

MSU-NSCL

The delayed neutron emission has a critical impact on the  $r$  process, affecting the final abundance pattern after freeze-out. For the purpose of measuring the neutron emission probabilities, a new low energy neutron detector has been designed and built at the NSCL. We discuss performance, results of  $P_n$  values measured in 2005, and future perspectives.

## 22.31 The $^{13}\text{C}(\alpha, n)^{16}\text{O}$ reaction rate at stellar temperatures

ROGACHEV, Grigory

Florida State University

The reaction  $^{13}\text{C}(\alpha, n)^{16}\text{O}$  is considered to be the main source of neutrons for the  $s$  process in AGB stars. Data from direct measurements of the cross section for this process are only available for  $\alpha$  energies above 279 keV. At lower energies the cross section is dominated by a  $1/2^+$ , 6.356 MeV

sub-threshold resonance in  $^{17}\text{O}$ . Due to the large uncertainty associated with the structure of this resonance, the rate of  $^{13}\text{C}(\alpha, n)^{16}\text{O}$  reaction was uncertain by 500% at stellar temperatures. The  $S_\alpha$  factor of this resonance was measured recently by Kubono *et al.* via the  $^{13}\text{C}(^6\text{Li}, d)$  reaction using a  $^6\text{Li}$  beam of 60 MeV. These authors claim that the  $S_\alpha$  factor of this resonance is very low (0.011) and that the cross section enhancement due to this resonance is considerably smaller than assumed in the NACRE compilation, which would imply a reduction of the reaction rate by a factor of four. Keeley *et al.* reanalyzed these data and argued that they are, in fact, consistent with a large  $S_\alpha$  factor for the resonance in question, supporting an assumption made in the NACRE compilation regarding the strong alpha-cluster structure of this state. The goal of the present work is to address this issue and to determine the contribution of the 6.356 MeV resonance to the  $^{13}\text{C}(\alpha, n)^{16}\text{O}$  reaction at low energies. We performed measurements of the asymptotic normalization coefficient (ANC) of the 6.356 MeV,  $1/2^+$  resonance in  $^{17}\text{O}$ , using the  $\alpha$ -transfer reaction  $^{13}\text{C}(^6\text{Li}, d)^{17}\text{O}$  at sub-Coulomb energies. The DWBA analysis of the  $\alpha$ -transfer reaction at sub-Coulomb energies is significantly simplified because the cross section is almost independent of the nuclear potential parameters in the entrance and exit channels, thus eliminating the corresponding uncertainty in the theoretical interpretation. By using the ANC approach one can completely eliminate the uncertainty associated with the freedom in choosing the potential parameters for the  $^6\text{Li}$  and  $^{17}\text{O}$  form factors. Our experimental result shows conclusively that the contribution of the 6.356 MeV state to the cross section of the  $^{13}\text{C}(\alpha, n)^{16}\text{O}$  reaction at low energies is 10 times lower than assumed in NACRE, although it is somewhat higher than reported by Kubono *et al.* The uncertainty of the  $^{13}\text{C}(\alpha, n)$  rate at stellar temperatures is now reduced to  $\approx 20\%$ .

### 22.32 Analysis of the $^{16}\text{O}(d, p)^{17}\text{O}$ and $^{16}\text{O}(d, n)^{17}\text{F}$ transfer reactions to determine astrophysical direct capture cross sections

ASSUNÇÃO, Marlete

Instituto de Física da Universidade de Sao Paulo

Coupled channel calculations have been performed for transitions to ground and first excited states of  $^{17}\text{F}$  and  $^{17}\text{O}$  at incident deuteron energies from  $E_d = 2.29$  MeV up to 3.27 MeV. The astrophysical direct capture cross sections were calculated using the spectroscopic factors from  $^{16}\text{O}(d, p)^{17}\text{O}$  and  $^{16}\text{O}(d, n)^{17}\text{F}$  transfer reactions based on the asymptotic normalization coefficient (ANC) method. The astrophysical S-factors were compared to recent experimental data. The Maxwellian-averaged neutron capture cross section at  $kT=30$  keV was obtained as  $22(3) \mu\text{barn}$ .

### 22.33 Sensitivity of type I X-ray bursts to $rp$ -process reaction rates

AMTHOR, Matthew

Department of Physics and Astronomy, Michigan State University, USA

First steps have been taken in a more comprehensive study of the dependence of observables in type I X-ray bursts on uncertain  $(p, \gamma)$  reaction rates along the  $rp$ -process path. These studies focus on reactions important during burst rise that are experimentally accessible at current rare-isotope facilities. We use the multi-zone hydrodynamics code KEPLER which implicitly couples a full nuclear reaction network of more than 1000 isotopes, as needed, to follow structure and evolution of the X-ray burst layer and its ashes. This allows us to incorporate the full  $rp$ -process network, including all relevant nuclear reactions, and individually study changes in the X-ray burst light curves when modifying select key nuclear reaction rates. When varying specific reaction rates within currently assumed uncertainties, our early results show changes in the burst light curves that are large compared to the current sensitivity of X-ray observations. More precise reaction rates are therefore needed to test current X-ray burst models of the burst rise with observational data and to constrain astrophysical parameters.

### 22.34 Neon abundances in B-stars of the Orion association: Solving the solar neon problem?

CUNHA, Katia

National Optical Astronomy Observatory, Tucson, USA

Recent results from 3-D hydrodynamical and time dependent model atmospheres calculations for the Sun advocate significantly lower photospheric C, N and O abundances. It soon became apparent that these significantly lower solar abundances resulted in severe inconsistencies between the solar models and measurements from helioseismology. One possibility to reconcile the solar models with observations, however, is to allow for a larger neon abundance in the Sun. The solar Ne abundance is considered to be uncertain because it is measured in the solar corona and from active solar regions only and not in the solar photosphere. In this study, we focus on the Ne content of the OB stars. In particular, we report on Ne abundances for a sample stellar members of the Orion Association. Our abundance calculations were done fully in non-LTE with non-LTE model atmospheres and line formation theory. Our results indicate very homogeneous Ne abundances for the young Orion stars and considerably higher than the most recent assessment of the solar value by 0.35 dex. Given that there is very good agreement between the B-star abundances and the Sun in all other elements, we advocate that the solar Ne abundance should follow the B stars as well. This significantly higher neon abundance in the B stars and, thus, in the Sun helps to reconcile the solar models with observations from helioseismology.

### 22.35 Nucleosynthesis relevant conditions in neutrino-driven supernova outflows

ARCONES, Almudena

Max-Planck-Institute for Astrophysics, Munich, Germany

We perform long-time hydrodynamic simulations of the neutrino-driven mass outflow from the surface of the newly formed neutron star in a supernova. In agreement with previous relativistic wind studies, we find the outflow to accelerate to supersonic velocities and in case of a compact  $\sim 1.4 M_{\odot}$  (gravitational mass) neutron star with a radius of about 10 km to reach entropies of about  $100 k_B$  per nucleon. The wind, however, is decelerated and shock-heated abruptly when it runs into a wind termination shock between the fast outflow and the slower preceding supernova ejecta. We demonstrate that the entropy jump through this reverse shock can be larger than a factor of three. Seconds after the onset of the explosion the entropies therefore can reach values in excess of  $250 k_B$  per nucleon. The temperature of the shocked wind at this time has dropped to about  $10^9$  K, and density and temperature continue to decrease only very slowly. Such conditions have previously been recognized as very favorable for  $r$  processing, a possibility which seems supported by the fact that the very fast expansion of the wind should enable a high neutron-to-seed ratio in case of neutron-rich conditions.

### 22.36 Electron capture rates for neutron star crusts

BECERRIL, Ana

National Superconducting Cyclotron Laboratory, Michigan State University, USA

Temperature and density dependent electron capture rates for low temperature astrophysical applications have been calculated using an analytic formulation. In this work we present a comparison of these calculated EC rates to those calculated by Fuller, Fowler and Newman [1]. Similarities and differences between the two models are presented.

[1] G.M. Fuller, W.A. Fowler, and M.J. Newman, ApJ. Suppl. 42, 447 (1980)

## Index

- ÄYSTÖ, J., 64  
ÖZKAN, N., 72
- A. P. SUAIDE, A., 79  
A. SOUZA, F., 79  
ACHOURI, L., 9  
ADACHI, T., 69  
ADEKOLA, A., 61, 71  
AGUILERA, E.F., 60  
AGVAANLUVSAN, U., 89  
AKIMUNE, H., 63  
AL-ABDULLAH, T., 80  
ALCORTA, M., 66  
ALEXANDER, T. K., 80  
ALIOTTA, M., 40, 46  
ALKSNIS, O., 54  
AMADIO, G., 17, 29, 91  
AMARI, S., 15  
AMAUDRUZ, P., 95  
AMRO, H., 60  
AMTHOR, M., 103  
ANDO, H., 64  
ANDREYEV, A.N., 80  
ANGULO, C., 9, 40, 46, 89  
AOI, N., 62  
AOKI, W., 14, 23, 34, 64  
APRAHAMIAN, A., 49, 75, 88  
ARCILLA, R., 94  
ARCONES, A., 104  
ARNDT, O., 88  
ASPLUND, M., 25  
ASSUNÇÃO, M., 103  
ATHANASSIADOU, T., 27  
AUDOUIN, L., 11, 55  
AUSTIN, S., 29  
AVRIGEANU, M., 99, 100  
AVRIGEANU, V., 100  
AXIOTIS, M., 30  
AYSTO, J., 87  
AZUMA, R., 83
- BABA, H., 62  
BACHARI, F., 53, 81  
BADENES, C., 44  
BAIRD, M.L., 84  
BALDOVIN, C., 36  
BALL, G.C., 80  
BANU, A., 80  
BARDAYAN, D.W., 56, 59, 71, 77, 88  
BARIONI, A., 60  
BARKLEM, P., 14  
BARUAH, S., 30  
BARZYK, J., 15  
BEARD, M., 17
- BEAUMEL, D., 55  
BECCHETTI, F.D., 60  
BECERRIL, A., 88, 104  
BECK, C., 39  
BECKER, F., 11  
BECKER, H.W., 30, 40  
BEER, H., 84  
BEERS, T., 14, 64  
BENLLIURE, J., 11  
BERTULANI, C., 25  
BESSERER, U., 84  
BEUN, J., 84  
BEYER, R., 32  
BICHLER, M., 51  
BISHOP, S., 62  
BISTERZO, S., 40, 51, 57, 66  
BLACKMON, J.C., 37, 56, 59, 71, 77, 79, 88  
BLANK, B., 11  
BLAUM, K., 30  
BLOCK, M., 99  
BORGE, M.J.G., 66  
BORKOWSKI, K., 44  
BORZOV, I., 79  
BOSCH, F., 19  
BRAVO, E., 44  
BREITENFELDT, M., 30  
BROWN, E., 28, 86  
BRUNE, C.R., 20, 59, 61, 71  
BUCHINGER, F., 100  
BUCHMANN, L., 9, 10, 20, 95, 96  
BURAS, R., 85  
BURROWS, A., 21  
BUSSO, M., 16  
BYELIKOV, A., 69  
BYRNE, A., 41
- CAGGIANO, J., 9, 20, 100  
CAMARGO, O., 60  
CARLIN, N., 39, 79  
CARPENTER, M.P., 41  
CASAREJOS, E., 9, 11, 40, 46  
CAURIER, E., 26  
CAYREL, R., 35  
CHAE, K.Y., 56, 59, 71, 77, 88  
CHAKRAWARTHY, R.S., 80  
CHAMPAGNE, A., 71, 83  
CHAMULAK, D., 86  
CHANKOVA, R., 89  
CHARBONNEL, C., 23, 59  
CHEN, A., 9, 17, 20, 91  
CHERUBINI, S., 79, 91  
CHIAPPINI, C., 94  
CHICOINE, M., 80  
CHIEFFI, A., 23

- CHOMAZ, P., 52  
CHRISTLIEB, N., 14  
CHUN, S., 81  
CHURCHMAN, R., 80  
CIZEWSKI, J.A., 88  
CLARK, J., 9, 100  
COC, A., 9, 12  
COQUARD, L., 42  
CORTINA-GIL, D., 11  
COSTANTINI, H., 8, 83  
COUDER, M., 17, 40, 46, 87  
COUTURE, A., 17, 40, 87  
COWAN, J., 13, 40  
CRAWFORD, H., 9  
CRAWFORD, J.E., 100  
CRISTALLO, S., 36, 40  
CUNHA, K., 38, 104  
CZERSKI, K., 27, 81, 94
- D'AURIA, J., 9, 10, 20  
DÖNAU, F., 32  
DÖRR, L., 84  
DA SILVA, L., 38  
DABABNEH, S., 51, 66, 84  
DALY, J., 17  
DAVIDS, B., 9, 20, 80  
DAVIDSON, P.M., 41  
DAVIDSON, P.O., 41  
DAVINSON, T., 9, 46  
DAVIS, A., 15  
DAVIS, C., 9  
DE FRENNE, D., 69  
DE MOURA, M.M., 39  
DE SEREVILLE, N., 9, 79  
DE SMET, L., 45  
DEAN, D., 11  
DEARBORN, D., 35  
DECRESSIN, T., 59  
DEIBEL, C., 9, 100  
DEL PELOSO, E., 38  
DELAHAYE, P., 30, 91  
DEMETRIOU, P., 30  
DESCOUEMONT, P., 26, 46, 92  
DI LEVA, A., 55  
DIEBELE, I., 54  
DIEHL, R., 8  
DIETRICH, F., 85  
DIGET, C.A., 18  
DILLMANN, I., 29, 42, 43, 51  
DOHERTY, C., 90  
DOMINGO PARDO, C., 34  
DOMINGUEZ, I., 36  
DOMIZIOLI, C., 71  
DORSCH, T., 94  
DOSSA, D., 35  
DRACOU LIS, G.D., 41  
DRAKE, N.A., 82
- DWARKADAS, V., 23  
DWORSCHAK, M., 30
- EGGLETON, P., 35  
EKSTRÖM, S., 49, 94  
ELISEEV, S., 64  
ELLIOT, T., 88  
ELLIS, J., 27  
ELOMAA, V.-V., 64, 87  
ERHARD, M., 32  
ERIKSON, L., 9  
ERONEN, T., 64, 87  
ESCHER, J., 85  
ESTRADE, A., 88, 101
- FÜLÖP, Zs., 99, 102  
FAESTERMANN, T., 43, 97  
FALAHAT, S., 17  
FAROUQI, K., 40, 76  
FENNER, Y., 74  
FERNANDEZ-ORDOÑEZ, M., 11  
FERRO, F., 81  
FIELDS, B., 27  
FIGUERA, P., 9  
FIRNSTEIN, M., 97  
FISKER, J.L., 78  
FOGARTY, L., 9, 20  
FORCADA, R., 74  
FORSSÉN, C., 26, 84, 85  
FORSTER, J.S., 80  
FORTIER, S., 55  
FOX, S., 9, 95  
FRÖHLICH, C., 22  
FREIBURGHaus, C., 60  
FREKERS, D., 9, 20, 69  
FU, C., 80  
FUJII, K., 32  
FUJIKAWA, H., 29, 91  
FUJIMOTO, M., 52  
FUJIMOTO, S., 49, 70  
FUJITA, H., 69  
FUJITA, Y., 69  
FULTON, B., 40, 95  
FYNBO, H., 66, 71
- GÖRRES, J., 17, 19, 40, 72, 83, 84, 87  
GAGLIARDI, C.A., 80  
GALAVIZ, D., 13, 78, 88, 99  
GALAZUTDINOV, G.A., 82  
GALLINO, R., 32, 36, 40, 45, 51, 57, 66  
GAMEIRO MUNHOZ, M., 79  
GARCÍA-BERRO, E., 22  
GARCÍA-SENZ, D., 74  
GARCIA BORGE, M.J., 71  
GARCIA, G., 66  
GARCIA, H., 60  
GARNAVICH, P., 27

- GAUDEFROY, L., 55  
GEIER, S., 68  
GEORGE, S., 30  
GERVINO, G., 48  
GIALANELLA, L., 86  
GIGLIOTTI, D., 95  
GIL-PONS, P., 22  
GIMENEZ DEL SANTO, M., 79  
GIOVINAZZO, J., 11  
GOKO, S., 33  
GOLSER, R., 29  
GOMI, T., 62  
GONCHAROV, G., 67  
GOPKA, V., 82  
GORIELY, S., 21, 50, 82  
GOSSELIN, G., 26  
GREENE, J.P., 100  
GREGORY, D., 56  
GREIFE, U., 9, 71, 76  
GRIMES, S.M., 61  
GROOMBRIDGE, D., 40  
GROSSE, E., 32  
GRYAZNYKH, A.I., 65  
GRYAZNYKH, D.A., 65  
GUEORGUIEV, V., 85  
GUIDRY, M., 56, 69  
GUIMARAES, V., 60  
GUJRATHI, S., 80  
GULICK, S., 100  
GULMINELLI, F., 52  
GUPTA, S., 28  
GUTTORMSEN, M., 89  
GUÉNAUT, C., 30  
GYÜRKY, G., 89, 99
- HACKMAN, G.C., 80  
HADIZADEH, M.H., 61  
HAGEN, G., 11  
HAGER, U., 30, 64, 87  
HAIGHT, R., 84  
HAKALA, J., 64, 87  
HAMMACHE, F., 9, 13, 55  
HAN, I., 82  
HANNAWALD, M., 44  
HANNES, W.R., 20  
HARDY, J.C., 100  
HARISSOPULOS, S., 30  
HARTMANN, D., 47  
HASHIMOTO, M., 46, 49, 50, 52  
HASNAOUI, K., 52  
HASPER, J., 33  
HASS, M., 21  
HAYAKAWA, T., 50, 53  
HE, J.J., 17, 29, 91  
HEBER, U., 68, 83  
HECHT, A.A., 100  
HEGER, A., 8, 21, 36, 69
- HEIDE, P., 27, 81, 94  
HEIL, M., 31, 32, 43, 48, 51, 57, 66, 72, 84  
HEINEN, Z., 61, 71  
HENKEL, C., 12  
HENNRICHS, S., 49, 75, 88  
HENZLOVA, D., 11  
HERFURTH, F., 30  
HERLERT, A., 30  
HERMAN, M., 94  
HERNANZ, M., 22, 79  
HERWIG, F., 35, 36  
HEYSE, J., 45  
HIRSCHI, R., 39, 94  
HIX, W.R., 59, 60, 77, 78, 84, 97  
HNATYK, B., 57  
HOFFMAN, R., 85  
HONDA, S., 23, 64  
HORNISH, M.J., 61, 71  
HOROI, M., 59  
HOWARD, J.A., 59  
HOWELL, D., 80  
HUGHES, J., 44  
HUJIKAWA, H., 17  
HUKE, A., 27, 81, 94  
HUSSEIN, A., 20  
HUTCHEON, D., 9, 20, 96
- ICHIKAWA, I., 62  
ICHIKI, K., 50, 92  
IGASHIRA, M., 31  
ILIADIS, C., 24  
IMAI, N., 62  
INAFUKU, K., 17, 29  
INOUE, S., 51  
IOCCO, F., 58  
ISHIMARU, Y., 24, 62, 64  
IVANS, I., 14  
IWAMOTO, N., 53  
IWASA, N., 17, 29, 62  
IWASAKI, H., 62  
IZZARD, R., 24
- JACHOWICZ, N., 63, 64  
JADHAV, M., 15  
JAKOBS, E., 69  
JANKA, H.-T., 85, 97  
JANSSENS, R.V.F., 21, 41  
JENA, S., 68  
JEPPESEN, H.B., 66  
JEWETT, C., 9  
JIANG, H., 60  
JOHNSON, M.S., 56, 59, 71, 88  
JOHNSON, R.C., 92  
JOKINEN, A., 64, 87  
JONES, K.L., 59, 71, 88  
JONSON, B., 71  
JOSÉ, J., 9, 10, 22, 65, 74, 79, 80

- JUNGHANS, A.R., 32  
JUODAGALVIS, A., 97  
JURADO, B., 11
- KÄPPELER, F., 29, 32, 40, 42, 43, 48, 51, 57, 66, 72, 84  
KAJINO, T., 23, 47, 53, 64, 92, 93, 96  
KALMYKOV, Y., 69  
KANKAINEN, A., 64  
KANUNGO, R., 80  
KARAKAS, A., 16, 24, 45  
KARL, C., 68  
KARLYKHANOV, N.G., 65  
KASHIV, Y., 21  
KATO, S., 17  
KAWAGOE, S., 93  
KAWAI, S., 62  
KELIĆ, A., 36, 79  
KELLERBAUER, A., 30  
KERN, L., 33, 88  
KESSLER, R., 88  
KHIEM, L.H., 29  
KIBEDI, T., 41  
KIENER, J., 9, 55  
KIM, A., 17  
KIM, J.C., 91  
KIM, J.Y., 17  
KIM, K.M., 82  
KIMURA, K., 47  
KING, J., 82  
KIRSEBOM, O., 66  
KISS, G., 99  
KLUGE, H.-J., 30  
KNAPP, G., 14  
KNIE, K., 43, 97  
KOLATA, J.J., 60  
KOLBE, E., 69  
KONDEV, F., 41  
KONDO, Y., 62  
KORNEEV, I., 74  
KORSCHINEK, G., 16, 43, 97  
KOSSEV, K., 32  
KOTAKE, K., 46, 49  
KOURA, H., 77  
KOZUB, R.L., 56, 59, 71, 88  
KRATZ, K.-L., 10, 28, 40, 49, 75, 76, 88  
KUBONO, S., 17, 29, 91  
KURTUKIAN-NIETO, T., 11  
KUSAKABE, M., 96  
KUTSCHERA, W., 20, 29, 42, 51  
KWON, Y.K., 17, 29
- LA COGNATA, M., 91  
LAGOYANNIS, A., 30  
LAIRD, A., 9, 40, 95  
LAMBERT, D.L., 82  
LAMEY, M., 20
- LAMIA, L., 79  
LANE, G.J., 41  
LANGANKE, K., 69, 79, 97  
LARSEN, A.-C., 89  
LATTANZIO, J., 35  
LAU, H.B., 58  
LAVAGNO, A., 47, 48  
LE HONG, K., 17  
LEBLANC, P., 17, 40  
LEE, C.S., 17  
LEE, H.Y., 17, 40, 87  
LEE, J.H., 17, 91  
LEE, J.K.P., 100  
LEEB, H., 100  
LEFEBVRE, A., 9, 55  
LELEUX, P., 9, 40, 46  
LENTZ, E.J., 84  
LESLIE, J.R., 80  
LEVAND, A.F., 100  
LEWIS, R., 9, 15, 100  
LI, ZH., 20  
LIANG, J.F., 59  
LICHTENTHALER, R., 60  
LIEBENDÖRFER, M., 22, 83  
LIGUORI NETO, R., 39, 79  
LIMATA, B.N., 75  
LIMONGI, M., 23  
LINDENBERG, K., 33  
LINDROOS, M., 10  
LINGERFELT, E., 59, 77  
LITVINENKO, I.A., 65  
LIU, WP., 20  
LIU, Z., 46  
LIVESAY, R.J., 56, 59, 71, 88  
LIZCANO, D., 60  
LORUSSO, G., 88  
LUBOWICH, D., 12  
LUCATELLO, S., 14  
LUGARO, M., 16, 24, 45, 73  
LUNDGREN, B.F., 100  
LUNNEY, D., 12, 30  
LUROSSO, G., 102  
LYKOV, V.A., 65
- M. DE MOURA, M., 79  
M. SZANTO, E., 79  
MÜLLER, P., 28  
MÜLLER, S., 33, 99  
MA, Z., 56, 71  
MADOKORO, H., 72  
MADURGA FLORES, M., 66, 71  
MAEDER, A., 14, 49, 90, 94  
MAERO, G., 81  
MAKII, H., 73  
MAKOTO, T., 54  
MANTICA, P., 49, 75, 88  
MANUKOVSKIY, K., 55

- MARIE-JEANNE, M., 91  
MARSTELLER, B., 14  
MARTÍNEZ PINEDO, G., 22, 37, 69, 79, 97  
MARTIN, L., 94  
MARTINEZ-QUIROZ, E., 60  
MASAKI, T., 31, 73  
MASSERON, T., 14  
MASSEY, T.N., 61, 71  
MATE, Z., 99  
MATEI, C., 20, 61  
MATHEWS, G., 23, 28, 92  
MATOS, M., 88  
MATTEUCCI, F., 94  
MCLAUGHLIN, G., 22, 63, 84  
MEDINA, A., 23  
MENGONI, A., 32, 84  
MEOT, V., 26  
MESSER, O.E.B., 84  
MEYNET, G., 14, 39, 49, 90, 94  
MEZZACAPPA, A., 84  
MILLAR, T., 12  
MISHIMA, K., 73  
MIYAMOTO, S., 63  
MOAZEN, B., 71, 88  
MOCHIZUKI, T., 63  
MOHR, P., 50, 99  
MONTES, F., 69, 88  
MOON, J.Y., 17, 91  
MOORE, I., 64  
MOREL, P., 26  
MORENO, F., 65  
MORTON, A.C., 80  
MOSCONI, M., 32  
MOTIZUKI, Y., 72  
MOTOBAYASHI, T., 19, 62  
MUGHABGHAB, S., 94  
MUKHAMEDZHANOV, A.Z., 42, 80  
MUMBY-CROFT, P., 9, 95  
MUNHOZ, M.G., 39  
MURPHY, A., 102
- NADYOZHIN, D., 54, 75  
NAGAI, Y., 31, 63, 70, 73  
NAGATAKI, S., 45, 47  
NAIR, C., 32  
NAKADA, H., 53  
NAKAMURA, K., 51  
NAKAMURA, R., 50  
NAKAO, T., 62  
NAKAYOSI, A., 31, 70  
NAKUMURA, T., 62  
NANKOV, N., 32  
NAOKO, Y., 54  
NAPIWOTZKI, R., 68  
NAPOLITANI, P., 52  
NASSAR, H., 21  
NAVRATIL, P., 26
- NAZARENKO, V., 82  
NEGRET, A., 69  
NESARAJA, C.D., 56, 71, 77, 88  
NIEMINEN, P., 41  
NIEVA, M., 48  
NIKURA, M., 29, 91  
NISHIMURA, N., 49  
NISHIMURA, S., 29, 62, 63, 91  
NISHIYAMA, J., 31  
NITTLER, L., 16  
NODA, T., 52  
NOMOTO, K., 53  
NOVIKOV, Y., 64  
NYMAN, G., 66, 71
- O'BRIEN, S., 17, 40, 84  
O'DONNELL, J.E., 61  
O'TOOLE, S., 83  
OBLOZINSKY, P., 94  
OBRADORS, D., 66  
OFAN, A., 21  
OGAWA, K., 53  
OHNISHI, T., 62  
OHTA, T., 31, 70  
ONG, H. J., 62  
ONISHI, K., 62  
OPENSHAW, R., 95  
ORMAND, W.E., 26  
ORR, N., 9  
OTA, S., 62  
OTSUKI, K., 23  
OTTEWELL, D., 9, 20, 96  
OUELLET, C.V., 9, 20
- PAIN, S.D., 56, 59, 71, 88  
PALUMBO, A., 17, 40  
PANOV, I., 74, 75  
PARDO, R., 21  
PARETE-KOON, S., 60  
PARIKH, A., 9, 100  
PARKER, P., 9  
PARKER, P.D., 100  
PASACHOFF, J., 12  
PATRONIS, N., 84  
PAUL, M., 20, 21, 29  
PAULAUSKAS, S., 56  
PAULUCCI, L., 102  
PAVAN, M., 95  
PEARSON, C.J., 80  
PEARSON, J., 9, 20, 91, 95  
PELLEGRITI, M.G., 55  
PELLIN, M., 15  
PEN, U.L., 83  
PENTTILÄ, H., 64  
PEREIRA, J., 11, 49, 75, 88  
PERERA, A., 62  
PEREZ GARCIA, A., 38

- PETRUK, O., 57  
PFEIFFER, B., 40, 76, 88  
PIERSANTI, L., 36  
PIGNATARI, M., 36  
PIZZONE, R., 91  
PLAG, R., 32, 43, 48, 84  
POPESCU, L., 69  
POPOV, A., 64  
PORTER-PEDEN, M., 56, 71  
PORTO DE MELLO, G., 38  
POUTIVTSEV, M., 43, 97  
PRANTZOS, N., 24, 34  
PREZADO, Y., 71  
PRILLER, A., 29  
PRITYCHENKO, B., 94  
PRUET, J., 85  
PRZYBILLA, N., 48, 98  
PUGLIA, S., 79
- QUARATI, P., 48, 53, 81  
QUINN, M., 49, 75, 88
- RAHAMAN, S., 64, 87  
RAIOLA, F., 65  
RAKERS, S., 69  
RAUSCHER, T., 43, 44, 76  
REHM, K.E., 21  
REIFARTH, R., 48, 84  
REJMUND, F., 11  
REKSTAD, J., 89  
RESSLER, J.J., 80  
RICHTER, A., 69  
RIISAGER, K., 71  
RINTA-ANTILA, S., 64, 87  
ROBERTS, H., 12  
ROBERTS, L.F., 77, 78  
ROBERTSON, D., 9  
ROCHMAN, D., 94  
ROGACHEV, G., 102  
ROLFS, C., 30  
ROMAN, F.L., 100  
ROMANO, S., 79  
ROSSI, S., 14  
ROSTOPCHIN, S.I., 82  
ROUSSEL, P., 55  
RUBBIA, C., 10  
RUGEL, G., 43  
RUIZ, C., 9, 20, 80, 96  
RUNDBERG, R., 84  
RUPRECHT, G., 9, 20, 27, 94-96  
RUSEV, G., 32  
RYAN, S., 14, 64, 86
- SÜMMERER, K., 13  
SAASTAMOINEN, A., 64  
SAITO, A., 17, 29, 91  
SAMPAIO, J., 97
- SANDULESCU, N., 56  
SARAZIN, F., 71  
SAVAJOLS, H., 80  
SAVARD, G., 21, 100  
SAVINA, M., 15  
SCHÜRSMANN, D., 19  
SCHATZ, H., 8, 28, 49, 75, 76, 88  
SCHILLER, A., 89  
SCHILLER, F., 48  
SCHILLING, K.D., 32  
SCHMIDT, K.-H., 11  
SCHMIDT, M., 54  
SCHULER, S., 82  
SCHUMAKER, M.A., 80  
SCHWEIKHARD, L., 30  
SCHWENGER, R., 32  
SCIELZO, N.D., 100  
SCOTT, J., 59, 77  
SEGAWA, M., 31, 70, 73  
SHARMA, K.S., 100  
SHAVRINA, A., 82  
SHERTZ, F., 88  
SHEVCHENKO, A., 69  
SHIGEYAMA, T., 51  
SHIMA, T., 31, 63, 70, 73  
SHIMBARA, Y., 69  
SHIMOURA, S., 62  
SHIZUMA, T., 50, 53  
SHRINER, J.F., 56, 71  
SHUSHLEBIN, A.N., 65  
SIEM, S., 89  
SIMONENKO, V.A., 65  
SIMPSON, E., 83  
SIVARANI, T., 14  
SKAKUN, Y., 44  
SMITH, E., 88, 101  
SMITH, M.S., 56, 59, 71, 76-78, 88  
SMITH, N., 56, 71  
SNEDEN, C., 40  
SOMORJAI, E., 99  
SONNABEND, K., 33  
SONODA, T., 64  
SONZOGNI, A., 94  
SOUZA, F.A., 39  
SPANOVA, G., 95  
SPITALERI, C., 79  
SPYROU, A., 30  
STANCLIFFE, R., 73  
STANOIU, M., 55  
STECH, E., 17, 40, 87  
STEFANO, M., 77  
STEIER, P., 29  
STRANDBERG, E., 17, 87  
STRANIERO, O., 36, 40  
SUADES, M., 79  
SUAIDE, A.A.P., 39

- SUBRAMANIAN, M., 80  
SUJKOWSKI, Z., 96  
SUMIYOSHI, K., 93  
SURMAN, R., 22, 84  
SUZUKI, D., 62  
SUZUKI, H., 62, 93  
SUZUKI, M. K., 62  
SUZUKI, T., 45  
SYED, N., 89  
SYLVIA, E., 14  
SZANTO DE TOLEDO, A., 39, 79  
SZANTO, E.M., 39
- TABACARU, G., 80  
TAGLIENTE, G., 91  
TAKAHASHI, J., 39  
TAKAMURA, A., 47  
TAKASHI, N., 54  
TAKEUCHI, S., 62  
TAKIBAYEV, N., 93, 95  
TAKUYA, S., 54  
TAMAKI, M., 62  
TAN, W., 17, 40, 87  
TANAKA, K., 62  
TANAKA, M., 17  
TANIHATA, I., 80, 100  
TANNER, J., 86  
TATISCHEFF, V., 9, 55  
TATSUYA, K., 54  
TELEZHINSKY, I., 57  
TEMM, Y., 31, 70  
TENGBLAD, O., 66  
TERANISHI, T., 29, 91  
THE, L.S., 82  
THIELEMANN, F.-K., 22, 43, 60, 76  
THOMAS, J.S., 56, 59, 71, 88  
THOMPSON, C., 83  
TIMMES, F., 76, 86  
TIMOFEYUK, N., 92  
TOGANO, Y., 29, 62, 91  
TOMOYUKI, I., 54  
TOUT, C., 58, 73  
TRACHE, L., 80  
TRAUTVETTER, H.P., 83  
TRAVAGLIO, C., 57  
TRIBBLE, R., 17, 80  
TRIMBLE, W., 100  
TRINCZEK, M., 9, 20  
TRURAN, J., 23, 40  
TSANGARIDES, S., 14  
TUDISCO, S., 79  
TULI, J., 94  
TUR, C., 29  
TYPEL, S., 13
- UBERSEDER, E., 72, 84  
UEDA, H., 73
- UGALDE, C., 17, 83, 87  
UHLIG, F., 13  
UMEDA, H., 53  
UTSUNOMIYA, H., 33, 50, 63
- VANDERBIST, F., 46  
VANTOURNHOUT, K., 64  
VAUGHAN, K., 9  
VILMAY, M., 55  
VISSER, D.W., 59, 71  
VOCKENHUBER, C., 9, 20, 29, 51, 96  
VOINOV, A.V., 61, 71, 89  
VON BRENTANO, P., 69  
VON NEUMANN-COSEL, P., 69  
VON OERTZEN, W., 100  
VONDRASEK, R., 21  
VOROBYEV, G., 64
- WAGEMANS, C., 45  
WAGNER, A., 32  
WAKABAYASHI, Y., 17, 29, 91  
WALDEN, P., 80, 95, 96  
WALLNER, A., 20, 29, 42, 43, 51, 97  
WALTER, S., 48  
WALTERS, W., 55, 88  
WANAJO, S., 24, 45, 47, 51, 61, 62, 64  
WANG, J.C., 100  
WANG, Y., 100  
WATANABE, H., 41  
WIESCHER, M., 17, 36, 40, 72, 76, 83, 84, 87  
WILHELMY, J., 84  
WILSON, A.N., 41  
WINCHELL, D., 94  
WINCKLER, N., 51, 66  
WOEHR, A., 49, 75, 88  
WOODS, P.J., 46  
WOOSLEY, S., 85  
WREDE, C., 9, 20, 100  
WUOSMAA, A., 29
- YAMADA, S., 46, 49, 93  
YAMAGUCHI, H., 17, 29, 91  
YAMAGUCHI, M., 54  
YAMAZAKI, D., 92  
YANAGISAWA, Y., 62  
YASUO, A., 54  
YASUTAKE, N., 46  
YAZIDJIAN, C., 30  
YEN, S., 80  
YOKOMAKURA, H., 47  
YORDANOV, O., 11  
YOSHIDA, T., 47  
YOSHIHIRO, T., 54  
YOSHINORI, Y., 54  
YUDIN, A., 54  
YUSHCHENKO, A., 82
- ZACS, L., 54

ZHAI, Y.J., 80  
ZHOU, Z., 100  
ZILGES, A., 33, 99  
ZINNER, E., 15  
ZINNER, N., 79

# Nuclei in the Cosmos IX

CERN, GENEVA, SWITZERLAND ● 25 – 30 June 2006

## NIC-IX SPONSORS



CERN Directorate



CERN – AB Department



CERN – PH Department



The n\_TOF-Collaboration



Forschungszentrum Karlsruhe  
in der Helmholtz-Gemeinschaft

Forschungszentrum Karlsruhe



The ISOLDE Collaboration



UNIVERSITÉ DE GENÈVE

University of Geneva

sc|nat

A Commission of  
the Swiss Academy of Sciences

Swiss Academy of Sciences

### CAEN

*Tools for Discovery*

CAEN spa, Italy



Mesytec GmbH & Co. KG



International Union of Pure and Applied Physics (IUPAP)



Astronomical Observatory of the Geneva University



Société Académique de Genève



Micron Semiconductor. Co. UK



### CANBERRA

Canberra Semiconductor NV



ACQIRIS, Geneva

